The Paradoxical Roles of Cell Death Pathways in Immune Cells

Scott McComb

Thesis submitted to the
Faculty of Graduate and Postdoctoral Studies
In partial fulfillment of the requirements
For the PhD degree in Microbiology and Immunology

Department of Biochemistry, Microbiology and Immunology

Faculty of Medicine

University of Ottawa

`

ABSTRACT

Cell death plays a vital role throughout the immune response, from the onset of inflammation to the elimination of primed T cells. Understanding the regulation of cell death within immune cells is of vital importance to understanding the immune system and developing therapies against various immune-disorders. In this thesis I have investigated the regulation of cell death and its functional role in of the innate and adaptive arms of the immune system.

The mechanisms that govern expansion and contraction of antigen stimulated $CD8^+$ T cells are not well understood. In the first section of this thesis, I show that caspase-3 becomes activated in proliferating $CD8^+$ proliferation, yet this does not result in cell death. I used both *in vivo* and *in vitro* models to demonstrate that caspase-3 activation is specifically driven by antigen presentation and not inflammation, and that it likely plays a role in promoting T cell proliferation.

Next, I present novel data regarding the regulation of a newly identified form of programmed cell death via necrosis, known as necroptosis. I show that the cellular inhibitor of apoptosis (cIAP) proteins act to limit activation of key necroptosis proteins in macrophage cells. Furthermore, I show that necroptosis can be exploited by intracellular bacterial pathogens to escape removal by the immune system. I also demonstrate that necroptosis is highly intertwined with the pathway of inflammation, and the autocrine production of type-I interferon constitutes a vital positive feedback loop in the induction of inflammatory cell death. In the final section of my thesis work, I delve into the specific regulation of Rip1 kinase and demonstrate that in addition to previously demonstrated regulation by caspase-8, cathepsins are also able to cleave Rip1 kinase and limit necroptosis.

This thesis presents a wide variety of novel data regarding the regulation of cell death within immune cells. In total, the results reveal a picture of two divergent forms of programmed cell death,

apoptosis and necroptosis. Through improving the understanding of the cross-regulation of these two key cell death pathways this work aims to improve the understanding of the immune function.

ACKNOWLEDGEMENTS

I would like to acknowledge all of the many people who helped me along the way in my graduate studies. The process of science is at its heart a collaborative one, and I have many people to thank. I would like to thank all current and former members of Krishnan and Sad (LKSS) labs; their help has been invaluable in my training and scientific work. Thank you to the many LKSS graduate students, postdoctoral researchers, and alumni; you have been an indispensable source of inspiration, discussion, collaboration and friendship. Thanks as well to the students I had the pleasure of mentoring both in the Sad lab and outside of it, your hard work and inquiring minds have helped me grow as a scientist and a teacher.

I would also like to thank the professors of the University of Ottawa Department of Microbiology and Immunology, who have instilled in me the knowledge and skills which I hope will enable me to pursue my own academic career. To my supervisor, Dr. Subash Sad, thank you for your patient guidance over the years. Thank you for encouraging me to think outside of the box and having the courage and trust for us to follow through on these ideas in the lab.

Finally, I would like to thank my family, who have given me the base of love and support that has allowed me to reach for and realize my dreams. I especially want to thank my wife Andrea for patiently bearing the idiosyncrasies of a scientific mind; I could not have accomplished this without you.

Thank you to the Canadian public for supporting scientific research. My work was supported by scholarships from the Ontario Graduate Scholarship Program and University of Ottawa. Research funds were provided by grants from the Canadian Institute for Health Research.

TABLE OF CONTENTS

ABSTRACT **1**
ACKNOWLEDGEMENTS **3**
TABLE OF CONTENTS **4**
LIST OF ABBREVIATIONS **7**
LIST OF FIGURES AND TABLES **9**
1.0 INTRODUCTION **11**
1.1 The Immune System 12
1.1.A Macrophages 13
1.1.A-I Innate Immune Cells and Inflammation – See Figure 1 15
1.1.A-II Macrophage Cell Death in Bacterial Infections 20
1.1.B $CD8^+$ T cells 22
1.1.B-I Cell Death Pathways in $CD8^+$ T Cell Function 25
1.2 Programmed Cell Death 26
1.2.A Apoptosis 28
1.2.A-I Extrinsic Apoptosis 28
1.2.A-II Intrinsic Apoptosis 32
1.2.A-III Caspase-3 34
1.2.A-IV SMAC and IAPs 35
1.2.B Necroptosis 37
1.2.B-I Necrotic Cell Death and Inflammation 42
2.0 SUMMARY **50**
2.1 Hypothesis 50
2.2 Aims 50
3.0 METHODS AND MATERIALS **51**
3.1 Animal Work 51
Adoptive transfer of OT1 splenocytes 51
In vivo Infection Models 51
Table 1: Mouse strains utilized in experiments, ... 52
In vivo Antigen Presentation 53
3.2 Bacterial Methods 53
CFU Assay 54
3.3 Cell Purification and Sorting 54
Magnetic Isolation of Cells 54
Cell Sorting by Flow Cytometry 55

3.4 Cell Culture 55

In vitro Antigen Presentation to $CD8^+$ T cells 55
In vitro LM-OVA Infection and Limiting Dilution Assay 55
Generation of Bone Marrow Macrophages and Dendritic Cells 56
In vitro Inhibitor Assays 57
RNA Interference 58
Mitochondrial Activity Cell Viability Assay (MTT) 58
Table 2: Inhibitors utilized in experiments 59
Cell death assay (LDH release) 60

3.5 Immunofluorescent Analyses 60

Flow Cytometry 60
Table 3: Antibodies and staining reagents 61
Intracellular Staining 62
Live Cell Flow-Cytometry 62
Confocal Microscopy 62
Live Cell Fluorescence Microscopy 63

3.6 Biochemical Analyses 64

Quantitative RT-PCR 64
SDS-PAGE and western blotting 64
Protein Dephosphorylation 65
Immunoprecipitation 65
Plasmid constructs and protein purification 66
Cell free cleavage assay 66

3.7 Statistics 66
3.8 Technical Acknowledgement 66

4.0 RESULTS 68

4.1 Caspase-3 Activation in $CD8^+$ T –Cell Function 68

4.1.A Caspase-3 is upregulated in proliferating $CD8^+$ T cells 68
4.1.B Active caspase-3 in proliferating $CD8^+$ T cells does not lead to cell death 70
4.1.C Proliferating $CD8^+$ T Cells show elevated caspase-3 in vivo 73
4.1.D The timing and magnitude of caspase-3 activation corresponds with the timing and 75
magnitude of antigen presentation 75
4.1.E Proliferating caspase-3+ CD8+ T cells show an apoptotic like phenotype 77
4.1.F Active caspase-3^{high} $CD8^+$ T cells do not progress to cell death 77
4.1.G Active caspase-3 is driven by antigen presentation and not inflammation 80
4.1.H Caspase-3 activation occurs before the emergence of differentiated $CD8^+$ effector cells 83
4.1.I Active caspase-3 promotes $CD8^+$ T cell proliferation 84

4.2 The Role of IAPs in Innate Immune Cell Function 87

4.2.A cIAPs limit cell death in innate immune cells 87
4.2.B SM-induced death is associated with increased inflammatory cytokine production 90

4.2.C SM induces programmed necrosis in macrophages 92
4.2.D cIAP1 and cIAP2 additively limit macrophage necroptosis 92
4.2.E xIAP limits SM-induced apoptosis 95
4.2.F Loss of cIAPs increases Rip1 activation 95
4.2.G Loss of cIAPs reduces constitutive degradation of Rip1 and Rip3 kinases 95
4.2.H Autocrine TNFR1 or 2 signaling is necessary for SM-induced necroptosis 97
4.2.I In vivo administration of SM results in macrophage cell death 99
4.2.J Loss of cIAP function in vivo decreases control of Listeria monocytogenes 99

4.3 *Salmonella* Induces Interferon Dependent Necroptosis 102

4.3.A cIAP1$^{-/-}$ or cIAP2$^{-/-}$ mice are more susceptible to Salmonella typhimurium 102
4.3.B ST infection of macrophages leads to delayed necroptosis 102
4.3.C ST induces necroptosis in macrophages in vivo 104
4.3.D Type-I interferon signaling is required for ST-induced necroptosis 104
4.3.E Treatment with IFN-β and zVAD induces necroptosis 107
4.3.F Type-I interferon is a key feedback in LPS induced necroptosis 107
4.3.G Type-I interferon induced death drives systemic shock in vivo 110

4.4 Cathepsins Regulate Necroptosis 110

4.4.A zVAD alone can induce macrophage necroptosis 110
4.4.B LPS stimulation drives Rip1 kinase activation independently of TNFR signaling 113
4.4.C Cysteine cathepsins cleave Rip1 kinase 116
4.4.D Cathepsin S and B both cleave Rip1 kinase 118
4.4.E Cathepsins associate with Rip1 kinase directly 121
4.4.F Cathepsins can directly cleave Rip1 kinase 121
4.4.G Cathepsins and caspase-8 cooperate to limit necroptosis 124

5.0 DISCUSSION 127

5.1 The role of Caspase-3 in CD8^{+} T Cells 127
5.2 The Role of IAPs in Innate Immune Cell Function 135
5.3 Necroptosis and Interferon 141
5.4 The Regulation of Necroptosis by Cathepsins 151

6.0 CONCLUSION 157
REFERENCES 160
CONTRIBUTIONS OF COLLABORATORS 179

LIST OF ABBREVIATIONS

ANT	Adeninine Nucleotide Transporter
BCL-2	B-Cell Lymphoma 2
BH-3	BCL2 Homology Domain 3
BMDM	Bone Marrow derived macrophage
C8I	Caspase-8 Inhibitor
cFLIP	Cellular FLICE-like Inhibitory Protein
CFSE	Carboxyfluorescein succinimidyl ester
CFU	Colony Forming Units
cIAP(1/2)	Cellular Inhibitor of Apoptosis
CLP	Caecal ligation and puncture
CTL	Cytolytic T cell
CYPD	Cyclophilin D
DAMP	Damage Associated Molecular Pattern
DD	Death Domain
DED	Death Effector Domain
DISC	Death inducing signaling complex
DSB	Double Strand Breaks
E64D	E64-D cysteine protease inhibitor
FADD	Fas-Associated Death Domain Protein
HMGB1	High-mobility Group Box Protein 1
IFN	Interferon
IFNAR	Interferon α/β Receptor
IL-(1...)	Interleukin
IRAK	Interleukin-1 Associated Kinase
IRF(3/7)	Interferon Regulatory Factor
Iκβ	Inhibitor of κβ
LCMV	Lymphocytic choriomeningitis virus
LM	Listeria monocytogenes
LM-OVA	Listeria monocytogenes expressing OVA
LPS	Lipopolysaccharide
MCMV	Mouse cytomegalorvirus
MHC	Major Histocompatibility Complex
MLKL	Mixed Lineage Kinase domain-Like
MOMP	Mitochondrial Outer Membrane Permeabilization
MPTP	Mitochondrial Permability Transition Pore
Myd88	Myeloid Differentiation Primary Response Gene 88
Nec	Necrostatin
NEMO	NF-κβ essential modulator
NF-κβ	Nuclear Factor Kappa-light-chain-enhancer of activated B cells
OT-1	Transgenic Mouse with OVA specific TCR
OVA	Ovalbumin
PAMP	Pathogen Associated Molecular Pattern
PBS	Phosphate buffered saline
PD-1	Programmed Death Marker 1
PI	Propidium Iodide
PKR	Protein Kinase R
PPL	PhiPhiLux - Fluorescent Caspase-3 Substrate
PRR	Pattern Recognition Receptor
R8	RPMI with 8% Fetal Bovine Serum
RHIM	Rip Homotypic Interaction Domain
Rip(1/3)	Receptor Interacting Protein Kinase
RNS	Reactive nitrogen species
ROS	Reactive oxygen species
SM	SMAC Mimetic
SMAC	Secondary Mitochondrial Activator of Cell Death
ST	Salmonella Typhimuirum

STAT	Signal Transducers and Activators of Transcription
ST-OVA	Salmonella Typhimuirum expressing OVA
TBS	Tris-buffered Saline
TCR	T-cell receptor
TLR	Toll-like Receptor
TNF	Tumour Necrosis Factor
TNFR	Tumour Necrosis Factor Receptor
TRADD	TNF-Receptor Associated Death Domain Protein
TRAF(1…)	TNF-Receptor Associated Factor
TRIF	TIR-domain Containing Adapter Inducing IFN-β
TUNEL	Terminal dUTP nick end labeling
xIAP	X-linked Inhibitor of Apoptosis
zVAD	z-VAD-FMK Pan-caspase Inhibitor

LIST OF FIGURES AND TABLES

Figure 1: *Inflammatory signaling pathways* 16
Figure 2: *Antigen presentation activates the T cell response* 23
Figure 3: *Extrinsic and intrinsic apoptotic signaling pathways* 29
Figure 4: *The many outcomes of TNF receptor signaling* 31
Figure 5: *The necrosome as a functional integrator of many signaling pathways.* 43
Figure 6: *The functional spectrum of necroptosis.* 45
Figure 7: *Active caspase-3 is upregulated in proliferating T cells.* 69
Figure 8: *Active caspase-3^{hi} CD8^{+} T Cells do not exhibit DNA fragmentation.* 71
Figure 9: *Active Caspase-3 in proliferating CD8 T cells does not lead to cell death.* 72
Figure 10: *Proliferating CD8+ T Cells show elevated Caspase-3 during in vivo response.* 74
Figure 11: *The timing and magnitude of caspase-3 activation corresponds with the timing and magnitude of antigen presentation.* 76
Figure 12: *Activated antigen specific CD8+ T cells simultaneously display markers for apoptosis and proliferation.* 78
Figure 13: *Caspase-3^{hi} proliferating CD8+ T cells in vivo do not show signs of progressing to cell death.* 79
Figure 14: *Caspase-3^{hi} proliferating CD8+ T cells do not undergo significant cell death when supplemented with supportive cytokine ex vivo.* 81
Figure 15: *Active caspase-3 is driven by antigen presentation and not inflammation.* 82
Figure 16: *Caspase-3 activation occurs before the emergence of differentiated CD8^{+} effector T cells.* 85
Figure 17: *Caspase-3 inhibition slows CD8+ T cell proliferation and enhances cell death* 86
Figure 18: *cIAPs inhibition does not have a significant impact on CD8+ T cell proliferation.* 88
Figure 19: *cIAPs limit cell death in bone marrow derived macrophages and dendritic cells.* 89
Figure 20: *SM-induced death is associated with increased inflammatory cytokine production.* 91
Figure 21: *SM treatment induces programmed necrosis in macrophages.* 93
Figure 22: *cIAP1 and cIAP2 are functionally redundant and additive in limiting macrophage necroptosis, while XIAP limits SM-induced apoptosis.* 94
Figure 23*: Loss of cIAPs increases Rip1 and Rip3 expression and activation.* 96
Figure 24: *Autocrine TNFR1 signaling is necessary for SM-induced necroptosis.* 98
Figure 25: *In vivo administration of SM results in cIAP degradation and macrophage cell death.* 100
Figure 26: *Decreased cIAP function in vivo decreases control of Listeria monocytogenes.* 101
Figure 27: *cIAP1 Deficient mice are more susceptible to infection with Salmonella typhimurium.* 103
Figure 28: *Infection of BMDM cells with ST induces delayed necroptotic cell death.* 105
Figure 29: *Rip3-deficient mice show less macrophage cell death during ST infection in vivo.* 106
Figure 30: *IFNAR-deficient BMDMs show less phosphorylation of Rip1 and Rip3 kinases and less necroptosis upon infection with ST.* 108

Figure 31: *Treatment of J774 macrophages with IFNβ drives necroptosis.* 109
Figure 32: *Autocrine production of type-I interferon is a key mechanism in the induction of necroptosis through the zVAD/LPS pathway.* 111
Figure 34: *zVAD alone can induce macrophage necroptosis.* 112
Figure 35: *LPS stimulation drives necroptosis independently of TNFR signaling* 114
Figure 36: *A non-caspase-8 cysteine protease cleaves Rip1 Kinase.* 117
Figure 37: *Cathepsin S and B can cleave Rip1 kinase.* 119
Figure 38: *Single knockouts for cathepsin S or cathepsin B show no change in susceptibility to necroptosis.* 120
Figure 39: *Cathepsins associate with Rip1 kinase directly.* 122
Figure 40: *Cathepsins can directly cleave Rip1 kinase in a cell free environment.* 123
Figure 41: *Cathepsins and caspase-8 cooperate to limit necroptosis.* 125
Figure 42: *CD8+ T cells become active caspase-3 high soon after activation and progressively lose this as cells proliferate.* 134
Figure 43: *Activation of Rip1 is kept in check by cIAP mediated degradation.* 142
Figure 44: *Model of how ST induces necroptosis* 146
Figure 45: *The role of interferon in LPS/zVAD induced necroptosis* 150
Figure 46: *The positive and negative regulators of necroptosis.* 155

Table 1: *Mouse strains utilized in experiments* 51
Table 2: *Inhibitors utilized in experiments* 58
Table 3: *Antibodies and staining reagents* 60

1.0 INTRODUCTION

Cell death is an indispensable mechanism for development and maintenance of all forms of complex life. Without the ability to trim unnecessary or damaged cells from the body, multicellular life would likely be impossible. Programmed cell death has even been observed within bacterial colonies in order to remove damaged cells[1,2]. Programmed cell death also plays a particularly important role at every level of an immune response. From the outset, cell death, induced by cellular damage or by pathogens directly, is thought to play a central role in the initiation of an inflammatory response[3]. In some cases, immune cells must also become resistant to normal cell death pathways in order to function within infected and cytotoxic microenvironments. In adaptive immune cells, these cells maintain the ability to rapidly expand massively by clonal proliferation in response to specific antigenic stimulation. Paradoxically, cell death pathways appear to play a role in this process of immune cell proliferation[4,5]. Following an adaptive response, the removal of the majority of activated immune cells while maintaining a reservoir of memory cells, also seems to rely on programmed cell death mechanisms[6,7].

A clear understanding of the regulation of cell death pathways within immune cells is essential to understanding of the immune system as a whole. In the work presented here, I will delve into new mechanisms that regulate cell death within innate and acquired immune cells. I will begin by presenting work in CD8 T cells, wherein we have uncovered novel data showing the activation of apoptotic cell death proteins without the induction of cell death in proliferating T cells. In follow up to this work, we next became interested in the role of non-apoptotic cell death pathways. Thus, I will next present work investigating the role of a new form of programmed necrotic cell death within innate immune cells, with a focus on macrophages. Finally, I will apply new understanding of the

regulation of programmed necrosis to bona fide models of infection and inflammation. Through revealing novel pathways by which immune cells have evolved to regulate cell death, I provide new insight into the regulation of key immune processes such as inflammation and T cell activation. Using both *in vitro* and *in vivo* techniques, I will demonstrate in a number of different systems how dysregulated immune cell death can lead to poorer immune response and pathology.

1.1 THE IMMUNE SYSTEM

The mammalian immune system can be broadly divided into the innate and adaptive arms. The innate immune system is made of the physical, chemical and cellular barriers which react directly to damage or infection. To accomplish this ends, the innate immune system has genetically fixed receptors which are programmed to be activated by a large number of molecules indicative of damage or infection. The specific cells of the innate immune system include macrophages, monocytes, neutrophils and dendritic cells, among others[8]. These cells usually react first to infection, often acting to induce the earliest inflammatory immune responses. In contrast to the innate immune system, the adaptive immune system is populated by cells that are constantly generated within specialized immune tissues, each carrying a specialized and specific immune receptor. These unique adaptive immune receptors are generated in developing T and B cells through a process of random shuffling of genetic elements known as VDJ rearrangement[8]. Only if adaptive immune cells encounter a molecule which can specifically bind their specific receptor will they become activated and able to perform their specific immune function. By combining the general ability of the innate immune system to initiate inflammatory immune reactions with the ability of the acquired immune system to focus its effects on particular targets, the mammalian immune system can effectively

recognize and defend against the staggering variety of bacteria, viruses and parasites present in the external environment (see [9] for more).

There is a large body of work covering the ways in which innate immune cells are able to respond to pathogens and initiate specific immune responses. Given that this thesis concentrates mainly on the functional role of macrophage cells, I will utilize these cells to introduce the important innate immunity concepts of pattern recognition receptors, cytokines, and inflammation. Similarly, within the adaptive immune compartment, the work described in this thesis examines the role of CD8 T cells. Thus, I will utilize the CD8 T cell section of this introduction to discuss important adaptive immune cell concepts such as antigen presentation, T cell activation, effector functions, and contraction of the response.

1.1.A *Macrophages*

Innate immune cells are found throughout the tissues of the body, where they continually scan the environment through phagocytosis. These tissue resident innate immune cells are formed when circulating monocytes extravasate from blood vessels and mature at peripheral sites. Macrophages are one important subtype of these highly phagocytic cells found in all tissues of the body[9]. Because they are found in high numbers throughout the body, macrophages are generally considered the first line of defense against pathogens. Upon encountering particles of appropriate size [0.5-2μM[10]], macrophages will ingest the particulate matter via phagocytosis. For smaller particles such as macromolecules and viruses, macrophages also show high levels of endocytosis through a variety of receptors, as well as performing pinocytosis[11]. The cell will then analyze the contents of this ingested material through an array of specialized immune pattern recognition receptors (PRRs)[12]. Depending on specific pathogen or damage associated molecular pattern (PAMPs and DAMPs) in the material ingested or in the environment around the macrophage, the

cells may become activated. Macrophages will then digest the particulate matter through proteolytic enzymes, become activated to produce various cytokines, and diminish pathogen replication[13]. Ultimately it is thought that inflammatory macrophage activation represents a key step in the initiation of the immune response to pathogens and in various inflammatory pathologies[14].

The role of macrophages in controlling bacterial infections has been well characterized. For example, mice lacking the key innate immune cell proliferation factor, GM-CSF, have been shown to be highly susceptible to *Streptococcus*[15] and *Listeria*[16] infections. While lack of GM-CSF might also have significant off-target effects on innate immune cells other than macrophages, the specific depletion of macrophages through a genetically encoded drug-inducible apoptosis system has also been shown to enhance susceptibility to *Yersinia pestis*[17]. Anti-bacterial macrophage activity has also been demonstrated as a vital element in control of *Salmonella enterica* serovar typhimurium (*Salmonella typhimuirum*) infection[18,19]. In a number of viral infection models, it has also been shown that macrophages are specifically important in limiting viral replication[20–22]. In dengue virus infections for example, it has been shown that depletion of macrophages actually had slightly lower virus within draining lymph nodes but allowed much higher systemic viral load, suggesting that macrophage cells act to pull virus into immune sites and limit peripheral spread[22].

While there is certainly strong evidence to support the vital role of macrophages in controlling acute infection, macrophages have deleterious effects in some infections. For example, in mouse models of necrotizing fasciitis it was shown that depletion of macrophages resulted in less systemic dissemination of *Streptococcus* bacteria from a site of subcutaneous infection, ultimately leading to improved survival[23]. Similarly, *Salmonella typhimuirum*[24], *Listeria monocytogenes*[25], *C. pneumoniae*[26] and several viruses[27–29] also utilize macrophage cells for systemic dissemination. In

the case of chronic pathogens such as HIV[29], *Salmonella*[30] and *Mycobacterium tuberculosis*[31] it is thought that macrophages can also act as a key reservoir, aiding in persistence of these diseases.

In addition to possible deleterious effects in various infection models, macrophages are also implicated in inflammatory pathologies. In a macrophage specific CD11b promoter driven diphtheria toxin (DT) receptor model of macrophage depletion, macrophages have been shown to play a key role in the acute peritoneal inflammatory response[32] and atherosclerotic plaque formation[33]. Similarly, liposome mediated macrophage depletion has been used to demonstrate the role of macrophages in many models of inflammatory pathology including endotoxic shock[34,35], rheumatoid arthritis[36], and implant-wear associated inflammation[37]. These experiments clearly place macrophages at the centre of inflammatory program. Whether such inflammation leads to a protective immune response or becomes pathological will ultimately be determined by a careful balance of key signaling factors which are not yet fully understood.

1.1.A-I Innate Immune Cells and Inflammation – See Figure 1

The innate immune system relies on an array of pattern recognition receptors (PRRs) to become activated in response to signals of damage or infection. When PRRs bind their cognate pathogen (PAMP) or damage (DAMP) associated ligands, it is thought that this generally drives clustering of two or more receptor monomers[38]. In the case of TLR proteins, ligand binding allows the toll/IL-1 domains (TIR domains) of two or more receptors to associate, inducing a conformational change which in turn allows signaling molecules such as Myd88 and TRIF to bind at the intracellular tail of the receptor[12]. Interactions with additional signal kinases leads to the formation of a larger complex of proteins that drives downstream signaling, eventually culminating in the activation of nuclear transcription factors such as NF-κβ, MAPK or IRFs[12].

Figure 1: *Inflammatory signaling pathways.* PAMPs and DAMPs are able to stimulate immune cells through specific PRRs. PRRs can be located on the cell surface, on vacuoles, or in the cytosol. Activation of these PRRs cause the translocation of various signaling elements to the nucleus which can induce the expression and release of inflammatory cytokines. Inflammatory stimulation can also have important metabolic affects, which may drive the release of ROS. Inflammatory cytokines can have a wide range of effects on the cell, including activation of additional transcriptional modifiers such as STATs or NF-κβ. Some cytokine receptors can also induce cell death, as is the case for the TNF-receptor.

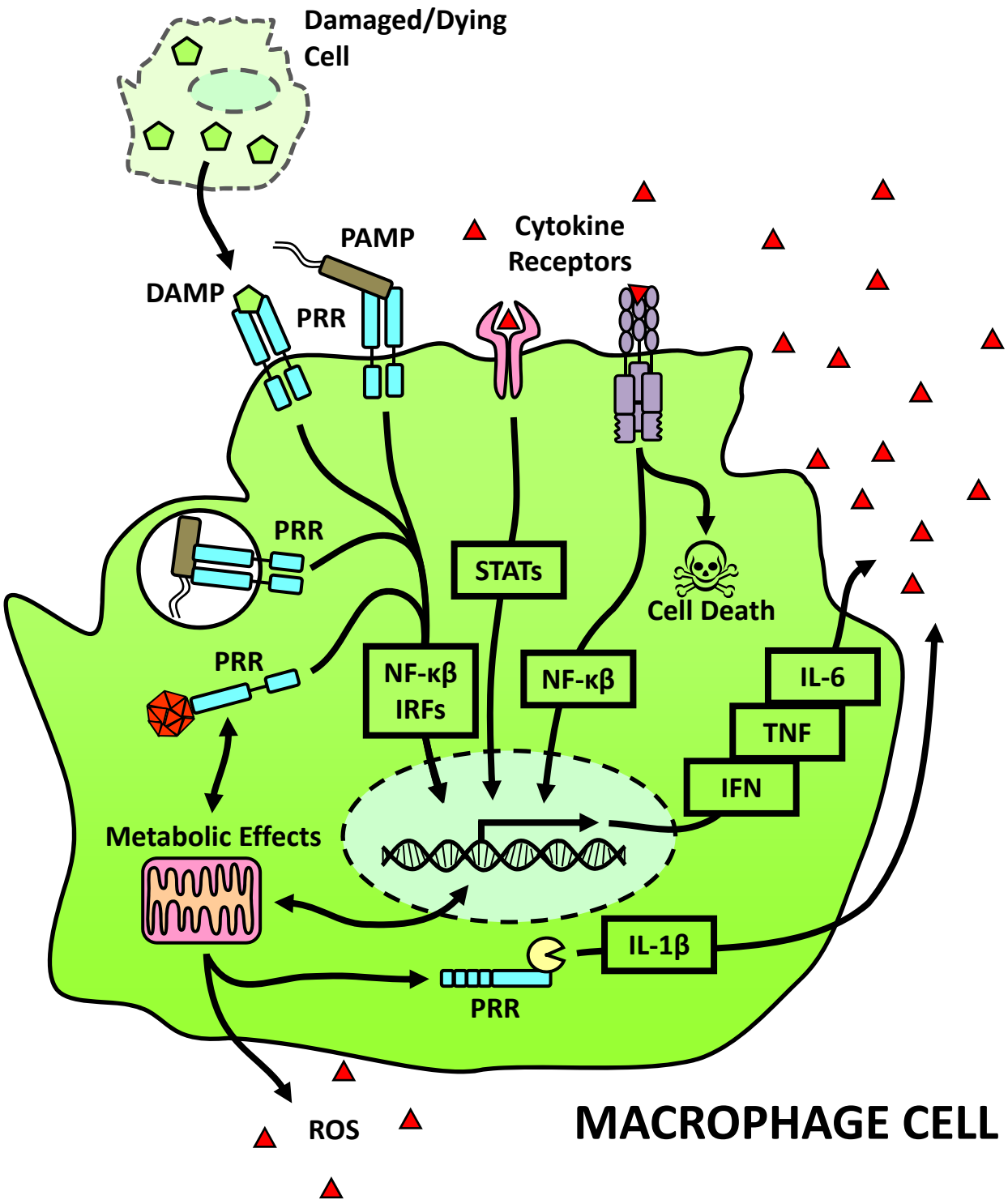
Damaged/Dying
Cell
PAMP
DAMP
PRR
Cytokine
Receptors
PRR
STATs
Cell Death
PRR
NF-κβ
IRFs
NF-κβ
IL-6
TNF
IFN
Metabolic Effects
IL-1β
PRR
ROS
MACROPHAGE CELL

Recently, many PRR signaling pathways have been demonstrated to also interact with key programmed necrosis proteins Rip1 and Rip3 (discussed in section 1.2.B-I).

The activation of nuclear transcription factors drives the expression of target genes. Taking the activation of NF-κβ by the PRR TLR4 for example, signaling is initiated by binding of bacterial lipopolysaccharide to the TLR4 receptor. This binding, which also involves extracellular factors such as CD14 and MD2, activates a conformational change in TLR4. This conformational change results in the recruitment of Myd88 to the intracellular tail of the receptor complex, which subsequently recruits members of the IL-1 receptor associated kinase (IRAK) family[39]. As the IRAKs (IRAK1, 2 and 4) become phosphorylated they associate with and catalyze the K63-autoubiquitination of TRAF6[40]. Non-degradative K63-ubiquitnation of TRAF6 allows the recruitment of the NF-κβ activating TAB2/TAK1/NEMO complex. Subsequently, NEMO becomes K63-ubiquitinated by TRAF6[41], which then allows it to associate with IKKα and IKKβ. Interestingly, NEMO seems to act as a signal integrator by receiving stimulus from a number of signalling pathways in activating NF-κβ, including TNF, Toll-like receptors, and genotxic stress[42]. This complex of NEMO/IKKα/IKKβ is then able to phosphorylate the key inhibitor of NF-κβ, Iκβ[43]. Phosphorylated Iκβ becomes rapidly degraded, which finally allows the translocation of NF-κβ into the nucleus (reviewed in [44]). Once in the nucleus, NF-κβ can interact with cell specific transcription factors and bind available genes depending upon methylation and histone interaction[45]. Contingent on the specific immune cells wherein NF-κβ is being activated, the transcription of a different subset of cytokines can be activated.

Similarly to NF-κβ, expression of type-I interferon is also activated downstream of a number of PRRs. In this case, TRIF drives the phosphorylation of the interferon-regulatory factor 3 and/or 7 (IRF3 and IRF7)[46]. The subsequent translocation of phosphorylated homo- and hetero-dimers

of IRF3 and IRF7 to the nucleus induces the expression and release of type-I interferons (IFNα and/or IFNβ) from innate immune cells[46]. Thus, through the translocation of various transcription factors into the nucleus in response to PRR stimulation, innate immune cells induce the expression of powerful inflammatory mediators. While these inflammatory mediators can include chemokines and cytokines; this thesis will focus on the role of cytokines in particular.

Inflammatory cytokines released by innate immune cells will quickly diffuse into the immediate areas surrounding the site of inflammation. While cytokines are released more widely into the body, the local effects of higher concentrations of cytokines are better defined in most cases. Cytokine receptors have varying expression patterns depending on their specific function, ranging from wide to highly specific expression on just a subset of immune cells[9].

Upon binding their cognate receptors, cytokines can also activate a range of signaling pathways. For example, the inflammatory cytokines IL-1 and TNFα activate NF-κβ, whereas IL-6 and interferons generally signal through the JAK/STAT1 signaling axis[47]. Similar to PRR signaling, the movement of transcription factors to the nucleus induces cells to increase expression of various genes involved in lowering the susceptibility of cells to infection, induction of cell death, or attraction of immune cells[48]. In addition, cytokine signaling often drives negative feedback cycles, as occurs with increased suppressor of cytokine signaling (SOCS) expression in response to interferon, as well as other inflammatory stimuli[49]. In some cases, cytokines can also drive cell death, as is sometimes the case in TNF signaling (see section 1.2.A-I).

Inflammatory stimulation also induces important metabolic changes within the target cell, in particularly within immune cell types. Specifically, both PRRs[50,51] and cytokine receptors[52–54] have been shown to increase glucose uptake and glycolytic metabolism. In the case of innate immune cells, such as neutrophils and macrophages, investigations have revealed a significant

shift in the cellular metabolism away from mitochondrial respiration and towards aerobic glycolysis during inflammation[55,56]. It is believed that this switch to glycolysis actually provides faster access to energy in inflamed tissue, despite being significantly less efficient than mitochondrial respiration[57]. In addition, the glycolytic shift is thought to lower cellular susceptibility to infection[55], allow cells to resist the hypoxic environment of inflamed tissue[50], and increase cellular proliferation[58].

Coincident with the metabolic shift to glycolysis, there is also an increase in the production of reactive oxygen and reactive nitrogen species (ROS and RNS)[59]. Within macrophages and other innate immune cells, ROS production occurs both at the plasma membrane, by NADPH oxidase, and within the cytosol, by the mitochondria[60]. ROS and RNS can damage sensitive biological molecules[61]. Some forms of these small ROS and RNS are also able to diffuse across membranes and into neighbouring cells where they can propagate the effects of inflammation[60]. In recent reports, some of the more specific connections between inflammation and ROS have been defined. In particular, it has been shown that the cytosolic protein NLRP3 undergoes a conformational change when it is exposed to elevated ROS levels[62]. In turn, NLRP3 forms a complex with ASC and caspase-1, termed the inflammasome, which activates the cleavage and release of a mature form of the inflammatory cytokine IL-1β[63]. Thus, the production and release of ROS/RNS represents an important step in the inflammatory program (see Figure 1).

Inflammation significantly alters the metabolic state and gene expression patterns of surrounding cells. Specific genes induced include those that code for adhesion molecules, kinases, proteases, chaperones and various other factors[48]. The expression and release of cytokines and chemokines from sites of infection leads to recruitment of innate immune cells to the site of infection. Increased adhesion protein expression on vascular endothelial cells attracts phagocytic

innate immune cells to the site of infection, where they can extravasate from blood vessels[64]. Cell specific effects of inflammation can also decrease the cells 'infectability'. Taking the case of interferon for instance, several anti-viral genes are induced: (1) ISG15 is a small protein modifying factor akin to ubiquitin that lowers susceptibility to some viruses[65,66]; (2) the expression of OAS pathway factors induces the activation of RNAse-L which in turn leads to the transient degradation of all RNA within the cell, potentially nullifying a viral infection[67]; (3) Protein Kinase R (PKR) is activated by long strands of dsRNA and leads to the phosphorylation of eIF2a, shutting down protein translation and limiting viral replication[68].

In addition to the induction of an anti-viral state, it has been demonstrated that interferon signaling also increases cell death. By inducing a number of pro-apoptotic genes, it is thought that interferon can promote a pro-cell death state[69]. There is also evidence for a more direct pathway for interferon induced cell death. Dendritic cells, for example, have been shown to undergo a type-I interferon dependent cell death in response to poly-I:C treatment[70]. Similarly, there is evidence that interferon-β is able to induce apoptosis directly in a number of cancer cell lines[71,72]. By promoting cell death in this way, type-I interferons function to increase death of infected cells and prevent the propagation of viral pathogens[68]. It has yet to be investigated what effect interferon signaling might have on programmed necrotic cell death (see section 1.2.B).

1.1.A-II Macrophage Cell Death in Bacterial Infections

Given the central role of macrophage activity in the inflammatory program outlined above, cell death of macrophages may have particularly important implications for the pathology of an infection. In particular, the specific mode of cell death (see section 1.2) may have important implications for the inflammatory effect of macrophages. Interestingly, death of macrophages is consistently observed during early stages of microbial infection[73]. For the most part, this death

has been previously attributed mostly to apoptotic cell death[74], but new forms of cell death have recently been shown to be of importance.

Work in *Shigella* infection was the first to show that IL-1β converting enzyme (ICE), also known as caspase-1, was vital for both production of the inflammatory cytokine IL-1β and death of macrophages[75]. This caspase-1 dependent inflammatory death of macrophages occurs in the first few days of infection with both intracellular pathogens *Shigella* and *Salmonella typhimurium* (ST)[76]. In this form of death, caspase-1 is activated through the assembly of a protein complex known as the inflammasome, which normally cleaves pro-IL-1β to produce active cytokine[77]. Activation of caspase-1 can also lead to an inflammatory form of cell death now known as pyroptosis[78]. Importantly, caspase-1 has not been implicated in the pathways of extrinsic and intrinsic apoptosis (see section 1.2.A). It was shown that pyroptosis aids in the dissemination of ST from the gut, with pyroptosis resistant caspase-1/11-deficient mice showing less ST invasion[79]. In contrast, caspase-1/11 deficient mice are more susceptible to intravenous infection with ST[80,81], underlining the complex relationships of immune response and cell death. Similarly, components of the caspase-1 activating complex (known as the inflammasome) have also been associated with improved responses to viral infections[82,83], but a clear characterization of the role of cell death through pyroptosis in this model was not made.

In contrast to the rapid pyroptotic form of cell death, which can be induced in macrophages under conditions of LPS priming or high infection loads[84], ST infection has also been observed to induce a delayed mode of cell death[85]. For delayed ST-induced death, it has been demonstrated that expression of PKR and TLR4 are key players in the death of infected macrophage cells[86]. Somewhat similarly, the delayed death in *Listeria monocytogenes* infected macrophages was found to be mediated by type-I interferon signaling[87]. *In vivo*, mice deficient in IFNAR

expression were also shown to be resistant to *Listeria monocytogenes* challenge, but viability of macrophages was not assessed[88]. A deleterious role for type-I interferon signaling in bacterial infection is somewhat paradoxical, given the well-established role of type-I interferons as key anti-viral cytokines (discussed above). This emphasizes the need for immune responses to be suited to specific pathogens.

1.1.B *$CD8^+$ T cells*

Whereas innate immune cells are primed to react directly to a wide range of pathogen molecules, acquired immune cells, such as B and T cells, must receive highly specific stimulus in order to become activated (see Figure 2A). New T cells are formed throughout the lifetime of an organism. As T cells develop, they undergo a random rearrangement of V(D)J DNA elements, to create a highly specific, and highly unique T cell receptor (TCR). T cells will continually interrogate antigen loaded MHC molecule displayed on the surface of target cells. Generally, only if the TCR has a high affinity for the antigen-MHC complex will it be able to form a long lasting interaction, resulting in signals necessary for activation. In some cases, lower affinity TCRs and MHC/antigen complexes can also form activating connections, as occurs in T cell selection and some immune diseases. T cells can be classified by their ability to bind type-I or type-II MHC-antigen complexes. MHC-II molecules usually present extracellular antigens to CD4 T cells, and are mostly expressed on specialized antigen presenting cells. In contrast, MHC-I molecules are expressed on all cell types, and present cytosolic antigens to CD8 T cells (reviewed in [9]).

Following activation, antigen specific T cells will begin to proliferate. The affinity of the TCR for the MHC-antigen complex, as well as amount of MHC-antigen complexes available on the antigen presenting cell will determine the potency of stimulus delivered to the T cell. In addition, the expression of costimulatory molecules and inflammatory cytokines by the APC will also impact

Figure 2: *Antigen presentation activates the T cell response.* Unlike innate immune cells, T cells must receive very specific stimulation in order to become activated. (A) T cells will continually scan the MHC-peptide complexes presented by antigen presenting cells. If the T cell encounters a high affinity MHC-peptide complex, it receives an activation signal involving the TCR. The activation signal for T cells is communicated through complex interaction of many molecules on or released from the APC (including MHC/antigen complex, CD28 and inflammatory cytokines) and molecules present on the T cell (including the TCR, CD3, and CD8 receptors). (B) Co-stimulatory molecules are engaged by signalling through PAMPs. T cell response can be divided into 4 phases. First the antigen specific T cells expand rapidly, then they reach a peak and differentiate into effector cells. Majority of T cells are removed during contraction phase, leaving a small stable pool of memory T cells.

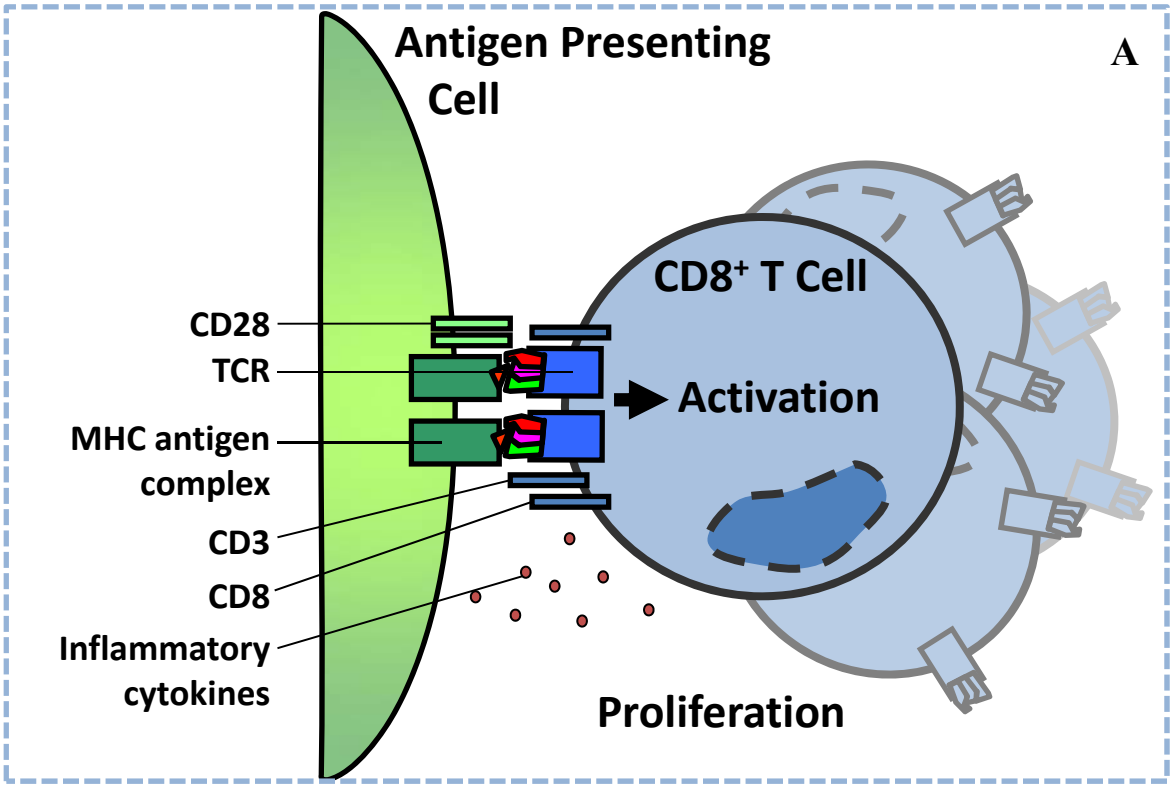
A
Antigen Presenting Cell
CD8+ T Cell
Activation
CD28
TCR
MHC antigen complex
CD3
CD8
Inflammatory cytokines
Proliferation

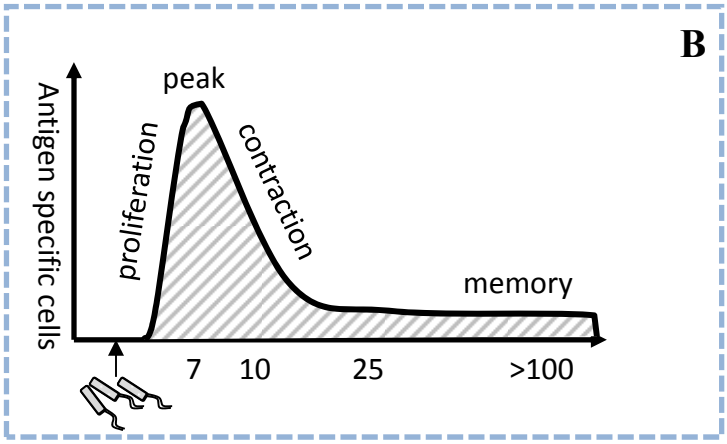
B
Antigen specific cells
peak
proliferation
contraction
memory
7
10
25
>100

the ultimate level of T cell activation. Depending on this multitude of stimulatory factors, activated T cells will proliferate slowly or very rapidly, up to 10 000 fold within 7 days[89]. Activated T cells will undergo a differentiation program into effector cells and are then endowed with the ability to perform specific functions, such as killing target cells and producing cytokines which aid in elimination of specific pathogens.

CD4 T cells produce cytokines that aid in the generation of antibody responses by B cells. In addition, activated CD4 and CD8 T cells can emigrate into the periphery, homing to sites of inflammation by following cytokine and chemokine gradients. In contrast to CD4 T cells, CD8 T cells can scan all peripheral cells via the ubiquitously expressed MHC-I. Upon binding their cognate antigen-MHC complex in the periphery $CD8^+$ T cells can induce apoptosis in target cells, in order to eliminate intracellular infections. For this reason, $CD8^+$ T cells are commonly known as cytotoxic T lymphocytes (CTL) [reviewed in [90]].

Following activation of T cells, the expanding numbers of antigen specific $CD8^+$ T cells eventually reach a point where competition of clonal cells outstrips the local resources of activation (e.g. IL-15, antigen-MHC complexes etc…). This loss of activating stimulus pushes T cells to stop proliferating. In acute viral and some intracellular bacterial infections, the peak of expansion typically occurs approximately 7-8 days after challenge[91–94]. It is important to note that most bacterial pathogens are extracellular and thus predominantly activate an MHC-II dominated response, as their antigens are not present in the cytosol. Following this peak, a significant proportion of effector $CD8^+$ T cells emigrate to the periphery to mediate immune-surveillance and effector function in non-lymphoid tissue. Between days 7-20 of an acute response, the majority of primed cells are eliminated through a poorly understood process known as contraction. For example, in an acute antigen specific responses to lymphocytic choriomeningitis virus (LCMV) or

Listeria monocytogenes, responding $CD8^+$ T cells populations will contract to form a stable memory population of ~5-10% of the peak number of cells[94,95] (see Figure 2B). The exact mechanisms that control the expansion, activation, contraction and memory of T cells are an area of intensive investigation. While some of the key molecular interactions that control $CD8^+$ T cell activation have been well identified (eg MHC/TCR, costimulation, cytokine production), the interaction of these pathways with cell death is not yet well understood.

1.1.B-I Cell Death Pathways in $CD8^+$ T Cell Function

The role of cell death pathways in regulating T cell function is a prime example of the complex and often paradoxical functions cell death pathways can have. When lymphocytes lack the death receptor Fas or its ligand, this results in a serious lymphoproliferative disorder in both mouse and human[96]. While this defect in the homeostatic balance of T cell numbers might seem predictable, mutations in Fas or its signaling partners FADD and caspase-8, also result in perplexing defects in antigen induced T cell proliferation[97,98]. The importance of caspases in T cell activation is reiterated by defective T cell activation observed in humans lacking functional caspase-8[99]. Furthermore, chemical inhibitors of caspases have been shown to inhibit T cell activation[4]. This adds to a growing paradigm whereby apoptotic mechanisms, normally associated with cell death, seem to also play a role in cell proliferation and differentiation[100]. Specifically, caspase-3 activation without cell death has been observed associated with the normal differentiation of skeletal muscle cells[101], macrophages[102], and erythroblasts[103].

Recently it has been revealed that the reason that caspase-8 expression is needed in $CD8^+$ T cells is that it specifically limits the induction of a specialized type of cell death known as programmed necrosis[104]. Consistent with this, defective T cell responses can thus be rescued by concurrent knockdown of Rip3 in order to eliminate the activation of programmed necrosis[105].

These Rip3/caspase-8 double knockout animals do show an accumulation of atypical lymphocytes similar to Fas deficient animals[106]. At this time while it is clear that caspases are expressed and activated within *in vitro* stimulated T cells[97,107,108], it is unclear what processes drive this activation. Through examination of apoptotic markers during the entirety of the $CD8^+$ T cell response to a constant antigen (OVA) under divergent conditions, we hope to gain insight into the link between the signaling networks of immune stimulation and cell death.

Interestingly, Rip3/caspase-8 double knockout T cells also showed a normal contraction of an antigen specific response, suggesting that neither extrinsic apoptosis (see section 1.2.A-I) nor programmed necrosis (see section 1.2.B) are required for T cell contraction[105]. Treatment of mice with caspase inhibitors during T cell contraction has similarly been shown to have no effect on contraction[109]. In contrast to this view, mice deficient in the pro-apoptotic mitochondrial outer membrane protein, Bim, have been demonstrated to show less T cell contraction following a CD8 T cell response[110,111]. A protein which is very similar to Bim, Puma, has also been shown to function in the removal of activated T cells[112]. Furthermore, double knockout mice for Fas and Bim show almost no contraction following an antigen specific T cell response and severe autoimmune pathology[7,113,114]. Given the additive effects that observed for these pro-apoptotic mediators, it seems likely that overlapping death pathways are at play in the removal of activated T cells by contraction.

1.2 PROGRAMMED CELL DEATH

Death of tissues of the body following extreme injury and/or infection has been referred to as necrosis since the time of Galen in ancient Rome[115]. By the mid-19th century, medical journals were publishing many accounts of painful necrosis of tissue, mostly within damaged bones in a process

that would now be known as osteonecrosis[116]. Even at this early time, it was recognized that damage effecting the vascular conveyance of nourishment was likely driving the 'mortification' of tissues[117]. The association of necrosis with infections and immune reactions was also becoming clear by 1885, as scientists observed the 'inflammatory exudation' of fibrous tissue associated with tissue necrosis induced by experimental models of diphtheria[118].

In parallel with these observations of necrosis, the first scientific observations were also being made of a quieter (non-inflammatory) type of cell death associated with natural fetal development. In a seminal 1885 paper, after having recently coined the term mitosis, the German biologist Walther Flemming observed that the maturing ovarian follicle was littered with cellular debris released from cells with shrunken (pyknotic) nuclei[119]. In beautiful camera obscura drawings, Flemming clearly showed the nucleus of the cell breaking into smaller fragments in a process he coined chromatolysis[120]. While it was proposed that this form of cell death might provide a key function in all organs of the body whenever cells must be eliminated, the subject remained largely restricted to developmental biology throughout the early part of the 20th century. It wasn't until 1972 when this type of cell death was rediscovered and coined apoptosis[121]. At this time, scientists quickly saw the potential role of this form of cell death and acknowledged that it was a "basic biological phenomenon" which occurred throughout all tissues[121].

Today, several more forms of cell death have been defined (such as autophagy or pyroptosis), but the two most studied remain apoptosis and necrosis. Owing to its association with various inflammatory tissue pathologies, necrosis has usually been seen as a 'death by default' caused by cellular damage or nutrient withdrawal. However, recent work has shown that necrosis can also occur by specific programmed mechanisms (discussed below)[122]. The existence of this specialized pathway of necrosis has now led some to question whether necroptosis might have a specific

functional relevance. Can a controlled level of inflammatory cell death be beneficial for the rapid activation of an immune response at the site of an infection? What role does this type of cell death potentially play in pathologies? These questions have become the subject of intensive research, and are the subject of much of this thesis.

1.2.A *Apoptosis*

Apoptosis has been specifically defined as cellular death characterized by cell rounding, chromatin condensation, nuclear fragmentation, and plasma membrane blebbing (release of small membrane vesicles) by the Nomenclature Committee on Cell Death[123]. Generally, apoptosis is differentiated into that induced by extrinsic signaling (death receptors, see section 1.2.A-I) and intrinsic signaling (mitochondrial signaling, see section 1.2.A-II)[124]. Both of these pathways usually involve the activation of apical caspases (caspase-8 or caspase-9) which in turn activate downstream effector caspases such as caspase-3 (see Figure 3). Ultimately, the activation of the caspase cascade leads to the activation and/or translocation of various factors to the nucleus which begin to fragment the DNA[125]. Concurrently, the plasma membrane of apoptotic cells becomes highly active, displaying rapid blebbing which can extend over the course of several hours. The final demise of the cell can eventually lead to loss of plasma membrane integrity known as secondary necrosis; although, it is thought that phagocytic removal of apoptotic cells mostly prevents this process from happening *in vivo*[126].

1.2.A-I Extrinsic Apoptosis

Extrinsic apoptosis occurs when death receptors on the cell surface are stimulated. Upon ligand binding, pre-assembled trimers of death receptors undergo conformational changes which allow

Figure 3*: Extrinsic and intrinsic apoptotic signaling pathways.* Apoptosis is initiated by intrinsic and extrinsic signaling. In extrinsic signaling, binding of death receptors to their specific ligands causes a change in the intracellular domains of the receptors and leads to the binding of additional factors in the DISC. This can either directly lead to cell death or the release of a cytosolic 2° signaling complex. In intrinsic apoptosis, changes in the expression levels of mitochondrial outer membrane proteins can lead to the formation of a mitochondrial outer membrane channel. The subsequent release of cytochrome c leads to the formation of the apoptosome. Both extrinsic and intrinsic apoptosis drive the activation of initiator caspases (8 or 9) which in turn will activate effector caspases (3, 6, and 7). Ultimately this leads to apoptotic cell death characterized by DNA fragmentation and membrane blebbing.

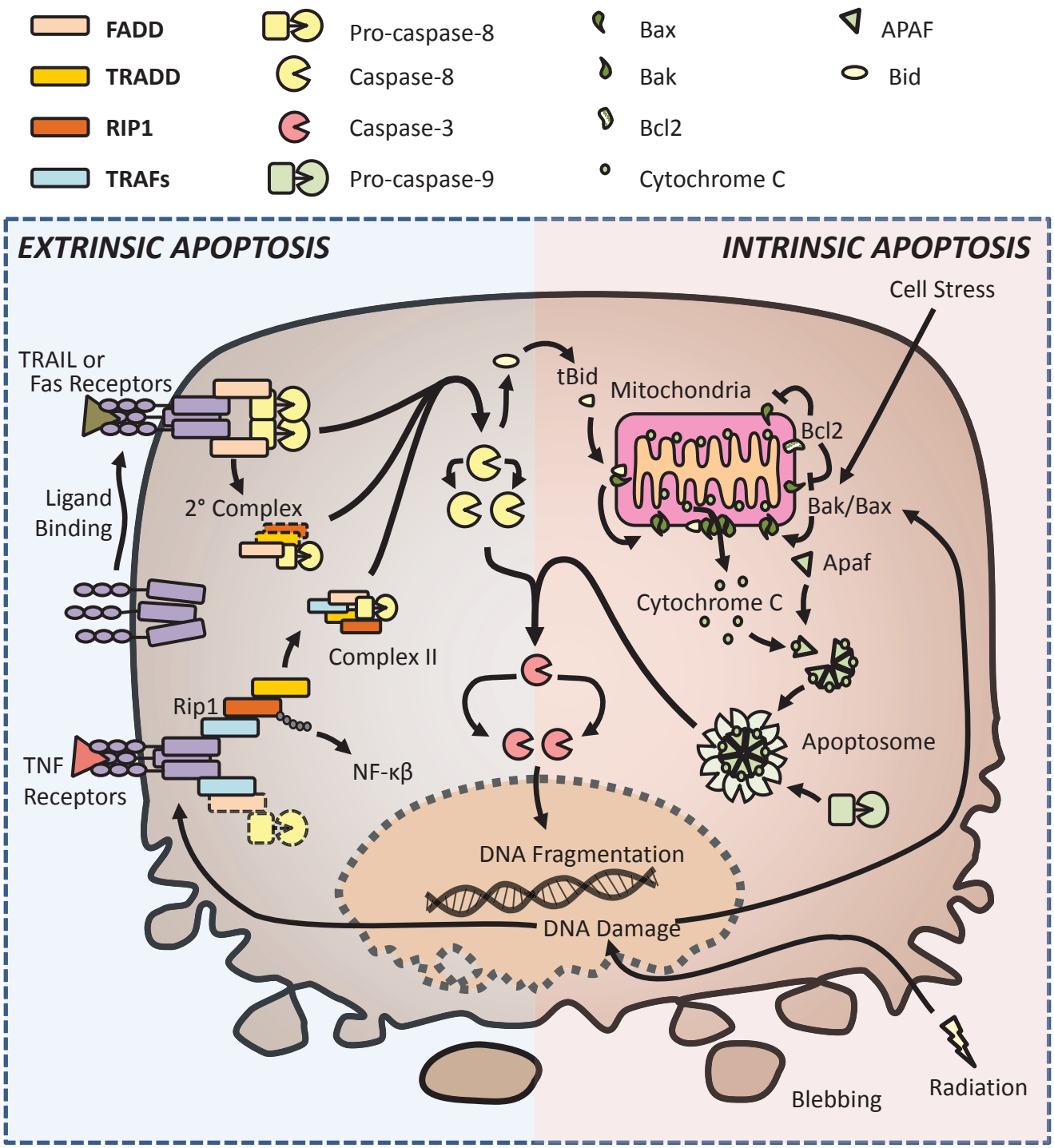
FADD
TRADD
RIP1
TRAFs
Pro-caspase-8
Caspase-8
Caspase-3
Pro-caspase-9
Bax
Bak
Bcl2
Cytochrome C
APAF
Bid
EXTRINSIC APOPTOSIS
INTRINSIC APOPTOSIS
Cell Stress
TRAIL or
Fas Receptors
tBid
Mitochondria
Bcl2
Ligand
Binding
2° Complex
Bak/Bax
Apaf
Cytochrome C
Complex II
Rip1
TNF
Receptors
NF-κβ
Apoptosome
DNA Fragmentation
DNA Damage
Blebbing
Radiation

the assembly of the death inducing signaling complex (DISC) at the intracellular tail of the receptor[127]. The first member of the DISC to be recruited is the Fas-Associated Death Domain protein (FADD), through homotypic interaction of death domains (DD) found in both the death receptor and FADD[128]. FADD also contains a death effector domain (DED) which can form homotypic interactions with a DED in caspase-8[129]. There is also evidence that higher level clustering of death receptors aid in the initiation of death signaling[130].

In addition to the membrane associated DISC complex, the caspase-8 and FADD containing complex can be released into the cytosol where it forms what is known as the secondary complex[131]. The Fas/TRAIL induced secondary complex may contain additional signaling factors such as the TRADD, TRAF2 and Rip1-kinase which can drive other non-cell death signaling such as cytokine or chemokine production[132]. Overall, both the membrane associated DISC and cytosolic secondary complex are thought to function by allowing multiple caspase-8 molecules into close proximity with each other, leading to their mutual cleavage and activation[133]. This active form of cleaved caspase-8 can in turn cleave and activate caspase-3, eventually resulting in apoptotic cell death. Interestingly, new data suggests that propagation in the activation of apical caspases may also rely on feedback from effector caspases[134,135].

While death receptors can drive cytokine or chemokine expression in some cases, the typical outcome of signaling through FAS/TRAIL receptors is considered to be apoptosis. In contrast to this, TNF receptor (TNFR) signaling is chiefly associated with pro-inflammatory signaling and will only induce apoptosis under certain conditions[136] (See Figure 2). Instead of binding to FADD, the TNFR recruits the TNFR-associated death domain protein (TRADD) which lacks a DED, and thus cannot recruit caspase-8 directly[137]. Through homotypic interaction between their death domains, TRADD then recruits receptor interacting protein kinase 1 (Rip1)[138]. Other

members of the TNFR membrane complex (known as Complex I), also include TNFR-associated factor 2 (TRAF2) and cellular inhibitors of apoptosis (cIAP)[136]. Currently it is thought that cIAP proteins mediate non-degradative (K63) ubiquitination of Rip1, which in turn allows the recruitment of the NF-kB signaling factors, and the initiation of pro-inflammatory signaling[139].

In contrast to the view that cIAPs are required for NF-κβ signaling, Rip1 knockout fibroblast cells were recently shown to only have only minor defects in NF-κβ activation and normal cytokine production in response to TNF stimulation[140,141]. It has also been shown that treatment of some cancer cells with a cIAP inhibitor actually results in an increase in constitutive NF-κβ activation[142,143], which in turn can drive the autocrine secretion of TNF-α[144]. Genetic deficiency for cIAP expression can also increase non-canonical NF-κβ signaling downstream of the TNF-receptor[145], and is associated with B-cell cancers such as multiple myeloma[146]. While the exact role of cIAPs in NF-κβ remains unclear, there is strong evidence to show that cIAPs are key regulators of Rip1 dependent cell death (discussed further in section 1.2.B). Regardless of the specific signaling axis responsible, TNFR signaling typically leads to the activation of NF-kB, ultimately resulting in the production of pro-inflammatory cytokines such as IL-6 and TNF-α[147].

For TNFR signaling to result in apoptosis instead of cytokine production, the membrane associated TNFR complex must be released into the cytosol to form what is known as complex II. Similar to the secondary complex sometimes formed in FAS/TRAIL signaling, complex II involves the association of the cytosolic TRADD/Rip1/TRAF2 complex with FADD and caspase-8[148]. In addition to these factors, cytosolic death signaling complexes may recruit the cellular FLICE/caspase-8 like inhibitory protein (cFLIP)[149]. Because cFLIP lacks the protease function of caspase-8, it will inhibit caspase-8 cleavage and activation of apoptosis[150]. Thus, depending on the mix of components present in complex II, it may or may not result in cleavage and activation

of caspase-8. As in other death receptor signaling, active caspase-8 amplifies the apoptotic signal through further cleavage of caspase-8, eventually resulting in activation of effector caspases and apoptotic cell death[151].

1.2.A-II Intrinsic Apoptosis

The other major form of apoptosis is known as intrinsic apoptosis (see Figure 3). Unlike extrinsic apoptosis, this form of cell death is controlled by signals intrinsic within the cell, specifically by signals derived from the mitochondria. This form of cell death can be triggered by a number of cell stressors such as DNA damage, oxidative stress, growth factor deprivation or hypoxia[124]. For instance, cell exposure to ionizing radiation results in double strand breaks (DSB) in DNA, which in turn recruits a DSB complex and activates ATM kinase[152]. Active ATM kinase then activates the key tumor suppressor transcription factor p53 through phosphorylation[153]. Active p53 induces increased expression of many target genes, including death receptors such as FAS and the pro-apoptotic protein Bax[154].

Bax is a member of a group of pro-apoptotic and anti-apoptotic regulatory proteins known as the BCL-2 family. The namesake of this family of proteins was initially identified for its overproduction in B cell lymphomas (hence BCL-2)[155]. Since its discovery, a number of BCL-2 homology (BH) proteins have been discovered, which are further subdivided according to the number of BH domains the proteins contain. Those containing 4 BH (numbered 1-4) domains are anti-apoptotic and include Bcl-2, Bcl-XL and Bcl-w. Proteins with only 3 BH domains are pro-apoptotic and include Bax and Bak. Finally, there are several pro-apoptotic proteins which have only one BH domain (BH3-only); these include Bid, Bim and PUMA (reviewed in [156]).

Under optimal conditions, Bax is located in the cytosol of cells, where protein chaperones such as 14-3-3 silence its activity[157]. Phosphorylation of 14-3-3 allows Bax to then translocate to the mitochondrial outer membrane. The translocation of Bax to the mitochondria is not adequate for activation of apoptosis, however, as anti-apoptotic Bcl-2 proteins are also located at the mitochondrial membrane and will act to bind and inhibit Bax or Bak[155]. Similarly, the expression of BH3-only proteins is thought to inhibit anti-apoptotic Bcl-2 family proteins, thus de-inhibiting Bax and Bak and precipitating mitochondrial apoptosis[158]. In addition to this, Bid cleavage by caspase-8 has been shown to produce a truncated Bid (tBid) which can directly interact with Bax and encourage apoptosis induction[159]. As the amount of Bax or Bak at the mitochondrial membrane begins to outweigh the amount of Bcl-2, this will allow Bax and Bak to increasingly associate. Eventually 9 or 10 Bax and/or Bak monomers will associate into oligomeric channels in the outer mitochondrial membrane[160].

The assembly of Bax/Bak channels on the mitochondrial surface results in mitochondrial outer membrane permeabilization (MOMP). This leads to the release of several pro-apoptotic factors from the mitochondria, including cytochrome c[161]. Once in the cytosol, cytochrome c is able to interact with APAF, which drives the association of up to 7 APAF-1/cytochrome c molecules into a macromolecular complex[162]. This oligomerization process exposes the CARD domains of APAF-1 which results in the recruitment of caspase-9 through homotypic interaction[163], similarly to the DD interactions between FADD and caspase-8 noted above. In contrast to caspase-8, it is thought that cleavage of caspase-9 is not strictly necessary for the activation of caspase-9; rather, simple dimerization of caspase-9 within the apoptosome is adequate to activate catalytic activity of caspase-9[164]. Assuming there is adequate caspase-9

available, the apoptosome will drive cleavage of effector caspases and apoptotic death in a similar fashion as described for caspase-8 in extrinsic apoptosis[165].

1.2.A-III Caspase-3

Activation of the effector caspases, caspases-3, -6, and/or -7, occurs downstream of both the extrinsic and intrinsic apoptosis pathways. The gene homologous to human caspase-3 was initially discovered for its role in programmed death of specific cells during C. elegans development, and was thus coined *C. elegans* death protein 3 (CED-3)[166]. It was later shown that this protein was homologous to the protease then referred to as IL-1β converting enzyme (ICE), now known as caspase-1[167]. This family of cysteine-aspartic acid proteases was eventually renamed caspases in 1996[168]. The vital need for caspase-3 and apoptosis in development is exemplified by the fact that caspase-3 deficient mice show perinatal death due to abnormalities in brain formation, although some strains of mice are viable[169]. It is thought that compensatory upregulation of caspase-7 is responsible for survival within these mice[170]. Consistent with this, thymocytes deficient in caspase-3 show some delays in death but are still able to undergo apoptosis in response to a number of stimuli[171], whereas caspase-3/7 double knockout thymocytes were shown to be deficient for intrinsic apoptosis[172].

Generally, the function of these effector caspases is to activate a variety of mechanisms associated with cell death through promiscuous cleavage of a large number of substrates[173]. One well characterized target is the DNAse inhibitor ICAD; cleavage of ICAD by caspase-3 results in de-inhibition of DNA fragmentation[174]. Similarly, caspase-3 also cleaves and inactivates multiple members of focal adhesion kinases[175] and the actin filament network[176] contributing to the cell detachment, shrinkage, and rounding associated with apoptosis. Thus, by targeting a

variety of proteins for cleavage, effector caspases directly affect the terminal phases of apoptosis and drive cell death.

In addition to its role in precipitating apoptosis, caspase-3 has been shown to have some non-apoptotic roles in various cell signaling pathways. In *Drosophila*, the connection of caspase activation to proliferation has been well characterized. Studies have shown that expression of an exogenous inhibitor of caspases can allow the activation of caspase-analogues without cell death in the insect cells; fascinatingly, this activation of caspases leads to enhanced cellular proliferation[177]. Caspase-3 has specifically been implicated in the differentiation of neurons, and in the maintenance of synaptic plasticity[178]. In both inhibitor studies and caspase-3 deficient mice, it has been shown that memory formation is affected, although the exact mechanism of this action is not entirely clear[179]. Similarly, caspase-3 has also been shown to act in the differentiation of macrophage cells through an unknown mechanism, although it seems to involve protection from cell death[102]. Finally, there is evidence to indicate that caspase-3 as well as other caspases are important for normal T cell activation, proliferation and differentiation (see section 1.1.B-I).

1.2.A-IV SMAC and IAPs

In addition to the release of cytochrome c following MOMP (as described in section 1.2.A-II), many other regulators of apoptosis are also released from the mitochondria. Among these factors is a small protein which acts to drive the degradation of the inhibitor of apoptosis proteins (IAPs), known as SMAC. SMAC was first identified when a research group noticed that detergent lysed membrane fractions had novel caspase activating properties[180]. These researchers were able to specifically identify and isolate a novel protein which they coined as the second mitochondrial activator of cell death (hence SMAC)[180]. Published simultaneously, the work of

another group was focusing on finding an IAP binding protein[181], analogous to the known pro-apoptotic mediators in *Drosophila*[182]. This group showed that a specific protein was capable of binding and inhibiting the X-linked inhibitor of apoptosis (xIAP); they coined this protein as the direct IAP binding protein with low pI (DIABLO). Thus, SMAC/DIABLO (henceforth referred to as SMAC) was shown to be a key de-inhibitor of caspases and promoter of apoptosis.

It was later shown that SMAC can form homodimers, greatly increasing their ability to inhibit the xIAP[183]. It has also been demonstrated that SMAC is able to induce the auto-ubiquitination and degradation of the cellular-IAPS (cIAP1 and cIAP2)[184]. Both xIAP and cIAPs were initially identified to directly bind apoptotic caspases, and were thus thought to act as inhibitors of apoptosis[185,186]. While xIAP is generally accepted to be a bona fide caspase inhibitor, cIAPs are no longer thought to directly inhibit caspases[187]. Rather, cIAPs have been identified to have important alternative roles in NF-κβ signaling[187]. The best studied mechanism of cIAPs is their E3 ubiquitin ligase activity. In particular, cIAP seem to have a key role in ubiquitination and regulation of Rip1 kinase in the TNFR complex (discussed further in section 1.2.B, see Figure 2)[188,189]. Interestingly, monoubiquitylation of caspases 3 and 7 by cIAPs has been observed[190], but at this time it remains unclear what the functional consequences of this might be. Thus, through interaction with many targets, poly-, mono- and auto-ubiquitylation, IAP proteins perform many complex functions in the regulation of apoptotic signaling.

Since the discovery of SMAC, there has been intense scientific interest in the role of IAPs and SMAC. This interest has been accelerated by the discovery that cIAPs are overexpressed in many forms of cancer[145]. Given that TNF-α is also overexpressed in many tumours[191], the ability of cIAPs to convert the TNF-α signal from pro-apoptotic to pro-survival/inflammatory NF-κβ signaling (see section 1.1.A-I) may be important in the enabling the process of oncogenesis[145].

With the goal of inhibiting the activity of IAPs within cancer cells, small molecule SMAC mimetics (SMs) have been developed. While these SMs were initially intended as a means to inhibit xIAP and thus induce caspase mediated apoptosis, a number of papers have shown that these compounds are often dependent on the degradation of cIAPs[192]. This loss of cIAP expression drives cell death via a TNF-α dependent apoptosis pathway involving Rip1kinase and caspase-8[142–144,193] (discussed further below).

1.2.B Necroptosis

Since the term apoptosis was coined in the 1970's, the bulk of research into cell death has concentrated on discovering the mechanisms that regulated this form of cell death (as described above). During this time, apoptosis was often used synonymously with any form of programmed cell death, whereas necrosis described unregulated mechanisms such as nutrient deprivation or cellular damage[119]. This over-simplified paradigm was never truly accurate. Rather, types of cell death are better defined based on their morphological characteristics; with apoptosis showing blebbing and nuclear condensation (see above), whereas necrosis exhibits rapid membrane collapse and release of cytosolic material[123].

Over the last 15 years, findings have conclusively demonstrated that necrosis can be the result of programmed signaling[194,195]. It was only a short time after the canonical apoptosis inhibitor z-VAD-FMK (zVAD) was demonstrated to specifically inhibit caspases[196], researchers reported that death receptor stimulation combined with zVAD could result in necrotic-like cell death[197]. This observation was quickly followed up with a number of other publications showing that something akin to necrosis occurs in caspase inhibited cells[198–201]. It has now been conclusively shown that caspase-8 is the key inhibitor of programmed necrosis, as embryonic lethality observed in caspase-8 knockout mice can be rescued by also knocking out the key programmed necrosis protein

Rip3[106]. Now known as necroptosis, programmed necrosis is often thought of as a back-up mechanism of apoptosis, normally inhibited by caspases[202], although it is now clear that caspase inhibition is not always required in order to activate necroptosis.

It was in work examining the induction of this caspase-independent cell death by Fas-receptor signaling, wherein Rip1-kinase activity was first shown to be required for programmed necrosis[203], but a similar effect for TNF soon followed[122]. The next big leap forward for the field of programmed necrosis came with a seminal paper from the Yuan group at Harvard Medical School, wherein they coined the term necroptosis to refer to programmed necrosis[204]. In this paper, they also identified a novel small molecule inhibitor of cell death induced by combined TNF-α and zVAD treatment, which they called necrostatin-1 (nec)[204]. This group also later confirmed that nec specifically inhibits Rip1 kinase activity to block necroptosis[205]. Rip3 was later demonstrated to also be essential for sensitivity to necroptosis[206].

With the advent of an unambiguous name for Rip1-dependent programmed necrosis and an easily employed inhibitor, research into necroptosis has greatly accelerated in recent years. As discussed above, cIAPs function as E3 ubiquitin ligases for Rip1[188]. Through this ubiquitination of Rip1 it has been proposed that cIAPs prevent the activation of necroptosis in response to TNF-α signaling[148,207], whereas other enzymes such as A20 and CYLD can deubiquitinate Rip1 and promote necroptosis[208–210]. Similar to the initiation of apoptosis through TNFR signaling, necroptosis also relies on the formation of a secondary cytosolic complex known as complex IIb or the necrosome[211] (see Figure 4). It is unclear at this point whether additional factors in the TNFR DISC are responsible for the initial phosphorylation of Rip1, but the ultimate formation of the necrosome complex is known to depend on the sequential phosphorylation of Rip1 and Rip3 kinases[206].

Figure 4: *The many outcomes of TNF receptor signaling.* Depending on the specific mediators that are present in the cell, activation of TNF signaling by binding of the receptor to TNF can result in a variety of outcomes. (1) cIAP1 or cIAP2 have been considered to ubiquitinate Rip1. This enables the docking of the TAB/TAK complex and drives downstream NF-κβ signaling. Degradation of cIAPs can be activated by release of SMAC from the mitochondria. (2) In the absence of cIAP1 and cIAP2, TNF signaling can lead to either apoptosis through successive formation of complex I and complex II, followed by activation of caspase-8. (3) In the absence of caspase-8, or caspase-8 activity, TNF signaling can drive the phosphorylation of Rip1 which subsequently associates with and phosphorylates Rip3, in a complex known as the necrosome. The formation of the necrosome drives cell death via the necroptosis pathway.

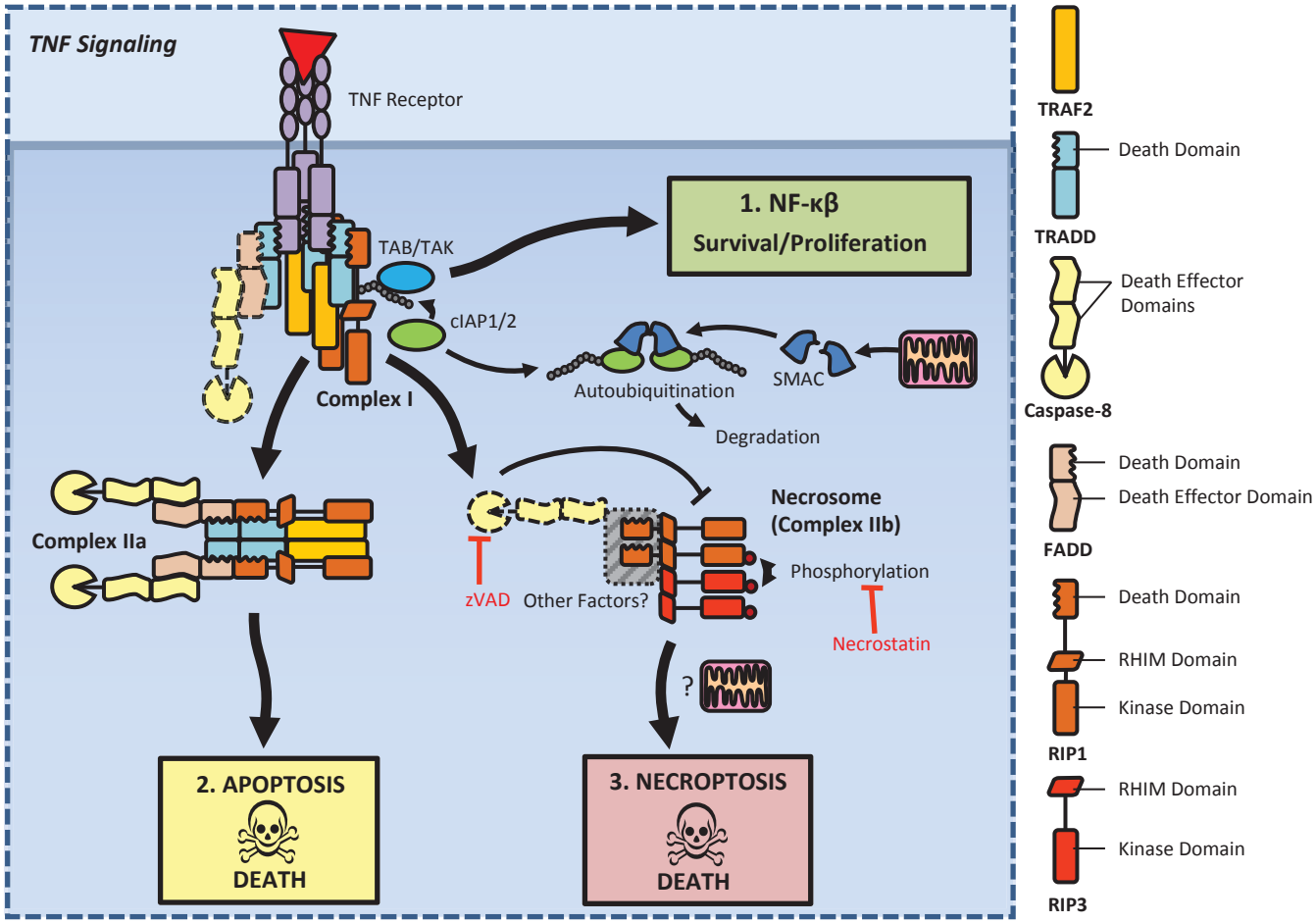
TNF Signaling
TNF Receptor
TAB/TAK
cIAP1/2
Complex I
1. NF-κβ
Survival/Proliferation
Autoubiquitination
SMAC
Degradation
Complex IIa
Necrosome
(Complex IIb)
zVAD
Other Factors?
Phosphorylation
Necrostatin
?
2. APOPTOSIS
DEATH
3. NECROPTOSIS
DEATH
TRAF2
Death Domain
TRADD
Death Effector
Domains
Caspase-8
Death Domain
Death Effector Domain
FADD
Death Domain
RHIM Domain
Kinase Domain
RIP1
RHIM Domain
Kinase Domain
RIP3

The involvement of factors other than Rip kinases in the necrosome complex is unclear at this point. It has been shown that genetic depletion of either FADD or caspase-8 results in embryonic lethality due to uncontrolled necroptotic cell death in the developing embryo[150], suggesting that the formation of FADD and caspase-8 containing complexes (ie Fas 2° complex or TNFR complex II) inhibits the formation of the necrosome. Consistent with this, knocking out of either Rip3 or Rip1 rescues embryonic lethality in FADD$^{-/-}$ mice[140,150]. It is not known what role TRADD plays in the formation of the necrosome, although knockdown of this gene seemed to have little impact on sensitivity to necroptosis in L929 fibroblast cells[212]. Importantly, an apoptosis inducing complex similar to the necrosome, involving Rip1 kinase activity, caspase-8 and FADD has recently been reported[207]. This complex is also inhibited by cIAP activity, and is known as the Ripoptosome[213].

Generally, the phosphorylation driven assembly of the Rip1 and Rip3 necrosome has been consistently associated with the initiation of necroptosis; although, new evidence has shown that when Rip3 is overexpressed, TNF stimulation is able to induce necroptosis in the absence of Rip1[214]. This suggests that Rip1 may simply act as a signal amplifier in activating the downstream necroptotic activity of Rip3. Rip1 and Rip3 associate through binding of their RIP homotypic interaction domains (RHIMs)[215]. One recent paper has shown that many phosphorylated Rip1 and Rip3 proteins can assemble in amyloid like structures via interactions of their RHIM domains[216]. This raises the possibility that the amyloid-like oligomerization of the necrosome could constitute a feedback mechanism to amplify pro-necroptotic signaling and drive cell death.

Downstream of the activation of Rip1 and Rip3 phosphorylation, recent work has also shown that Rip3 associates with, and phosphorylates the mixed-lineage kinase like protein (MLKL), which leads to necroptotic cell death[217]. In addition to the MLKL dependent pathway, Rip1 activation has also been shown to lead to the inhibition adenine nucleotide translocase (ANT) pores

on the mitochondria; this drives the release of ATP from the mitochondria[218]. Some cells can also be protected from programmed necrosis through the inhibition of cylophilin D (CYPD) by cyclosporine A[219]. CYPD is a key protein for generating the mitochondrial permeability transition pore (MPTP), which allows unregulated movement of ions into the mitochondria[220].

Necroptosis has also been associated with the elevated production of reactive oxygen species (ROS)[221]. The release of mitochondrial ROS during necroptosis has been documented to steadily increase preceding necroptotic cell death in fibroblast cells, followed by a rapid collapse as the plasma membrane integrity is lost[221]. Consistent with this, some results have shown that treatment with ROS scavengers can protect some cell lines from necroptotic cell death (eg. L929 fibroblast or HT-22 neuronal cells)[222,223]. Complicating the situation, however, it appears that cells of hematopoietic origin (eg. U937 or Jurkat lymphocyte cells) are not protected from necroptosis by ROS scavengers[218,224]. To resolve this dissonance, it has been proposed that there exist at least two classes of cells which are susceptible to necroptotic cell death. In type-I cells, death relies on activation of the MPTP pathway without requiring ROS, whereas type-II cells require the generation of high levels of ROS in order to undergo necroptosis[215]. The recently discovered Rip3/MLKL necroptosis pathway has been associated with ROS production[217], but it remains unclear whether it might also play a role in ROS independent necroptosis.

While the best characterized mode of inducing necroptotic cell death is through the death receptors TNFR, FAS and TRAIL[203,225], it has very recently been shown that certain immunoreceptors can also activate necroptotic signaling. In particular it has been shown that stimulation through toll-like receptors 3 and 4 (TLR3 and TLR4, see section 1.1.A-I) can induce necroptosis when combined with the zVAD to block caspase activity[226]. Specifically, it was shown that ligand binding by TLR3 or 4 caused TRIF to interact directly with Rip3 via a RHIM contained

in TRIF. Thus TRIF drives activation of the necrosome and necroptosis[226]. Similar to TRIF, it has also recently been demonstrated that the cytoplasmic DNA sensor DAI is able to interact with both Rip1 and Rip3 via its RHIM domain[227]. The DAI dependent pathway was also shown to be important in murine cytomegalovirus (MCMV) induced cell necrosis[228]. In addition to these pathogen associated molecular pattern (PAMP) sensing pathways, new work has demonstrated that genotoxic stress can activate assembly of a Rip1 and Rip3 dependent complex similar to the necrosome, and which promotes both apoptotic and necroptotic cell death[213,229]. These examples add to a new paradigm wherein the necrosome acts as a functional integrator of multiple signaling axes in the initiation of necroptosis (see Figure 5, reviewed in [230]).

The activation of Rip1 and Rip3 kinases and downstream effectors eventually leads to rapid necrotic release of cytoplasmic material into the extracellular space. It is thought that this cytosolic release likely represents a potent inflammatory stimulus. The specific cytoplasmic components responsible for this effect are collectively known as damage associated molecular patterns (DAMPs). The archetypal DAMP, HMGB1, has been well associated with inflammatory pathologies such as rheumatoid arthritis[231], lupus[232], and sepsis[233]. While it can also be secreted by mechanisms independent of cell death, release of HMGB1 is usually associated with the loss of plasma membrane integrity[234], and has been recently observed following Rip1 kinase dependent death[207,235].

1.2.B-I Necrotic Cell Death and Inflammation

There is ample evidence to show that inflammation is an important activator of cell death (as discussed above), but the reverse question should also be asked: how important is necrotic cell death as a source of inflammation? The existence of a programmed pathway of necrosis begs the

Figure 5: *The necrosome as a functional integrator of many signaling pathways.* Many different pathways have been demonstrated to induce phosphorylation of Rip1 including TLRs, cytosolic PRRs, genotoxic stress and death receptor stimulation. Under pro-necrotic conditions (usually involving caspase inhibitors) this can also lead to the association of Rip1 with Rip3 in the necrosome complex. Downstream, Rip1 activation has been shown to promote NF-κβ signaling and inflammasome activation. Downstream of Rip3, MLKL and PGAM5 have been recently shown to activate mitochondrial fission, which leads to necroptosis, associated ROS production may also be implicated in inflammasome activation.

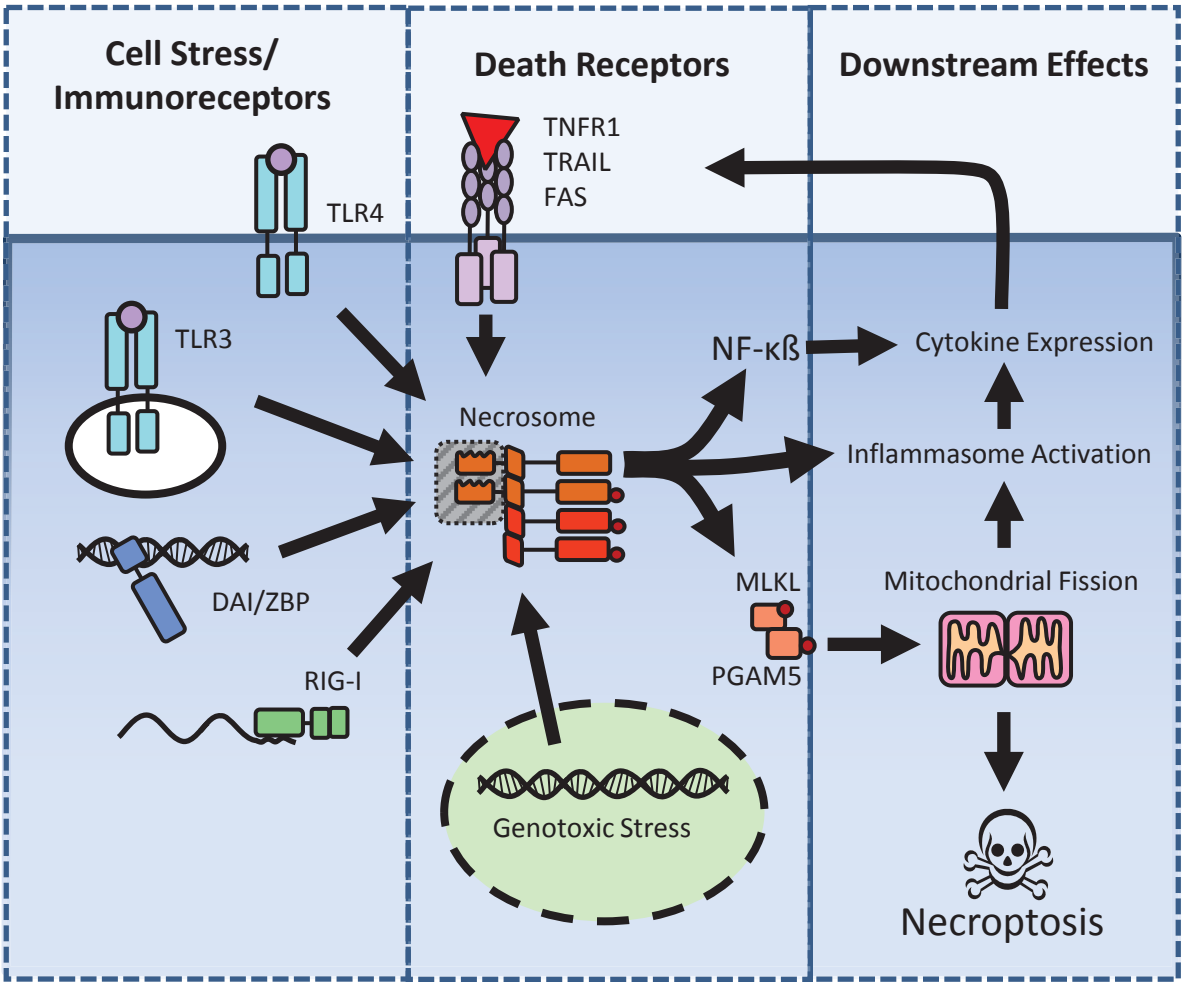
Cell Stress/
Immunoreceptors
Death Receptors
Downstream Effects
TNFR1
TRAIL
FAS
TLR4
TLR3
DAI/ZBP
RIG-I
Necrosome
NF-κß
Cytokine Expression
Inflammasome Activation
MLKL
PGAM5
Mitochondrial Fission
Genotoxic Stress
Necroptosis

question as to its potential functional role. Through active (cytokines) and passive (DAMPs) mechanisms, necroptosis is clearly associated with the local release of inflammatory mediators. Ultimately this necroptosis induced inflammation could be a driver of wider processes, ranging from a normal immune response to acute pathological inflammation, depending on the context and extent of cell death (see Figure 6).

The initial study which coined the term necroptosis, also demonstrated that *in vivo* application of the inhibitor of Rip1 kinase significantly reduces infarct size in a model of ischemic brain injury[204]. While inflammation plays a complex role in ischemic disease etiology, it is thought that the immediate inflammation following brain ischemia acts to aggravate tissue injury[236]. In particular, it has been shown that HMGB1 released by the initial ischemic injury plays an important role in tissue damage and disease pathology[237,238]. Similarly, both Rip1 dependent necroptosis[239] and HMGB1[240] have been shown to play a role in ischemic tissue damage associated with myocardial infarction models. Thus, in these cases of extreme cell stress, it seems that the induction of necroptotic cell death is a significant factor in exacerbating disease pathology.

The release of HMGB1 can also have a range of inflammatory effects on cells. Once released, extracellular HMGB1 is able to interact with a variety of immune receptors, including TLR2, TLR4, and TLR9[241]. HMGB1 stimulation of TLR4 has been shown to drive further release of inflammatory cytokines such as TNF, IL-6, and Il-1β[242,243]. HMGB1 can also interact with the RAGE receptor which can drive chemotaxis, proliferation and differentiation of immune cells[244,245]. Other DAMPs released by necrotic cells include ATP, mitochondrial DNA, heat-shock proteins, uric acid, and others[246], although the specific release of these DAMPs by necroptotic cell death has yet to be shown. Interestingly, the recently established roles for necroptosis[247] in

Figure 6: *The functional spectrum of necroptosis.* Depending on the context and extent of programmed necrosis there is evidence that death can range from inadequate to pathological. In cases of some viral infections, such as vaccinia, it has been shown that mice deficient in key necroptosis proteins do not mount a normal immune response. There is also evidence that in some cases necroptosis is associated with inflammatory pathology. This occurs in ischemic injury models as well as models of systemic shock.

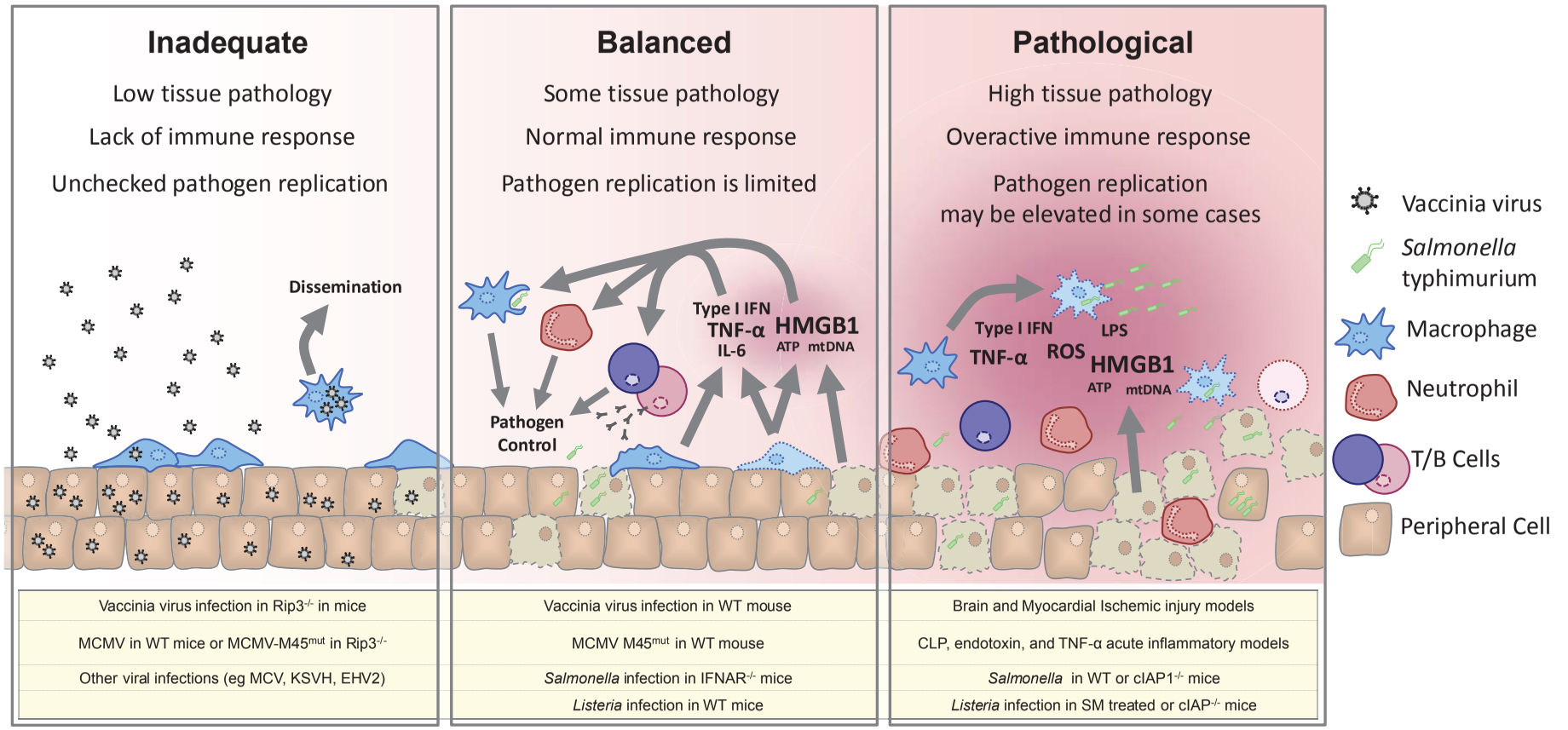
Inadequate
Low tissue pathology
Lack of immune response
Unchecked pathogen replication
Dissemination
Balanced
Some tissue pathology
Normal immune response
Pathogen replication is limited
Type I IFN
TNF-α
IL-6
HMGB1
ATP mtDNA
Pathogen Control
Pathological
High tissue pathology
Overactive immune response
Pathogen replication may be elevated in some cases
Type I IFN
TNF-α
ROS
LPS
HMGB1
ATP mtDNA
Vaccinia virus
Salmonella typhimurium
Macrophage
Neutrophil
T/B Cells
Peripheral Cell
Vaccinia virus infection in Rip3-/- in mice
MCMV in WT mice or MCMV-M45mut in Rip3-/-
Other viral infections (eg MCV, KSVH, EHV2)
Vaccinia virus infection in WT mouse
MCMV M45mut in WT mouse
Salmonella infection in IFNAR-/- mice
Listeria infection in WT mice
Brain and Myocardial Ischemic injury models
CLP, endotoxin, and TNF-α acute inflammatory models
Salmonella in WT or cIAP1-/- mice
Listeria infection in SM treated or cIAP-/- mice

various inflammatory pathologies are mirrored by work investigating the role of HMGB1[234], underlining the likelihood of an intimate connection of DAMPs and necroptotic cell death.

In addition to the indirect inflammatory effects of necroptotic release of DAMPs, current evidence also suggests a more direct impact of Rip1/3 kinase signaling on inflammatory cytokine expression. The dual role of Rip1 in death and cytokine signaling is well accepted, particularly downstream of TNFR. Commonly, it has been thought that these functions of Rip1 can be separated based on kinase activity, wherein the phosphorylation activity is associated with death and is dispensable for its role in cytokine expression[248]. In contrast to this simple bifurcation of Rip1 activity, it was also recently shown that production of TNF-α in macrophage cell lines can be inhibited using necrostatin[229,249]. This work suggests that increased Rip1 kinase activity can actually drive expression of inflammatory cytokines. Consistent with this, DNA damage induced expression of IL-8 has also been shown to require Rip1 kinase activity[229]. Work examining TLR3/4 signaling has also shown that Rip1 phosphorylation and ubiquitination is required for TRIF mediated NF-κβ signaling[250]. Furthermore, TLR4 mediated inflammasome activation and IL-1β production in response to LPS stimulation can be blocked through either overexpression of caspase-8 or treatment with necrostatin[251]. These data clearly show that across diverse signaling pathways Rip1 kinase is a key inducer of inflammatory cytokine expression (see Figure 5).

Similar to the kinase activity of Rip1, the lack of an overt phenotype of Rip3-deficent mice has led to it being disregarded in cytokine signaling. Consistent with this view, expression of Rip3 is dispensable for NF-kB signaling in response to B-cell, T-cell, TLR, and TNF receptors[252,253]. In contrast however, Rip3 has been shown to play a key role in NF-kB activation downstream of the cytosolic DNA sensor, DAI[227]. In the case of inflammasome activation, the ROS production downstream of Rip3 expression has also been specifically implicated in

inflammasome mediated IL-1β activation[254]. Production of IL-6 and TNF in response to endotoxin injection *in vivo* is also significantly decreased in Rip3 knockout animals, although this may be a secondary effect of necrotic cell death[226]. Based on these data, it seems clear that in at least some cases, activation of the necrosome can directly drive inflammatory cytokine expression.

This type of induction of inflammatory cytokine expression by Rip1/Rip3 kinase signaling may constitute a key step in driving the ultimate death of the cell. Case in point: autocrine TNF-α signaling has been consistently shown to be both induced by necroptotic stimulus and ultimately to be necessary for necroptosis[255,256]. Thus, the release of TNF induced by Rip1 kinase activity[249] could be acting as a positive feedback for the induction of necrotic cell death. It is unclear at this time whether the expression of other inflammatory cytokines, such as interferon or IL-1β, plays a role in the induction of cell death.

One recently published commentary has suggested that the immediate function of Rip1/Rip3 kinases may be to induce cytokine expression, with the induction of necroptotic death being a secondary effect of this inflammatory stimulation[257]. Whether it turns out to be the 'chicken or the egg' in this case, the data clearly underlines a complex intertwining of inflammation and necroptotic cell death. Additional experiments to examine the timecourse of events preceding necroptosis may be highly informative regarding the interaction of these pathways.

Necroptosis has recently been demonstrated in models of sepsis. Mice deficient in Rip3 show lower cytokine release and significantly improved survival in the caecal ligation and puncture (CLP) and LPS injection models of sepsis [226,258]. In TNF-injection induced inflammation, similar protection by Rip3-deficiency was observed, but pathology was exacerbated by the Rip-1 kinase inhibitor[259], underlining important as of yet undistilled complexities. Findings showing

necroptosis in sepsis are mirrored by an established role for HMGB1 in acute inflammation models. Antibody treatment targeting extracellular HMGB1 in the (CLP) mouse model of sepsis have shown a significant benefit in terms of cytokine release and mouse survival[260,261]. These results clearly point to a model by which necroptosis and associated HMGB1 release could be the key driver acute pathological inflammation in sepsis; further studies are well justified to further characterize the mechanisms regulating this effect.

Very recently, Rip3 dependent necroptosis of macrophages has been associated with the formation of advanced atherosclerotic plaques[262]; a pathology which also has a well-established connection to HMGB1[263,264]. Given the medical significance of atherosclerosis to Canadians, further research is needed to investigate how this occurs, and whether interventions targeting necroptosis could be effective in treating advanced atherosclerosis.

While the inflammation induced by necrotic cell death can be associated with the pathologies described above, it also appears that necroptosis can aid in the activation of an immune response. In a clear example of this effect, Rip3-deficient mice infected with vaccinia virus showed significantly lower tissue pathology in response to infection but eventually succumbed to high viral loads. In contrast, WT mice infected with the same virus which showed tissue pathology but were able to control the infection[206]. Similar results were observed in vaccinia virus infection of $TNFR2^{-/-}$ mice[265]. It has also been discovered that the MCMV virus has evolved means of inhibiting necroptosis by targeting Rip1 kinase with its M45 (or vIRA) protein[266]. MCMV mutants lacking vIRA are unable to infect WT mice, but show normal infection in Rip3 knockout mice[228]. Other viruses also appear to modulate programmed necrosis through expression of viral FLIP-like proteins, such as K13 in Kaposi sarcoma virus, E8 in equine herpesvirus-2, and MC159

in poxvirus Molluscum contagiosum[265]. These studies clearly demonstrate that necroptosis can have a pro-inflammatory effect which aid in immune response and viral clearance.

While the results discussed above illustrate how programmed necrotic cell death can have a positive role in the initiation of an appropriate inflammatory response to pathogens, key questions remain regarding the role death of particular cell types might play in this response: Is the death of infected cells the primary source of this of necrotic inflammation? Do innate immune cells undergo inflammatory suicide to enhance the inflammatory cascade? What is the role of necroptosis in chronic inflammation? What is the role of necroptotic cell death during bacterial infections? Experiments to address the complex role of cell death of specific cell types across the full-spectrum of inflammation are essential to a more complete understanding of the function of the immune system.

2.0 SUMMARY

2.1 HYPOTHESIS: Cell death pathways have significant impact on the immune function in both innate and acquired immune responses.

2.2 AIMS:

1. **To determine the factors which regulate the induction of caspase-3 activity during $CD8^+$ T cell activation.**
    a. Careful experiments will confirm whether caspase-3 high cells are undergoing cell death during $CD8^+$proliferation.
    b. The relative impact of inflammation and antigen presentation to caspase-3 will be investigated.
    c. Experiments will investigate the timing and magnitude of caspase-3 activation during *in vivo* $CD8^+$ responses to the same antigen (OVA) under varying conditions of presentation.
    d. Experiments will probe the role of caspase-3 in promoting $CD8^+$ proliferation.
2. **To investigate the factors which regulate programmed necrosis within innate immune cells, with particular focus on macrophages.**
    a. The newly developed small molecule mimetic of SMAC, SM-164, will be employed to investigate the regulation of necroptosis by IAPs
    b. The relative sensitivity of macrophages and dendritic cells to the induction of necroptosis will be studied.
    c. The relative release of inflammatory cytokines in the response of dendritic cells and macrophages to immunostimulatory and/or necroptotic stimulus will be assessed.
    d. Specific knockout models will be used to delineate the specific roles of cIAP1, cIAP2, and xIAP in the regulation of necroptosis.
    e. Knockout models and SM-164 treatment *in vivo* will be utilized to investigate the importance of necroptotic control during the immune response to intracellular bacterial infections.
3. **To investigate the relationship of the necroptosis death program with the production of inflammatory cytokines.**
    a. The role of necroptosis in *Salmonella*-induced death of macrophages will be investigated
    b. The specific interaction of the type-I interferon pathway in necroptosis of macrophages will be investigated.
4. **To examine the proteolysis of RIP kinases in the regulation of necroptosis.**
    a. The relative effect of immune-activating TLRs in necroptosis will be investigated.
    b. The canonical model of necroptosis induction using the pan-caspase inhibitor zVAD will be utilized to examine changes in Rip1 cleavage products during the necroptotic program.
    c. Using various small-molecule protease inhibitors, the relative role of different proteases to limiting necroptosis will be investigated.
    d. Using a totally cell free cleavage assay, the ability of cathepsins to directly cleave Rip1 kinase will be demonstrated.

3.0 METHODS AND MATERIALS

3.1 ANIMAL WORK: All animals were housed at the animal facilities of the National Research Council Institute for Biological Science, or at the University of Ottawa. Animals were maintained in accordance with CCAC guidelines. Protocols and procedures were approved and monitored by the National Research Council of Canada-Institute for Biological Sciences Animal Care and Ethics Board and/or the University of Ottawa Animal Care Committee. The strains of mice utilized for experiments and their sources are listed in Table 1. Any genetic analysis necessary for strain determination was performed utilizing tail clips and genomic PCR. Experiments utilizing multiple transgenic mice utilized age and sex matched mice.

***Adoptive transfer of OT1 splenocytes*:** For experiments requiring adoptive transfer of OVA-specific T cells, OT1 TCR transgenic mice were sacrificed and spleens were removed. Cells were counted and resuspended at appropriate concentrations in HBSS. Generally 10^6 splenocytes were transferred to each recipient mouse unless otherwise stated in the text. Sex-matched recipient mice were injected intravenously (iv) with cells followed by 1 week of equilibration prior to further manipulations.

***In vivo Infection Models*:** Animal infections were performed by iv or intraperitoneal route according to descriptions given in the text. In brief, stated pathogens were resuspended at appropriate concentration in HBSS and 200 µL was injected into mice. Daily monitoring was utilized to assess animal health, and mice were sacrificed at established humane endpoints (>20% weight loss or symptoms of illness such as lethargy, hunched, shivering etc…). Mice were euthanized by carbon dioxide inhalation followed by cervical dislocation. Various inhibitors (see Table 2) were also injected into mice as described in the text. In brief, inhibitors were

Table 1: *Mouse strains utilized in experiments*, their source and the derivation of the strain are also given.

Mouse Strain	Source	Origin/Notes
C57BL/6J	Jackson Laboratories Stock #000664	
***OT1 Transgenic Mouse (CD45.2$^+$)**	Bred in house	OT1 mice have transgenic CD8$^+$ TCR expression. >90% of CD8$^+$ T cells were confirmed to be OVA specific via FACS
***OT1 Transgenic Mouse (CD45.1$^+$)**	Bred in house	OT1 transgenic mice were backcrossed to CD45.1 expressing C57BL mice to provide a marker for identifying adoptively transferred cells
C57BLx129SvJ "F1 mice"	Bred in house	F1 mice show resistance to *Salmonella* infection yet are immunologically compatible with OT1 adoptive transfer
***cIAP1$^{-/-}$**	Bred in house (University of Ottawa)	As described in [267]
***cIAP2$^{-/-}$**	Bred in house (University of Ottawa)	As described in [268]
***IFNAR$^{-/-}$**	Bred in house A kind gift from K Murali-Krishna	Backcrossed to C57BL in [269] from mice generated as described in [270]
***Rip3$^{-/-}$**	Bred in house A kind gift from V. Dixit	As described in [253]
***CTSB$^{-/-}$**	Bone marrow samples received from collaborator	
***CTSS$^{-/-}$**	Bone marrow samples received from collaborator	As described in [271]

*Note: all transgenic mice were bred on the C57/BL background.

suspended at appropriate concentration in phosphate buffered saline (PBS) to achieve desired dose/kg and injected intraperitoneally.

For experiments examining immune cells in other tissues (lungs or brain), mice were first bled to obtain blood samples, then anaesthetized and perfused using 50 mL of PBS before sacrificing. Following this, organs were removed and placed in RPMI (Invitrogen 31800-022) on ice. Tissues were dissociated in RPMI using a Potter-Elvehjem homogenizer and a cell strainer to obtain a single cell suspension before FACS analysis as described below.

Following euthanasia, for peritoneal lavage studies, the skin was first removed to expose the peritoneal membrane. 10 mL of cold PBS was then injected into the peritoneal cavity using a washing motion 4-5 times before removing the lavage liquid. Samples were then placed immediately on ice. For splenic examinations, the spleen was removed and placed immediately in RPMI media and placed on ice. For experiments requiring bone marrow cells, mouse hind- and forelimbs were removed, taking care to include the ischium with the hind limbs. The skin was removed and samples were placed on ice in RPMI before further processing (see section 3.3).

***In vivo Antigen Presentation*:** For evaluation of antigen presentation *in vivo*, CFSE labeled OT-1 cells were injected (5×10^6) into mice iv. After allowing 3–4 days for cells to equilibrate, mice were infected with bacteria through the iv route as described in the text. Four to five days after infection, spleens were removed from the recipient mice. The presence of donor OT-1 $CD8^+$ T cells ($CD45.1^+$) and the reduction in CFSE intensity of donor cells was evaluated by FACS (see below).

3.2 BACTERIAL METHODS: Bacterial lines utilized for experiments outlined in this thesis include SL1344 strain *Salmonella enterica* serovar typhimurium, OVA expressing *Salmonella* SL1344

(ST-OVA as described in [272]), *Listeria monocytogenes* strain 10403S , and OVA expressing *Listeria* (LM-OVA as described in [273]).

***CFU Assay*:** For *in vivo* infection models, the bacterial load in the peritoneum and/or spleen was assessed at various timepoints after infection as described in the text. Bacterial colony-forming units (CFU) assessment was performed by diluting peritoneal lavage, or splenic suspension to varying extent in saline and plating on BHI-agar plates. CFU numbers were then counted after incubation for 24 hours at 37°C.

3.3 CELL PURIFICATION AND SORTING: In order to obtain high concentrations of different cell types, various cell purification and sorting procedures were utilized.

***Magnetic Isolation of Cells*:** $CD8^+$ T cells were enriched by negative selection (Stem cell Cat#19753) according to the manufacturer's instructions. In brief, a single suspension of splenic cells was stained with a cocktail of biotinylated antibodies targeted against the non-$CD8^+$ cells of the spleen (e.g. B cells, CD4 T cells, macrophages, stromal cells etc…). These cells were then combined with streptavidin conjugated to magnetic beads. Using a magnetic field, the non-$CD8^+$ cells can then be retained as the cell suspension is decanted, leaving only the enriched $CD8^+$ cells.

Similarly, macrophages were isolated using positive magnetic separation. In this case peritoneal cells were placed in single cell suspension in PBS with 1% BSA, then stained using anti-F4/80 PE (BD Biosciences, Franklin Lakes, NJ, USA; 123109). Magnetic isolation was then performed using anti-PE magnetic beads (StemCell Technologies Inc., Vancouver, BC, Canada; 18554). Purification was performed according to manufacturer's protocol, similar as described above but retaining magnetically retained $F4/80^+$ cells. Cell purity was confirmed to be >90% by flow cytometry (see below).

***Cell Sorting by Flow Cytometry*:** For studies examining $CD8^+$ cell populations, splenic cells were first enriched for $CD8^+$ by negative selection as described above. A single cell suspension of $CD8^+$ cells was then stained for CD45.1 APC and caspase activity using PhiPhiLux (see antibodies and stains in table 3). Cells were then sorted on MoFlo cell sorter into $CD45.1^+$ OVA-specific $CD8^+$ T cells that express low or high levels of caspase 3 activity. Sorted cells were then placed in 96 well plates with or without the addition of supporting IL-7 (1 ng/ml) using limiting dilutions. Cells were examined for viability over several days using TMRE staining similar as described above.

3.4 CELL CULTURE: Cells used for experiments outlined in this thesis were primarily bone marrow derived macrophages and dendritic cells, J774 macrophage cells (C57BL6 mouse background) were also employed. Unless otherwise stated, all cell culture experiments were performed in RPMI supplemented with 8% fetal bovine serum, 50μM 2-mercaptoethanol, and 50 μg/mL gentamicin. Cells were incubated at 37°C at 5-7% CO_2.

***In vitro Antigen Presentation to $CD8^+$ T cells*:** For evaluation of antigen-presentation *in vitro*, a single cell suspension of OT-1 splenocytes was seeded in a 24-well plate at 5×10^6 cells/well in 1 ml of media. Soluble SIINFEKL ($OVA^{257–264}$) peptide was added directly to the culture (0.1 pg to 1 mg). Cells were allowed to proliferate for 24–72 hours and then analyzed by FACS (as described below). In some cases OT-1 cells were first labeled with 1 mM of carboxyfluorescein succinimidyl ester (CFSE, See Table 3) for 8 minutes before antigen presentation. After 3–4 days of culture, cells were harvested from the wells and stained, and the expression of CFSE or other markers evaluated by flow cytometry.

***In vitro LM-OVA Infection and Limiting Dilution Assay*:** OT1 spleen cells were obtained from a naïve donor animal and placed in a flask at approximately 5×10^6 cells/ml. 10^4 LM-

OVA bacteria were then added to the flask and the infected culture was incubated overnight at 37°C. At this time, cells were spun down and washed in fresh media to remove bacteria from the culture. Gentamicin (50 mg/ml) was also added to prevent further bacterial replication. Cells were washed and returned to a flask at 2×10^6 cells/ml and allowed to proliferate overnight. At 48 hours after initial infection, the cells are split to allow further proliferation to occur; at this time supporting IL-7 is also added to the culture at 1 ng/ml. After a total of 3 days in culture, an aliquot of cells was stained using a similar procedure as detailed above to confirm that >90% of cells are $CD8^+$ and active-caspase-3+. Cells were then counted and placed in a 96-well round bottom plate at approximately 200 cells/well. Two fold dilutions were performed row-wise to approximately 6.25 cells/well. At various time intervals, TMRE was added at 1 nM and live cells were examined using Olympus IX81 fluorescent microscope after 18 h. At least 6 wells were examined for every dilution of cells. 12.5 cells/well was chosen for daily analysis because the number of cells was adequate for counting, while providing a small enough number to preclude the possibility that a sub-population outgrowth accounts for the majority of the culture. Similarly as described, cells were also plated for limiting dilution analysis after 12 days in post-infection culture with regular media changes (every 2-3 days) and added IL-7 cytokine.

***Generation of Bone Marrow Macrophages and Dendritic Cells*:** In order to generate primary bone marrow derived macrophages (BMDMs) and dendritic cells (BMDCs) for *in vitro* experiments, mouse bone marrow was used as a cell source. In brief, mouse femurs and radius bones were removed from mice of the appropriate genotype (as described in the text) and the muscle and tissue was removed using scissors and forceps. Gentle rubbing using a paper towel

wetted with 70% ethanol was also employed to clean the bone of muscle. The bones were then flushed with PBS using a small-gauge needle to obtain the bone marrow.

To generate macrophages, cells were then placed in RPMI with 8% FBS (R8 media) in 50mm plastic petri dishes. It is of note that non-tissue culture grade petri dishes were employed here, as macrophages seem to develop better on adherent plastics[274]. In developing the protocol for BMDM cells, I also observed that spreading the M-CSF (at 5 ng/ml) on the petri dish before plating bone marrow lead to higher yields of macrophages. Cells were then given 7-12 days (as described in the text) to allow cell differentiation before being used for experiments. Flow cytometry was used to confirm the purity of macrophages ($F4/80^+/CD11b^+$).

The generation of BMDCs was performed in T150 tissue culture flasks. Bone marrow cells were placed at ~$20\text{-}30\times10^6$ cells per flask with GM-CSF (at 5 ng/mL). After 3 and 5 days, the media was changed to remove non-adherent cells with very gently washing in order to retain the less adherent dendritic cell population, with the addition of more GM-CSF at each media change. After 7 days in culture, the non-adherent cells were then utilized for experiments as described in the text.

***In vitro Inhibitor Assays*:** BMDMs and BMDCs were treated with a variety of different small molecule inhibitors over the course of experiments as described in the text. A full list of inhibitors employed and their sources can be found in Table 2. A variety of techniques were used, with pertinent details given in the text. In general, cells were differentiated from bone marrow as described above for 7-10 days, before being placed in R8 media within 96-well plates at ~50 000 cells/well. Cells were given 24 hours to adhere to the plates before treatment with inhibitors was initiated. At this time, cells were treated with appropriate concentrations of

inhibitors and left for 24 hours before assessing cell death or viability, unless otherwise stated in the text. Experiments to generate protein lysates from cells were performed with 250 000 cells/well in 24-well plates, and terminated at various timepoints.

***RNA Interference*:** siRNA targeted against specific genes was obtained from various commercial sources as follows: scrambled control (Santa Cruz sc-37007), cathepsin S (Santa Cruz sc-29941), cathepsin B OnTarget SMARTpool siRNA (Thermo Scientific L-044712-00-0005), TRIF (Santa Cruz sc-106845). J774 macrophages were transfected with siRNA using Dharmafect 4 (Thermo Scientific T-2004-02) according to manufacturer's instruction. In brief, cells were plated at low density (~15 000 cells/well) in 96-well plates 24 hours before transfection. 0.2 µL of Dharmafect was combined with 0.5µL of 5µM siRNA in 20µL of total serum free RPMI and incubated at room temperature for 20 minutes to allow complexes to form. 80µL of R8 medium without antibiotics was then added and the total volume was placed on the cells. For bone marrow derived macrophages, cells were transfected using the Lonza electroporation kit for bone marrow macrophages (Lonza VPA-1009) in accordance with manufacturer's protocol. In brief, siRNA and cells were combined in the specialized transfection buffer and electroporated. For both J774 and BMDMs, 24 hours after transfection, cells were then treated with various inhibitors and incubated for an additional 24 hours. At this time, cells were assessed for protein expression or viability as described in the text.

***Mitochondrial Activity Cell Viability Assay (MTT)*:** Cell viability was assessed using the MTT assay. MTT staining reagent was added to cells at a final concentration of 0.5 mg/ml and incubated at 37°C for 4 h. Cells were then lysed and the MTT crystals solubilized using 5mM HCl in isopropyl alcohol. Results were quantified by measuring absorption at 570 nm with a reference wavelength of 650 nm on a Molecular Devices Emax plate reader.

Table 2: *Inhibitors utilized in experiments*

Inhibitor	Source	Cat#	Notes	Conc. Used and Solvent
z-VAD-FMK (zVAD)	EMD Millipore	627610	Pan-caspase inhibitor	10-200µM DMSO
z-IETD-FMK (Caspase-8 Inhibitor)	EMD Millipore	218759	Caspase-8 Selective Inhibitor	10-100µM DMSO
z-DQMD-FMK (Caspase-3 Inhibitor)	EMD Millipore	219002	Caspase-3 Selective Inhibitor	50µM DMSO
YVAD-CHO (Caspase-1 Inhibitor)	EMD Millipore	400010	Caspase-1 Selective Inhibitor	50µM DMSO
Necrostatin (Nec)	Sigma-Aldrich	9037	Rip1-kinase Inhibitor	25-50µM DMSO
SM-164	Dr. Shaomeng Wang (Collaborator)	As in [275]	SMAC Mimetic targets cIAP1, cIAP2 and xIAP	100nM-5µM PBS
E-64-D (E64D)	Santa Cruz Biotech	sc-201280	Inhibitor of cysteine cathepsins	10µg/mL DMSO
Calpeptin (Cal)	Tocris	0448	Inhibits cathepsins and calpains	10µg/mL DMSO
Ca-074-Me	EMD Millipore	205531	Specific inhibitor of cathepsin B	10µg/mL DMSO
Bacterial Lipopolysaccharide (LPS)	Sigma-Aldrich	L2630	Used to stimulate macrophage activation via the TLR4 Receptor	*in vitro*: 10ng/mL *in vivo*: 10mg/kg RPMI
Poly-I:C	Sigma-Aldrich	P9582	Used to stimulate macrophage activation via the TLR3 Receptor	100 ng/mL PBS

***Cell death assay (LDH release)*:** Cell death was assessed using a commercial LDH release assay (Sigma-Aldrich #TOX7). Supernatants were collected from SM-treated cell cultures and subjected to analysis for total LDH according to manufacturer's instructions. In brief, the assay mixture was first prepared by mixing equal parts of LDH substrate, LDH dye and LDH cofactor. This was then combined in equal parts with supernatants generated experimentally. After 20-30 minutes of incubation the reaction was stopped with 1/10 volume of 1N HCl and the signal was measured at 490nm with background subtracted using 650nm reading on a Molecular Devices Emax plate reader. Cell death was alternatively measured using various fluorescent staining techniques (described below).

3.5 IMMUNOFLUORESCENT ANALYSES: Various commercial antibodies were used for FACS and immunofluorescence staining, see Table 3 for a complete list of antibodies employed.

***Flow Cytometry*:** For surface staining, aliquots of cells derived from various *in vitro* or *in vivo* experiments as described above (5×10^6 cells) were incubated in 100 µl of PBS with 1% BSA (PBS-BSA) with Fc block (anti-CD16/32) at 4°C. After 10 min., cells were stained various antibodies of interest for 30 min. at room temperature. When OVA-tetramer was utilized, cells were stained first with tetramer for 15 minutes before the addition of other antibodies. Cells were washed, fixed in 0.5% formaldehyde and acquired on BD Biosciences FACS Canto analyzer.

For analysis of apoptosis, annexin V staining for phosphatidylserine exposure was employed as follows. Aliquots of cells (5×10^6 cells) were first surface stained with desired surface markers as described above. This was followed by washing cells with PBS and resuspension in 3 ml annexin binding buffer (provided in Annexin staining kit). Annexin V was then added,

Table 3: *Antibodies and staining reagents*

Antibody/Stain	Source	Cat#	Notes
Flow Cytometry (Conjugated) Antibodies			
Anti-F4/80 APC-Cy7	BioLegend	122614	
Anti-CD11b PE-Cy7	BD	552850	
Anti-CD3 APC	BD	557030	
PE-H-2K^{b}OVA$_{257-264}$ (Tetramer)	Beckman Coulter		
Anti-CD8^{+} Percp-Cy5.5	BD	553036	
Anti-PD1 PE	BD	551892	
Anti-CD128 (IL7Rα)	BD	560733	
Anti-CD62L	BD	510516	
Anti-Ki67	BD	556026	
Anti-active caspase-3	BD	554714	Specific antibody only reacts with the cleaved active form of caspase-3
Fluorescent Stains			
Propidium Iodide (w RNAse)	BD	51-6551AZ	In unfixed samples, PI only stains dead cells after loss of plasma membrane integrity
Annexin V Staining Kit	BD	556419	Detects phosphatidylserine exposure on apoptotic cells
PhiPhiLux	OncoImmunin	A304R1G-3	Fluorescence activated when cleaved by Caspase-3
Apo-Direct TUNEL Kit	BD	556381	Labels terminal nicks in DNA found in apoptotic cells
CFSE			
Hoechst Stain			
Tetra-Methyl Rhodamine Ester (TMRE)			
Western Blot and Microscopy Antibodies			
Mouse Anti-Rip1	BD	610458	
Mouse Anti-Rip3	ProSci Inc.	2283	
Goat Anti-cathepsin S	Santa Cruz Biotech	sc-6505	
Rabbit Anti-cathepsin B	Santa Cruz Biotech	sc-6490	
Mouse Anti-actin	BD	612656	
Rabbit Anti-cIAP1/2	Santa Cruz Biotech	sc-12410	
Rabbit Anti-cIAP2	Abcam	ab23423-100	Detects both cIAP1 and cIAP2
Goat Anti- TNFR1	Santa Cruz Biotech	sc-1070	
Secondary Antibodies			
Goat-anti rabbit Alexa-fluor 488	Invitrogen	A11070	
Goat anti-mouse Alexa-fluor 594	Invitrogen	A11020	
Donkey anti-Goat Alexa-fluor 546	Invitrogen	A11056	
Goat anti-mouse HRP	Bio Rad	172-1011	
Goat anti-mouse HRP	Bio Rad	170-6515	

and the cells were incubated with annexin V for 15 minutes. Cells were then analyzed by flow cytometry as above, leaving the cells in annexin binding buffer.

***Intracellular Staining*:** Staining for intracellular markers was also employed to examine cells for active caspase-3 and Ki67 expression. Cells were first stained with surface markers as above, then washed and fix/permeabilized for 15 minutes on ice (BD – Cat#554714). Cells were then washed in permabilization/wash buffer (PW, BD – Cat#554723) and resuspended in 100µL PW and stained with a biotin conjugated antibody against active caspase-3 and Ki67. The cells were subsequently washed and resuspended in 100µL PW for streptavidin labelling. Finally the cells were analyzed by flow cytometry as described above.

DNA cleavage was also examined using the Apo-Direct TUNEL kit. Briefly, cells were stained with surface markers of interest, then fixed using the combination fixative/permeabilization solution described above. Cells were washed, resuspended in TUNEL buffer, and incubated at 37°C with a solution containing terminal transferase enzyme and a FITC labeled dNTP. After incubation for 1 hour, cells were then fixed in 0.5% formaldehyde and read by flow cytometry.

***Live Cell Flow-Cytometry*:** For live staining techniques, cells (up to 5×10^6) were resuspended in 100µL of RPMI and surface markers were directly added to the mixture. Cells were then incubated at 37°C for 20 minutes. Cells were then washed and resuspended in RPMI for flow cytometric analysis. Live cell flow cytometric analysis was used to determine the cleavage activity of caspase-3. This was accomplished using a cell permeable fluorogenic substrate, PhiPhiLux, according to the manufacturer's recommended protocol.

***Confocal Microscopy*:** Cells obtained by various *in vitro* experimental techniques, as described in the text and above, were examined via fluorescence microscopy. Cells were first fixed using

4% paraformaldehyde and washed with PBS containing 1% FBS. Cells were then permeabilized using 0.4% Triton X-100 for 15 minutes at room temperature. Cells were rinsed 3× in PBS with 0.1% Triton X-100. Primary antibody was then diluted in PBS with 0.1% TX-100 and 0.5% FBS and incubated on the cells overnight at 4°C. Cells were again rinsed 5× in PBS with 0.1% Triton X-100. Appropriate fluorescently conjugated secondary antibodies (see Table 3) were diluted in PBS with 0.1% TX-100 and 0.5% FBS and incubated on the cells for 1 hour at room temperature. Appropriate unstained and secondary only controls were utilized to confirm the specificity of antibodies in initial testing. Images were captured using an extended focus image constructed from 10 exposures on the Olympus Fluoview 1000 confocal microscope.

***Live Cell Fluorescence Microscopy*:** Cell viability and function were tested using live cell fluorescence microscropy in various experiments as described in the text. For experiments measuring mitochondrial activity via TMRE staining, the stain was added directly to fresh R8 media and the cells were pre-incubated for 15 minutes before measurement. Cells were then examined for TMRE signal at 37°C using an Olympus IX81 fluorescence microscope. Dead cells were determined by lack of TMRE signal and clear dead cell morphology (i.e. small, rounded and granular). Time-lapse monitoring of cell viability following treatment with various inhibitors as described in the text was also performed. In this case, cells were maintained at 37°C with 5% CO_2 and images were acquired every 30 seconds over an extended time period.

An additional technique used to confirm cell viability results determined by techniques described above was the use of propidium iodide (PI) to identify loss of plasma membrane integrity. Hoechst and PI stains were added directly to R8 media, and cells were incubated for

15 minutes at 37°C. Images of cells after various treatments were then acquired using an Olympus IX81 fluorescence microscope. The percentage of dead cells was then determined using Image Pro Software (Mediacybernetics) to perform automated counting of Hoechst versus PI positive nuclei.

3.6 BIOCHEMICAL ANALYSES:

***Quantitative RT-PCR*:** RNA for qRT-PCR was isolated from cells after various inhibitor treatments as described in the text. RNA was converted to cDNA using Superscript III Reverse Transcriptase (Invitrogen). cDNA was then analyzed using Sybr green fast method performed on an Applied Biosystems 7500-Fast qRTPCR System. Specific primers for mRNA of interest were synthesized using the NCBI primer tool in order to amplify 150-200bp sequences spanning at least one exon junction. The qRTPCR amplification of a fragment of the correct length was also confirmed by electrophoresis.

***SDS-PAGE and western blotting*:** Cell lysates were obtained during various experiments by lysing cells directly in SDS lysis buffer with 0.5% β-mercaptoethanol and boiling immediately to minimize protein degradation. SDS-PAGE and PVDF membrane transfer was performed by standard protocol. In brief, 10% or 8% polyacrylamide gels were poured with stacking gels and allowed to set. Gels were then loaded with 15-20µL of lysates and gels were run at 120 V for 1-1.5h. Transfer to PVDF was then performed via wet transfer using 20% methanol transfer buffer. Membranes were subsequently blocked in a blocking buffer of 5% skim milk in Tris Buffered Saline (TBS, 0.5M Tris 1.5M NaCl pH7) for 1 hour at room temperature. Western blotting was performed with varying concentrations of primary antibody (see Table 3, dilutions were 1/1000 or in accordance with manufacturers' suggestions) overnight in blocking buffer. Washes were done using TBS with 0.5% Tween-20 before probing with appropriate

secondary antibody for 2 h. Finally, blots were visualized using either luminol ECL reagent (Thermo Scientific #32106) the highly sensitive West Femto ECL (Thermo Scientific #34095) for proteins with low expression. Results were obtained by exposing photosensitive film (Sigma-Aldrich, Carestream Health 785019). Densitometric measurement was performed for some blots using Image-J software.

***Protein Dephosphorylation*:** Some proteins ran as two forms which migrated slightly differently by SDS-PAGE. Because it has been reported that these bands correspond to the phosphorylated form of the proteins, we wished to confirm this by dephosphorylation of the proteins. In this case, cells were plated at 250 000 cells/well in 24-well plates, and treated with various inhibitors as described in the text. Cells were then lysed using RIPA buffer containing a protease inhibitor cocktail (Roche Applied Science, 04693132001). Phosphatase treatments were performed using 500 units of lambda phosphatase (Santa Cruz Biotechnology sc-200312) for 30min at 30°C. SDS lysis buffer was then added and the samples were boiled before analysis via western blot (as describe above).

***Immunoprecipitation*:** Co-immunoprecipitations were performed as follows. Cells were plated at 250 000/well in 24-well plates. Cells were subsequently treated with inhibitors as described in the text and lysed with RIPA buffer containing a protease inhibitor cocktail (Roche Applied Science 04693132001) and phosphatase inhibitor cocktail (Sigma-Aldrich P5726). Lysates were then sonicated for 5 minutes and pre-cleared using unconjugated protein-G sepharose beads (GE Healthcare, Waukesha, WI, USA; 51-3478-CO-EG) and mouse control IgG. Specific antibodies targeting protein of interest (see Table 3) were incubated with cell lysates overnight at 4°C. Lysates were then incubated with protein-G sepharose beads for 1 hour with agitation on ice. Finally, immunoprecipitates were collected by centrifugation and washed with

PBS several times. Immunoprecipitates were then denatured by boiling in SDS for 5 minutes before analysis by western blot (as described above).

***Plasmid constructs and protein purification*:** Bacterial strain *E. coli* DH5α harboring plasmid encoding for mouse RIPK1 with N terminal GST tag was obtained from Addgene, plasmid 11972[276]. By the use of restriction free cloning strategy[277], a plasmid encoding the shorter version of mouse RIPK1 from 280aa to 656aa also with N terminal GST tag was generated and *E. coli* BL21 was transformed with it. The GST-RIP$^{280-656}$ protein was purified with GE Healthcare GSTrap FF (17-5130-01) according to manufacturer recommendations and eluted at pH-8.0.

***Cell free cleavage assay*:** Cell free cleavage of GST-Rip1$^{280-656}$ was performed as follows. Purified GST-Rip1$^{280-656}$ (6μg) was combined with active mouse Cathepsin S (Sino Biologicals 50769-M08H) or mouse Cathepsin B (R&D Systems 965-CY) or cathepsin L (R&D Systems 1515-CY-010). Reactions were performed as recommended by manufacturers under following conditions. Cathepsin S reaction was set for 2 hours at 37°C, pH-7.4; the cathepsin B reaction for 4 hours at 37°C, pH-6.3; cathepsin L 2 hours at 37°C, pH-7.4. At appropriate times after each reaction, SDS lysis buffer was added and samples were boiled immediately. The results were subsequently examined by western blot (as above).

3.7 STATISTICS: All error bars show standard error of the mean; where shown in the text Student T tests were used to determine the significance of results. All statistical analyses were performed using Graphpad Prism software.

3.8 TECHNICAL ACKNOWLEDGEMENT: The following technical procedures described in this thesis were carried out under my supervision by students and technicians, or in collaboration with post-doctoral researchers in the lab of Dr. Subash Sad: (**1)** Renu Dudani – intravenous injections

for ST and LM infection models, (**2)** Edmund Yao – performed some of the ELISAs for TNF and IL-6 measurements following BM cell SM treatments, (**3)** Dr. Nirmal Robinson – performed *in vitro* infection of macrophage cells with ST with necroptosis inhibitors (Fig. 28, 29 used with permission of Dr. Robinson), (**4)** Susan Thurston – performed some of the western blotting to examine degradation of Rip1 kinase (Fig. 36, 37), (**5)** Dr. Bojan Shutinoski – performed molecular biology for generating GST-Rip1$^{280\text{-}654}$, and part of the cell-free cleavage of Rip1 experiments (Fig. 40), (**6)** Erin Cessford – aided in the generation of macrophage cell and zVAD/LPS necroptosis assay in IFNAR$^{-/-}$ macrophages (Fig. 32).

4.0 RESULTS

4.1 CASPASE-3 ACTIVATION IN CD8$^+$ T –CELL FUNCTION

4.1.A Caspase-3 is upregulated in proliferating CD8$^+$ T cells: The first goal of this thesis was to investigate how antigen specific stimulation of CD8$^+$ T cells *in vitro* would affect caspase-3 activation. OVA-specific CD8$^+$ TCR transgenic mouse (OT-1) splenocytes were isolated and resuspended in a single cell suspension. Cells were then placed in culture with various concentrations of OVA peptide (SIINFEKL). The CD8$^+$ T cells began proliferating within 24 hours of initial stimulation, as confirmed by the presence of blasting cell clusters. After allowing 48 hours for activation, CD8$^+$ cells were examined via intracellular staining using fluorescently labeled antibodies as described in the methods section. Those OT-1 CD8$^+$ T cells that were stimulated with peptide levels that were greater than ~0.1 nM (10^{-4} μg/ml) showed active proliferation, as identified by high expression of the active cell cycle marker Ki67 (Fig. 7A). Based on calculations, this amount of OVA peptide corresponded with only about 1000 molecules of SIINFEKL per cell. Proliferation of these cells was also confirmed by the sequential loss of CFSE staining after activation with OVA peptide (Fig. 7B). In direct correlation with the increase in CD8$^+$ proliferation, a significant increase in the level of active caspase-3 within the proliferating CD8$^+$ population was observed (Fig. 7). Co-staining revealed direct correlation between the level of caspase-3 activation and expression of a marker for cell proliferation, Ki67, within the CD8$^+$ population (Fig. 7D). I also confirmed that caspase-3 cleavage activity was upregulated in OVA stimulated CD8$^+$ T cells using the fluorogenic caspase-3 substrate PhiPhiLux (data not shown).

Figure 7: *Active caspase-3 is upregulated in proliferating T cells.* A single cell suspension of OT1 TCR transgenic splenocytes were placed in culture with varying concentrations of SIINFEKL peptide for 48 hours and analyzed by intracellular flow cytometry ($n \geq 3$). Cells were stained with extra- and intra-cellular stains as described in the methods section (A) MFI of active caspase-3 versus Ki67 shows a linear correlation in their expression levels ($P<0.05$). (B) MFI of CFSE versus active caspase-3 shows a significant inverse correlation ($P<0.01$). (C) MFI of TUNEL stain versus active caspase-3 shows a significant inverse correlation ($P<0.01$). (D) Scatterplots show the relative expression of active caspase-3 versus Ki67 in gated $CD8^+$ cells of splenocyte cultures treated for 48 hours with varying concentrations of SIINFEKL peptide as shown. Data shown is representative for two repeated experiments performed in triplicate.

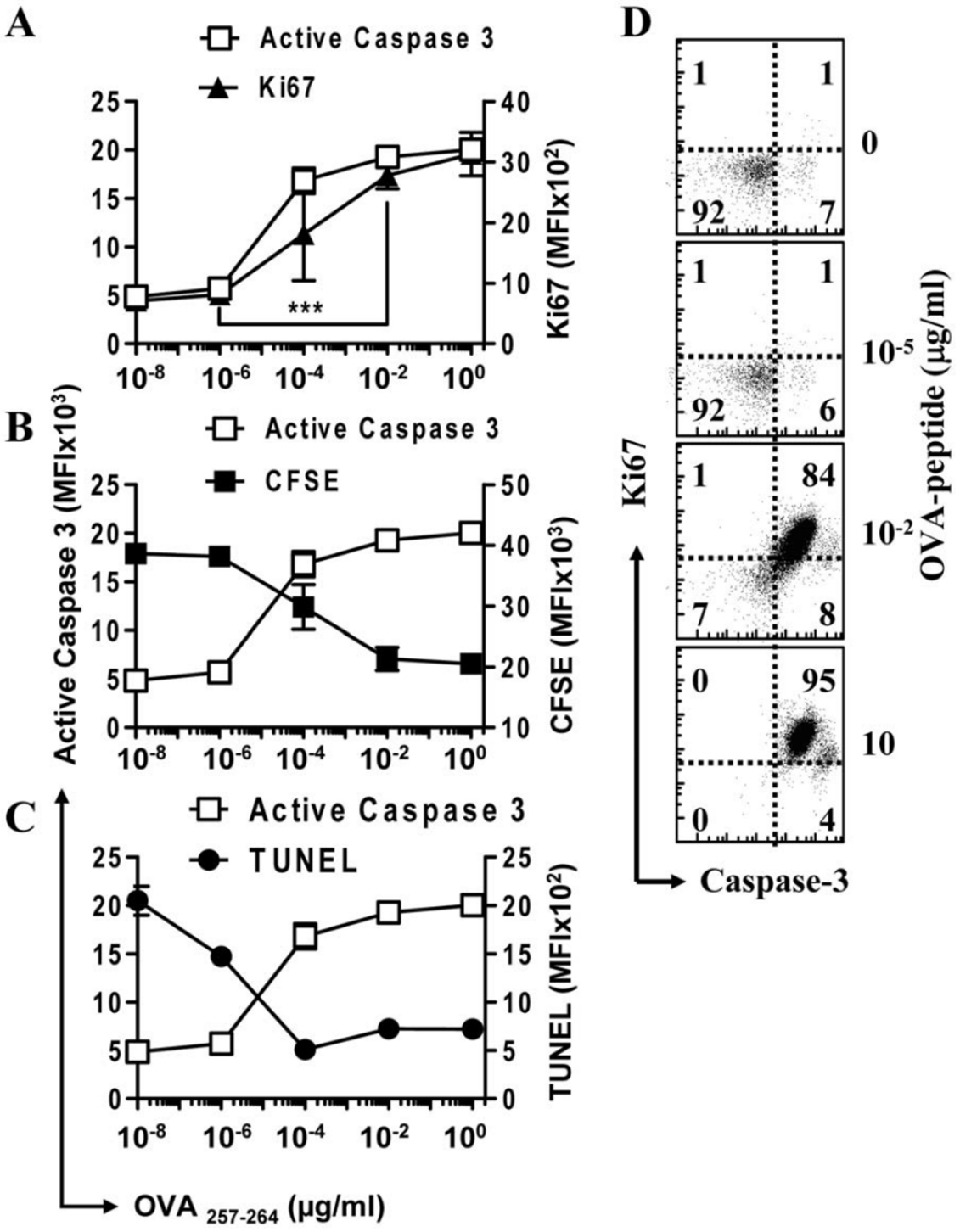
A
Active Caspase 3
Ki67
***
Ki67 (MFIx10²)
B
Active Caspase 3
CFSE
Active Caspase 3 (MFIx10³)
CFSE (MFIx10³)
C
Active Caspase 3
TUNEL
TUNEL (MFIx10²)
OVA 257-264 (µg/ml)
D
Ki67
Caspase-3
OVA-peptide (µg/ml)
0
10-5
10-2
10
1
1
92
7
1
1
92
6
1
84
7
8
0
95
0
4

4.1.B Active caspase-3 in proliferating CD8$^+$ T cells does not lead to cell death: Next, I wished to confirm whether this increase in active caspase-3 corresponded with an increase in cell death in primed CD8$^+$ T cells. The terminal dUTP nick end labeling (TUNEL) assay labels cleaved DNA by enzymatically conjugating free 3' ends of DNA molecules with one or more fluorescently labeled deoxyuridyl molecules. In cells with elevated DNA cleavage due to apoptosis, TUNEL should show much higher signal. In this case, a drop in the TUNEL signal was observed following stimulation with OVA peptide (Fig. 7C). Interestingly, CD8+ T cells were TUNEL-positive only when they were cultured with very low amounts of peptide, a situation wherein CD8$^+$ T cells are well known to die due to lack of stimulation. OVA-peptide stimulated active-caspase-3$^+$ cells do not show TUNEL staining by fluorescence microscopy (Fig. 8).

Despite the lower overall decrease in the level of TUNEL staining associated with OVA peptide stimulation, it remained possible that the rapid proliferation of CD8$^+$ T cells was masking a concurrent increase in cell death associated with active caspase-3 expression. To address this possibility, OT1 CD8$^+$ T cells were monitored directly for their death. OT1 spleen cells were first activated by *in vitro* infection with OVA expressing *Listeria monocytogenes* (LM-OVA) as described in the methods section. After allowing 3 days for proliferation to occur, CD8$^+$ T cells were confirmed to express a high level of active caspase-3 (Fig. 9A *top*). In contrast, after 12 days in culture, the majority of CD8$^+$ proliferation had ceased and cells expressed only a basal level of active caspase-3 (Fig. 9A *bottom*).

In order to monitor the absolute level of cell proliferation and cell death on a per-cell basis, cells were placed in a 96-well plate by limiting dilution to achieve a countable number of cells

Figure 8: *Active caspase-3^{hi} CD8^{+} T Cells do not exhibit DNA fragmentation.* OT1 spleen cells were stimulated *in vitro* for 48 hours with SIINFEKL peptide or left unstimulated. Control cells were treated with 1 μg/ml staurospaurine for 24 hours to induce apoptosis. Cells were stained with anti-CD8 antibody, fixed and permeabilized before TUNEL and caspase-3 staining. Cells were mounted on slides and examined by fluorescence microscopy. Images show TUNEL staining (green), and active caspase-3 (red) in CD8 labeled T cells (blue). The images are representative of 3 repeated examinations for each differentially stimulated culture. Arrows shown identify cells with positive staining for both caspase-3 and TUNEL.

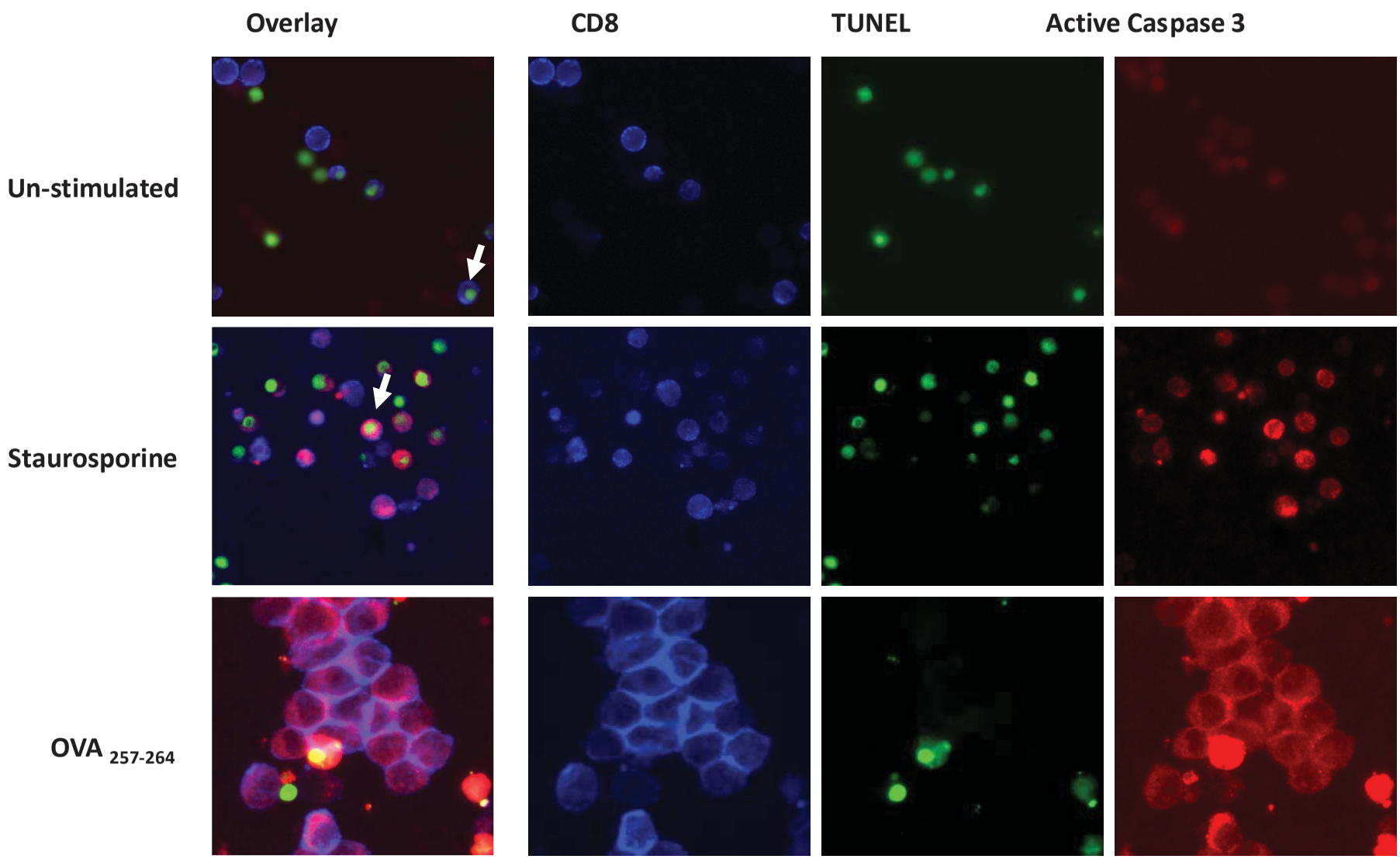
Overlay
CD8
TUNEL
Active Caspase 3
Un-stimulated
Staurosporine
OVA 257-264

Figure 9: *Active Caspase-3 in proliferating CD8 T cells does not lead to cell death.* OT1 splenocytes were placed in a flask and infected at low MOI (0.001) *in vitro* with LM-OVA overnight. Extracellular bacteria were then washed from the culture using a high does of gentamicin. (A) After 3 or 12 days after stimulation with LM-OVA, OT1 cultures were confirmed to be >90% $CD8^+$ cells. The expression of active caspase-3 was also examined. (B) Cells were placed at low numbers in 96-well plates and monitored for cell viability using TMRE staining for mitochondrial activity. (C) Line graphs show the number of live and dead cells in culture over several days.

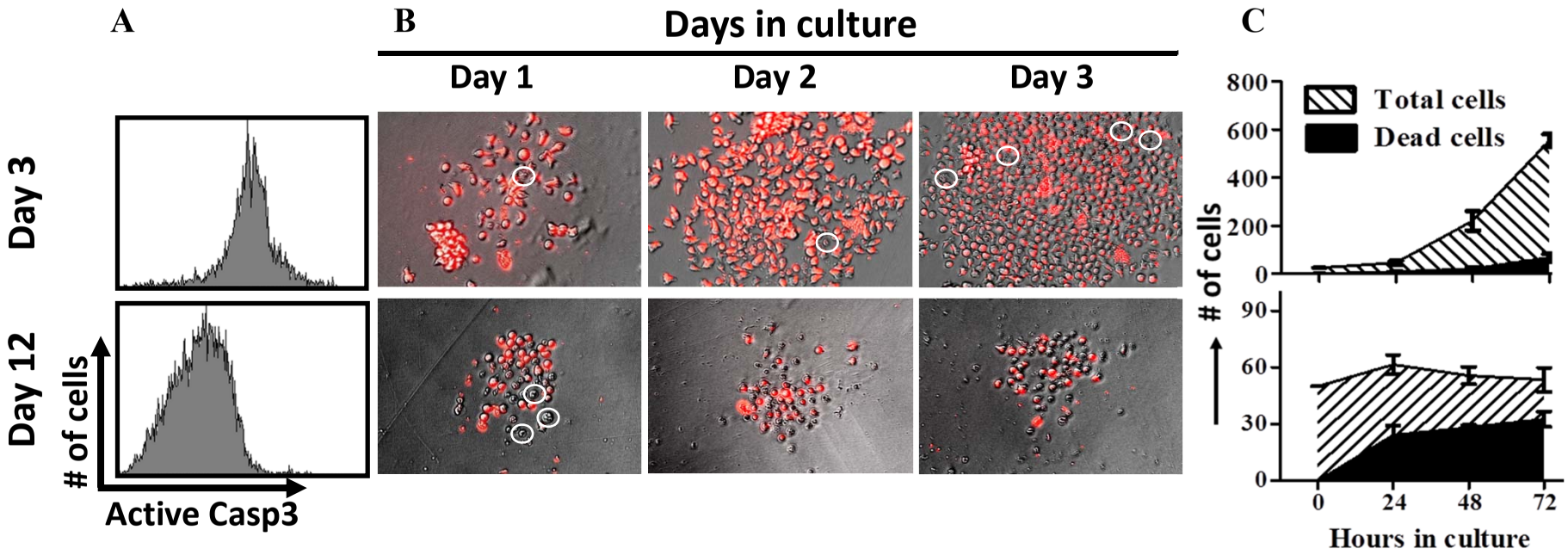
A
B
Days in culture
Day 1
Day 2
Day 3
Day 3
Day 12
# of cells
Active Casp3
C
800
600
400
200
0
Total cells
Dead cells
# of cells
90
60
30
0
0
24
48
72
Hours in culture

(~25/well). After 24, 48 and 72 hours in sub-culture the total number of cells, and the number of dead cells was quantified, using the active-mitochondrial stain TMRE to identify the cell viability. Results clearly show that despite high caspase-3 expression, there is only a very low level of cell death concurrent with $CD8^+$ proliferation (Fig. 9A-C). Conversely, after 12 days in culture, $CD8^+$ T cells show low levels of caspase-3, low proliferation, and a steady increase in the level of cell death when placed in limiting dilution culture (Fig. 9A-C). These data indicate that proliferating $CD8^+$ T cells express a high level of active caspase-3 without a significant level of cell death.

4.1.C Proliferating $CD8^+$ T Cells show elevated caspase-3 in vivo: While the above data, as well as previous work[4,107,108] has consistently shown that *in vitro* stimulation of $CD8^+$ T cells can drive caspase activation, few studies have examined the activation of caspase-3 in an *in vivo* $CD8^+$ T cell response. Thus to accomplish this, OT1 splenocytes were adoptively transferred to WT recipient mice 7 days before the mice were infected with OVA expressing *Listeria monocytogenes* or *Salmonella typhimurium* (LM-OVA or ST-OVA) as described in the methods section. Following this, OVA specific $CD8^+$ T cells were examined at various timepoints using OVA-tetramer and other intracellular stains.

By as early as 3 days after infection with LM-OVA the level of active caspase-3 expression was elevated within the OVA-specific $CD8^+$ T cell population (Fig. 10A). Specifically, the population of proliferating OVA-specific $CD8^+$ T cells showed elevated active caspase-3 at 3 and 4 days post-infection. By 7 days post-infection, the OVA-specific $CD8^+$ response was at its peak, but the active caspase-3 expression had returned to a basal level (Fig. 10B), and remained as such up to at least 40 days post-infection (Fig. 10A). I also confirmed similar results using a sensor

Figure 10: *Proliferating $CD8^+$ T Cells show elevated Caspase-3 during in vivo response.* Recipient C57/BL6 (LM-OVA) were parked with 10^6 OT1 T cells After 7 days of equilibration, mice were then challenged intravenously with 10^4 LM-OVA as shown. At various time points challenged mice were sacrificed and a single-cell suspension obtained from spleens and other organs. Cells were then stained for $CD8^+$, OVA-tetramer binding, active caspase-3 or caspase-3 activity (PhiPhiLux). (A-B) The % OVA-specific and % active caspase-3^{high} in OVA-specific $CD8^+$ T cell population is shown (C) The relative level of caspase-3 activity in OVA-specific $CD8^+$ T cell population is shown. (D) The % OVA-specific $CD8^+$ T cells in various organs, and the caspase-3^{hi} cells in the OVA-specific CD8+ population is shown. n≥3 mice/time point.

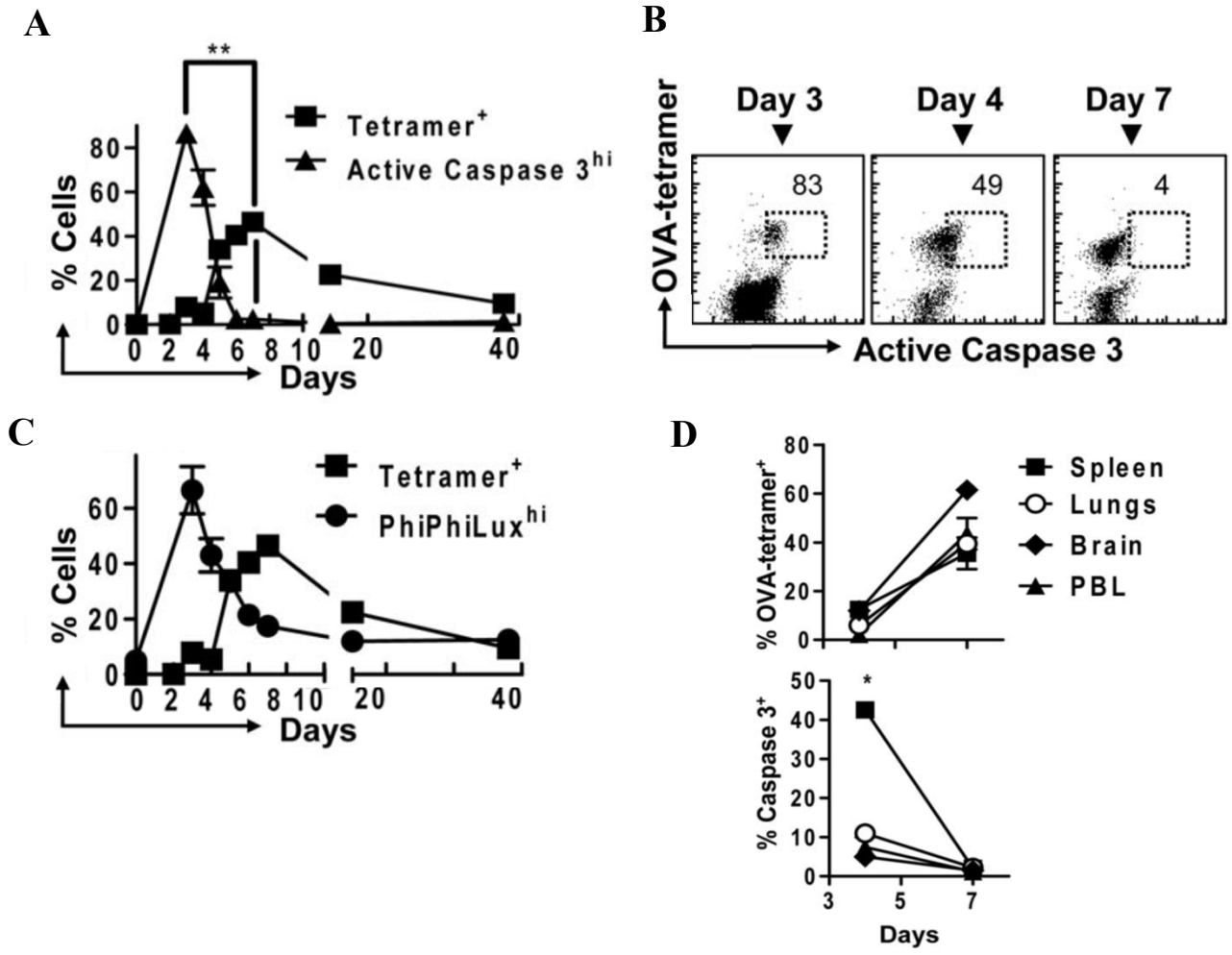
A
**
Tetramer+
Active Caspase 3hi
% Cells
80
60
40
20
0
0 2 4 6 8 10 20 40
Days
B
Day 3
Day 4
Day 7
OVA-tetramer
83
49
4
Active Caspase 3
C
Tetramer+
PhiPhiLuxhi
% Cells
60
40
20
0
0 2 4 6 8 10 20 40
Days
D
% OVA-tetramer+
80
60
40
20
0
Spleen
Lungs
Brain
PBL
% Caspase 3+
*
50
40
30
20
10
0
3 5 7
Days

of caspase-3 cleavage activity PhiPhiLux, which only fluoresces when it is cleaved by caspase-3 type protease activity (Fig. 10C). These results elevated caspase-3 activity coincides with the proliferation phase of the $CD8^+$ T cell response (day 2-7), and it returns to base line levels of throughout the contraction and memory phases of the response (day 7-40). It was also observed that caspase-3^{high} OVA-specific $CD8^+$ T cells are primarily found within the spleen, whereas OVA-specific $CD8^+$ T cells found in the lungs, brain or blood showed very few active caspase-3^{high} $CD8^+$ T cells (Fig. 10D). This is also consistent with the view that proliferating $CD8^+$ T cells specifically express active caspase-3, as T cell proliferation occurs primarily in lymphoid tissues and not in the periphery[9].

4.1.D The timing and magnitude of caspase-3 activation corresponds with the timing and magnitude of antigen presentation: Next, I was interested to analyze how the magnitude and timing of antigen presentation *in vivo* effects the onset of caspase-3 activation. To accomplish this two OVA expressing bacterial models, each which induce divergent modes of $CD8^+$ T cell activation, were utilized. In contrast to infection with LM-OVA, ST-OVA infection induces a muted and protracted proliferation of OVA –specific $CD8^+$ T cells due to a phagosomal lifestyle and very low levels of antigen expression[272,278,279]. In this case, it was observed that there was a significant decrease and delay in the activation of active caspase-3, correlating with the delay and decrease in the magnitude of the OVA specific $CD8^+$ T cell response in ST-OVA infection relative to a response to LM-OVA (Fig. 11A,B). I also confirmed that the timing and magnitude of proliferation in both infection models of OVA-specific $CD8^+$ T cells using Ki67 staining (Fig. 11C). These data indicate that poor antigen presentation in the ST-OVA model drives delayed and protracted proliferation and activation of caspase-3 in OVA-specific $CD8^+$ T cells. Furthermore, these results support the connection of active caspase-3 to proliferation specifically.

Figure 11: *The timing and magnitude of caspase-3 activation corresponds with the timing and magnitude of antigen presentation.* Recipient 129xC57 (B6F1) mice were parked with 10^6 OT1 T cells. After 7 days of equilibration, mice were challenged intravenously with 10^4 LM-OVA 10^3 ST-OVA as shown. At various time points post-infection mice were sacrificed and a single-cell suspension of splenic cells was stained for $CD8^+$, OVA-tetramer binding, active caspase-3 or Ki67. (A) The % OVA-specific $CD8^+$ T cells at various time points are shown. (B) The % active caspase-3^{high} in OVA-specific $CD8^+$ T cell population are shown. (C) The %$Ki67^+$ in OVA-specific $CD8^+$ T cells are shown. $n \geq 3$ mice/time point.

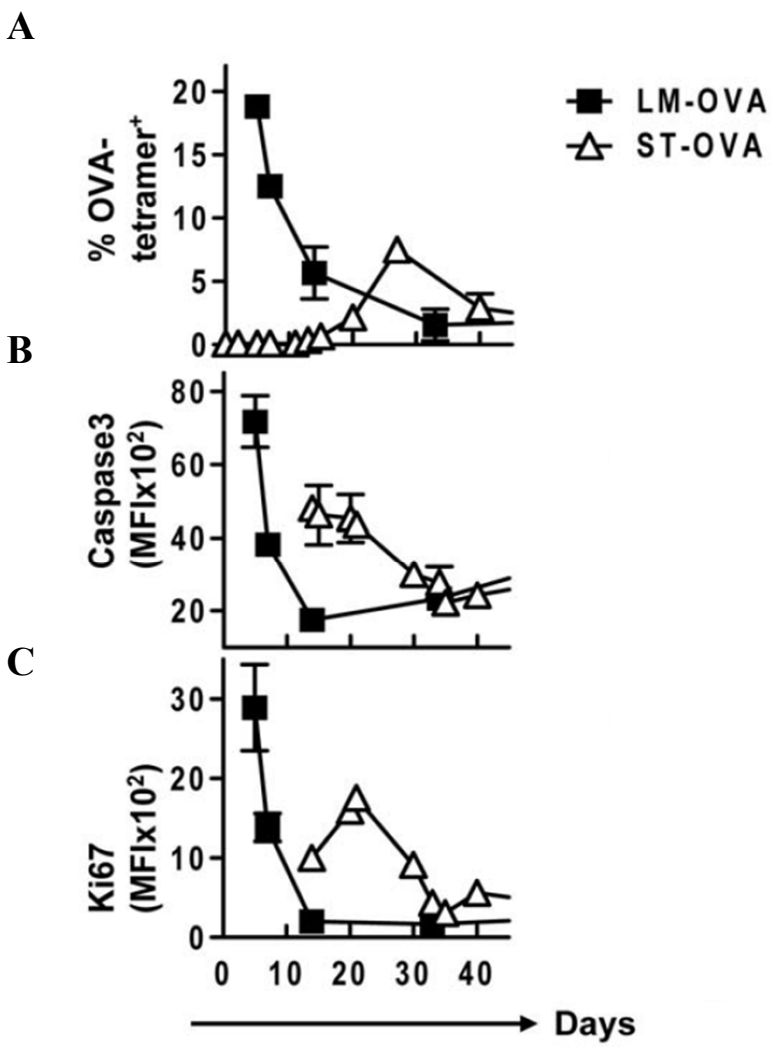
A
B
C
% OVA-tetramer+
Caspase3 (MFIx10²)
Ki67 (MFIx10²)
LM-OVA
ST-OVA
Days
0
5
10
15
20
40
60
80
30
0
10
20
30
40

4.1.E Proliferating caspase-3+ CD8+ T cells show an apoptotic like phenotype: *In vitro* results showed the surprising result that $CD8^+$ T cells expressing active-caspase-3 co-express the marker for proliferation Ki67, thus I next wanted to confirm similar results *in vivo*. At day 3 after infection with LM-OVA, cells showed a high expression of both Ki67 and active caspase-3; conversely, by the peak of OVA-specific $CD8^+$ numbers at day 7, the population showed low expression of both Ki67 and active caspase-3 (Fig. 12A). Interestingly, at time points during the proliferative phase of the $CD8^+$ response, all active-caspase-3+ cells were also high for Ki67 expression, but not all $Ki67^+$ cells were high for active caspase-3 (Fig. 12A, day 4). This data suggests that active caspase-3 is specifically expressed in proliferating $CD8^+$ T cells early after antigen stimulation.

In addition to expression of active caspase-3, proliferating $CD8^+$ T cells also showed an apoptotic like phenotype. At day 3 after infection with LM-OVA, proliferating OVA-specific $CD8^+$ T cells had elevated exposure of phosphatidylserine as measured by Annexin V binding (Fig. 12B). Similarly, it was observed that activated OVA-specific $CD8^+$ T cells co-expressed elevated levels of active caspase-3, annexin binding (Fig. 12C) and programmed death marker 1 (PD1, data not shown). These results indicate that following antigen specific activation, $CD8^+$ T cells not only express active caspase-3, but also exhibit other hallmarks of apoptosis.

4.1.F Active caspase-3^{high} $CD8^+$ T cells do not progress to cell death: Given the apoptotic-like phenotype of activated $CD8^+$ T cells *in vivo*, it was next necessary to confirm whether active caspase-3^{high} $CD8^+$ T cells were progressing to cell death. During the antigen specific $CD8^+$ T cell response to LM-OVA infection, a moderate increase in the staining for TUNEL within the active-caspase-3^+ population was observed (Fig. 13A). Similar moderate increases in TUNEL staining have previously been associated with proliferating cells[280]. During delayed proliferation

Figure 12: *Activated antigen specific CD8$^+$ T cells simultaneously display markers for apoptosis and proliferation.* Recipient mice were injected with 10^6 OT1 splenocytes 7 days before challenge with LM-OVA (iv). Infected mice were sacrificed and spleens were examined via flow cytometry at various time points after infection as shown. The co-expression of (A) Ki67 and active caspase-3, (B) OVA-Tetramer binding and annexin-V, or (C) annexin-V binding and active caspase-3 is shown.

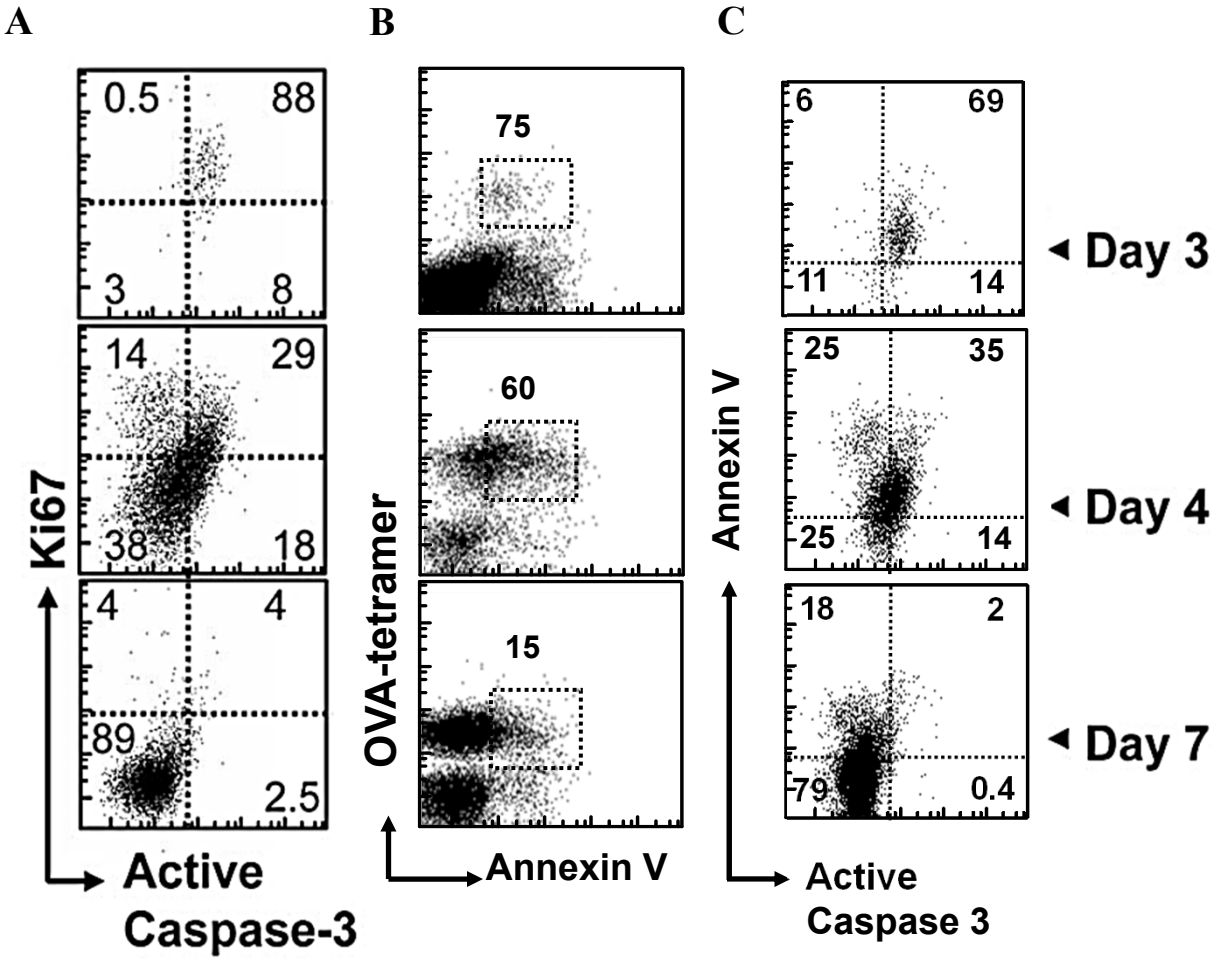
A
B
C
0.5
88
3
8
14
29
38
18
4
4
89
2.5
Ki67
Active
Caspase-3
75
60
15
OVA-tetramer
Annexin V
6
69
11
14
25
35
25
14
18
2
79
0.4
Annexin V
Active
Caspase 3
Day 3
Day 4
Day 7

Figure 13: *Caspase-3^{hi} proliferating CD8^{+} T cells in vivo do not show signs of progressing to cell death.* Recipient B6.F1 mice were injected with 10^6 OT1 splenocytes 7 days before challenge with **(A)** LM-OVA (iv) or **(B)** ST-OVA. At various time points after infection, mice were sacrificed and a single cell suspension of splenocytes was stained for CD8^{+}, OVA-tetramer, active caspase-3 and TUNEL. Scatterplots show caspase-3 and TUNEL staining for CD8^{+} OVA-tetramer^{+} cells.

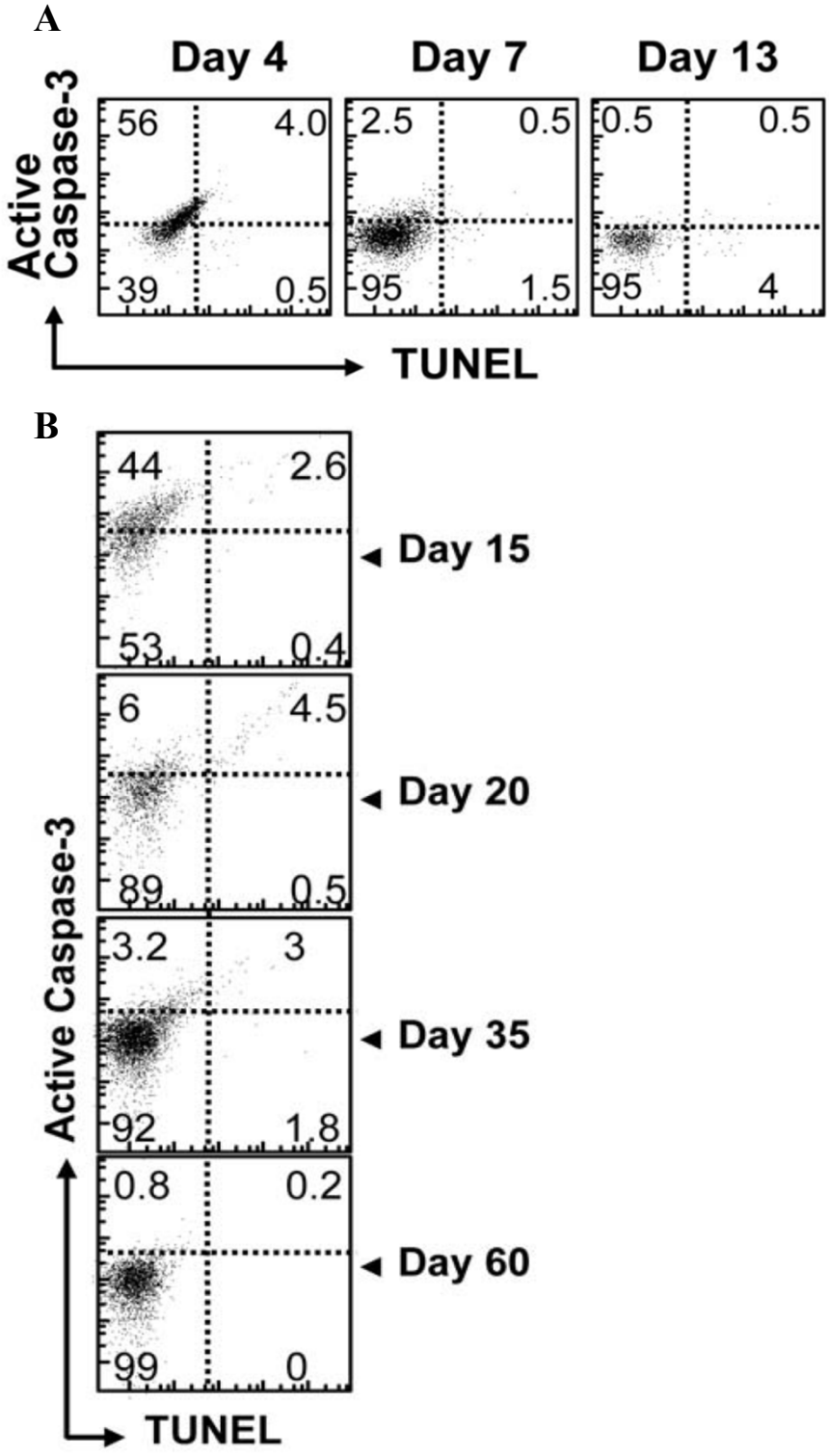
A
Day 4
Day 7
Day 13
Active Caspase-3
56
4.0
39
0.5
2.5
0.5
95
1.5
0.5
0.5
95
4
TUNEL
B
44
2.6
53
0.4
Day 15
6
4.5
89
0.5
Day 20
3.2
3
92
1.8
Day 35
0.8
0.2
99
0
Day 60
Active Caspase-3
TUNEL

of OVA-specific $CD8^+$ T cells in response to ST-OVA, only a small increase in TUNEL staining with active caspase-3^{high} population was again observed (Fig. 13B). These results suggest that there is little ongoing apoptotic DNA fragmentation and cell death in either the proliferating active caspase-3^{high} $CD8^+$ T cell population or the contracting caspase-3^{low} population *in vivo*.

The lack of a population of terminally dead $TUNEL^+$ $CD8^+$ T cells in the proliferating caspase-3^{high} cells may be alternatively explained by rapid clearance of dying cells by phagocytic cells in the spleen. Thus I employed PhiPhiLux to sort proliferating $CD8^+$ T cells, at day 5 of LM-OVA infection, into caspase-3 high and low populations (Fig. 14A), which were subsequently placed in low density culture so as to monitor the absolute level of death and proliferation *in vitro*. When placed in culture with supporting IL-7, both caspase-3 high and low populations did not show a significant difference in capacity to proliferate or the level of cell death (Fig. 14B,C). Similarly, both populations showed rapid progression to cell death with little proliferation when no supporting IL-7 was added to the culture (Fig. 14B,C). These results show that the expression of active caspase-3 during $CD8^+$ T cell expansion is not associated with cell death either *in vivo* or *in vitro*.

4.1.G Active caspase-3 is driven by antigen presentation and not inflammation: Our data thus far showed that activation of $CD8^+$ T cells drives an increase in active caspase-3, but it remained unclear what signals regulated this activation of caspase-3. To investigate this purified $CD8^+$ T-cells were exposed to OVA peptide and/or inflammatory stimulus in the form of heat-killed *Listeria* bacteria. I observed that while antigen stimulation led to a significant increase in active caspase-3^{high} cells, inflammatory stimulus alone did not (Fig. 15A). Furthermore, the addition of inflammatory stimulus to OVA stimulated cultures did not appreciably alter the level of active caspase-3 in antigen stimulated cultures (Fig. 15A).

Figure 14: *Caspase-3^{hi} proliferating CD8^{+} T cells do not undergo significant cell death when supplemented with supportive cytokine ex vivo.* Mice were parked with 10^4 CD45.1+ OT1 spleen cells and challenged with 10^4 LM-OVA (iv). Mice were sacrificed at day 5 post LM-OVA infection and CD8^{+} T cells were magnetically isolated by negative selection. Cells were stained with anti-CD45.1 antibody and PhiPhiLux. (A) Cells were sorted into CD45.1+ caspase-3 activity^{high} and CD45.1+ caspase-3 activity^{low} fractions. (B) Sorted cells were then plated at low cell densities (~12.5 cells/well) and examined for viability over several days using TMRE staining. (C) The total number and number of dead cells were counted directly in at least 6 replicate wells and the changes observed over 72 hours in the plates. (D) Cells were also maintained at higher concentrations (~100 000/well) and stained for DNA cleavage (TUNEL) after 1 day in culture.

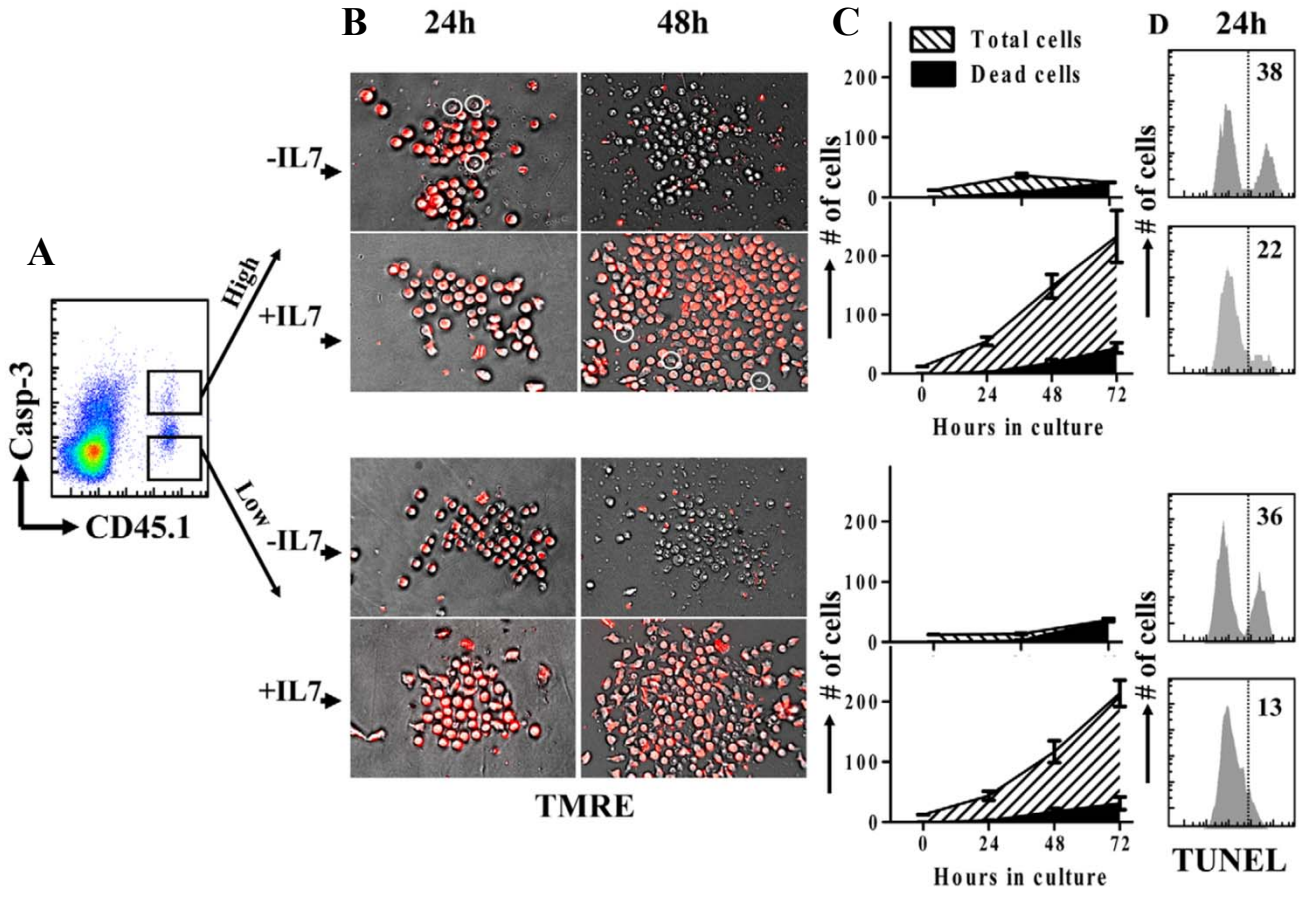
A
Casp-3
CD45.1
High
Low
+IL7
-IL7
+IL7
-IL7
B
24h
48h
TMRE
C
Total cells
Dead cells
# of cells
Hours in culture
D
24h
38
22
36
13
TUNEL

Figure 15: *Active caspase-3 is driven by antigen presentation and not inflammation.* (A) OT-1 cells were placed in culture and either stimulated with 1 μg/ml of SIINFEKL peptide or left unstimulated. Additional inflammatory stimulation was added to some cultures by adding 10^4 heat killed *Listeria monocytogenes* (HK-LM). After 48 hours in culture cells were intracellular stained for active caspase-3 and Ki67 and examined by FACS. Data is representative of at least 3 repeated experiments. (B) WT mice were injected with 10^5 CFSE stained OT1 cells concurrent with PBS, LM-OVA, or ST-OVA (10^4, iv). Four days later mice were sacrificed and spleen cell suspensions stained with anti-CD8 antibody, OVA-tetramer, followed by intracellular staining with anti-caspase-3 antibody. (C) $Rag1^{-/-}$ mice were injected with 10^4 CFSE stained OT1 cells. The expression of active caspase-3 was examined at 4 days after adoptive transfer as described above. All scatterplots show data is obtained from gated OVA specific $CD8^+$ T cells and is representative of 3 mice per group

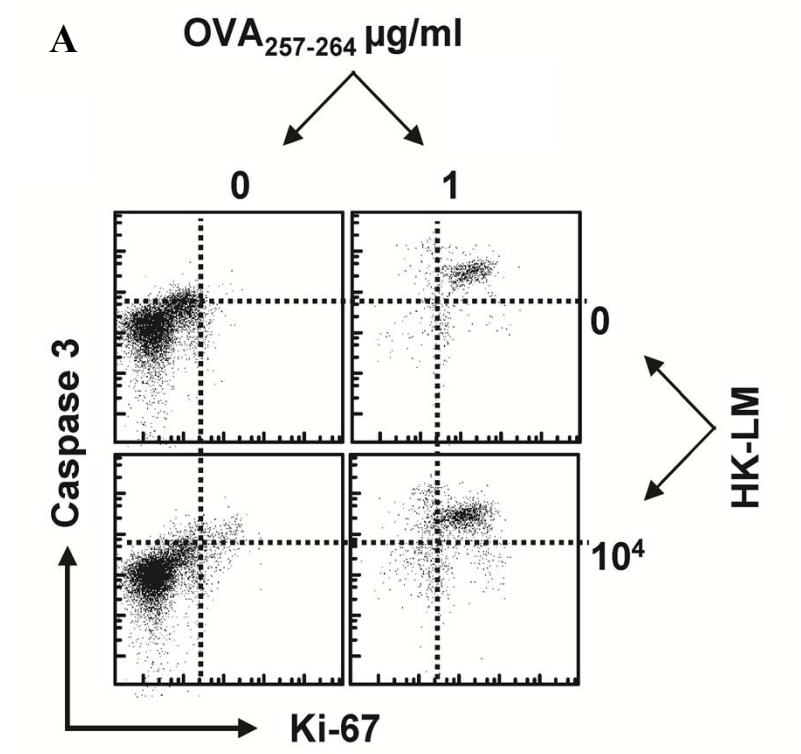
A
OVA257-264 µg/ml
0
1
0
HK-LM
10^4
Caspase 3
Ki-67

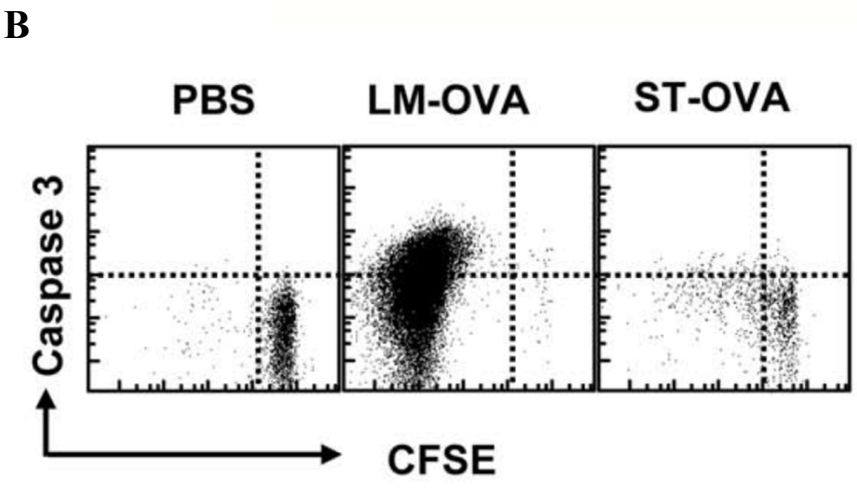
B
PBS
LM-OVA
ST-OVA
Caspase 3
CFSE

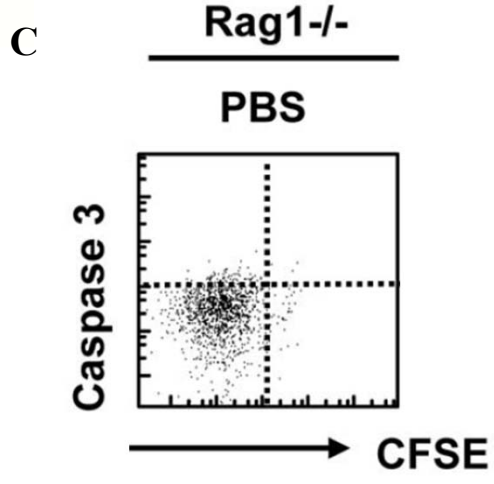
C
Rag1-/-
PBS
Caspase 3
CFSE

Similar results were also confirmed *in vivo*, where mice parked with CFSE-labeled OT1 T cells were challenged with LM-OVA, ST-OVA, or a vehicle control. Within our lab, we have observed that ST-OVA presents little antigen early on in infection, despite significant induction of inflammation[278]. At day 5 after infection, ST-OVA stimulated cells showed some low level proliferation but had little induction of active caspase-3, whereas those cells which received strong antigenic stimulus from LM-OVA infection showed significant proliferation and induction of active caspase-3 (Fig. 15C). Thus, these results show that both *in vitro* and *in vivo*, the strength of antigenic stimulation and not inflammation corresponds with the increase in active caspase-3 within proliferating T cells.

Given the correlation between activation of caspase-3 and T cell proliferation, I was also interested to examine whether antigen independent, homeostatic proliferation of $CD8^+$ T cells also led to an increase in active caspase-3. To test this I adoptively transferred CFSE-stained OT1 $CD8^+$ T cells into $Rag1^{-/-}$ animals, which lack T cells. After 4 days in this lymphopenic environment, a significant "homeostatic expansion" of $CD8^+$ T cells was observed, but there was no significant increase in the level of active caspase-3 within these cells (Fig. 15D). These data show that it antigenic stimulation specifically drives increased expression of caspase-3 within proliferating $CD8^+$ T cells.

4.1.H Caspase-3 activation occurs before the emergence of differentiated $CD8^+$ effector cells: I next wanted to further probe the phenotype of active caspase-3 expressing $CD8^+$ T cells. To do this, I examined the expression of markers of $CD8^+$ T cell differentiation, CD62L and IL7Rα. CD62L and IL7R are lymphoid homing markers that aid in retaining proliferating $CD8^+$ T cells in secondary lymphoid tissue. Effector $CD8^+$ T cells have low expression of these markers to allow their T cell emigration to peripheral sites[281]. Examining cells at day 3 and 4 of LM-OVA

infection *in vivo*, proliferating OVA specific $CD8^+$ cells displayed an activated $CD62L^{high}/IL7R\alpha^{high}$ phenotype, while also being active caspase-3^{high} (Fig. 16A). By day 7 of infection, the majority of cells showed a $CD62L^{low}/IL7R\alpha^{low}$ effector phenotype, but active caspase-3 expression had returned to a basal level.

To further investigate the relationship of expression of active caspase-3 and lymphoid homing markers kinetically, I next examined CFSE-stained adoptively transferred OT1 $CD8^+$ T cells as they were proliferating in response to LM-OVA. At day 4 of infection, those cells that retained the most CFSE, and thus had undergone less division, also showed the highest levels of active caspase-3 and CD62L (Fig. 16B,C). Conversely, those cells which had undergone the most proliferation had the lowest levels of CD62L and active caspase-3 (Fig. 16B,C). These data show that proliferating $CD8^+$ T cells rapidly upregulate active caspase-3 in the earliest cell divisions following antigenic stimulus, and then progressively lose both active caspase-3 and lymphoid homing markers as proliferation proceeds.

4.1.I Active caspase-3 promotes $CD8^+$ T cell proliferation: Given the clear evidence that antigenic stimulation drives early activation of caspase-3 without cell death in proliferating $CD8^+$ T cells, the question remained as to what the function of caspase-3 is in this context. To probe this question, CFSE-stained $CD8^+$ T cells were treated with antigen, or left unstimulated for control cells, with the caspase-3 specific inhibitor z-DQMD-FMK. After 48 hours, those cells treated with a caspase-3 inhibitor showed significantly less proliferation compared to control cells (Fig. 17A). It was also observed that caspase-3 inhibited cells showed significantly more cell death when compared to stimulated control cells (Fig. 17B). It should be noted that because death was not significantly different than observed in unstimulated cells, this death cannot be specifically ascribed to either inhibition of cytokine production in activated T cells[4] or induction of an

Figure 16: *Caspase-3 activation occurs before the emergence of differentiated CD8$^+$ effector T cells.* C57BL/6 mice were initially parked with 10^4 OT1 spleen cells. After infection with 10^4 LM-OVA, mice were sacrificed at various time points and spleens were harvested. Single cell suspensions were co-stained for CD8$^+$, OVA-Tetramer, CD62L, IL7Ra and active caspase-3. (A) Scatter plots show the relative staining of OVA-tetramer+ CD8$^+$ cells for activation markers and active caspase-3. (B) 10^6 CFSE stained OT1 splenocytes were injected concurrently with 10^4 LM-OVA. Scatterplots show expression of active caspase-3 versus CFSE and CD62L in OVA-tetramer+ CD8$^+$ T cells after 4 days *in vivo*. (C) OVA specific CD8$^+$ T cells at specific division number were examined for expression of active caspase-3 and CD62L/IL7Ra as cell proliferation proceeds (**P<0.01, *P<0.05, n = 3 per time point)

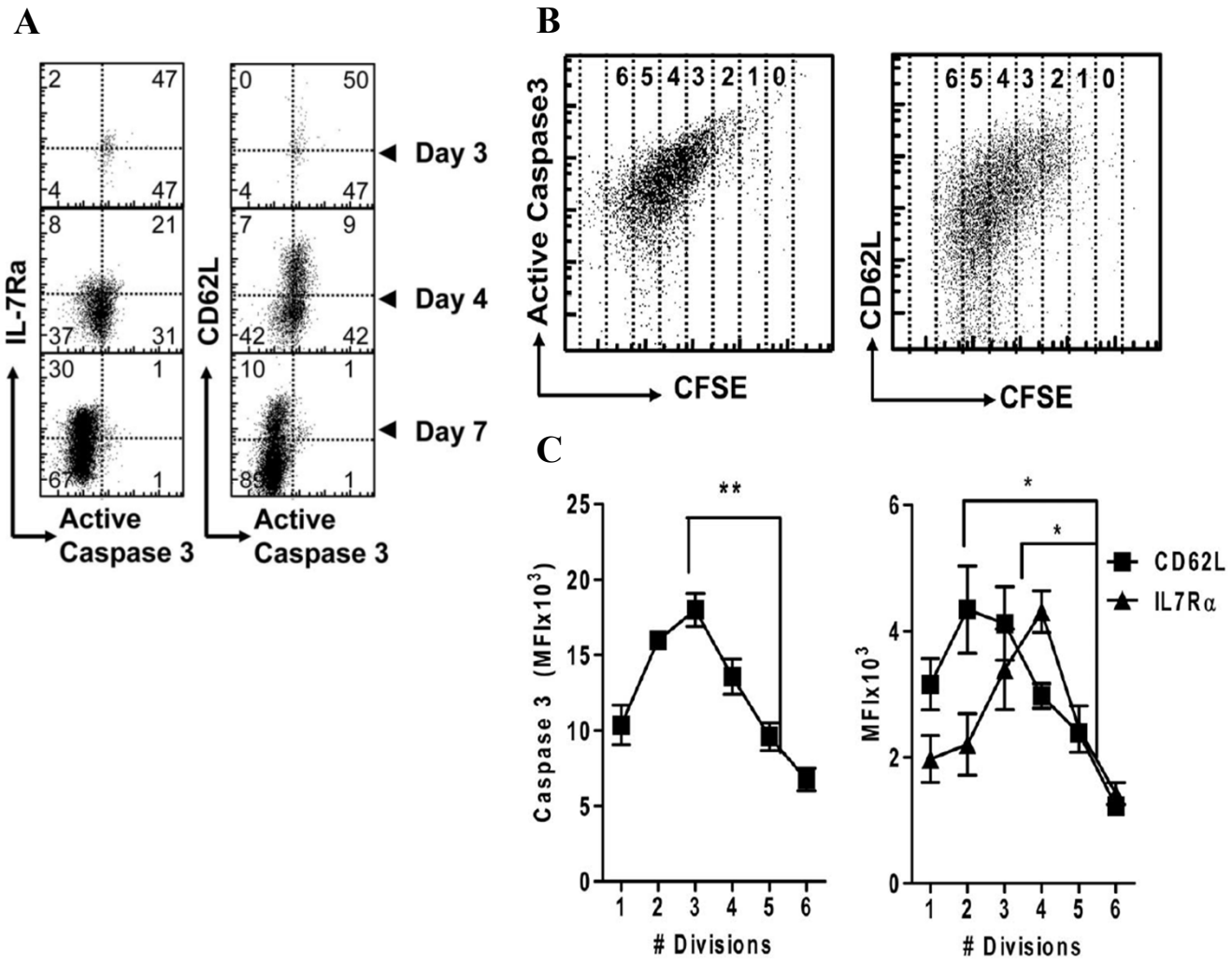
A
2
47
4
47
8
21
37
31
30
1
67
1
IL-7Ra
Active Caspase 3
0
50
4
47
7
9
42
42
10
1
89
1
CD62L
Active Caspase 3
Day 3
Day 4
Day 7
B
Active Caspase3
6 5 4 3 2 1 0
CFSE
CD62L
6 5 4 3 2 1 0
CFSE
C
Caspase 3 (MFIx10^3)
**
Divisions
MFIx10^3
*
*
CD62L
IL7Rα
Divisions

Figure 17: *Caspase-3 inhibition slows CD8$^+$ T cell proliferation and enhances cell death*. 10^5 CFSE stained OT1 cells were stimulated *in vitro* with SIINFEKL peptide in the presence or absence of 50 μM caspase-3 inhibitor (z-DQMD-FMK) and examined for proliferation after 48 hours. Proliferation was examined by FACS staining for Ki67. (A) There is a significant decrease in proliferation induced by OVA peptide in the presence of caspase-3 inhibitor. (B) Cells were also examined for viability using loss of propidium iodide exclusion as a marker for loss of plasma membrane integrity (* $P<0.05$). Experiments shown are representative of at least 3 repeated experiments.

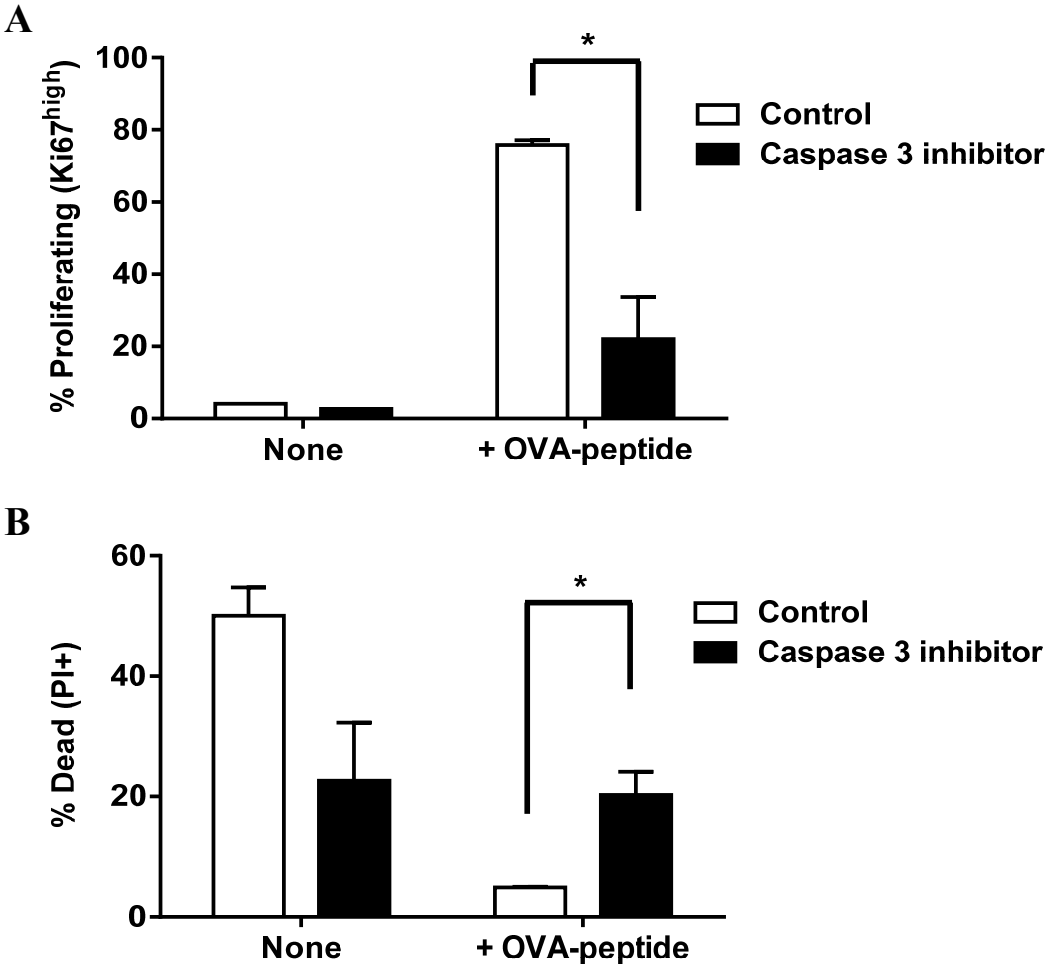
A
% Proliferating (Ki67high)
100
80
60
40
20
0
*
Control
Caspase 3 inhibitor
None
+ OVA-peptide
B
% Dead (PI+)
60
40
20
0
*
Control
Caspase 3 inhibitor
None
+ OVA-peptide

alternative death pathway[104]. These data support a model wherein caspase-3 activation promotes $CD8^+$ T cell proliferation, potentially by limiting alternative modes of cell death.

4.2 THE ROLE OF IAPS IN INNATE IMMUNE CELL FUNCTION

Given our discovery of a protective role for caspase-3 in proliferating $CD8^+$ T cells, I next questioned why the antigen stimulated $CD8^+$ T cells did not progress to cell death despite high levels of caspase activation. Thus, in consultation with my thesis advisory committee, I turned my focus to the inhibitor of apoptosis proteins (IAPs), which can act to limit cell death in various cell types. In order to probe the role of the IAPs, we obtained the IAP antagonist SM-164 through a collaboration with the lab of Dr. Shaomeng Wang at the University of Michigan. SM-164 (SM) is part of a newly developed class of small molecule inhibitors of cIAP1, cIAP2, and xIAP proteins. SM is a mimetic of the death promoting protein SMAC released from the mitochondria during apoptosis. Treating activated $CD8^+$ T cells with SM had relatively little effect on the proliferation and survival of antigen stimulated $CD8^+$ T cells (Fig. 18A). Treating mice *in vivo* with SM yielded no significant difference in the magnitude or timing of an OVA-specific $CD8^+$ T cell response (Fig. 18B). These data suggest that the expression of IAPs do not play a role in limiting cell death induction by active caspase-3 within proliferating $CD8^+$ T cells.

***4.2.A cIAPs limit cell death in innate immune cells*:** While there has been no report of dysfunction in $CD8^+$ T cells within cIAP1- or cIAP2-deficient mice, several reports have demonstrated that mice deficient for either cIAP show significantly altered macrophage function[268,282]. Consistent with a view that cIAP is particularly important in innate immune cells, it was observed that splenic macrophages showed significantly higher expression of cIAP1 and cIAP2 relative to B cells, T cells or dendritic cells (Fig. 19A).

Figure 18: *cIAPs inhibition does not have a signifiant impact on CD8$^+$ T cell proliferation*. OT1 cells were stimulated *in vitro* with OVA peptide in the presence or absence of 1μM of SM-164 SMAC mimetic. After 48 hours, cell proliferation was evaluated by Ki67 staining and cell death by propidium iodide staining. (A) No significant impact on the number of proliferating cells or cell death was observed with SMAC mimetic treatment. (B) Mice were parked with 10^6 CD45.1$^+$OT1 splenocyte 7 days before challenge with LM-OVA (10^4, iv). Mice were bled and the blood was examined by flow cytometry for the number of CD45.1+ CD8$^+$ T cells at various time points after infection as shown (n≥3 mice/treatment group).

A

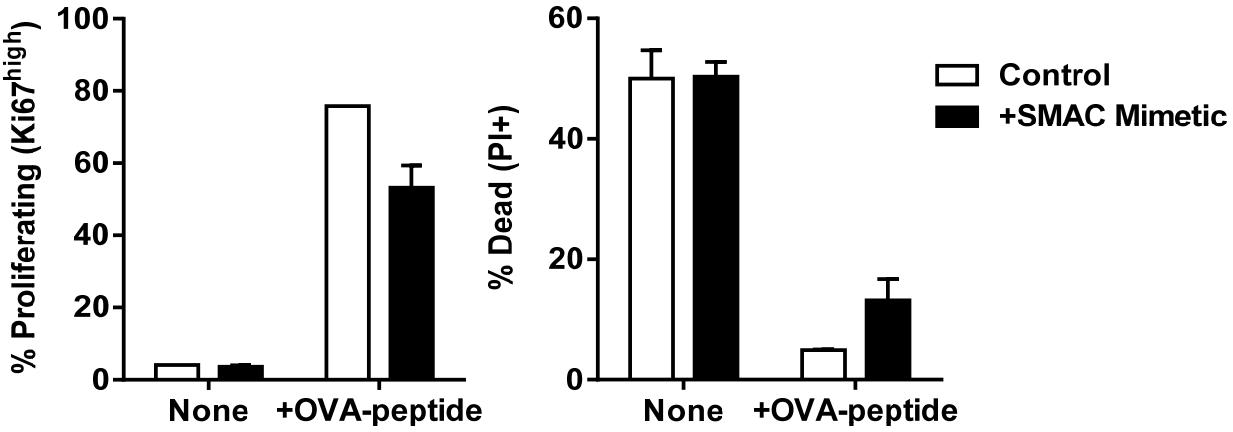
% Proliferating (Ki67high)
100
80
60
40
20
0
None
+OVA-peptide
% Dead (PI+)
60
40
20
0
None
+OVA-peptide
Control
+SMAC Mimetic

B

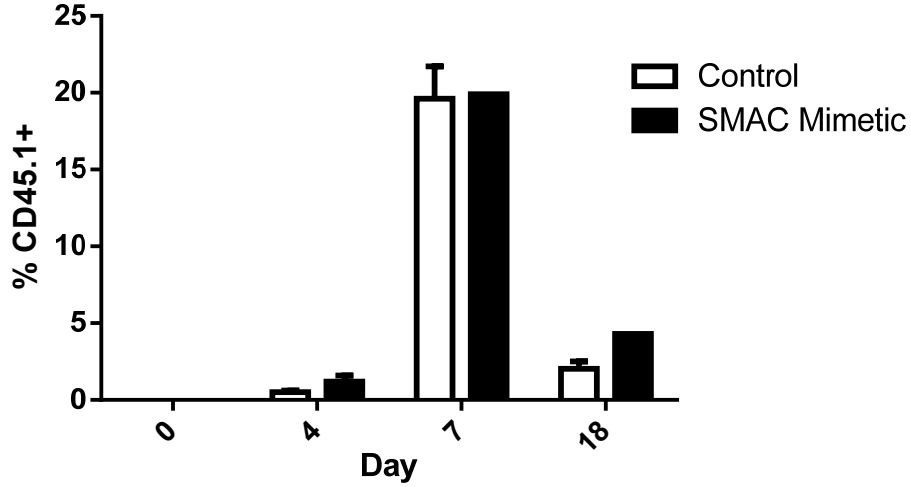
% CD45.1+
25
20
15
10
5
0
0
4
7
18
Day
Control
SMAC Mimetic

Figure 19: *cIAPs limit cell death in bone marrow derived macrophages and dendritic cells.* (A) Spleen cells were obtained from WT C57BL6/J mice and a single cell suspension was prepared. Cells were sequentially isolated via positive magnetic selection of CD11b+ macrophages, B220+ B cells, CD3+ T cells and CD11c+ dendritic cells as described in the methods section. Isolated cells were then examined for cIAP expression via western blot. (B) Bone-marrow derived dendritic cells (BMDC) and macrophages (BMDM) cells were differentiated for 7 days as described in the methods. Cells were then plated in 96 well plates and treated with various doses of SM as shown. Viability was determined 24 hours after treatment using MTT. (C) BMDM cells treated with SM for 1 hour were examined for expression of cIAPs via western blot. (D) BMDM cells were derived from WT, cIAP1$^{-/-}$ or cIAP2$^{-/-}$ mice and treated for 1 or 4h with SM, then examined for expression of cIAPs or XIAP via western blot. Experiments are representative of at least 3 repeated experiments.

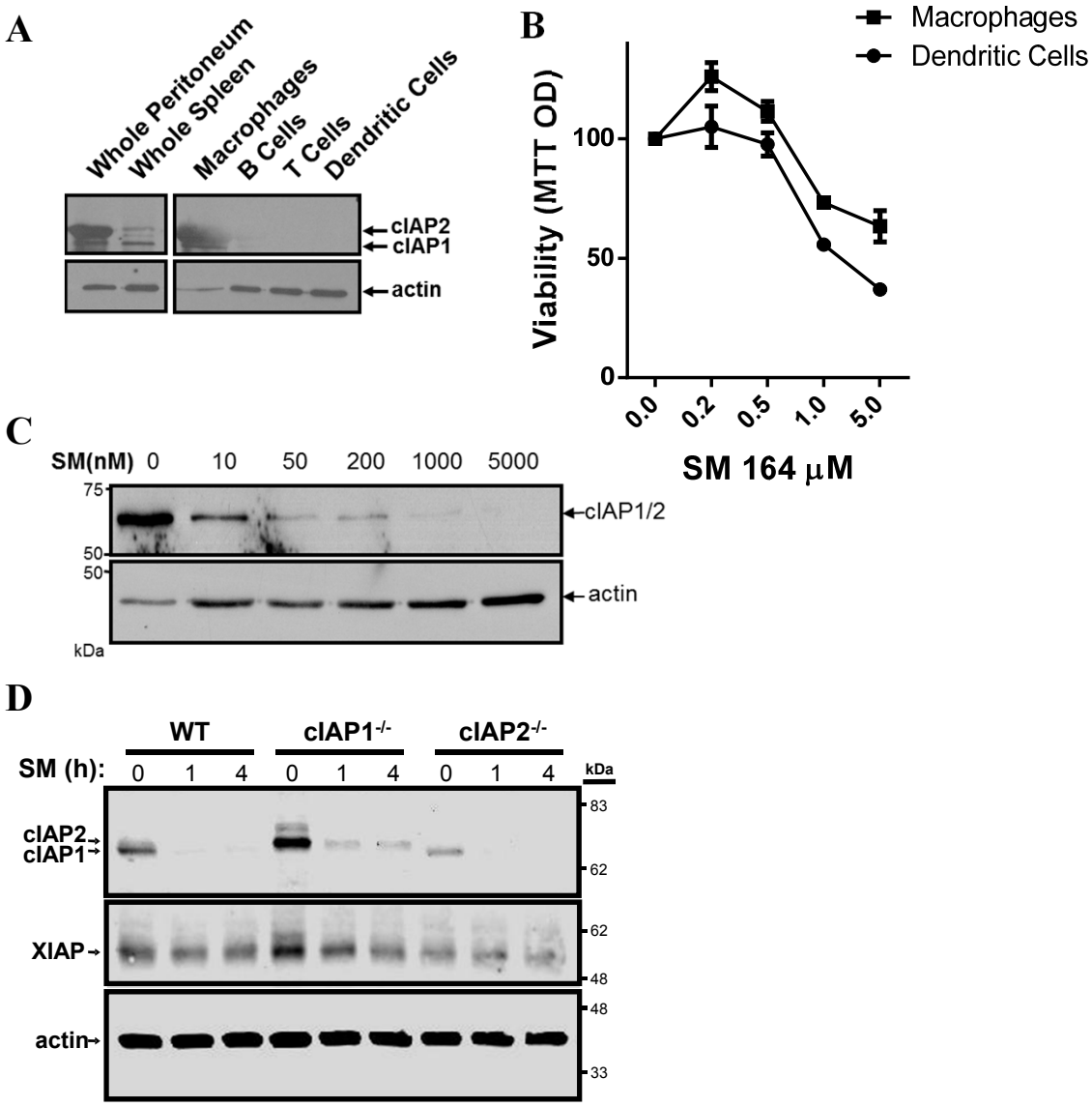
A
Whole Peritoneum
Whole Spleen
Macrophages
B Cells
T Cells
Dendritic Cells
cIAP2
cIAP1
actin
B
Macrophages
Dendritic Cells
Viability (MTT OD)
100
50
0
0.0
0.2
0.5
1.0
5.0
SM 164 μM
C
SM(nM) 0 10 50 200 1000 5000
75
50
50
cIAP1/2
actin
kDa
D
WT
cIAP1-/-
cIAP2-/-
SM (h): 0 1 4 0 1 4 0 1 4
kDa
cIAP2
cIAP1
XIAP
actin
83
62
62
48
48
33

To probe the function of cIAP expression within innate immune cells, I treated bone marrow derived dendritic cells (BMDCs) and bone marrow derived macrophages (BMDMs) with varying concentrations of SM. Both BMDMs and BMDCs showed a concentration dependent loss of viability in response to treatment with SM-164 (Fig. 19B). SM-164 is known to function by inducing the proteasomal degradation of cIAP1 and cIAP2[283], thus the dose-dependent degradation of cIAP expression with SM treatment was confirmed (Fig. 19C). Finally, cIAP1- or cIAP2-deficient macrophages were employed to confirm that treatment with SM-164 was able to target and deplete both cIAPs (Fig. 19D). It was noted that there was only a very modest effect on the expression level of xIAP (Fig. 19D), but this is not necessarily indicative of xIAP function, as SM has been shown to impact xIAP function in a non-degradative fashion[283].

***4.2.B SM-induced death is associated with increased inflammatory cytokine production*:** In addition to their role in various cell death pathways, cIAPs have also been extensively implicated in various inflammatory signaling pathways, for instance in TNF-α induced NF-κβ signaling[189] (see introduction). Thus, in order to investigate the role of cIAPs in the production of inflammatory cytokines, BMDCs or BMDMs were treated with SM and/or varying amounts of the TLR4 agonist, LPS. In response to LPS, both BMDC and BMDM cells increased their production of IL-6 and TNF cytokines (Fig. 20A,B). Furthermore, the addition of SM treatment resulted in a significant increase in LPS-induced production of both IL-6 and TNF, although SM treatment alone resulted in only a low level of TNF production (Fig. 20A,B). It is of note that treatment with LPS did not have a significant impact on the sensitivity of macrophages to SM-induced loss of cell viability (unpublished results from our lab). These results indicate that cIAP inhibition increases pro-inflammatory signaling within innate immune cells.

Figure 20: *SM-induced death is associated with increased inflammatory cytokine production.* (A) BMDC and (B) BMDM cells were examined for inflammatory cytokine production in response to SM treatment and/or LPS. Cells were plates at 50 000 cells/well in 96 well plates and treated for 24 hours with varying concentrations of SM and LPS as shown. The level of TNF in the supernatant was evaluated by a bioassay and IL-6 was determined by a sandwich ELISA as described in the methods section. Results show the mean of at least 3 experiments performed in duplicate.

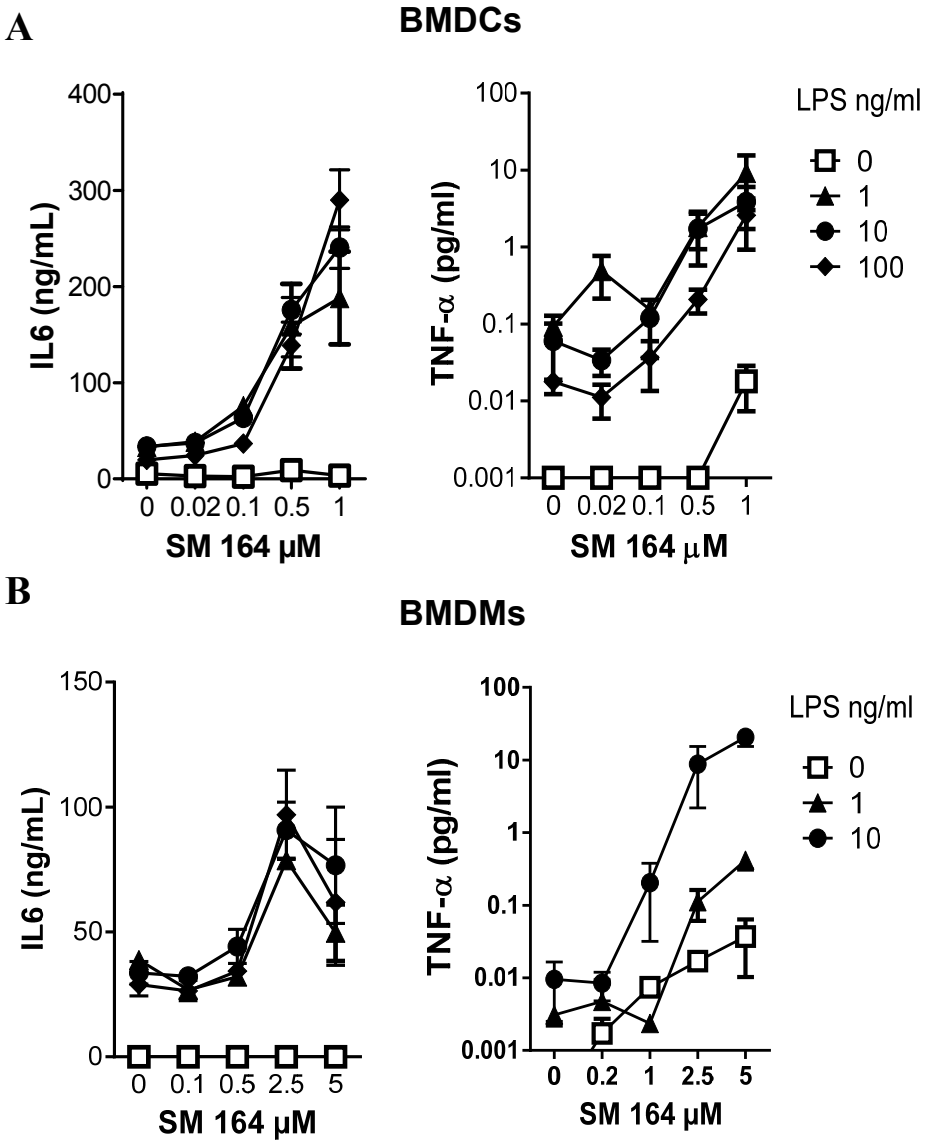
A
BMDCs
IL6 (ng/mL)
400
300
200
100
0
0 0.02 0.1 0.5 1
SM 164 µM
TNF-α (pg/ml)
100
10
1
0.1
0.01
0.001
0 0.02 0.1 0.5 1
SM 164 µM
LPS ng/ml
0
1
10
100
B
BMDMs
IL6 (ng/mL)
150
100
50
0
0 0.1 0.5 2.5 5
SM 164 µM
TNF-α (pg/ml)
100
10
1
0.1
0.01
0.001
0 0.2 1 2.5 5
SM 164 µM
LPS ng/ml
0
1
10

***4.2.C SM induces programmed necrosis in macrophages*:** Due to the highly similar results obtained between BMDM and BMDC cell types thus far, I decided to examine only macrophages for the remainder of experiments. In order to probe the exact mode of cell death induced by SM, I next combined SM-treatment with inhibitors of death pathways. Addition of the pan-caspase inhibitor z-VAD-FMK (zVAD) resulted in a significant increase in sensitivity of cIAP inhibition at lower concentrations of SM (Fig. 20A,B). Notably, treatment with high levels of SM (~2.5-5μM) alone was a potent inducer of cell death and was not significantly affected by the addition of zVAD (Fig. 21A,B).

In contrast to caspase inhibition, treatment with the specific inhibitor of necroptosis, necrostatin, resulted in a consistent rescue of SM-induced cell death (Fig. 21A, B). Necrostatin functions by specifically inhibiting the kinase function of Rip1, preventing the downstream phosphorylation of Rip3, which in turn drives necroptotic cell death[205]. Thus to confirm our results, the response of necroptosis deficient $Rip3^{-/-}$ macrophages were also examined [253]. Indeed, results showed that $Rip3^{-/-}$ were highly resistant to SM-induced cell death (Fig. 21C), implicating the pathway of necroptosis as the specific death pathway induced by SM treatment.

***4.2.D cIAP1 and cIAP2 additively limit macrophage necroptosis*:** In order to delineate possible differences in the function of cIAPs, the relative response to SM treatment of WT, $cIAP1^{-/-}$, and $cIAP2^{-/-}$ macrophages was next examined. A significant increase in sensitivity of $cIAP1^{-/-}$ and $cIAP2^{-/-}$ macrophages to a sub-lethal dose of SM-164 (1μM) was observed (Fig. 22A). Rescue by necrostatin was similar to WT in the cIAP1 and 2 knockout macrophages (Fig. 22A). These results indicate that cIAP1 and cIAP2 can function redundantly in an additive fashion to limit necroptosis.

Figure 21: *SM treatment induces programmed necrosis in macrophages.* (A) BMDM cells were treated with various concentrations of SM and necrostatin or zVAD as shown. Cell viability was examined via MTT assay (A) or by counter-staining with Hoechst and propidium iodide to mark all cells and dead cells respectively (B) BMDM cells were treated with various concentrations of SM and 10μg/mL of necrostatin or zVAD (or nothing for control cells). Cells were then left for 24 hours before being examined for viability via microscopic analysis. Graph shows the average % of dead cells by counting images from 3 repeated experiments (C) BMDM cells were derived from WT or $RIP3^{-/-}$ mice and treated with SM and/or necrostatin as shown. *$P<0.05$ **$P<0.01$. Experiments show the mean of 3 experiments performed in duplicate.

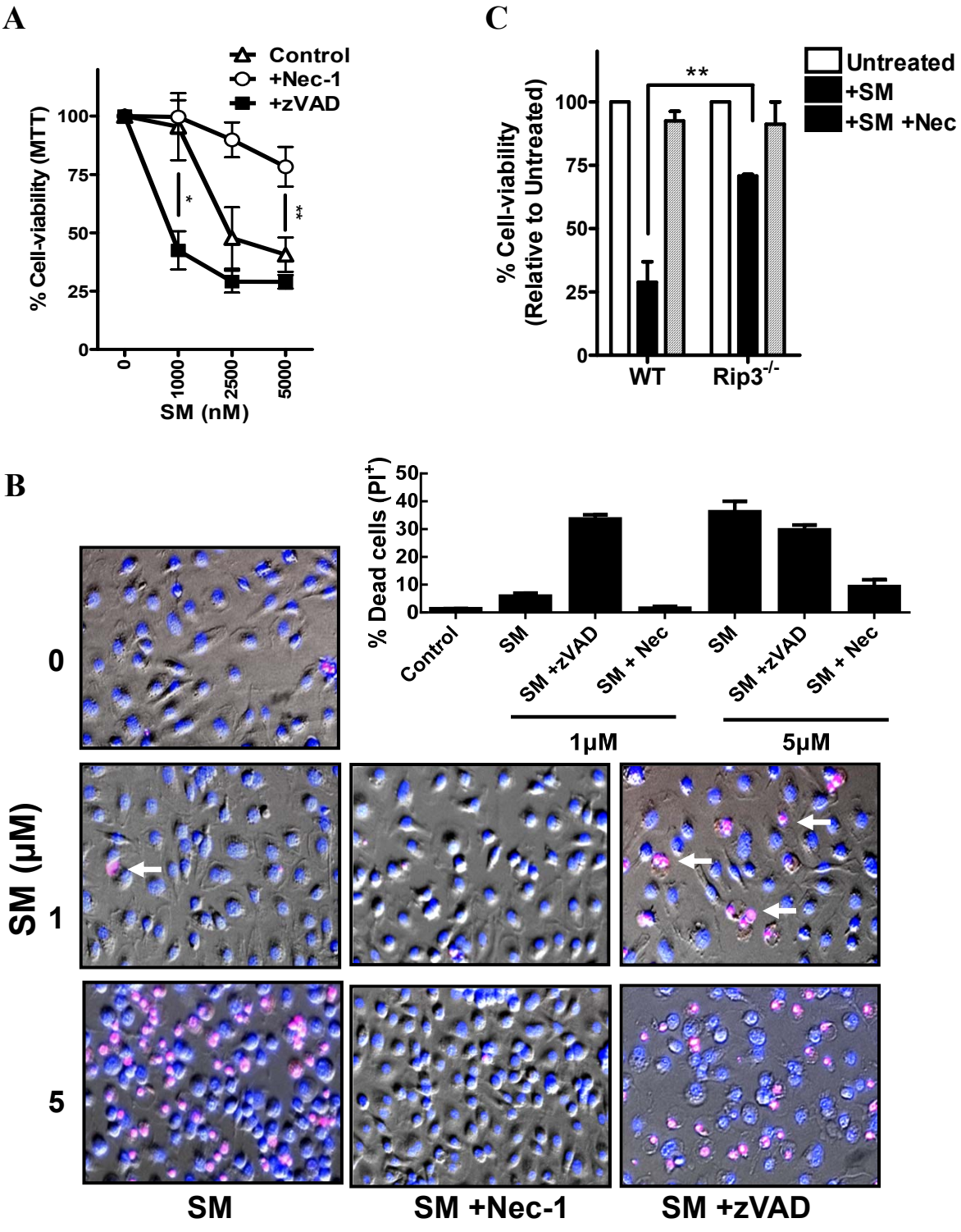
A
Control
+Nec-1
+zVAD
% Cell-viability (MTT)
100
75
50
25
0
0
1000
2500
5000
SM (nM)
*
**
C
Untreated
+SM
+SM +Nec
% Cell-viability
(Relative to Untreated)
**
WT
Rip3-/-
B
% Dead cells (PI+)
50
40
30
20
10
0
Control
SM
SM +zVAD
SM + Nec
1μM
5μM
SM (μM)
0
1
5
SM
SM +Nec-1
SM +zVAD

Figure 22: *cIAP1 and cIAP2 are functionally redundant and additive in limiting macrophage necroptosis, while XIAP limits SM-induced apoptosis.* (A) BMDM cells derived from WT, cIAP1$^{-/-}$ and cIAP2$^{-/-}$ mice were treated with 5μM SM and/or necrostatin as shown. 24 hours after treatment cells were examined for viability using the MTT assay. (B) BMDM cells derived from XIAP and WT mice were treated with various concentrations of SM and necrostatin as shown. 24 hours after treatment cells were examined for viability using MTT. *P<0.05 **P<0.01 ***P<0.001. Results show the average result of 3 experiments performed in duplicate.

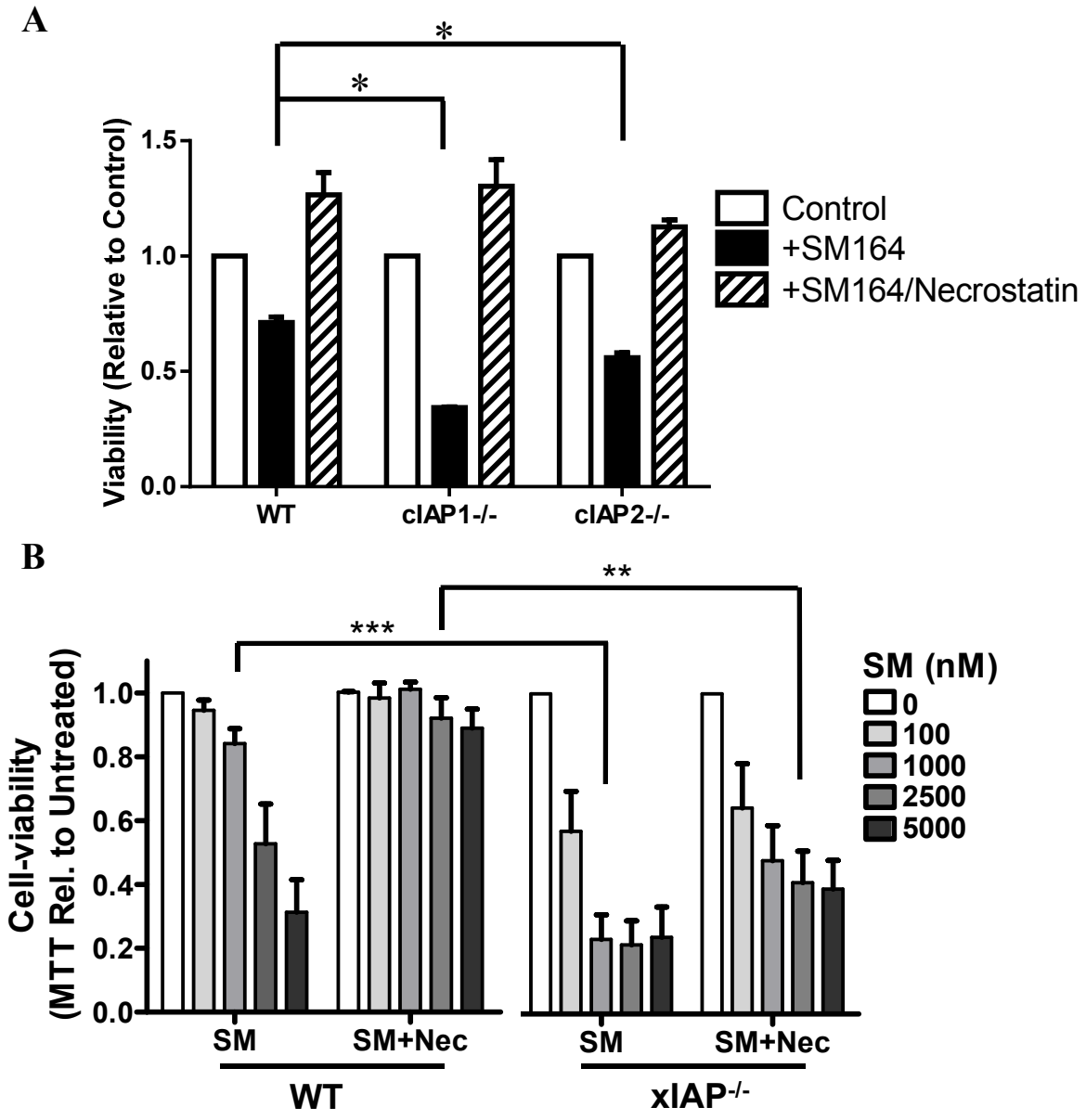
A
*
*
Viability (Relative to Control)
1.5
1.0
0.5
0.0
WT
cIAP1-/-
cIAP2-/-
Control
+SM164
+SM164/Necrostatin
B
**
***
Cell-viability
(MTT Rel. to Untreated)
1.0
0.8
0.6
0.4
0.2
0.0
SM (nM)
0
100
1000
2500
5000
SM
SM+Nec
SM
SM+Nec
WT
xIAP-/-

***4.2.E xIAP limits SM-induced apoptosis*:** While both cIAPs have been previously demonstrated to ubiquitinate Rip1 and thus limit the induction of necroptosis[188], the role of xIAP in the programmed necrosis has remained enigmatic. Thus, I next treated macrophages deficient in xIAP with SM. It was observed that xIAP-deficient macrophages showed a significant increase in sensitivity to SM treatment, and more importantly these cells could not be rescued by the addition of necrostatin (Fig. 22B). Unlike the cIAPs, xIAP is thought to be a bona fide inhibitor of caspases[284]. Taking this combination, our data supports a view that xIAP may act to limit SM-induced apoptosis and allow the alternative necroptotic pathway to be revealed.

***4.2.F Loss of cIAPs increases Rip1 activation*:** In order to more directly investigate how cIAPs specifically regulate necroptosis, the expression of Rip1 and Rip3 kinases over the timecourse of cIAP degradation were next investigated. Consistent with its reported activity[275], SM-164 induced the rapid degradation of cIAPs within 10 minutes following treatment (Fig. 23A). As macrophages lost their cIAP expression, a coincident increase in a secondary slightly slower-migrating form of Rip1 was observed (Fig. 23A). It has been previously reported that this slower migrating band is the phosphorylated form of Rip1 kinase[248]. I also confirmed this by dephosphorylating Rip1 with λ-phosphatase, causing it to resolve as a single band (Fig. 23B). These results indicate that the loss of cIAP expression causes Rip1 to become phosphorylated.

***4.2.G Loss of cIAPs reduces constitutive degradation of Rip1 and Rip3 kinases*:** In addition to increased expression of Rip1 kinase, it was also observed that a significant increase in the expression of Rip3 kinase (Fig. 23A). Densitometry measurements averaged over 3 repeated experiments show a greater then 15-fold increase in the expression of Rip3 kinase, and an approximately 4- to 5-fold increase in Rip1 expression (Fig. 23C). To investigate whether this increase in expression might be transcriptional, the transcript levels for Rip1 and Rip3 following

Figure 23*: Loss of cIAPs increases Rip1 and Rip3 expression and activation.* BMDMs were placed in a 24-well plate at 30 000 cells/well. Cells were then stimulated for various time with SM and/or Nec-1 as indicated. (A) Cell lysates were analyzed or expression of cIAP, Rip1, and Rip3 via western blot. (B) Cell lysates were also treated with λ phosphatase as shown to confirm that phosphorylated Rip1 can be resolved as a secondary band. (C) Three separate western blot experiments were performed (as described in A) and examined by densitometry using ImageJ software. The mean expression level of Rip1 and Rip3 normalized to actin and relative to untreated control is shown. *$P<0.05$. (D) BMDM cells were stimulated with SM for 1 or 4 h as indicated. mRNA levels for Rip1 and Rip3 were then quantified by qRT-PCR analysis. The average relative transcript level of Rip1 and Rip3 relative to untreated control and normalized to actin is shown from three separate experiments performed in duplicate (E) BMDM cells were treated with zVAD or lactacystin for 1h and examined for the level of Rip1 and Rip3 expression via western blot.

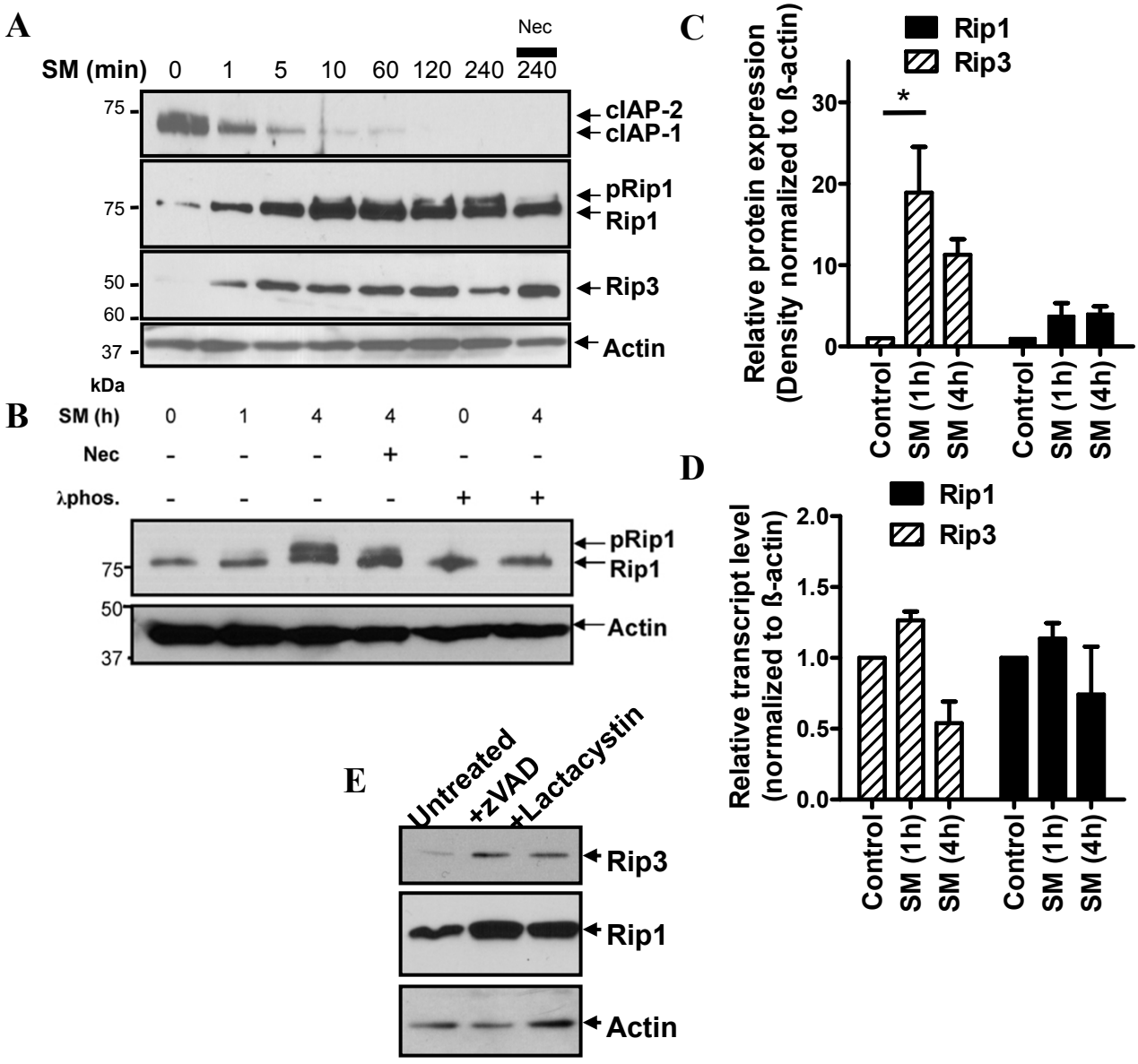
A
Nec
SM (min) 0 1 5 10 60 120 240 240
75
75
50
60
37
kDa
cIAP-2
cIAP-1
pRip1
Rip1
Rip3
Actin
B
SM (h) 0 1 4 4 0 4
Nec - - - + - -
λphos. - - - - + +
75
50
37
pRip1
Rip1
Actin
C
Rip1
Rip3
Relative protein expression
(Density normalized to ß-actin)
30
20
10
0
*
Control
SM (1h)
SM (4h)
Control
SM (1h)
SM (4h)
D
Rip1
Rip3
Relative transcript level
(normalized to ß-actin)
2.0
1.5
1.0
0.5
0.0
Control
SM (1h)
SM (4h)
Control
SM (1h)
SM (4h)
E
Untreated
+zVAD
+Lactacystin
Rip3
Rip1
Actin

treatment with SM were next examined. While results showed a small increase in mRNA levels at 1 hour following SM treatment, this was consistently much smaller than the increase observed in protein levels (Fig. 23C,D). To test whether constitutive degradation of Rip1 and Rip3 kinase might be occurring, macrophages were next treated with either the 20S proteasome inhibitor, lactacystin, or the caspase inhibitor, zVAD. Treatment with either inhibitor resulted in a small increase in both Rip1 and Rip3 protein levels (Fig. 23E). In total these data suggest that cIAPs may function to promote constitutive degradation of both Rip1 and Rip3 kinases.

***4.2.H Autocrine TNFR1 or 2 signaling is necessary for SM-induced necroptosis*:** Generally, studies have shown that necroptosis requires exogenous death receptor signaling[211], although it has been shown that autocrine production of TNF can fill this role in some cell types[256]. Given that I had identified the production of TNF in response to SM treatment (Fig. 20), I wished to investigate what role this might play in the ultimate induction of macrophage necroptosis. TNFR1/2-deficient ($TNFR^{-/-}$) macrophages showed almost complete resistance to TNFR-induced cell death (Fig. 24A). Upon examining Rip1 directly by western blot, it was observed that no SM-induced phosphorylation occurred in $TNFR^{-/-}$ macrophages (Fig. 24B). Interestingly, there also appeared to be no changes in the expression levels of Rip1 or Rip3 following SM treatment in TNFR-deficient macrophages, suggesting that the receptor may play a role in the degradation of Rip1 and Rip3.

I also wished to probe the role of TNFR signaling within WT cells by confirming association of Rip1 with the receptor following SM treatment. Confocal fluorescence microscopy also showed increased colocaliztion of both Rip1 and Rip3 with the TNFR following treatment with SM (Fig. 24C). In addition, I was also able to immunoprecipitate Rip1 along with the TNFR (Fig. 24D). Interestingly, only the phosphorylated form of Rip1 appeared to precipitate with TNFR,

Figure 24: *Autocrine TNFR1 signaling is necessary for SM-induced necroptosis.* (A) The viability of WT and TNF-R$^{-/-}$ cells after SM treatment was measured using MTT assay. (B) Bone marrow macrophages from WT and TNFR1/2$^{-/-}$ mice were exposed to SM and/or Nec for varying time intervals as indicated. Cell lysates were then examined for Rip1 and Rip3 expression via western blot. (C) BMDM cells were grown on cover slips in six-well plates and exposed to SM for 4 h. After staining with primary and secondary antibodies for TNF-R (blue), Rip1 (red) and Rip3 (green), cells were examined via fluorescent confocal microscopy. (D) WT macrophages were treated with SM and Nec for various time intervals as shown. Cells were then lysed using RIPA buffer and co-immunoprecipitation was then performed using Protein-G sepharose beads and an antibody targeting TNF-R1 (E) TNFR-deficient and WT BMDM cells were treated with zVAD, zVAD/SM, or zVAD/SM/Nec as shown. Viability was assessed after 24 hours by MTT assay. All graphs show the average result for at least 3 experiments performed in duplicate. ***P<0.001

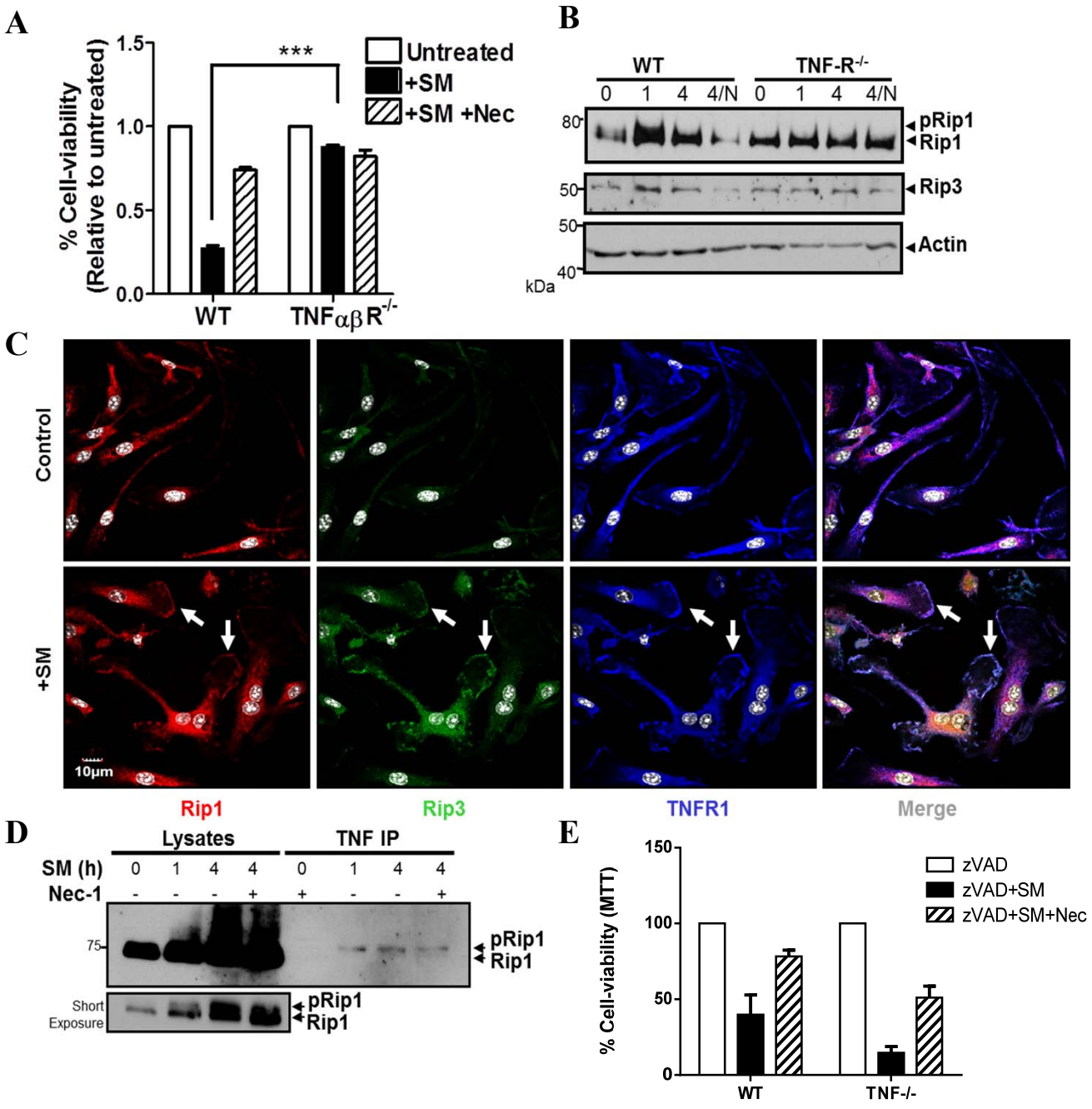
A
% Cell-viability (Relative to untreated)
1.5
1.0
0.5
0.0
***
Untreated
+SM
+SM +Nec
WT
TNFαβR-/-
B
WT
TNF-R-/-
0 1 4 4/N 0 1 4 4/N
80
pRip1
Rip1
50
Rip3
50
Actin
40
kDa
C
Control
+SM
10μm
Rip1
Rip3
TNFR1
Merge
D
Lysates
TNF IP
SM (h) 0 1 4 4 0 1 4 4
Nec-1 - - - + + - - +
75
pRip1
Rip1
Short Exposure
pRip1
Rip1
E
% Cell-viability (MTT)
150
100
50
0
zVAD
zVAD+SM
zVAD+SM+Nec
WT
TNF-/-

supporting a model wherein phosphorylation of Rip1 occurs at the receptor. Unfortunately, the size of Rip3 precluded visualization by western blot following immunoprecipitation using our system, as it migrates very closely to the immunoprecipitation antibody heavy chain.

Taken together, these results show that autocrine TNF signaling is necessary for SM-induced necroptosis. However, I was interested in whether additional pro-necroptotic stimuli could push TNF-receptor 1 and 2-deficient ($TNFR^{-/-}$) macrophages to undergo programmed necrosis. By combining zVAD with SM, a significant induction of necroptosis within $TNFR^{-/-}$ macrophages was induced. This data demonstrates that TNF receptor signaling is not strictly necessary for the induction of necroptosis if multiple necroptosis inhibitors are simultaneously targeted (Fig. 24E).

***4.2.I In vivo administration of SM results in macrophage cell death*:** Given the discovery that SM treatment of macrophages results in cell death *in vitro*, I next wanted to investigate what effect SM treatment would have *in vivo*. Intraperitoneal injection of SM results in a rapid loss of cIAP expression in both the peritoneum and the spleen (Fig. 25A). Staining of cells obtained by peritoneal lavage 6 hours after injection of SM164 or vehicle showed a significant increase in macrophage death, as measured by uptake of propidium iodide (Fig. 25B). Furthermore, daily injections of SM over 4 days resulted in a significant depletion of the macrophage pool (Fig. 25C). These data show that SM treatment can also drive increased death of macrophages *in vivo*.

4.2.J Loss of cIAP function in vivo decreases control of Listeria monocytogenes: To assess what effect the depletion of macrophages by SM treatment might have upon immune function, mice were next challenged intraperitoneally with the intracellular bacterial pathogen, *Listeria monocytogenes* (LM), concurrent with daily injections of SM. At day 3 of infection, significantly higher bacterial loads in both the spleen and peritoneum of mice treated with SM relative to vehicle treated mice were observed (Fig. 26A). Examining the cells within the peritoneum of

Figure 25: *In vivo administration of SM results in cIAP degradation and macrophage cell death.* C57BL/6J mice were injected intraperitoneally with 100 µg of SM164. After 6 h, control and treated mice were sacrificed and peritoneal lavage was performed. (A) An equal number of spleen and peritoneal cells were lysed and analyzed by western blot for expression of cIAP. (B) Peritoneal cells were stained for macrophage cell markers and cell death (propidium iodide). Histograms show gated populations of $F4/80^{+}CD11b^{+}$ macrophages or $CD3^{+}$ T cells as labeled. Results are representative of at least three mice analyzed per treatment group. The mean percentages of dead cells for three mice per group (±S.E.M.) are shown. (C) Mice were injected daily (IP) with 100 µg (85mg/kg) of SM164. At day 4, mice were killed and peritoneal lavage was performed. Cells were stained and analyzed by flow cytometry. Graphs show the average number of $F4/80^{+}$ and $CD3^{+}$ cells within these populations. Similar results were obtained in two experiments each with $n \geq 3$ mice per group. ***$P<0.001$

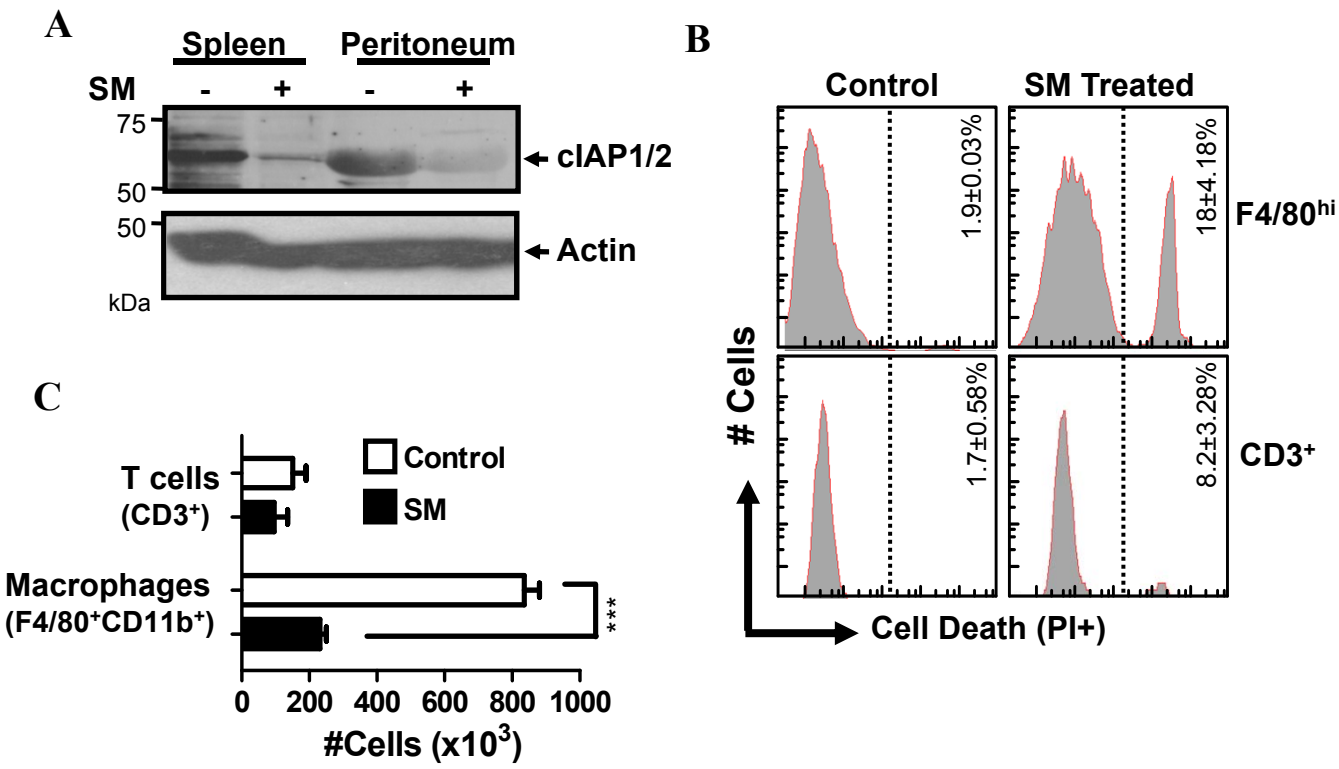
A
Spleen
Peritoneum
SM
-
+
-
+
75
50
50
kDa
cIAP1/2
Actin
B
Control
SM Treated
1.9±0.03%
18±4.18%
F4/80hi
1.7±0.58%
8.2±3.28%
CD3+
Cells
Cell Death (PI+)
C
Control
SM
T cells
(CD3+)
Macrophages
(F4/80+CD11b+)
***
0
200
400
600
800
1000
#Cells (x10^3)

Figure 26: *Decreased cIAP function in vivo decreases control of Listeria monocytogenes.* C57BL/6J mice were injected intraperitoneally with 10^4 LM bacteria. Mice were also injected intraperitoneally with 100 µg (~5mg/kg) of SM or vehicle control daily. At day 4 post infection, mice were killed and peritoneal lavage was performed. (A) Bacterial burden in the spleen and peritoneum of mice was assessed. (B) Peritoneal cells were also stained for F4/80 and CD3 expression as well as cell death (propidium iodide). (C) The percentage of cell death (PI^+) in the macrophage and T-cell populations from peritoneum as assessed by flow cytometry is shown. (D) Similarly as described, WT, $cIAP1^{-/-}$ and $cIAP2^{-/-}$ mice were challenged with 10^6 LM intravenously. Numbers of macrophages and T cells in the peritoneum (E), and their commitment to cell death (F, propidium iodide) were assessed at day 3 post-infection. The mean values of five mice per group are shown. *P<0.05; **P<0.01, ***P<0.001, n≥3 mice/group

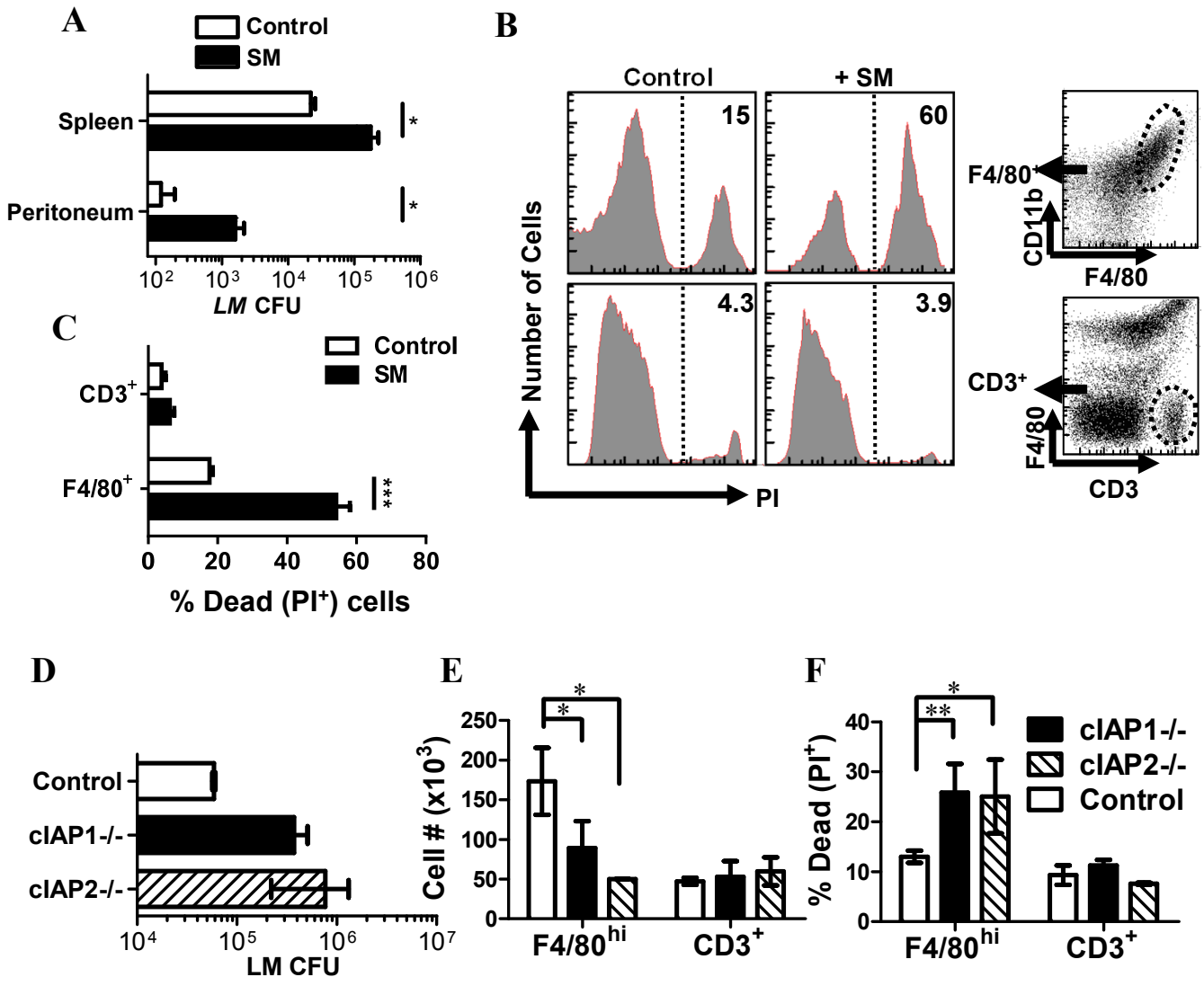
A
Control
SM
Spleen
Peritoneum
*
*
10^2 10^3 10^4 10^5 10^6
LM CFU
B
Control
+ SM
15
60
4.3
3.9
Number of Cells
PI
F4/80+
CD11b
F4/80
CD3+
F4/80
CD3
C
Control
SM
CD3+
F4/80+
***
0 20 40 60 80
% Dead (PI+) cells
D
Control
cIAP1-/-
cIAP2-/-
10^4 10^5 10^6 10^7
LM CFU
E
Cell # (x10^3)
250
200
150
100
50
0
*
*
F4/80hi
CD3+
F
% Dead (PI+)
40
30
20
10
0
*
**
cIAP1-/-
cIAP2-/-
Control
F4/80hi
CD3+

treated mice also showed a significant increase in cell death of macrophages ($F4/80^{+}CD11b^{+}$) in SM-treated mice relative to control mice (Fig. 26B,C).

Next, mice deficient in either cIAP1 or cIAP2 were challenged with LM. Consistent with our observations using SM, genetic deficiency for either cIAP1 or cIAP2 also resulted in a significantly higher burden of LM bacteria (Fig. 26D). These mice also showed significantly lower numbers of macrophages (Fig. 26E) and elevated cell death within the macrophage population (Fig. 26F). Overall this data showed that cIAP1 and cIAP2 expression act redundantly and additively to regulate cell death in macrophages, with decreased activity of either cIAP leading to a deficient immune response to intracellular bacterial infection.

4.3 *SALMONELLA* INDUCES INTERFERON DEPENDENT NECROPTOSIS

***4.3.A cIAP1$^{-/-}$ or cIAP2$^{-/-}$ mice are more susceptible to Salmonella typhimurium*:** Having identified that a defect in cIAP function leads to overactive necroptosis and less control of LM infection, I next wanted to test whether a similar effect occurs in infection with *Salmonella typhimurium* (ST). Thus, cIAP1$^{-/-}$ and WT mice were injected with 10^3 CFU of ST intravenously. At day 3 after infection, mice deficient in cIAP1 expression showed significantly more splenic CFUs compared to WT mice (Fig. 27). Based on this and our previous work demonstrating that cIAPs regulate macrophage necroptosis, it was inferred that death of macrophages by necroptosis might be driving a deficient immune response to ST infection similar to LM.

***4.3.B ST infection of macrophages leads to delayed necroptosis*:** In order to further probe whether ST infection indeed leads to necroptosis, *in vitro* infections of macrophages were next performed. Unstimulated bone marrow-derived macrophages (BMDMs) were plated in round bottom plates and allowed 24 hours for cells to adhere. Infections were then performed as

Figure 27: *cIAP1 Deficient mice are more susceptible to infection with Salmonella Typhimurium.* WT and cIAP1$^{-/-}$ mice (C57BL/6J background) were challenged with 10^3 ST bacteria intraperitoneally. At 3 days post-infection mice were sacrificed and the bacterial CFU in the peritoneum was assessed as described in the methods section. n=3 mice/group.

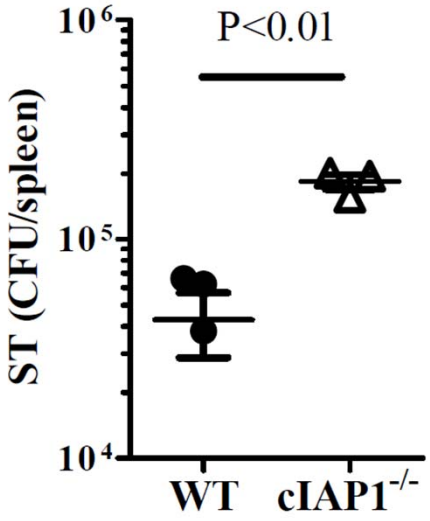
P<0.01
10^6
10^5
10^4
ST (CFU/spleen)
WT
cIAP1$^{-/-}$

described in the materials and methods section at an MOI of 10. In this model, it was observed that delayed death of infected macrophages occurred after 24-48 hours. Macrophages have previously been shown to undergo an inflammatory caspase-1 dependent form of cell death known as pyroptosis. At 48 hours after infection, a significant rescue of ST infected cells with a caspase-1 specific inhibitor was noted (Fig. 28A). However, the addition of necrostatin resulted in a significantly better rescue of macrophage viability (Fig. 28A). The involvement of necroptotic mechanisms in ST-induced macrophage cell death was also confirmed through an siRNA knockdown of Rip3 (Fig. 28B), which resulted in significantly less ST-induced macrophage cell death (Fig. 28C). This evidence indicates that infection with ST induces necroptotic cell death within macrophages.

***4.3.C ST induces necroptosis in macrophages in vivo*:** I next wanted to confirm whether death of macrophages following ST infection *in vivo* was occurring by necroptosis. Thus, WT and Rip3-deficient were infected mice intravenously with 10^3 CFU of ST and examined the numbers of macrophages in the spleen at day 3 of infection. Consistent with an induction of necroptosis by ST infection, significantly less death of Rip3-deficient than WT macrophages was observed, as determined by uptake of propidium iodide (Fig. 29A). Importantly, there was no significant change in the survival of Rip3-deficient mice (Fig. 29B), signifying a complex phenotype of ST pathogenesis occurring within these mice. Overall, this data supports the model that ST induces macrophage necroptosis *in vivo*, but resistance to this effect alone is inadequate to protect from infection.

***4.3.D Type-I interferon signaling is required for ST-induced necroptosis*:** At this time, several members of the lab were studying the role of type-I interferon in ST pathogenesis. In their work, they had observed that interferon receptor alpha-deficient ($IFNAR^{-/-}$) mice showed significantly

Figure 28: *Infection of BMDM cells with ST induces delayed necroptotic cell death.* BMDM cells were plated in round bottom 96-well plates at 50 000 cells/well and infected with ST at 10 MOI. After 30 minutes of infection, cells were washed with high concentration of gentamicin (50 micrograms/ml) to remove extracellular bacteria. Infected cultures were also treated with various inhibitors (at 10μg/mL) as shown. (A) 48 hours after infection BMDM viability was assessed using neutral red assay (for lysosomal activity). (B) WT BMDM cells were transfected with control or Rip3 target siRNA as shown. After 24 hours, knockdown of Rip3 was assessed by western blot. (C) Following siRNA knockdown cells were challenged with ST bacteria as described above, and assessed for viability after an additional 48 hours of infection. All experiments are representative of at least 3 experiments performed in duplicate. **P<0.01

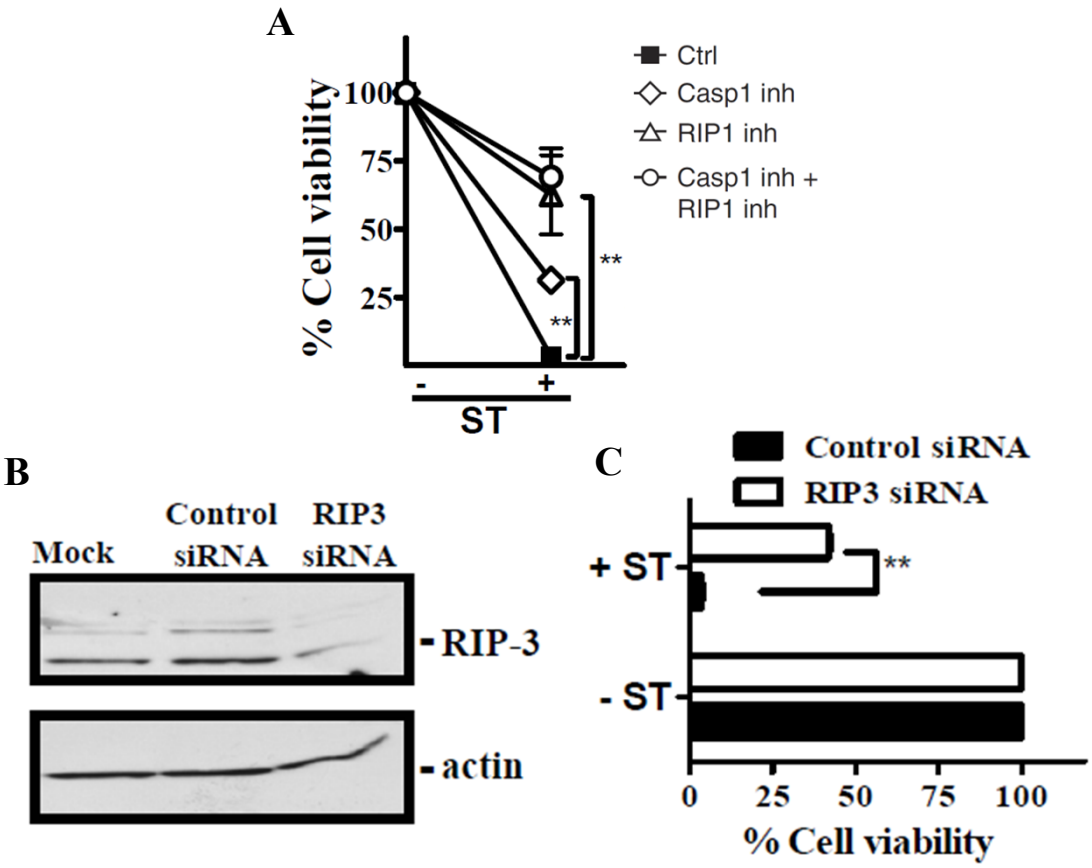
A
% Cell viability
100
75
50
25
- +
ST
Ctrl
Casp1 inh
RIP1 inh
Casp1 inh +
RIP1 inh
**
**
B
Mock
Control
siRNA
RIP3
siRNA
RIP-3
actin
C
Control siRNA
RIP3 siRNA
+ ST
- ST
**
0
25
50
75
100
% Cell viability

Figure 29: *Rip3-deficient mice show less macrophage cell death during ST infection in vivo.* WT and Rip3$^{-/-}$ mice (C57BL background) were challenged with 10^3 ST intraperitoneally. (A) At day 3 post-infection mice were sacrificed and the number of macrophages in the spleen was assessed. The level of cell death within the macrophage population was also assessed by propidium iodide staining (n=3 mice per group) (B) Survival or WT and Rip3$^{-/-}$ mice during ST-infection was also examined. (n=4 mice per group)

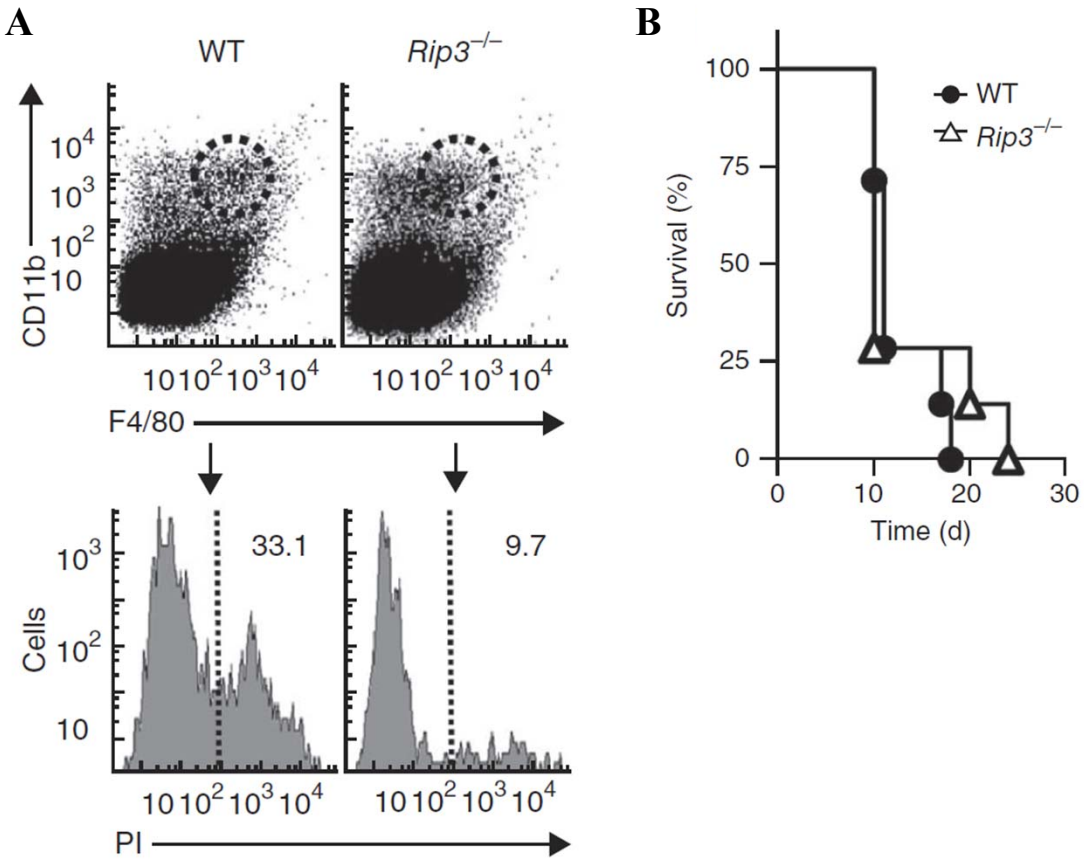
A
WT
Rip3−/−
CD11b
F4/80
Cells
PI
33.1
9.7
B
Survival (%)
Time (d)
WT
Rip3−/−

extended survival following ST infection (see [285]). In addition, mice also showed higher numbers of macrophage cells during infection with ST, suggesting the possibility that type-I interferon could be participating in the death of macrophages during ST pathogenesis. To test this hypothesis, WT and IFNAR macrophages were infected with ST *in vitro*. It was observed that IFNAR-deficient macrophages showed much more resistance to cell death induced by infection with ST (Fig. 30A). To confirm that type-I interferon is indeed inducing increased necroptotic signaling, the induction of Rip1 and Rip3 phosphorylation was also examined. In ST infected $IFNAR^{-/-}$ macrophages there was less of the slower migrating phosphorylated forms of Rip1 and Rip3 (Fig. 30B). I also confirmed that treatment with lambda phosphatase caused these phosphorylated forms of Rip1 and Rip3 to largely disappear (Fig. 30B). These results confirm that IFNAR signaling is a key signaling factor for ST-induced necroptosis within macrophages.

***4.3.E Treatment with IFN-β and zVAD induces necroptosis*:** Follow-up work performed by Dr. Nirmal Robinson in the lab showed that necroptotic signaling derived from type-I interferon receptor is driven specifically by interferon beta (IFN-β). He also showed that treatment of cells with IFN-β alone leads to a transient phosphorylation of Rip1 but was unable to drive significant cell death (see [285]). Thus, I next wanted to test whether blocking the anti-necroptotic activity of caspases in combination with IFN-β would lead to full blown necroptosis. Indeed, treatment of J774 macrophages with IFN-β and zVAD resulted in a potent induction of cell death which could be inhibited by the addition of necrostatin (Fig. 31). This data supports the model that interferon-β signaling directly induces activation of the necrosome but requires caspase inhibition for progression to cell death.

***4.3.F Type-I interferon is a key feedback in LPS induced necroptosis*:** A combination of zVAD and LPS has been recently shown to be a potent inducer of necroptosis[226]. This means of

Figure 30: *IFNAR-deficient BMDMs show less phosphorylation of Rip1 and Rip3 kinases and less necroptosis upon infection with ST.* (A) WT and IFNAR$^{-/-}$ mice were challenged with ST *in vitro* as described in the methods section. At 24 and 48 hours after infection the viability of cells was examined using the neutral red assay. Results show the average % viability for at least 3 experiments performed in duplicate. (B) After 24 hours of infection as described, WT and IFNAR macrophages were examined for Rip1 and Rip3 phosphorylation as shown. Some lysates were also treated with λ phosphatase to confirm phosphorylation bands for Rip1 and Rip3.

Experiments presented in this figure were performed in collaboration with N. Robinson.

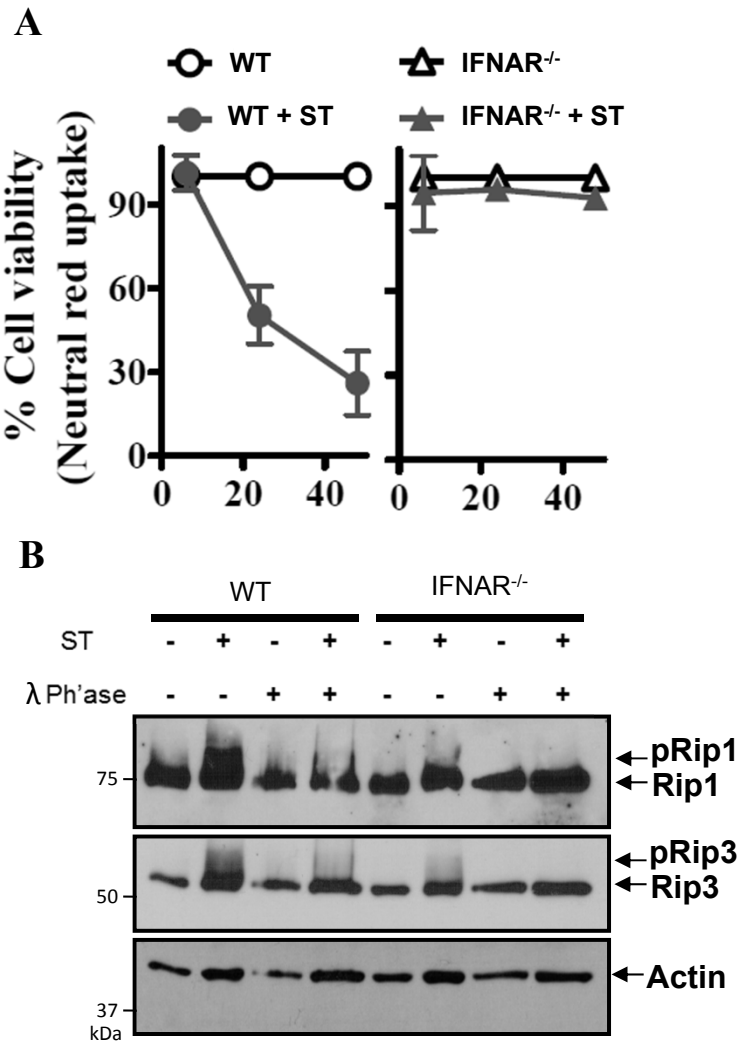
A
WT
IFNAR-/-
WT + ST
IFNAR-/- + ST
% Cell viability
(Neutral red uptake)
90
60
30
0
0
20
40
0
20
40
B
WT
IFNAR-/-
ST
- + - + - + - +
λ Ph'ase
- - + + - - + +
75
50
37
kDa
pRip1
Rip1
pRip3
Rip3
Actin

Figure 31: *Treatment of J774 macrophages with IFNß drives necroptosis.* J774 macrophages were plated at 50 000 cells/well in a 96-well plate. Cells were then treated with varying concentrations of IFNß, zVAD, and necrostatin as shown. Viability was assessed after 24 hours of treatment via the MTT assay. Results show the average viability of at least 3 experiments performed in duplicate.

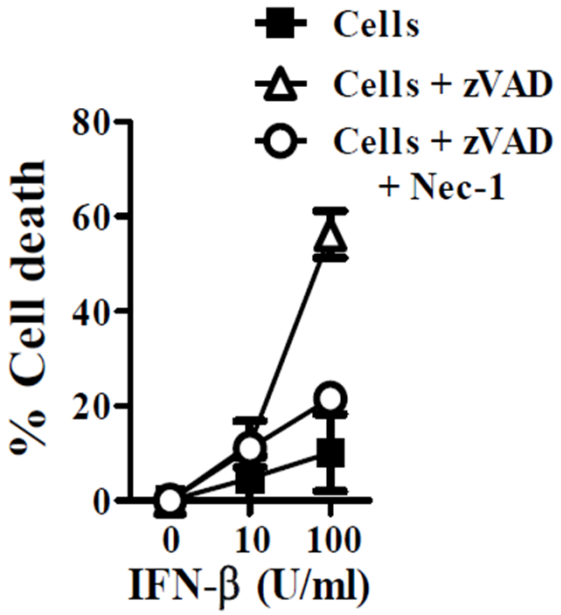
Cells
Cells + zVAD
Cells + zVAD
+ Nec-1
% Cell death
80
60
40
20
0
0
10
100
IFN-β (U/ml)

inducing necroptosis by stimulating PAMP receptors recapitulates some elements of ST infection, and is known to induce release of type-I interferon[286]. Thus, I was interested to test whether induction of necroptosis by this method is also dependent upon IFNAR signaling. Whereas WT macrophages showed a significant loss of viability 24 hours after treatment with zVAD and LPS, $IFNAR^{-/-}$ macrophages were highly resistant to this effect (Fig. 32). This result supports the highly novel conclusion that type-I interferon signaling is a key feedback for the induction of macrophage cell death by LPS/zVAD-induced necroptosis.

***4.3.G Type-I interferon induced death drives systemic shock in vivo*:** Next, I wished to confirm the role of interferon in zVAD/LPS induced necroptosis within an *in vivo* setting. Following injection with a combination of zVAD and LPS, WT mice displayed a hunched posture and were moribund by 18 hours after injection. In stark contrast, IFNAR mice appeared relatively normal. At this time, all mice were sacrificed and a peritoneal lavage was performed. Both IFNAR and WT mice showed a drop on the total number of peritoneal macrophage cells (Fig. 33A,B), although IFNAR mice had significantly less cell death occurring within the macrophage pool (Fig. 33C). These results support the view that interferon-induced macrophage necroptosis may exacerbate the effects of LPS induced shock within mice.

4.4 CATHEPSINS REGULATE NECROPTOSIS

***4.4.A zVAD alone can induce macrophage necroptosis*:** Next, a further investigation of how Rip1 and Rip3 kinases are regulated to within macrophages was initiated. To accomplish this, I wished to examine how the canonical inducer of necroptosis, zVAD, drives changes in Rip1 and Rip3 expression, and results in necroptosis of macrophages. High doses of zVAD have been previously documented to induce cell death within macrophage cell lines[287]. In our model, we

Figure 32: *Autocrine production of type-I interferon is a key mechanism in the induction of necroptosis through the zVAD/LPS pathway.* WT and IFNAR$^{-/-}$ BMDM cells were plated at 50 000 cells/well in 96-well plates. Cells were then treated with LPS (100 ng/mL) and various doses of zVAD as shown. After 24 hours cell viability was assessed using the MTT assay. Results show the mean of at least 3 experiments performed in duplicate. ***P<0.001

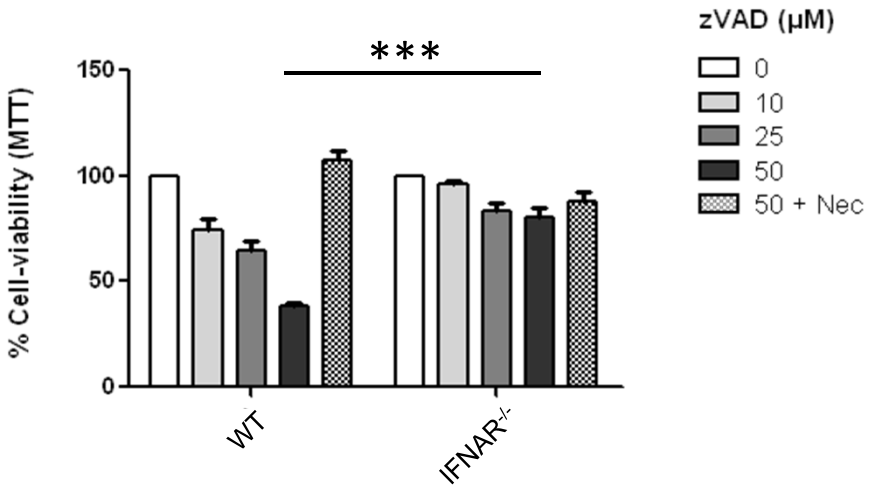
zVAD (μM)
0
10
25
50
50 + Nec
***
% Cell-viability (MTT)
150
100
50
0
WT
IFNAR-/-

Figure 33: *Macrophages in INAR-deficient mice undergo less death following LPS/zVAD injection in vivo.* WT and IFNAR$^{-/-}$ mice were injected with 10mg/kg of LPS and 50 μg of zVAD suspended in PBS. After 18 hours, mice were sacrificed and a peritoneal lavage was performed. (A) FACS staining for CD11b and F4/80 expression was utilized to assess the number of macrophages in the peritoneal lavage. (B) The average % of macrophages is shown. (C) The viability of macrophages in the peritoneal lavage was also assessed using propidium iodide staining. n=3 mice/group, *P<0.05

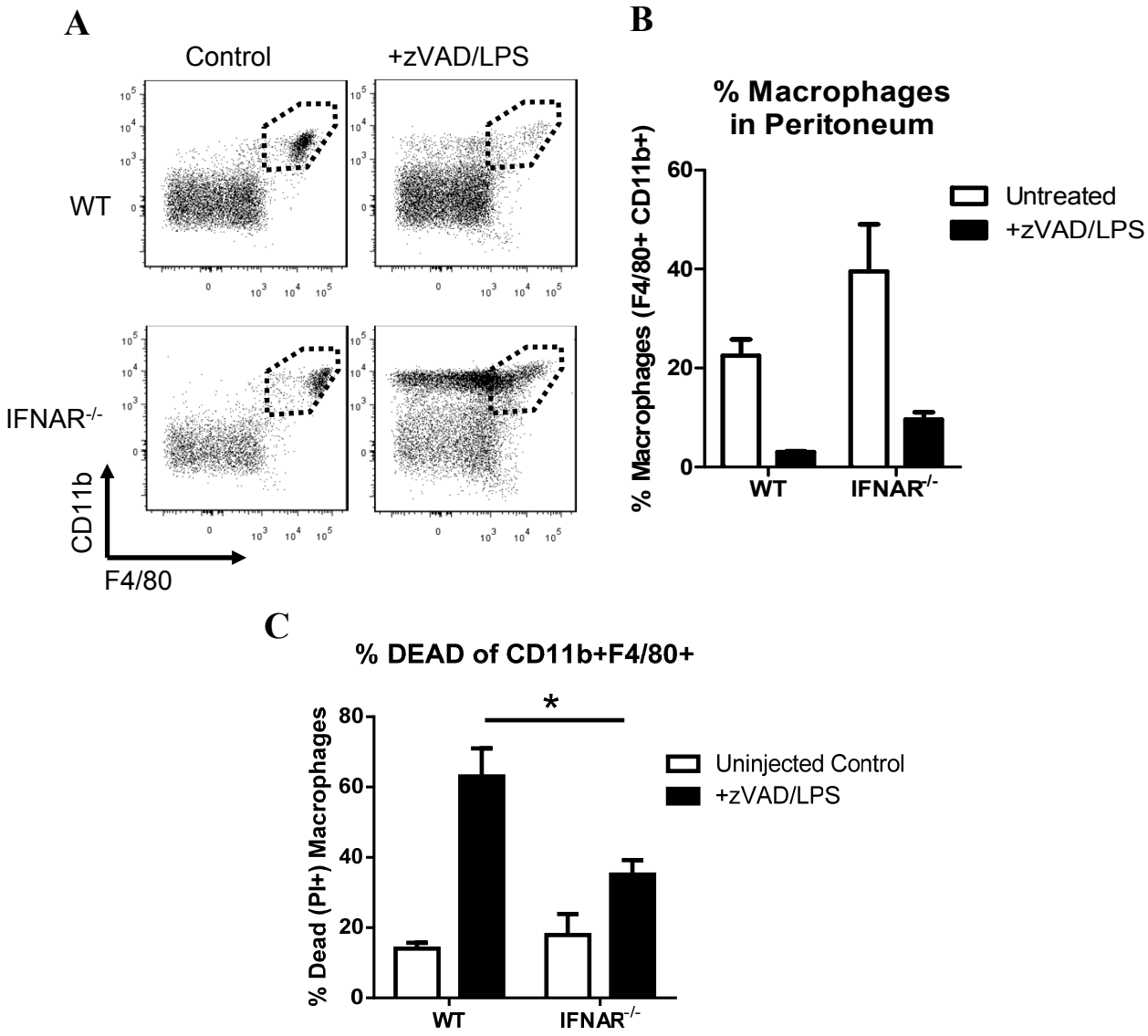
A
Control
+zVAD/LPS
WT
IFNAR-/-
CD11b
F4/80
B
% Macrophages in Peritoneum
% Macrophages (F4/80+ CD11b+)
60
40
20
0
WT
IFNAR-/-
Untreated
+zVAD/LPS
C
% DEAD of CD11b+F4/80+
% Dead (PI+) Macrophages
80
60
40
20
0
*
WT
IFNAR-/-
Uninjected Control
+zVAD/LPS

observed that treatment of BMDMs with 50-200μM of zVAD lead to a significant loss of viability (Fig. 34A). It was confirmed that zVAD was in fact inducing necroptosis by combining zVAD with necrostatin, wherein macrophages were completely rescued from cell death (Fig. 34B). Similar to what I reported for SM, zVAD drove a dose-dependent increase in Rip1 phosphorylation (Fig. 34C). Furthermore, macrophages deficient in Rip3 kinase were highly resistant to treatment with zVAD-FMK (Fig. 34D,E). These results indicate that treatment of macrophages with high doses of zVAD is sufficient to induce necroptosis.

***4.4.B LPS stimulation drives Rip1 kinase activation independently of TNFR signaling*:**

Much work in recent years has underlined the connection between immunostimulatory signaling and the necroptosis pathway (see section 1.2.B). Thus, I next wished to investigate what impact LPS stimulation would have upon zVAD-induced necroptosis. Stimulation with a low level of LPS (100ng/mL) led to a significant increase in sensitivity of macrophages to zVAD treatment (Fig. 35A). Whereas normally at least 50-100μM of zVAD was necessary for necroptosis induction, treatment with LPS sensitized macrophages to necroptotic cell death at as low as 25-50μM of zVAD (Fig. 35A). Interestingly, LPS treatment alone was able to induce phosphorylation of Rip1 kinase, but this did not result in phosphorylation of Rip3 kinase (Fig. 35B). Only when LPS signalling was combined with zVAD treatment did Rip3 phosphorylation occur (Fig. 35B). These results indicate that zVAD acts to somehow de-inhibit the phosphorylation of Rip3 downstream of Rip1 activation.

It has recently been reported that LPS specifically induces necroptotic signaling through TLR4 via the TRIF signaling axis[226]. To test this in our model, targeted siRNA knock down of TLR4 or TRIF expression was performed in BMDMs. Macrophages showed significantly lower sensitivity to zVAD/LPS-induced necroptosis following siRNA knockdown (Fig. 35C). I was

Figure 34: *zVAD alone can induce macrophage necroptosis.* (A) BMDM cells were treated with various concentrations of zVAD (as shown) for 24 hours and viability was assessed using the MTT assay. (B) Macrophages were treated with 100 μM of zVAD with or without the addition of necrostatin for 24 hours and stained with Hoechst, dead cells were identified using propidium iodide staining. The % of dead cells was obtained using automated counting of Propidium Iodide^{+} cells versus Hoechst^{+} cells (*top bar graph*). An MTT assay was also performed in parallel to confirm inverse correlation of cell death and viability results. (*bottom bar graph*) (C) Macrophages were treated with various concentrations of zVAD for 1 hour and examined via western blot for Rip1 protein expression. (D) Bone marrow macrophages were derived from WT and Rip3$^{-/-}$ mice. Cells were treated with 100μM zVAD for 24 hours and cell death was assessed via MTT assay. (E) WT and Rip3 BMDMs were examined for viability as described for (B). All experiments were performed a minimum of 3 times in duplicate. ***P<0.0001 **P<0.005

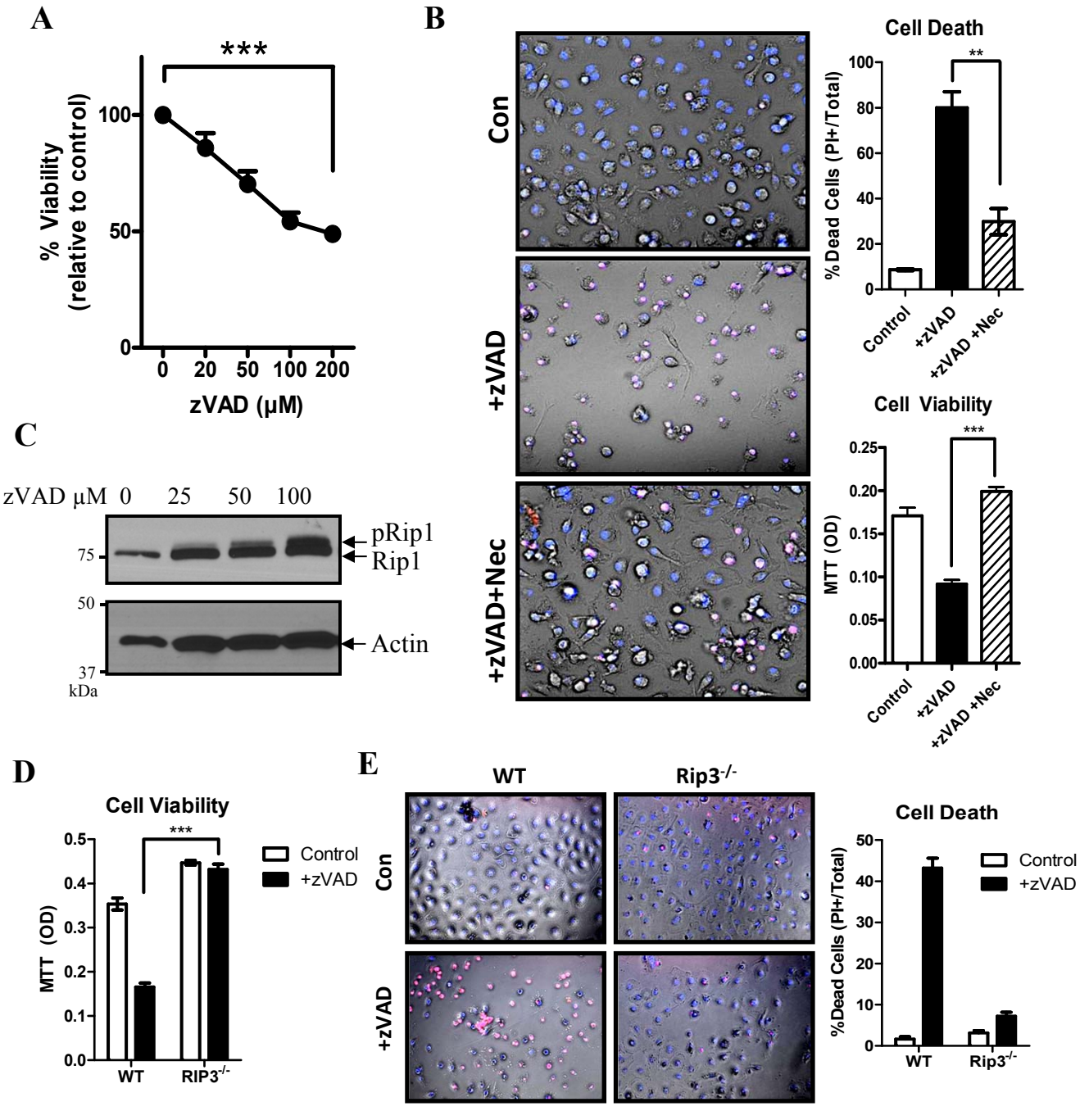
A
***
% Viability (relative to control)
100
50
0
0 20 50 100 200
zVAD (μM)
B
Con
+zVAD
+zVAD+Nec
Cell Death
**
% Dead Cells (PI+/Total)
100
80
60
40
20
0
Control
+zVAD
+zVAD +Nec
Cell Viability
***
MTT (OD)
0.25
0.20
0.15
0.10
0.05
0.00
Control
+zVAD
+zVAD +Nec
C
zVAD μM 0 25 50 100
75
50
37
kDa
pRip1
Rip1
Actin
D
Cell Viability
***
MTT (OD)
0.5
0.4
0.3
0.2
0.1
0.0
WT
RIP3-/-
Control
+zVAD
E
WT
Rip3-/-
Con
+zVAD
Cell Death
%Dead Cells (PI+/Total)
50
40
30
20
10
0
WT
Rip3-/-
Control
+zVAD

Figure 35: *LPS stimulation drives necroptosis independently of TNFR signaling* (A) Macrophages were treated with 100 ng/mL of LPS in combination with various concentrations of zVAD as shown, with or without the addition of necrostatin. Viability was assessed after 24 hours by MTT assay. (B) Macrophages were treated with LPS and zVAD or zVAD/necrostatin for one hour, after which cells were lysed and examined for Rip1 and Rip3 expression via western blot. (C) J774 macrophages were transfected with TRIF, TLR4 or untargeted control siRNA for 24 hours and lysates were examined for TRIF knockdown (*right*). Cells were then treated with various concentrations of zVAD and LPS and incubated for an additional 24 hours, and viability measured using MTT assay. (D) Macrophages were derived from WT or TNFR1/2$^{-/-}$ mice and treated with LPS and various concentrations of zVAD as shown. After 24 hours viability was examined via the MTT assay. All graphs show cell viability relative to controls without zVAD. All experiments were performed a minimum of 3 times in duplicate. ***$P<0.0001$ **$P<0.005$

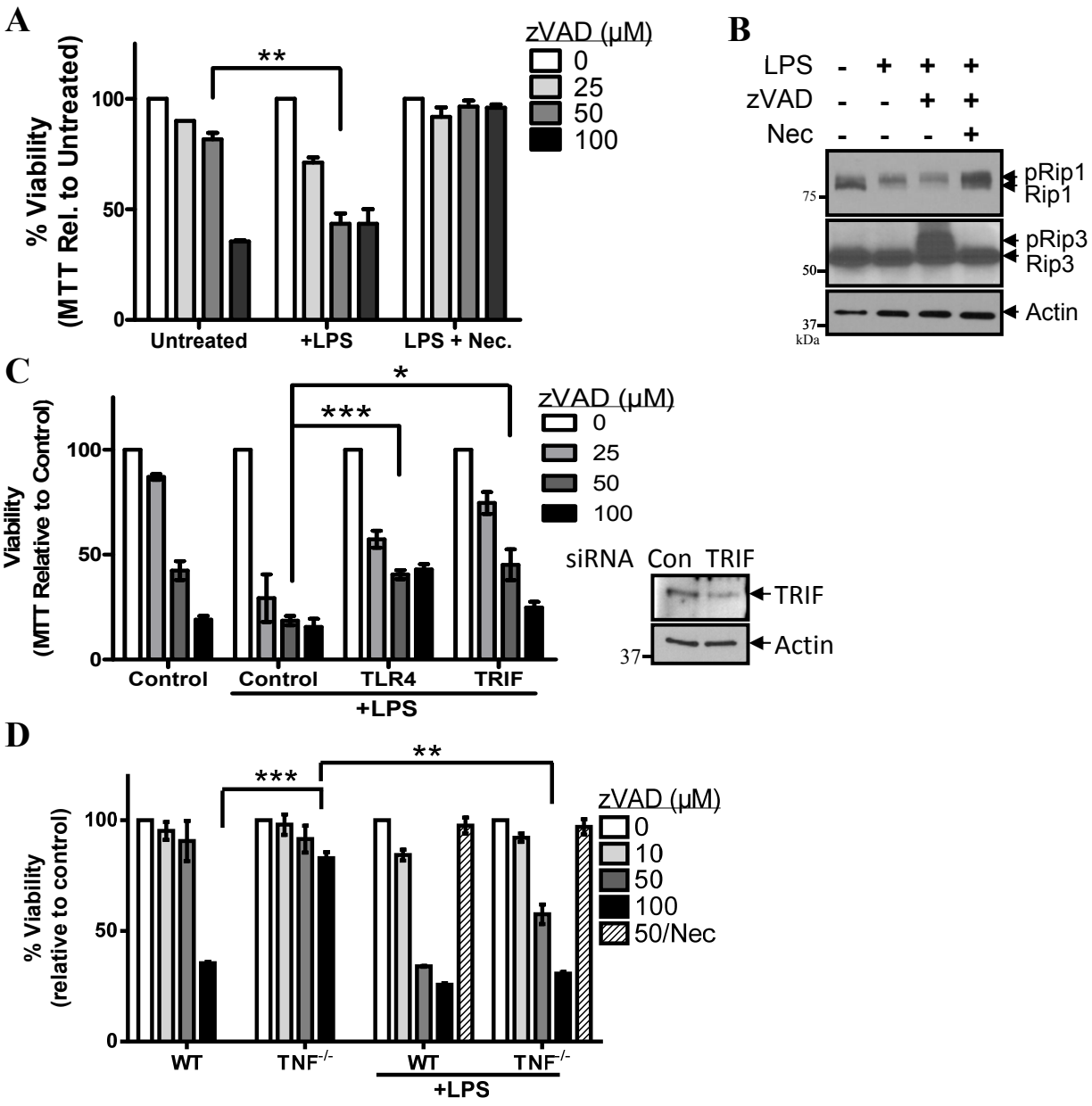
A
% Viability
(MTT Rel. to Untreated)
100
50
0
**
zVAD (μM)
0
25
50
100
Untreated
+LPS
LPS + Nec.
B
LPS - + + +
zVAD - - + +
Nec - - - +
75
50
37
kDa
pRip1
Rip1
pRip3
Rip3
Actin
C
Viability
(MTT Relative to Control)
100
50
0
*
***
zVAD (μM)
0
25
50
100
Control
Control
TLR4
TRIF
+LPS
siRNA Con TRIF
37
TRIF
Actin
D
% Viability
(relative to control)
100
50
0
***
**
zVAD (μM)
0
10
50
100
50/Nec
WT
TNF-/-
WT
TNF-/-
+LPS

next interested to test whether this TLR4/TRIF-dependent induction of the necroptotic signaling cascade occurred independently of TNFR signaling. While $TNFR^{-/-}$ BMDMs were highly resistant to zVAD-induced necroptosis, these cells were highly susceptible to necroptosis as induced by zVAD/LPS. Taken together, this data clearly demonstrates that LPS can directly activate the phosphorylation of Rip1 kinase through the TRIF pathway, while zVAD allows the activation Rip3 downstream of Rip1.

***4.4.C Cysteine cathepsins cleave Rip1 kinase*:** To more directly examine the regulation of Rip1 and Rip3 kinase following treatment with zVAD/LPS, western blotting experiments were next performed. Cells were treated with various combinations of inhibitors and LPS for 1 hour and the expression of Rip1 and Rip3 was examined. Western blots using the highly sensitive West Femto enhanced chemiluminescence reagent revealed several lower molecular weight bands in Rip1 and Rip3 blots. I hypothesized that these bands were likely cleavage products of Rip1 kinase. Supporting this view, there was a consistent loss of these cleavage bands following treatment with zVAD (Fig. 36A Lane 3). It should be noted that the anti-Rip1 antibody employed targets the C-terminal portion of the protein (385-650), and thus these cleavage products would likely be C-terminal fragments of Rip1 kinase protein. In the case of Rip3, several lower molecular weight bands were also observed, however only one band (~20 kDa) was affected by the application of zVAD.

Next, macrophages were treated with a specific inhibitor for caspase-8 (z-IETD-FMK, 100 μM) for 1 hour. There appeared to be mostly no change in the cleavage of Rip1 kinase in macrophages, although one faint band at approximately 42 kD was absent with caspase-8 inhibition (Fig. 36A Lane 4). In addition to its ability to potently inhibit caspases, zVAD has also been previously demonstrated to also inhibit cysteine family cathepsins, such as cathepsins B and

Figure 36: *A non-caspase-8 cysteine protease cleaves Rip1 Kinase.* BMDM cells were treated with various combinations of LPS, zVAD, caspase-8 inhibitor (C8I), and/or cathepsin inhibitor (E64D) as shown. After 1 hour of treatment, cells were lysed and examined for expression of Rip1 and Rip3 via western blot. Short (1 min.) and long (15 min.) exposures were utilized in order to identify Rip1 expression by western blots. Actin expression was used as a loading control. Results are representative of at least 3 repeated experiments.

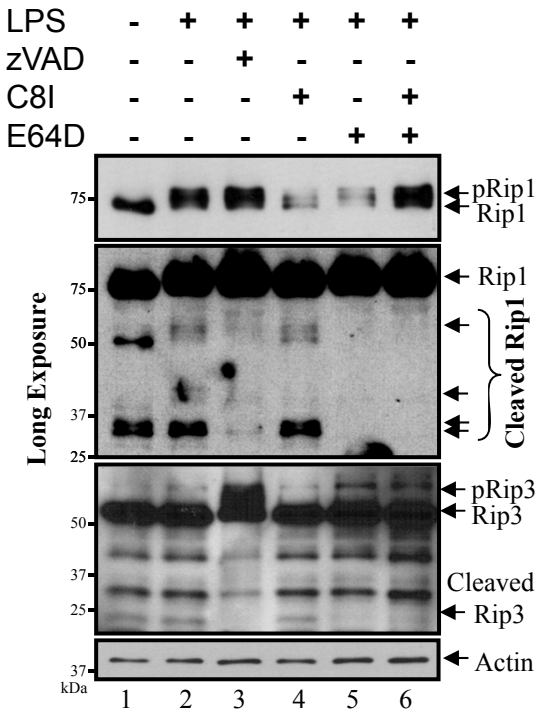
LPS - + + + + +
zVAD - - + - - -
C8I - - - + - +
E64D - - - - + +
75
pRip1
Rip1
Long Exposure
75
50
37
25
Rip1
Cleaved Rip1
50
37
25
pRip3
Rip3
Cleaved
Rip3
37
kDa
Actin
1 2 3 4 5 6

S, at the concentration ranges which were necessary to induce necroptosis (~50-100 μM)[288]. Based on this, I hypothesized that cathepsins may also cleave Rip1 and Rip3. Application of a cell-permeable cysteine cathepsin/calpain inhibitor, E64-D, completely abrogated the cleavage bands of Rip1 kinase, similar to zVAD treatment (Fig. 36A Lane 5). Also similar to zVAD, possible cleavage of Rip3 kinase was only effected for the ~20kDa band. Finally, a caspase-8 inhibitor was combined with the cathepsin inhibitor, where I observed elevated Rip1 phosphorylation and expression along with a decrease in cleavage bands (Fig. 36A Lane 6). Thus, these data imply that the inhibition of cathepsins by zVAD may be a considerable factor in the induction of necroptosis.

***4.4.D Cathepsin S and B both cleave Rip1 kinase*:** To further confirm cathepsin mediated cleavage of Rip1, an siRNA knockdown targeting two key members of the cysteine cathepsin family was next performed[289]. Knockdown of either cathepsin S or cathepsin B resulted in less cleavage of Rip1 kinase (Fig. 37A), as well as a small but significant increase in the sensitivity of macrophages to zVAD-induced cell death (Fig. 37B). Importantly, siRNA knockdown of an alternative cysteine protease, calpain-1, actually resulted in less necroptosis of macrophages (Fig. 37C). Based on this, it was hypothesized that cysteine cathepsins may have a redundant role in regulating Rip1 activity. Consistent with this, there was no significant differences in the induction of necroptosis in macrophages specifically deficient in either cathepsin S or cathepsin B (Fig. 38A,B). We also attempted combined siRNA knockdown of multiple cathepsin family members. Unfortunately, I was unable to achieve efficient simultaneous knockdown of both cathepsins, potentially due to deleterious effects on cell viability. Thus, these data suggest that cysteine family cathepsins may act redundantly to cleave Rip1 kinase and limit necroptosis within macrophages.

Figure 37: *Cathepsin S and B can cleave Rip1 kinase.* (A) BMDM cells were transfected using the Lonza system (as described in the methods section) with untargeted, cathepsin S, or cathepsin B targeting siRNA via electroporation for 24 hours. Cells were then treated with LPS for 2 hours and examined via western blot for Rip1, cathepsin S (CatS), and cathepsin B (CatB) expression. Actin was used as a loading control. (B) Macrophages transfected for 24 hours with untargeted control, cathepsin S, or cathepsin B targeted siRNA were treated with LPS and varying concentration of zVAD as shown. After an additional 24 hours, cells were tested for viability using MTT assay. Similar experiments were repeated at least 3 times. (C) To confirm the role of cathepsins specifically, BMDM cells were also transfected with control or calpain siRNA and examined for sensitivity to zVAD/LPS induced necroptosis as described in (B) **$P<0.01$ All graphs show the average cell viability relative to untreated control from at least 3 experiments performed in duplicate.

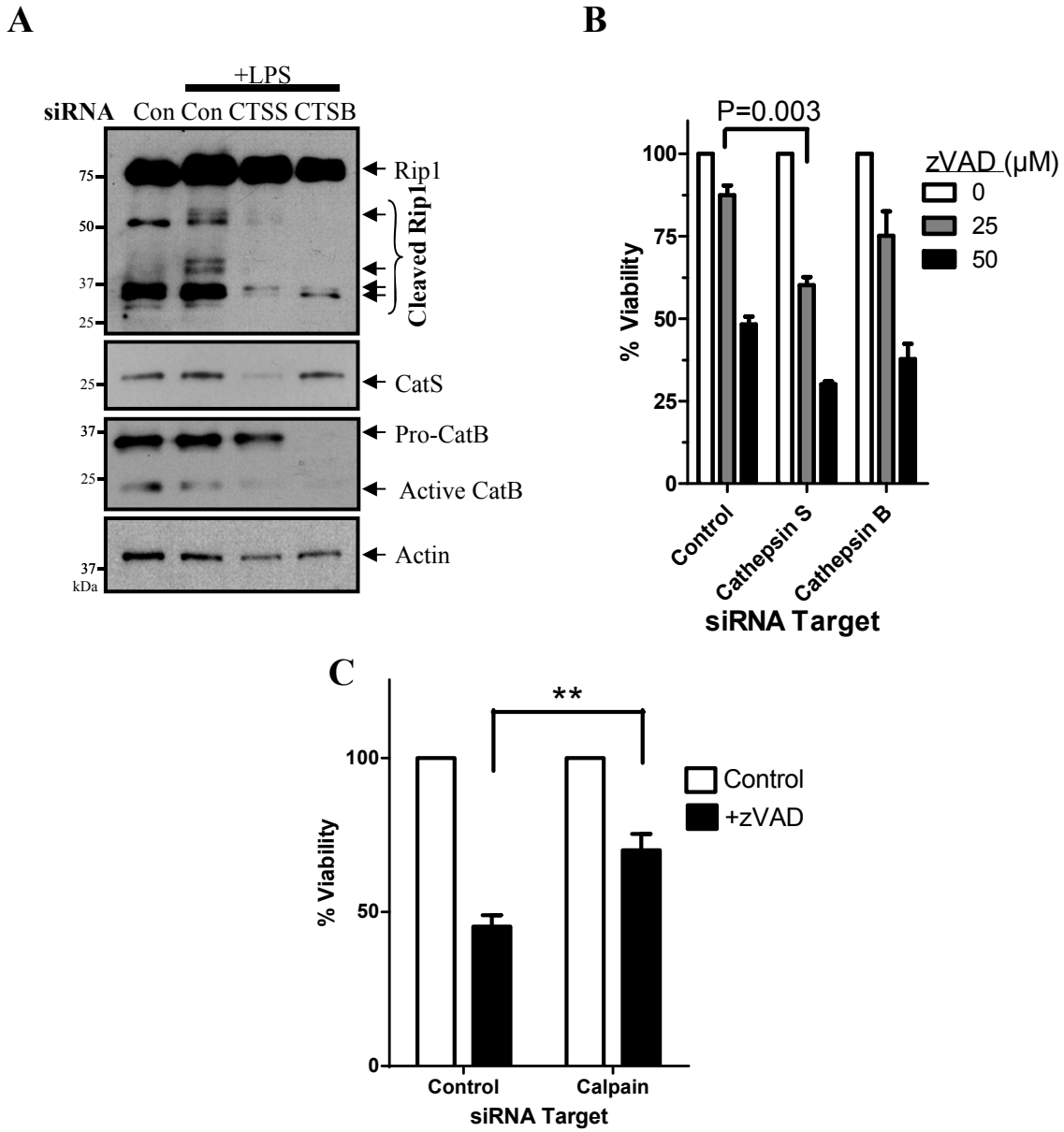
A
+LPS
siRNA Con Con CTSS CTSB
75
50
37
25
Rip1
Cleaved Rip1
25
CatS
37
25
Pro-CatB
Active CatB
37
kDa
Actin
B
P=0.003
100
75
50
25
0
% Viability
zVAD (μM)
0
25
50
Control
Cathepsin S
Cathepsin B
siRNA Target
C
**
100
50
0
% Viability
Control
+zVAD
Control
Calpain
siRNA Target

Figure 38: *Single knockouts for cathepsin S or cathepsin B show no change in susceptibility to necroptosis.* BMDM cells were generated from WT, CTSS- (A) and CTSB-(B) deficient mice as described in the methods section. Cells were then plated at 50 000 cells/well in 96-well plates and treated for 24 hours with LPS (100ng/mL) and various concentrations of zVAD and necrostatin as shown. Graphs show the average viability relative to untreated control from 3 repeated experiments performed in duplicate.

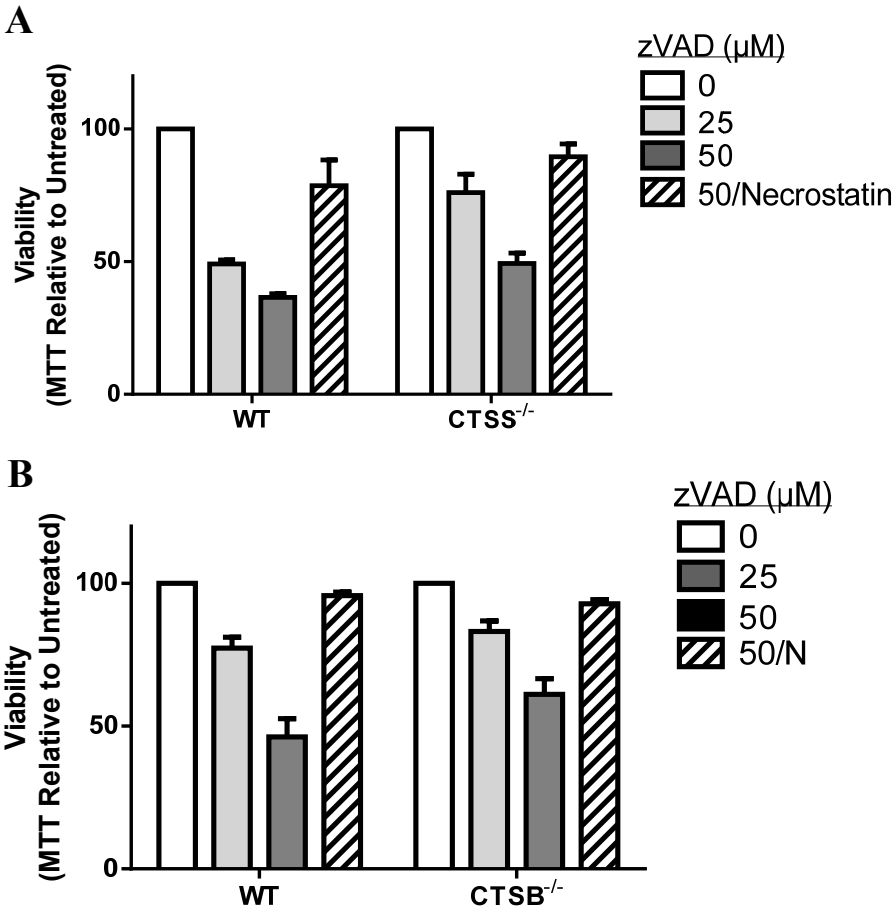
A
zVAD (μM)
0
25
50
50/Necrostatin
Viability
(MTT Relative to Untreated)
100
50
0
WT
CTSS-/-
B
zVAD (μM)
0
25
50
50/N
Viability
(MTT Relative to Untreated)
100
50
0
WT
CTSB-/-

***4.4.E Cathepsins associate with Rip1 kinase directly*:** To test whether Rip1 is indeed being targeted by cathepsins *in vivo* I performed experiments to examine colocalization of cathepsins with Rip1. Co-immunoprecipitation were able to pull down Rip1 kinase along with cathepsin S (Fig. 39A). Importantly, it was observed that a significant amount of cleaved Rip1was in association with cathepsin S, supporting a view that cathepsin S can directly cleave Rip1 kinase. Curiously, a detectable amount of cathepsin S was not immunoprecipitated in associated with Rip1 kinase (Fig. 39A), potentially due to a fairly small fraction of Rip1 being actually associated with cathepsin S. Finally, it was confirmed that Rip1 kinase colocalizes with cathepsins S and B in LPS-treated macrophages (Fig. 39B,C). In total these results support a view that cathepsin S and B directly associate with Rip1 in macrophages.

***4.4.F Cathepsins can directly cleave Rip1 kinase*:** Given the surprising nature of our finding that cathepsins can act in an anti-necroptotic role, I wanted to prove that cathepsins are indeed capable of cleaving Rip1 kinase. Thus, a cell-free cleavage assay was next performed using purified Rip1 and various cathepsins. We found that bacterial expression of full length Rip1 kinase was highly inefficient, and therefore we expressed a GST fusion protein with truncated Rip1 (GST-Rip1$^{280\text{-}656}$). Importantly, given the size of c-terminal fragments observed in our macrophage experiments, this truncated form of Rip1 should still contain putative cleavage site(s) for cathepsins based on the Rip1 cleavage fragments in experiments described above (Fig. 40A). By combining purified GST-Rip1$^{280\text{-}656}$ with active recombinant mouse cathepsin S at cytosolic pH, a clear dose-dependent cleavage of Rip1 kinase was observed (Fig. 40B). Cleavage of recombinant Rip1 by cathepsin S resulted in a ~35-40 kD cleavage product, consistent with what has been observed in macrophage cells. A similar cell free cleavage of Rip1 using cathepsin B and cathepsin L was also observed, although it was significantly less efficient. A number of

Figure 39: *Cathepsins associate with Rip1 kinase directly.* (A) BMDM cells were plated at 2.5×10^5 cells/well in 24-well plates. Cells were then treated for 1h with LPS and/or zVAD as shown. Cells were then lysed and immunoprecipitations were performed as described in the methods section. Lysates and immunoprecipitates were then examined by western blot for Rip1 and CTSS. (B-C) BMDM cells were treated with LPS for 1h and stained with CTSS or CTSB, and Rip1 specific antibodies as described in the methods section. Cells were then examined using confocal microscopy.

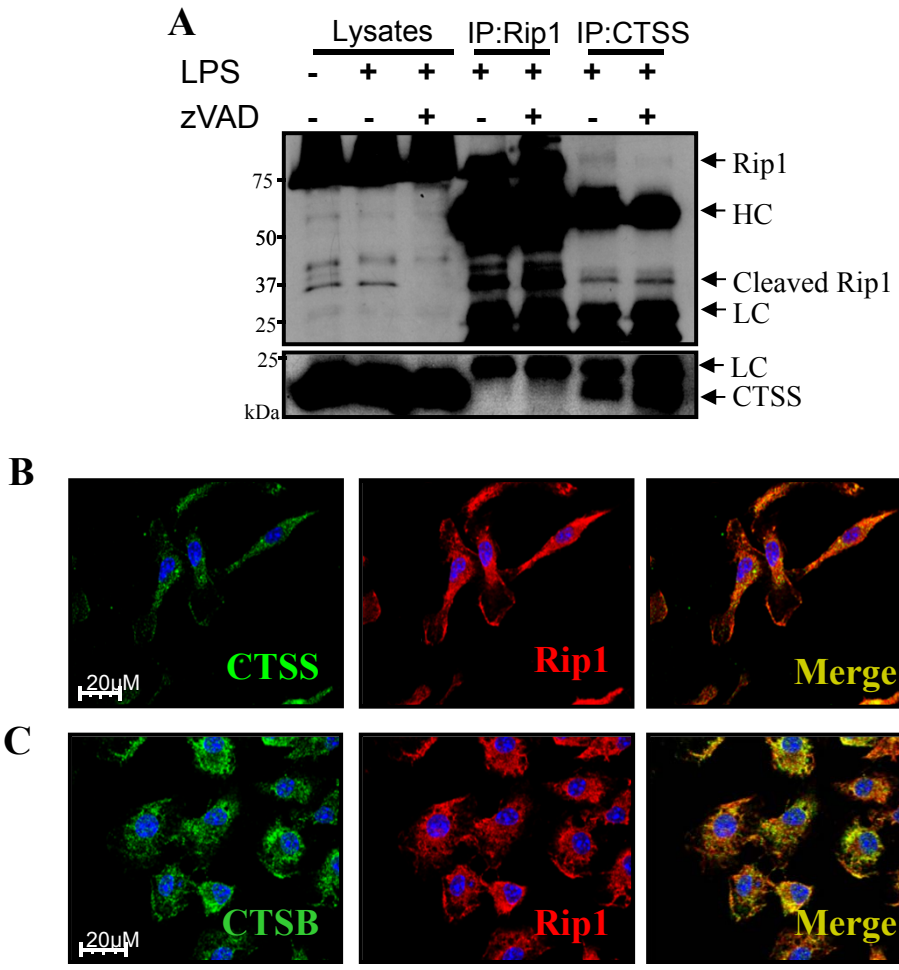
A
Lysates
IP:Rip1
IP:CTSS
LPS
zVAD
75
50
37
25
25
kDa
Rip1
HC
Cleaved Rip1
LC
LC
CTSS
B
CTSS
20μM
Rip1
Merge
C
CTSB
20μM
Rip1
Merge

Figure 40: *Cathepsins can directly cleave Rip1 kinase in a cell free environment.* (A) Diagram showing the domains of Rip1 kinase as identified in the conserved domain database. The approximate sites for cathepsin B cleavage were identified using online SitePrediction tool (*Tool can be found at: http://www.dmbr.ugent.be/prx/bioit2-public/SitePrediction/).* Diagram showing the recombinant GST fusion of Rip1 we employed in our cell free cleavage assays. (B) Recombinant GST-Rip1$^{280\text{-}656}$ was exposed under cell free conditions to CTSS, CTSB, and CTSL as described in the methods section. After treatment, the cleavage of recombinant Rip1 was examined by western blot as shown. Results are representative of at least 3 repeated experiments.

Experiments shown in this figure were performed in collaboration with B. Shutinoski

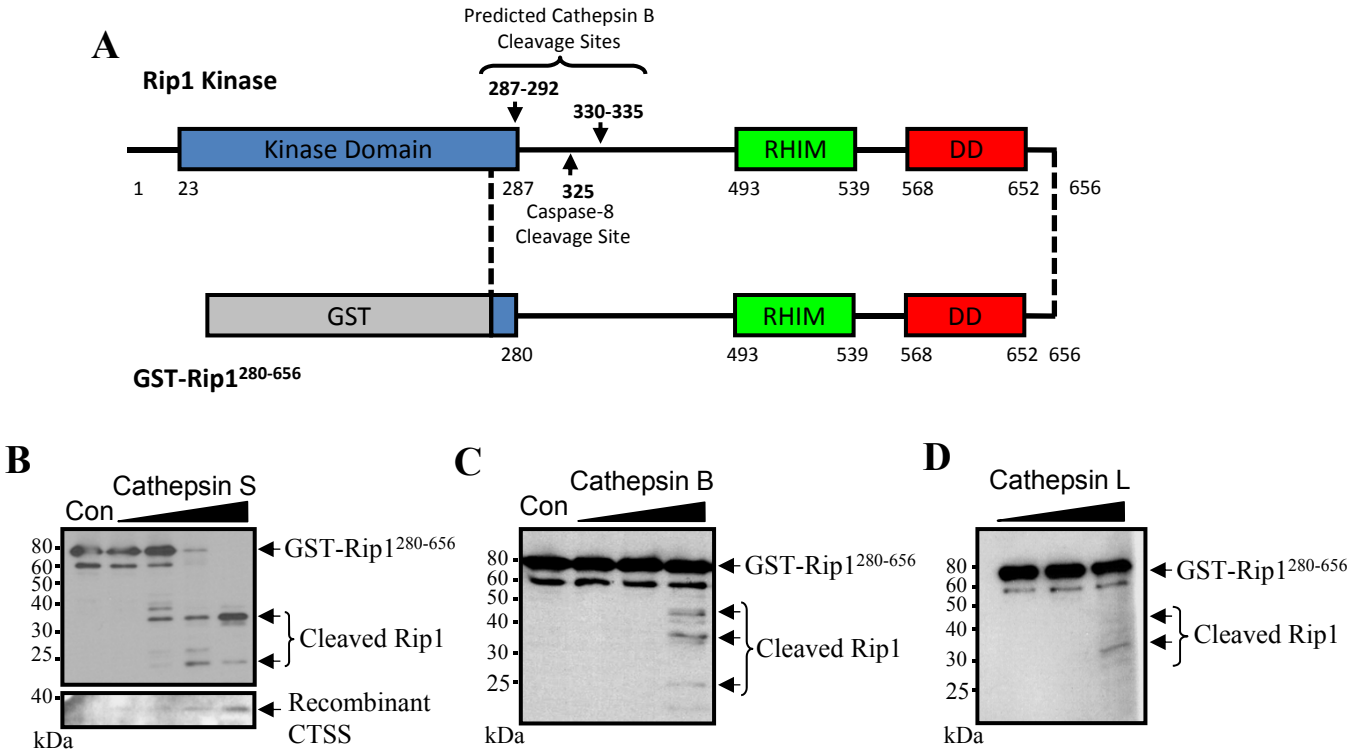
A
Predicted Cathepsin B
Cleavage Sites
Rip1 Kinase
287-292
330-335
Kinase Domain
RHIM
DD
1
23
287
325
Caspase-8
Cleavage Site
493
539
568
652
656
GST
RHIM
DD
280
493
539
568
652
656
GST-Rip1280-656
B
Cathepsin S
Con
80
60
50
40
30
25
40
GST-Rip1280-656
Cleaved Rip1
Recombinant
CTSS
kDa
C
Cathepsin B
Con
80
60
50
40
30
25
GST-Rip1280-656
Cleaved Rip1
kDa
D
Cathepsin L
80
60
50
40
30
25
GST-Rip1280-656
Cleaved Rip1
kDa

bands were visible which were generally consistent with those observed in LPS treated macrophages (Fig. 40C,D). Importantly, at the neutral pH utilized for cleavage experiments, cathepsin B has been reported to cleave targets much more selectively than at acidic pH[290]. These data provide clear evidence that cysteine cathepsins can directly cleave Rip1 kinase.

***4.4.G Cathepsins and caspase-8 cooperate to limit necroptosis*:** Finally, I wanted to directly assess the role cathepsin mediated cleavage of Rip1 might play in regulating necroptosis of macrophages. This was accomplished by applying various cathepsin inhibitors in combination with zVAD/LPS. The addition of cathepsin inhibitors E64D, Ca-074-Me or calpeptin resulted in a small but significant increase in sensitivity of macrophages to zVAD/LPS (Fig. 41A). The relatively minor effect of cathepsin inhibitors is likely due to overlapping effects of cathepsins and zVAD/LPS in terms of protease inhibition. Cathepsin inhibition alone did not result in any significant loss of viability of macrophages (Fig. 41A-D). These results indicate that, within macrophages, the induction of necroptosis by zVAD treatment occurs via its inhibition of cathepsins as well as caspase 8.

Previous work has clearly demonstrated that Rip1 is cleaved directly by caspase-8 [106]. Thus, to confirm the role of both caspase-8 and cathepsins in the regulation of necroptosis, macrophages were treated with LPS and a caspase-8 specific inhibitor, z-IETD-FMK (C8I). While treatment with C8I and/or LPS alone did not induce significant cell death, when it was combined with cathepsin inhibitors treatment resulted in increased macrophage necroptosis (Fig. 41B-D). Similar results were obtained with a number of different cathepsin inhibitors in combination with C8I (Fig. 41B-D). Consistent with necroptosis, this death was abrogated by the addition of necrostatin (Fig. 41B-D). Finally, other caspase inhibitors were utilized to confirm the specific role of caspase-8. Combined inhibition of cathepsins and caspase-9 or -3 inhibitors resulted in no

Figure 41: *Cathepsins and caspase-8 cooperate to limit necroptosis.* (A) BMDM cells were treated with LPS (10 ng/mL), cathepsin inhibitors (10μg/mL) and varying concentrations of zVAD as shown for 24 hours. Cell viability was then assessed by MTT assay. Graph shows cell viability relative to controls without zVAD. (B) BMDM cells were treated with LPS, zVAD (50μM), caspase-8 inhibitor (C8I - 100μM), necrostatin (Nec), and cathepsin inhibitors (10μg/mL) as shown. Cells were incubated for 24 hours with inhibitors and assessed for viability via MTT assay. Graph shows cell viability relative to cells treated with LPS alone. (C) Macrophages were treated with caspase-8 inhibitor (100μM) or zVAD (25μM) in the presence or absence of the cathepsin inhibitors. Cell death was then assessed using Hoechst and propidium iodide costaining. (D) The average cell death counts from 3 experiments performed as described for (C). (E) BMDM cells were treated for 24 hours with caspase inhibitors with LPS and calpain, then assessed for viability via MTT assay. All graphs show viability measurement relative to the untreated control. All experiments were repeated a minimum of 3 times in duplicate *P<0.05, **P<0.005, ***P<0.0001.

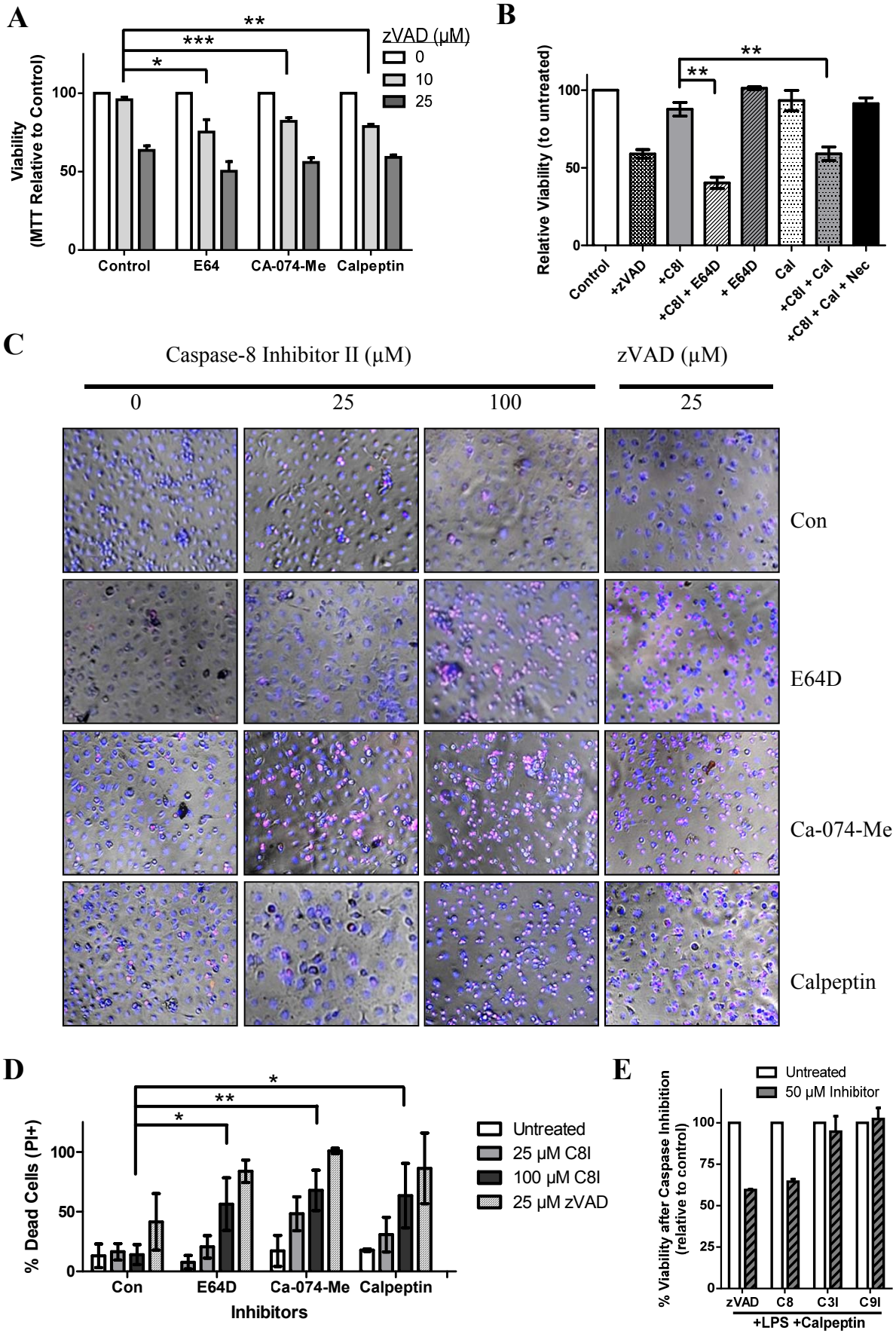
A
zVAD (μM)
0
10
25
Viability (MTT Relative to Control)
Control
E64
CA-074-Me
Calpeptin
B
Relative Viability (to untreated)
Control
+zVAD
+C8I
+C8I + E64D
+ E64D
Cal
+C8I + Cal
+C8I + Cal + Nec
C
Caspase-8 Inhibitor II (μM)
zVAD (μM)
0
25
100
25
Con
E64D
Ca-074-Me
Calpeptin
D
% Dead Cells (PI+)
Untreated
25 μM C8I
100 μM C8I
25 μM zVAD
Con
E64D
Ca-074-Me
Calpeptin
Inhibitors
E
Untreated
50 μM Inhibitor
% Viability after Caspase Inhibition (relative to control)
zVAD
C8
C3I
C9I
+LPS +Calpeptin

significant increase in necroptosis (Fig. 41E). Together, these results point to the novel conclusion that cathepsins and caspase-8 cooperate to regulate necroptosis in macrophages.

5.0 DISCUSSION

5.1 THE ROLE OF CASPASE-3 IN CD8$^+$ T CELLS

CD8$^+$ T cell responses are vital for effective clearance of intracellular pathogens, as well as long-term protection against re-infection[9]. Depletion of the CD8$^+$ T cell population in mice greatly enhances their susceptibility to infection with viruses such as LCMV[291] and HIV[292], as well as intracellular bacteria such as *Mycobacterium tuberculosis*[293], *Salmonella typhimurium*[294] (ST) and *Listeria monocytogenes*[295] (LM). It is thought that breakdown of normal CD8$^+$ T cell surveillance in the central nervous system is responsible for the re-emergence of latent viruses in leukoencephalopathy[296,297]. Despite the clear importance of CD8$^+$ T cells in immune response to many infections, the mechanisms that govern the highly dynamic processes of T cell proliferation, contraction and memory formation remain unclear. By better understanding the intricate interaction of the biochemical signaling pathways that control life and death of T cells during their differentiation, we may be better able to improve responses to vaccines, or to prevent or reverse undesirable T cell responses in cases of autoimmunity.

Previous work has revealed an unexpected and paradoxical link between the activation of the canonical regulators of apoptosis, the caspases, and cell proliferation[100]. In T cells specifically, work has connected caspase activation to both proliferation[107] and contraction[6,7] of primed CD8$^+$ T cells. While a link between T cell activation and apoptotic mechanisms has been repeatedly reported, previous studies have not specifically addressed what stimulatory mechanisms drive caspase activation. Furthermore, to our knowledge no study has yet confirmed that activation of caspases occurs in activated CD8$^+$ T cells during an *in vivo* response to bacterial infection. Thus, in this study I have used two divergent infection models, which differ in intensity and timing of antigen-

presentation, to evaluate the induction of caspase-3 activation in antigen-specific $CD8^+$ T cells during their proliferation, differentiation and contraction.

Caspase-3 cleavage is often referred to as the key downstream apoptotic event preceding cell death, and can be activated by a variety of pathways including death receptor driven caspase-8 cleavage, or mitochondrial driven caspase-9 cleavage (see section 1.2 of introduction). Our data clearly demonstrates that caspase-3 can also be activated downstream of antigen specific stimulation, while excluding a role for inflammation in regulating this process (Fig. 7, 14). This adds to previous work showing that caspase-3 mRNA is increased following TCR stimulation[108]. The question remains as to how caspase-3 is activated downstream of the TCR? Work in other cell types has shown that in some cases calcium flux can activate calpains which in turn can cleave and activate caspase-3[298,299]. It seems possible that activation of caspase-3 could be mediated by the high levels of calcium flux within activated T cells[300].

Probably the most interesting questions in regards to caspase-3 in T cell activation pertain to what function caspase-3 might have in a proliferating cell. Using targeted inhibitors of caspases, it has been shown that caspase activity is actually necessary for efficient T cell proliferation in response to anti-CD3 stimulation[4,107]. This suggests that caspase activation actually promotes T cell proliferation. In contrast to this, it has also been shown that caspase activation can function to cleave important TCR signaling mediators such as Vav and Grb2, and thus can drive T cell anergy in some cases[301,302]. In the data presented here, treatment of antigen stimulated $CD8^+$ T cells with a selective caspase-3 inhibitor led to less proliferation of $CD8^+$ T cells (Fig. 17). Furthermore, I show that cells expressing active caspase-3 consistently also show elevated levels of the cell cycling marker, Ki67 (Fig. 7). Taken together, these data indicate that caspase-3 plays a role in promoting T cell proliferation, but the molecular mechanism of this activity remains elusive.

While several careful studies of caspase activation in $CD8^+$ T cells have been performed *in vitro*, most have employed anti-CD3 stimulation with relatively few examining bona fide antigen presentation, and fewer still looking at caspases in T cell proliferation *in vivo*. In only one study was it previously observed that antigen specific $CD8^+$ T cells upregulate caspase-3 during proliferation in response to LCMV[303]. In this case, the authors suggest that this activation of caspase-3 might somehow prepare cells for a delayed form of apoptosis, which could occur during contraction. Given the fact that caspase-3 is known to be a terminal step in the process of apoptosis[171], this type of delayed cell death seems highly unlikely. In my observations, I saw that caspase-3 was most active during the proliferative activation of $CD8^+$ T cells in response to similar antigen in the context of two divergent infection models, and remained low during contraction phases of the response (Fig. 11). I also observed little evidence that these caspase-3^{hi} $CD8^+$ T cells are undergoing cell death *in vitro* or *in vivo (*Fig. 9, 11). These data support a model wherein caspase-3 likely plays a non-apoptotic role in the proliferative phases of $CD8^+$ T cell activation.

Several reports have previously indicated that caspase-3 induction does not drive the death of activated $CD8^+$ T cells *in vitro*[4,107], yet the possibility that a vigorous outgrowth of small population of caspase-3^{low} cells was masking a significant level of cell death remained a possibility. Thus, I diluted activated $CD8^+$ T cells to very low cell numbers *ex vivo*, greatly reducing the possibility of a minority contaminating population being responsible for significant outgrowth. In this case, there were few signs of cell death (cell debris, or $TMRE^{-ve}$ cells) in the active caspase-3^{hi} activated $CD8^+$ T cells (Fig. 9). I also confirmed these findings *in vivo,* where despite the relatively high level of active caspase-3, I was unable to detect a significant population of $TUNEL^+CD8^+$ T cells (Fig. 12). Even purified caspase-3^{hi} $CD8^+$ T cells *ex vivo* did not exhibit significantly elevated number of dead cells ($TMRE^{-ve}$) when compared to those cells with the lowest level of caspase-3 (Fig. 14). I

conclude that caspase-3 activation does not result in a significant amount of cell death concurrent with $CD8^+$ T cell proliferation.

Although early inflammation is an important determinant of $CD8^+$ T cell contraction[89,304], no programmed death mechanisms have yet come to light to explain the mechanism of contraction of the antigen specific population. Apoptosis might seem to be a likely candidate for the removal of activated cells following resolution of an infection, but in previous work the *in vivo* application of caspase inhibitors during T cell contraction had little effect on the dramatic drop in T cell numbers following the peak of the $CD8^+$ response[109]. Consistent with this, I also observed that active caspase-3 actually remained at basal levels throughout the contraction phases of the OVA-specific response to two divergent intracellular bacterial pathogens (Fig. 10). These data indicate that caspase-dependent apoptosis may not play an important role in T cell contraction. It should be noted that recent work in Bim, Bid, and/or Fas deficient mice indicates that redundant pro-death mediators cooperate to remove activated T cells during contraction[7,305,306]. It is an interesting possibility that these upstream activators of apoptosis might drive caspase-independent death mechanisms in contracting T cells, but more work will be necessary to address this possibility.

Following the realization that caspases do not seem to play a significant role in T cell death, it has been suggested that the alternative programmed death pathway of necroptosis might function to remove activated cells. Supporting this view, it has been shown that specific deficiency in caspase-8 in T cells or its adapter, FADD, leads to dysfunctional T cell responses[97], which was later shown to be due to overactive necroptosis[307,308]. Pharmacological or genetic ablation of the necroptosis pathway by targeting either Rip1 or Rip3 rescued the ability of these T cells to proliferate in response to stimulation[104,105,140]. These observations indicate that expression of caspase-8 is required in order to limit necroptosis in activated T cells.

While the findings that caspase-8 is needed to reign in Rip3 dependent death in activated T cells might point to necroptosis as the means of T cell contraction, it is important to note that deficiency for Rip3 alone does not seem to have any appreciable effect on the T cell activation or contraction[105,253]. I confirmed similar lack of any effect of Rip3-deficiency on the $CD8^+$ T cell response to LM-OVA (unpublished results from our lab). In addition, T cells with concurrent deficiency for Rip3 and caspase-8 show a normal contraction of $CD8^+$ T cells following an antigen specific response[105]. In contrast to the antigen specific contraction, these mice do suffer a progressive accumulation of dysfunctional T cells, although these cells seem to be restricted to an abnormal population of non-functional T cells [106,150]. This is highly reminiscent of what is seen in *lpr* or g*ld* mutations of the Fas pathway[96]. Based on these observations, it seems that necroptosis likely is not an important factor in contraction of an antigen specific T cell response under normal caspase-8 sufficient conditions.

Though the role of caspase-8 in limiting necroptosis has been well documented[309], the potential activity of caspase-3 in this process has not been thoroughly investigated. Unlike caspase-8 knockout which is embryonic lethal due to overactive necroptosis[106], caspase-3 knockout animals remain viable with no documented T cell defects. This may be due to significant redundancy between caspase-3 and caspase-7, as double knockout caspase-3/7 animals die immediately after birth[172]. Whether caspases-3 or -7 can inhibit necroptosis through cleavage of Rip1 kinase or other means remains to be investigated. Supporting this possibility, I saw both less proliferation and somewhat increased cell death in antigen stimulated T cells with the addition of a caspase-3 inhibitor (Fig. 15). One intriguing possibility may be that caspase-3 could also function to promote or maintain caspase-8 activation, as this type of retrograde activation of caspase-8 by caspase-3 has recently been

demonstrated[310,311]. Further work will be needed to investigate the role that effector caspases might play in the regulation of necroptotic cell death.

Interestingly, I have observed that in addition to elevated levels of active caspase-3, antigenic stimulation of $CD8^+$ T cells also led to more exposure of phosphatidylserine (Fig. 18), another cardinal signal of apoptotic cell death. This type of reversible exposure of phosphatidylserine in activated T cells has been previously reported[312]. The question remains as to how these cells, which show many of the hallmarks of apoptosis, manage to escape actual cell death. One possible explanation might be differential subcellular localization of caspase-3 in activated T cells versus apoptotic cells. In previous work, it has been shown that active caspase-3 preferentially localizes to the membrane in activated $CD8^+$ T cells[301,313,314], whereas caspase-3 would normally need to translocate to the nucleus to induce apoptotic death[315]. Consistent with this, immunofluorescent staining for active caspase-3 appeared to localize at the cell membrane in activated $CD8^+$ T cells, whereas it appeared more cytosolic in cells stimulated to undergo apoptosis by staurosporine exposure (Fig. 8).

In addition to the importance of controlled localization of caspases, I felt that the expression of inhibitors of apoptosis proteins (cIAP1, cIAP2, xIAP) might also have a significant impact on $CD8^+$ T cell function. Thus, I also attempted treating cells with a small molecule mimetic of SMAC, which would normally inhibit IAP function in apoptotic cells. SMAC mimetic (SM) treatment had little impact on $CD8^+$ T cell responses both *in vitro* and *in vivo*. Consistent with this, mice with single gene deficiencies for cIAP1, cIAP2 or xIAP do not appear to have significant defects in T cell responses[189,268,316]. Based on this, I conclude that IAP expression likely does not play a significant role in controlling caspase function within proliferating T cells in mice. Despite this, it should be noted that there is significant evidence supporting a role for IAPs in regulating T cell responses in

humans, with particular note to the X-linked lymphoproliferative disorder associated with xIAP muations[317].

Thus, by studying OVA specific $CD8^+$ T cell responses in a variety of *in vitro* and *in vivo* contexts, I have provided new evidence to support a model by which caspase-3 becomes activated and promotes $CD8^+$ T cell proliferation and precedes differentiation to effector cells (Fig. 16). Similarly, caspase-3 cleavage has been implicated in the normal differentiation of skeletal muscle cells[101], macrophages[102], erythroblasts[103], as well as others. The promiscuity of caspase-3 as a protease has hampered attempts to specifically dissect the molecular mechanisms by which caspase-3 affects its function in differentiation. This frustrating property of the apoptotic proteases to target many proteins[173] must surely be relevant to its function. Perhaps the ability of caspase-8 to cleave and limit the function of the pro-necrotic Rip1 kinase offers us a glimpse at a more general function of caspases to break down signaling networks. By targeting many proteins for cleavage, caspases could aid in degrading the established signaling pathways and precipitate change in the cellular signaling program from a naive latent state to one of active proliferation and differentiation.

Taken together, these results resolve some controversies surrounding caspases in $CD8^+$ T cell activation by providing strong evidence that active caspase-3 is: (a) directly stimulated by antigen, (b) expressed transiently and lost progressively during proliferation and differentiation of $CD8^+$ T cells, (c) not associated with contraction of the response, (d) coupled with activation of other canonical apoptotic mediators, and (e) does not lead to cell death (see Figure 42 for model). Our data using a specific inhibitor also indicates that caspase-3 activation plays some role in limiting death during T cell activation. This supports a model wherein the activation of caspases is key in limiting necroptosis during T cell proliferation[104], perhaps as a mechanism to remove activated T cells if they

Figure 42: *$CD8^+$ T cells become active caspase-3 high soon after activation and progressively lose this as cells proliferate.* Antigen presentation from antigen presenting cells drives the upregulation of caspase-3 at the cell membrane. As activated cells continue to proliferate they progressively lose expression of active caspase-3. Throughout later phases of the $CD8^+$ T cell response cells maintain a low level of caspase-3, suggesting that cell death by caspase 3 may not play a role in contraction and memory formation.

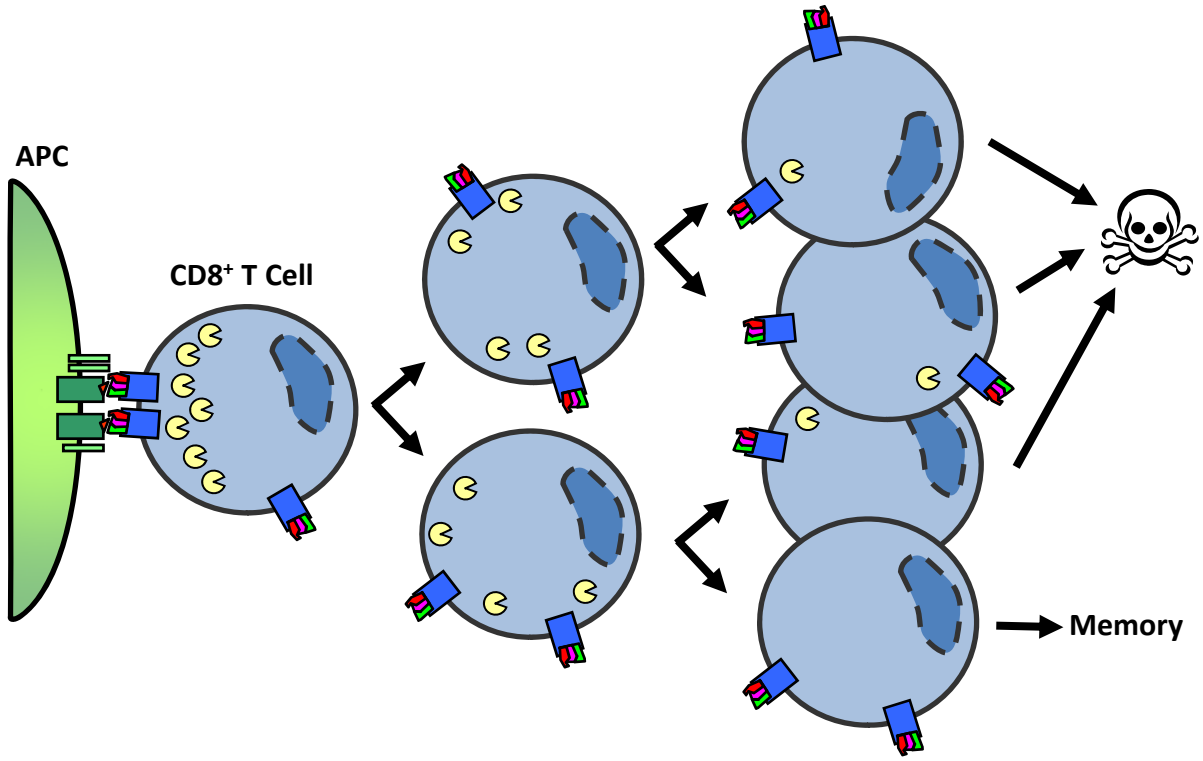
APC
CD8+ T Cell
Memory

fail to receive sustained stimulation. Further work will be necessary to fully characterize the role of caspase-3 in regulating T cell death and proliferation.

5.2 The Role of IAPs in Innate Immune Cell Function

As discussed above, there is no evidence that expression of inhibitor of apoptosis proteins (IAPs) such as cIAP1, cIAP2, and xIAP have a significant role in regulating T cell survival. In contrast, there have been several reports to show that expression of IAPs is important in regulating the survival of innate immune cells. For example, it is known that innate immune cells upregulate cIAP expression during differentiation and activation[318–320]. Furthermore, the inflammatory immune response to LPS and bacterial infection has been shown to be significantly altered in mice deficient for cIAP1[282], cIAP2[268], or xIAP[321] expression. Consistent with a key role in macrophage function in particular, I observed that purified macrophages expressed significantly higher levels of cIAPs than B cells or T cells (Fig. 19A). Despite the apparent importance of IAPs in regulating innate immune responses, the signaling mechanisms behind this function are not yet well understood. Thus, in this thesis I have employed a newly available SMAC mimetic (SM) as an inhibitor of IAPs, SM-164. In addition, I use genetically-deficient mice to explore the *in vitro* and *in vivo* role of cIAPs in protecting innate immune cells from programmed cell death.

Our data clearly demonstrates that treatment of bone marrow derived macrophages (BMDMs) or dendritic cells (BMDCs) treated with SM results in a dose dependent loss of viability (Fig. 19B, 20). These results seem to contradict a recent paper examining human innate immune cells, wherein it was found that monocytes were susceptible to SM-induced death but that macrophage cells were highly resistant to this effect[322]. The differences between our results and those presented by Muller-Sienerth *et al*. can potentially be explained by differences between human and mouse immune cells

in IAP function, as is exemplified by xIAP associated immunodeficiency observed in humans[317] but not mouse models[316]. In addition, in collaboration with other Sad lab members, I have recently examined the susceptibility of macrophage cells over several weeks of differentiation using M-CSF. In this case we observed a consistent loss of susceptibility to SM over time, with macrophages differentiated for 15 days being completely non-responsive to SM treatment (unpublished results from our lab). This data indicates that SM inhibition of cIAPs in freshly derived (~day 7) macrophages and dendritic cells drives a potent induction of cell death. It is likely that persistent culture of cells with M-CSF modulates pro- and anti-apoptotic mechanisms, and this may have significant influence on their resistance to cell death. This may provide an interesting avenue for future work in the Sad lab.

In most studies examining the effects of SMs in cancer cell lines, it has been shown that SM will induce apoptosis which can be inhibited by zVAD treatment[143,255]. In BMDM cells, I saw that co-treatment with zVAD in addition to SM actually resulted in a significant increase in loss of viability (Fig. 21). In contrast, necrostatin completely rescued SM treated macrophages, pinpointing the mechanism of death to be necroptosis (Fig. 21). Similar papers showing SM-induced necroptosis in cell lines have mostly also employed a caspase inhibitor, zVAD-FMK (zVAD), to allow robust activation of the programmed necrotic cell death pathway[148]. Interestingly, necroptosis induced by SM has also been reported to occur without addition of a caspase inhibitor[323]. Our data shows that cIAP inhibition through SM treatment alone is adequate to activate necroptotic cell death, but this can be further enhanced by the application of zVAD.

Many reports have implicated cIAPs in the evasion of programmed death within cancer cells[143,192], but results have been conflicting as to the roles of cIAP1 or cIAP2 specifically. In pancreatic cancer cells, it was shown that the knockdown both cIAP1 and cIAP2, through either

combined siRNA targeting or SM treatment, was necessary to sensitize pancreatic cancer cells to TNF-α/zVAD-induced cell death[148]. In contrast to this, work in L929 fibroblasts showed that knockdown of cIAP1 but not cIAP2 led to significantly increased sensitivity to TNF-α-induced cell death, although it was not tested whether simultaneous knockdown of cIAP1 and cIAP2 could further enhance cell death[323]. In this case primary macrophages lacking either cIAP1 or cIAP2 displayed increased sensitivity to SM-induced necroptosis; although this sensitization effect was more prominent cIAP1- than cIAP2-deficient cells (Fig. 22A). Based on this, our data supports a model whereby cIAP1 and cIAP2 act redundantly to limit the activation of necroptosis.

Similar to what has been observed in necroptosis, it was recently revealed that cIAP1, cIAP2 and xIAP function jointly to suppress the formation of a pro-apoptotic ripoptosome, a cell death signaling platform containing both Rip1 and caspase-8 which is similar to the necrosome[207,213]. Interestingly, these two simultaneous reports revealing the existence of the ripoptosome signaling complex differed in terms of their observed importance of Rip1 kinase activity. While the TLR3-induced ripoptosome required both zVAD and necrostatin (nec) for rescue[207], the genotoxic stress (etoposide)-induced ripoptosome was inhibited by necrostatin alone[213]. In my observations, I saw that xIAP knockout animals showed significantly elevated sensitivity to SM-induced cell death, but could not be rescued by necrostatin treatment alone (Fig. 22B). The addition of both zVAD and nec resulted in a somewhat increased but still incomplete rescue of SM-induced cell death (data not shown). These data suggest that in macrophages xIAP specifically functions to block the apoptotic axis of SM-induced death, although further work will be needed to confirm if this involves the formation of a ripoptosome. Importantly, this also suggests a qualitative difference between the inhibition of xIAP-induced by SM-164[275] and that achieved by complete genetic-deficiency.

Reports have previously implicated cIAPs in limiting cell death thorough their E3 ligase activity in the ubiquitination of Rip1 kinase[188,324]. Correspondingly, the deubiquitinating enzyme cylindromatosis has been shown to promote Rip1 dependent death pathways[148,323]. Importantly, although cIAP ubiquitination of Rip1 is generally associated with non-degradative K63-linked ubiquitin chains[139,189], it has been recently reported that cIAPs can participate in the ubiquitination of both Rip1 and Rip3 with degradative K48 as well as K63 ubiquitin chains[325]. Herein I report that SM-induced loss of cIAPs corresponds with an increased expression of both Rip1 and Rip3 (Fig. 23A), which appears to be mediated by post-translational mechanisms (Fig. 23C,D). Furthermore, I show that treatment of cells with the 20S proteasome inhibitor, lactacystin, results in an increase in expression of Rip1 and Rip3 (Fig. 23E). Taken together this data indicates that cIAPs increase the degradative turnover of Rip1 and Rip3 kinases, potentially through K48 ubiquitination.

In addition to the increased expression of Rip1 and Rip3 kinases associated with SM treatment, I also observed a consistent increase in a secondary slightly slower migrating form of Rip1 (Fig. 23A), which I confirmed to be phosphorylated Rip1 (Fig. 23B). It has been shown repeatedly that TNF-receptor (TNFR) signaling drives the activation (phosphorylation) of Rip1[194]. While exogenous TNF-α can serve this function, it has also been demonstrated that SM treatment of some cell lines can induce the autocrine production of TNF-α necessary for cell death[255]. BMDM cells appear to be no exception to this, as macrophage death was dependent upon the expression of TNFR1/2 ($TNFR^{-/-}$) (Fig. 24A). Interestingly, the addition of both zVAD and SM resulted in a potent induction of necroptosis even within $TNFR^{-/-}$ macrophages (Fig. 24E), suggesting that alternative pathways to necroptosis may become activated under conditions where multiple necroptosis inhibitors are blocked.

At first glance, an increase in TNF-α production in response to SM might seem somewhat confusing given that cIAPs have been reported to act in pro-inflammatory NF-κβ signaling[189]. It should be kept in mind however that the reported NF-κβ promoting effects of cIAPs apply primarily to signaling downstream of TNFR signaling and should not be generally applied to all pro-inflammatory signaling. Indeed, spontaneous production to cytokines has recently been reported to actually increase with application of a SM[326]. Furthermore, it has been shown that inhibition of Rip1 kinase activity through nec-1 can also inhibit the production of TNF-α[229,249]. Production of IL-1β has also been linked to SM-induced activation of the necrosome, although it appears to be Rip3 rather than Rip1 specific[254]. In my case, I observed increased inflammatory cytokine production in BMDM and BMDC cells in response to SM treatment, with a much more potent effect in combination with LPS (Fig. 20). This data supports a model whereby Rip1 activation promotes increased pro-inflammatory signaling and cytokine production.

Interestingly, I also observed no increase in Rip1/3 expression in TNFR1/2-deficient macrophages treated with SM (Fig. 24B), perhaps suggesting that the TNFR may itself participate in this turnover of Rip1 and Rip3. It seems plausible that cIAP1 and cIAP2 could function to specifically promote the degradation of Rip1 and Rip3 as they become associated with the TNFR complex, and thus limit downstream signaling. A similar effect of IAPs to limit the recruitment of Rip1 to the FAS receptor was recently reported[327], although the authors do not provide evidence to suggest whether degradation of Rip1 may be involved. Taken with our observations here I propose a model wherein cIAPs selectively degrade Rip1 and Rip3 as they become activated by the TNFR. Furthermore, given the lack of a plausible mechanism to explain spontaneous TNF-α production in the absence of TNF production, I speculate that this TNFR activation of the necrosome occurs constitutively at a low level which is kept in check cIAPs.

The extensive *in vitro* analysis of cIAPs and SMs has clearly shown that their expression is often important in preventing programmed cell death in cancer cells, but the role of cIAPs within normal immune cells has been much less clear. Recently, one study showed that cIAP1-deficient mice have higher *C. pneumoniae* burden[282], but the *in vivo* viability of macrophages was not assessed. Their finding of reduced macrophage numbers in infected lungs of knockout mice is compatible with increased cell death. Another study has shown that cIAP2-deficient mice are highly resistant to LPS-induced shock due to elevated macrophage cell death[268]. In this data, I show that loss of cIAP activity, either through genetic ablation or using a specific inhibitor, results in significantly increased necroptosis of macrophages (Fig. 26). This increased death of macrophages *in vivo*, led to poorer control of an intracellular bacterial pathogen (Fig. 26A,D). Thus, I conclude that cIAPs function to limit necroptosis in macrophages *in vivo*.

Based on recent data showing that mice deficient in Rip3 expression are significantly more susceptible to infection with vaccinia virus[206], it has been suggested that necroptosis provides an important means to eliminate infected cells. Furthermore, it is thought that necroptosis will cause the release of important DAMPs, driving acute inflammation which may be beneficial in initiating an immune response[247]. Consistent with this, cytomegalovirus has also been demonstrated to evade immune response by inhibiting Rip3; mutants of cytomegalovirus which lack this ability to inhibit Rip3 exhibit severely attenuated pathogenesis[328]. In contrast to this view, I show that overactive necroptosis associated with loss of cIAP activity leads to impaired control of *Listeria monocytogenes*. Taken together, these data underline the complexity of cell death regulation in immune cells, and the need for an appropriate balance between too little and too much cell death.

In conclusion, I have provided novel mechanistic insights into how cIAPs protect macrophages from cell death, through direct interaction with key members of the necrosome. I propose that

because activated macrophages can carry elevated levels of ROS and other cytotoxic inflammatory mediators, it is possible that the action of caspases and cIAPs may represent an important mechanism to counteract a natural predisposition toward necrotic cell death. In addition, as I have observed in SM treated cells, and has been reported by others, Rip1 phosphorylation seems to be an important driver of necroptosis[249]. Based on this I propose the following model: (1) Preclustering of the TNFR complex, or low level TNF release drives low level activation of the necrosome, (2) Constitutive necrosome activation is kept in check by cIAP mediated degradation of Rip1 and Rip3 kinase, (3) SM driven degradation of cIAPs leads to elevated necrosome activation, (4) Rip1 kinase activity drives increased release of TNF-α, (5) TNFR signaling results in a potent induction of both necroptosis and apoptosis, (6) xIAP prevents the induction of apoptosis, resulting in necroptotic cell death (see Figure 43 for model). Given the increasing push for clinical application of SMAC mimetics, it represents an interesting possibility that the pathway I have revealed here may also operate in some tumor cells.

5.3 NECROPTOSIS AND INTERFERON

I next wished to address the issue of necroptotic cell death in *Salmonella* infection. Our initial investigations into the infection of mice with *Salmonella typhimurium* (ST) somewhat mirrored the results of LM infection, namely that cIAP1-deficent animals had much worse control of ST infection (Fig. 27). Based on this, I formulated a hypothesis that necroptosis might play a significant role in the pathogenesis of ST.

Previous work investigating cell death of macrophages associated with ST infection has revealed two divergent forms of death. The faster of the two forms of cell death, pyroptosis, occurs within as little as 1 hour after infection and is dependent upon the activation of caspase-1[85]. This

Figure 43: *Activation of Rip1 is kept in check by cIAP mediated degradation.* Our data indicates that loss of cIAP expression following SM treatment leads to increased expression of Rip1 and Rip3. Loss of constitutive inhibition of necrosome activity leads to increased expression of inflammatory cytokines, including TNF. Ligation of the TNFR leads to high level activation of the necrosome and drives cell death through both apoptotic and necroptotic pathways. Expression of xIAP is necessary to dampen the TNFR induced apoptosis pathway.

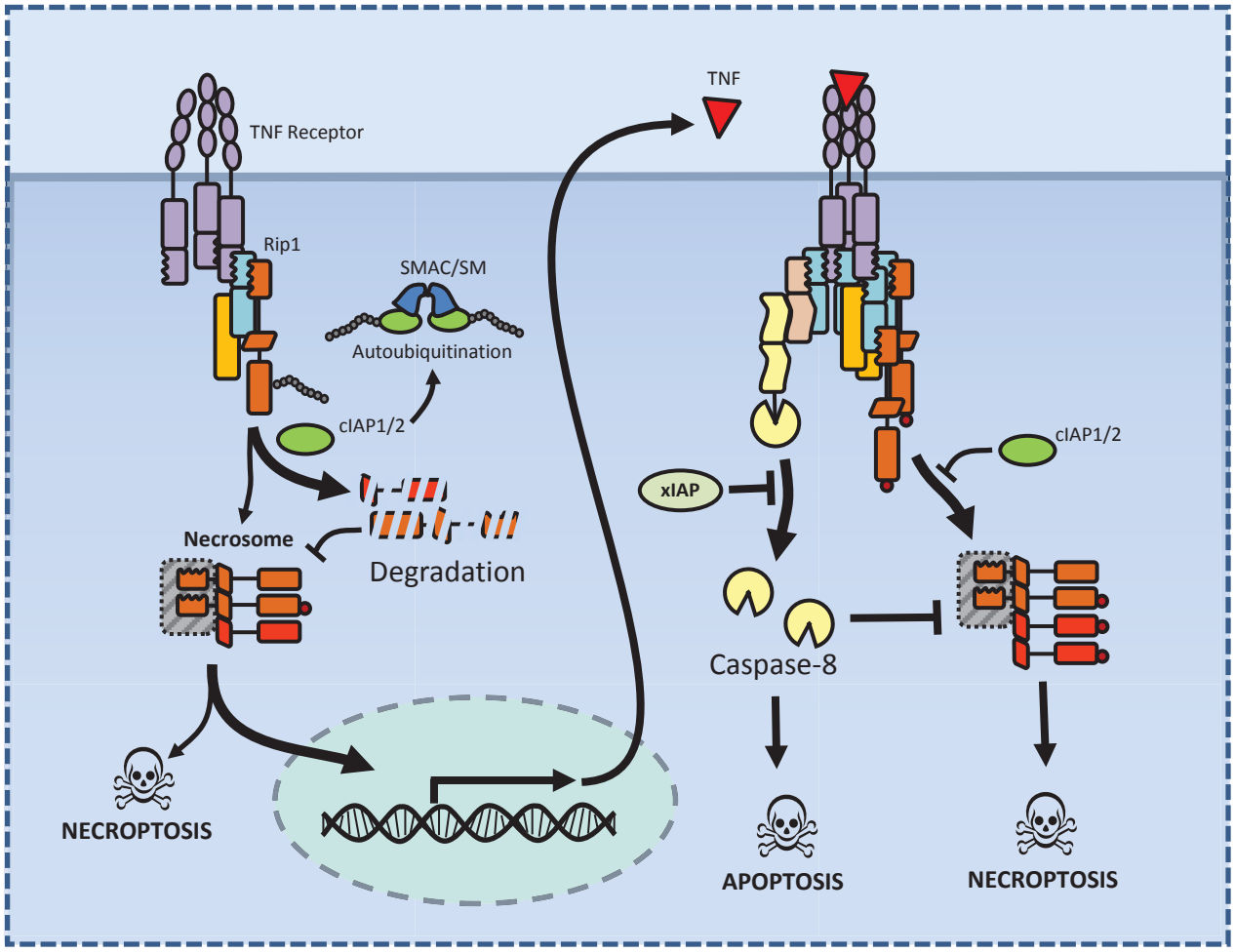
TNF Receptor
Rip1
SMAC/SM
Autoubiquitination
cIAP1/2
Necrosome
Degradation
NECROPTOSIS
TNF
xIAP
cIAP1/2
Caspase-8
APOPTOSIS
NECROPTOSIS

form of death was proposed to be to be a key mechanism for systemic dissemination of ST, as caspase-1-deficient mice were resistant to oral infection[79]. More recent studies have contrasted this earlier work however, instead showing that caspase-1-dependent inflammasome activation resistance to oral ST infection[329]. Caspase-1-deficient mice have also been shown to have higher susceptibility to intravenous delivery of ST[80,81]. While these conflicting results yielded from groups testing *Salmonella* infection have are still somewhat unresolved, the prevailing model now views caspase-1 as an inflammatory mechanism which aids the immune response to ST. In addition to pyroptosis, ST has also been demonstrated to elicit a delayed form of cell death occurring 6-18 hours or more after infection of macrophages[85]. This form of cell death appears to be primarily revealed in infections with *Salmonella* pathogenicity island-1 (SPI-1) deficient mutant strains[330,331]. Interestingly, this delayed macrophage cell death has also been reported to rely on activation of TLR4 signaling and protein kinase R[86].

In contrast to these previous reports, our lab had observed that cell death of infected macrophages primarily occurred between 24 and 48 hours of infection, more consistent with the delayed phenotype of ST-induced death. It is not entirely clear why rapid pyroptosis was not seen in our model, but it should be noted that pyroptosis has been previously induced by infecting either LPS-primed macrophages or using very high multiplicities of infection (MOI) of ST[84]. Consistent with such an explanation, it was observed that LPS pre-treatment of macrophages significantly accelerated cell death induced by ST (unpublished results from our lab).

Despite the delayed kinetics of macrophage death induced by ST in our infection model, cell death was significantly reduced using a specific inhibitor of caspase-1 (Fig. 28A). Interestingly, we found that the application of the Rip1 inhibitor, necrostatin, was significantly more effective at rescuing macrophages from delayed ST-induced cell death (Fig. 28A). I also confirmed that cell

death was occurring through activation of necroptosis by targeted siRNA knockdown of Rip3 followed by ST-infection of macrophages (Fig. 28B). This data provides the first evidence that *Salmonella* can indeed induce programmed necrosis in macrophages, although several previous reports investigating ST-induced cell death have repeatedly noted a necrotic like phenotype[85,332]. Given the well-established role for caspase-1 in ST-induced cell death, these data also seem to support a possibility that there may be points of molecular interaction between the pathways of the caspase-1 inflammasome and necrosome that are as yet undetermined.

At this time, ongoing work in our lab had also identified that IFNAR-deficient macrophages were highly resistant to ST-induced cell death (Fig. 30A). Based on this, it was hypothesized that IFNAR signaling might play a role in activating ST-induced macrophage cell death. Indeed, whereas WT macrophages showed elevated Rip1 and Rip3 phosphorylation following ST infection, IFNAR-deficient macrophages showed much less activation of Rip1 and Rip3 (Fig. 30B). Generally, type-I interferon is thought to drive the expression of anti-viral genes[68], and under some conditions has also been reported to induce apoptosis[69,70]. To my knowledge, this is the first data to show that type-I interferon can lead to programmed necrotic cell death, although one published study did identify members of the interferon gene family in a genome-wide screen to identify the regulators of necroptosis[210].

Work in our lab was also performed to confirm that the type-I interferon receptor directly associated with Rip1, and that treatment with interferon-β could drive a transient phosphorylation of Rip1 (see [285]). Nevertheless, treating macrophage cells with type-I interferon alone was insufficient to induce necrotic cell death. This was likely due to intact inhibitory effect of caspases when interferon alone was applied to the cells. Indeed, the addition of zVAD in combination with IFN-β induced a significant level of cell death in J774 macrophages (Fig. 31). These data indicate that

interferon can drive activation of Rip1 kinase, but a mechanism to block the inhibitory effects of caspases is necessary for full-blown necroptosis. Furthermore, these data indicated that ST must interfere with the functioning of caspase-8 in some way, which was later confirmed by western blot for caspase-8 cleavage (see [285]).

Thus, we have identified a novel model by which ST exploits the host type I interferon response to eliminate macrophages through RIP-dependent cell death and promote its own survival (see Figure 44 for model). Furthermore, this work shows how type-I interferon driven necroptosis can lead to massive inflammation. Interestingly, although type-I interferon is a key resistance factor for viral infection, this data agrees with recent results demonstrating that it can be highly detrimental in the context of bacterial infections such as *Listeria monocytogenes* infection[88]. This work highlights the need for a careful balance of cell death in the immune system, and provides a key demonstration that inflammatory cytokine signaling can drive massive inflammation through necroptotic cell death.

I next wanted to further probe how type-I interferon signaling was related to the more general process of necroptosis. In *in vitro* BMDM cultures, I observed that treatment with LPS and zVAD can lead to a potent induction of necroptosis (Fig. 35A,B), similarly as recently described[226]. Intriguingly, I observed that IFNAR-deficient macrophages are highly resistant to necroptosis as induced by zVAD/LPS treatment (Fig. 32). Canonically, the activation of TRIF by TLR4 is thought to a drive interferon expression through the activation of IRF3, with a positive feedback activation through IRF7[46]. These findings are somewhat in contrast with data indicating that there was no effect of IRF-3-deficiency on LPS/zVAD mediated induction of necroptosis[226]. I hypothesize that IRF-7 alone may be adequate to produce interferon necessary for necroptosis[333,334]. Our lab is actively addressing the pathway through which type-I interferon expression is activated in this model and how interferon is able to induce necroptosis.

Figure 44: *Model of how ST induces necroptosis*. (1) ST is rapidly phagocytosed by macrophage cells, where it remains in the phagosome (2) Exposure to ST induces a immune stimulation through PRRs leading to (3) the release of inflammatory cytokines such as IL-6, TNF and type-I interferon. (4) Type-I interferon induces an up-regulation of IFNAR signaling which (5) leads to activation of Rip1 kinase. It remains unclear what other factors such as JAKs and STATs might play in the activation of Rip1 kinase (6) Activation of Rip1 leads to formation and activation of the necrosome (7) Ultimately, this leads to necroptotic cell death and release of ST bacteria.

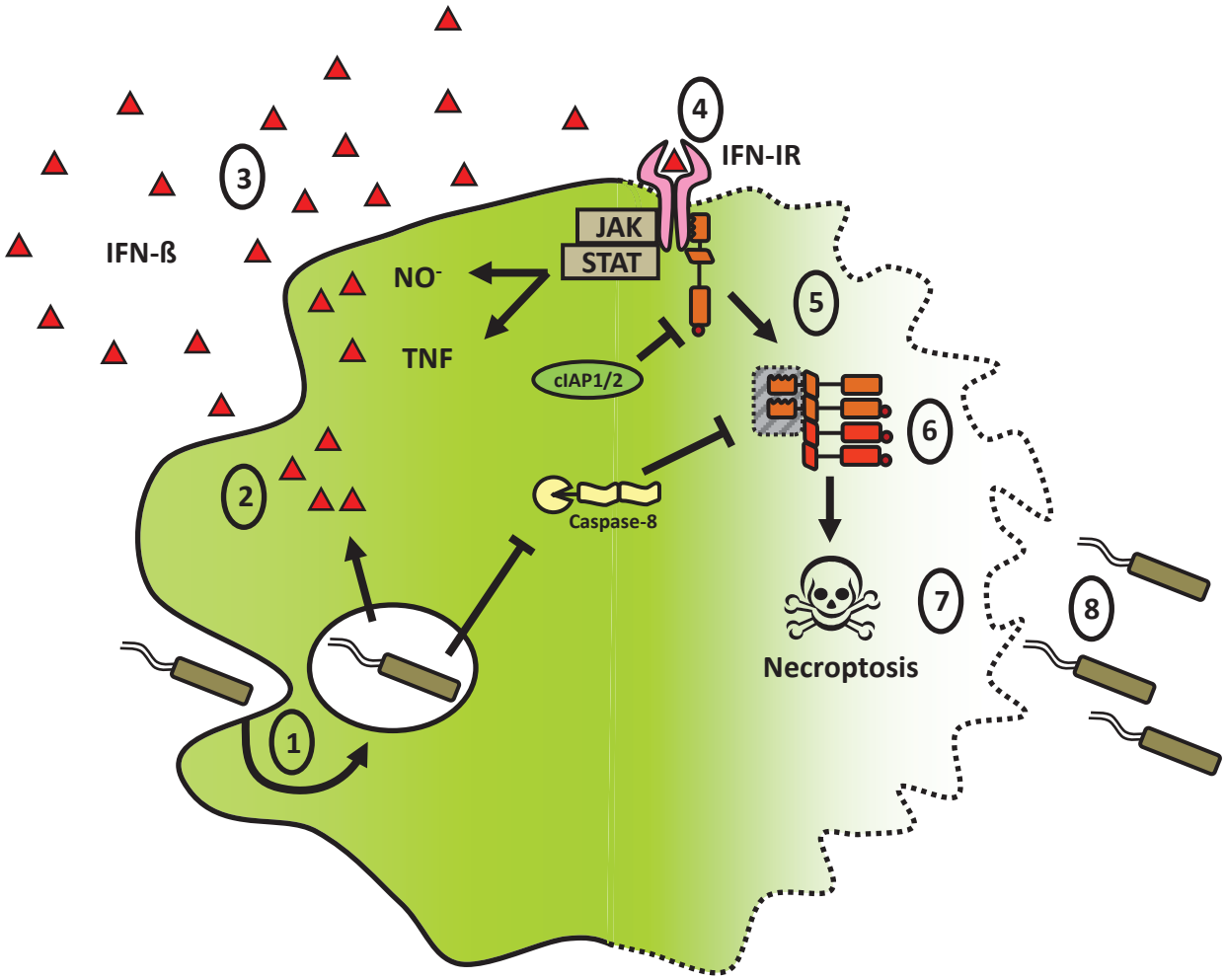
4
IFN-IR
3
IFN-ß
JAK
STAT
NO-
TNF
5
cIAP1/2
6
2
Caspase-8
7
8
Necroptosis
1

The *in vivo* relevance of necroptosis has been an important question since its identification of the specific mechanisms behind this cell death pathway. Newly published data shows that Rip3-deficient mice are resistant to systemic shock as induced by TNF injection or caecal ligation and puncture[258]. Given this view of necroptosis as a driver of systemic shock, I wanted to probe what role interferon might play in this effect. Intraperitoneal injection of LPS/zVAD led to significantly more cell death of macrophages in WT than IFNAR$^{-/-}$ mice (Fig. 33C). In addition, while WT mice were largely moribund, IFNAR mice showed drastically reduced symptoms at 18 hours after LPS/zVAD injection. These results lead to the highly novel conclusion that type-I interferon-induced necroptosis may constitute a significant factor in the pathology of acute systemic shock.

While work in our lab has recently confirmed Rip1 association with the IFNAR receptor complex (see [285]), it remains unclear what signaling component of the type-I interferon signaling complex might be responsible for the induction of Rip1 phosphorylation and necroptosis. To our knowledge, none of the key signaling kinases (JAK, Tyk2, STATs) have been previously found in association with Rip1 kinase. Several of these downstream mediators of IFNAR have however been implicated in the induction of sepsis. Mice deficient in the signaling components Tyk2 or STAT1 have been shown to be somewhat protected against septic shock[335]. JAK inhibitors have also been shown to have an inhibitory effect on septic shock[336]. STAT1 has previously been shown to be involved in a form of LPS-induced caspase-independent cell death within macrophages[337]. We are currently addressing which specific component(s) of IFNAR signaling machinery may be involved in the phosphorylation of Rip1 kinase.

There is strong evidence to support a role for type-I interferon in septic shock. Several publications have for instance shown that IFNAR-deficient mice are highly resistant to injection of TNF-α[338] or LPS[339,340]. Signaling components upstream of the production of type-I interferon, such

as IRF3[341] or TRIF[342], have also been shown to protect against LPS endotoxemia. TNFR1 deficient mice are not similarly protected from endotoxemia[343], underlining the importance of type-I interferon signaling specifically. Despite the abundance of evidence implicating type-I IFN signaling in endotoxic shock, a viable mechanism has not yet emerged to explain how interferon mediates this effect[344].

Fascinatingly, mice deficient in IFNAR signaling do not appear to have any significant defects in the early production of the inflammatory mediators (IL-6, IL1β, IL-12, NO or TNF) which occurs in response to LPS injection, despite their strong protection from death[335]. Recently, IFN-β-induced JAK signaling has been implicated in LPS-induced release of another key player in sepsis, HMGB1[336]. Elevated serum levels of HMGB1 are commonly seen in septic patients[345], and blocking HMGB1 has been shown to be somewhat protective in the mouse LPS injection model[346]. While HMGB1 is generally accepted as a key component in acute inflammation induced during sepsis[233], a mechanism for such massive release of this intracellular DAMP following endotoxic shock has also not yet been identified. The ability of interferon to induce necroptosis, which I have identified here, represents a highly novel mechanism by which such a release of HMGB1 could be occurring. Given the ability of HMGB1 released from necrotic cells to signal through TLR4, I speculate that it may be possible that HMGB1 itself acts to feedback and promote activation of necroptosis.

The discovery that type-I interferon signaling can directly induce Rip1 phosphorylation and necroptotic cell death potentially represents an important paradigm shift in the understanding of systemic shock. Based on this I propose the following temporal model of endotoxic shock: (1) exposure of innate immune cells to LPS initiates necroptotic pathway by inducing phosphorylation of Rip1 kinase, (2) activation of TRIF dependent signaling drives release of interferon-beta, (3) signaling through IFNAR directly activates Rip1 phosphorylation, potentially through as of yet

unknown mediators, (4) prolonged activation of the Rip1/Rip3 necrosome drives necroptotic cell death, (5) this leads to the extracellular release of inflammatory DAMPs such as HMGB1, driving intense inflammatory feedback (see Figure 45 for model).

Sepsis is clinically a highly significant disease. In Canada, approximately 9300 people die every year from sepsis, making up approximately 10% of all hospital deaths[347]. Despite this, there exist few effective strategies to deal with sepsis. Currently, standard protocol dictates that intravenous antibiotics should be administered as soon as a diagnosis of sepsis is made[348]. To date, no effective anti-inflammatory intervention has been developed to treat sepsis, although many are in development[349]. Targeting type-I interferon signaling has been suggested as a candidate for treatment of sepsis[344]. The identification of the molecular mechanism by which type-I interferon can induce inflammatory necrotic cell death may lead to novel treatment strategies for sepsis. For instance, significant synergistic effect might be achieved by combinatorial targeting of both the interferon pathway and the necrosome.

This novel mechanism of action of interferon may also lead to understanding of the clinical action of interferon therapy. Type-I interferon is utilized in a wide variety of diseases, ranging from Hepatitis C infection, to multiple sclerosis, and cancer[350]. Examining the possibility that type-1 interferon-induced necroptosis may play a therapeutic role in treatment of these diseases could lead to an improved understanding of these diseases more generally. For instance, is the induction of necroptosis a viable strategy for the removal of cancer cells? Perhaps this alternative form of inflammatory death may be desirable for cells that have escaped the normal processes of apoptotic death. In this case, combining interferon therapy with zVAD or SMAC mimetics may be a viable strategy to improve this type of cell death. Similarly, these types of strategies could potentially be employed to improve clearance of viral infection.

Figure 45: *The role of interferon in LPS/zVAD induced necroptosis.* Similarly to ST infection, induction of necroptosis via LPS/zVAD requires the release of type-I interferon for the activation of necroptosis. Upstream release of inflammatory cytokines is required for induction of necroptotic cell death.

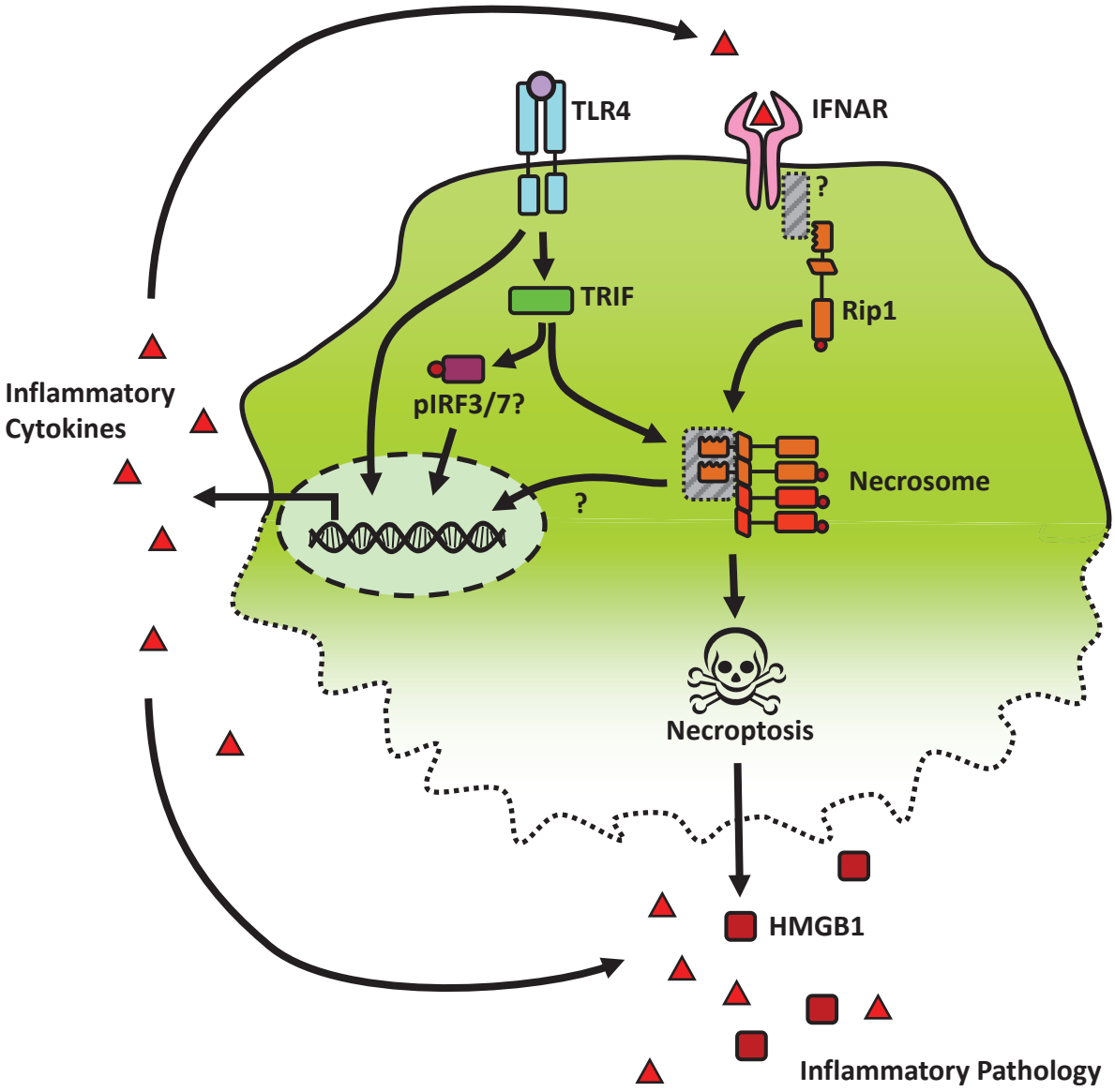
TLR4
IFNAR
?
TRIF
Rip1
pIRF3/7?
Inflammatory
Cytokines
Necrosome
?
Necroptosis
HMGB1
Inflammatory Pathology

5.4 THE REGULATION OF NECROPTOSIS BY CATHEPSINS

Innate immune cells, such as macrophages, must strike a careful balance between the need for cell death to prevent propagation of an infectious agent and the need to limit inflammatory cell death. Because necrotic cell death can lead to the release of potent intracellular danger signals, understanding the regulation of necroptosis may have important implications for the understanding of inflammation[211]. Currently, the prevailing model of inhibitory dampening of necroptotic signaling focuses on caspase-8 mediated cleavage of Rip1 kinase as the central mechanism[209,211]. As a novel addition to this, I have found that cysteine family cathepsins are also able to cleave Rip1 and regulate necroptosis in macrophages. Our data thus reveals that the dual-inhibitory effects of zVAD on both cathepsins and caspase-8 may explain why zVAD is such a potent inducer of necroptosis, while other caspase inhibitors fail to do so. Cathepsins acting as a backup mechanism to limit necroptosis makes biological sense, since redundant mechanisms to limit acute inflammation would likely be advantageous.

The process of zVAD-induced necroptosis has been observed in a number of different cell lines. A potent induction of necroptosis generally requires either exogenous [351] or autocrine TNFα signaling [256]. In macrophages specifically, zVAD has been shown to induce cell death in the RAW264.1 cell line, although the mechanism of death was not clear [287]. In bone marrow macrophages, I observe that zVAD alone drives necroptosis, which was dependent on autocrine TNF-α signaling (Fig. 34). I go on to show that LPS/zVAD stimulation is able to stimulate TNFR-independent necroptosis in macrophages (Fig. 35), as has recently been reported[226].

Stimulation of macrophages with LPS was able to initiate phosphorylation of Rip1 independently of zVAD. However, the addition of zVAD was necessary to drive downstream

phosphorylation of Rip3 and lead to necroptosis. I also demonstrate that the LPS-TRIF pathway specifically drives Rip1 activation, similarly to what has been described in the literature[226]. This indicates that caspase-8 does not appear to regulate the upstream activation of Rip1, but specifically inhibits the activation of the necrosome complex and phosphorylation of Rip3.

Interestingly, while zVAD was able to induce necroptosis, I found that a caspase-8 specific inhibitor, z-IETD-FMK (zIETD), did not result in cell death. A similar observation in L929 cells was previously ascribed to a lack of stimulation of autocrine TNF-α production with caspase 8 inhibitor (zIETD) relative to pan-caspase inhibitor (zVAD)[256]. Inconsistent with this explanation, the addition of LPS is able to drive necroptosis independently of TNF-α in our model. Even in combination with this exogenous signaling from LPS, zIETD fails to induce necroptosis. Given this fact, I questioned whether the lack of induction of necroptosis by zIETD indicates that alternative targets are being inhibited by zVAD in addition to caspase-8.

In examining the expression of Rip1 during necroptosis, I consistently observed smaller bands, which reacted with our anti-Rip1 antibody. Upon treatment with zVAD I saw a significant reduction in these bands, leading us to conclude that they were likely cleavage fragments of Rip1 kinase. In contrast to zVAD, treatment with zIETD did not affect the cleaved Rip1 forms. In addition to its effects on caspases, zVAD has been demonstrated to also inhibit cysteine protease family cathepsins, such as cathepsin B and S[352]. Thus I tested the application of targeted cathepsin inhibitors to macrophages. While zIETD failed to affect the level of cleaved Rip1, the addition of a pan cysteine cathepsin/calpain inhibitor, E64D, resulted in a total abrogation of cleaved Rip1 (Fig. 36). This data indicated that cathepsins could potentially be cleaving Rip1 kinase in macrophages.

Confirming the role of cathepsins in Rip1 cleavage, I also observed decreased cleavage of Rip1 using siRNA knockdown of either cathepsin S or B (Fig. 37A). Knockdown also resulted in a small

but significant increase in sensitivity to zVAD-induced necroptosis, whereas knockdown of calpain resulted in reduced necroptotic response (Fig. 37B). I also treated cathepsin S- or cathepsin B-deficient macrophages with zVAD and LPS, wherein I observed no significant change in the sensitivity to necroptosis induced by zVAD (Fig. 38). This data suggests that cysteine cathepsins may act redundantly to regulate Rip1 kinase. Consistent with such a model, single knockout mice for either cathepsin S or B show no defects in development or immune response[290]. Interestingly, double knockout mice for cathepsin B and cathepsin L die in the second to fourth week of postnatal due to overactive cell death in the brain[353].

Cell-free cleavage experiments, in collaboration with Dr. Shutinoski within the Sad lab, clearly show that at neutral pH, cysteine family cathepsins are able to directly cleave Rip1, producing fragments consistent with those observed in macrophages. I also observed some cleavage of Rip1 kinase with cathepsin L, but it was relatively inefficient in comparison to that observed with cathepsin S or B. Given the size of the Rip1 kinase fragments observed, I estimate that the most prominent cleavage of Rip1 likely occurs in the 310-340 amino acid range. This may be consistent with a predicted cathepsin B site at position 330-335 (Fig. 40A) [354]. Prediction for cathepsin S sites was unavailable. At this time it is unclear exactly how cleavage of Rip1 effects necroptotic signaling given that the pool of full-length Rip1 remains relatively unchanged.

Cathepsins have previously been thought of as aggressive proteases, which once released from the lysosomes will mediate rapid proteolytic breakdown of the cell[355]. While, massive cathepsin release may result in necrosis under some conditions[356], slow release of cathepsins actually results in selective cleavage of few targets[357]. Specifically, controlled lysosomal breakdown enhances apoptotic cell death via cathepsin-mediated cleavage of Bid into its pro-apoptotic form[358,359]. In the case of necroptosis, cathepsins have been proposed to aid in rapid cellular disintegration[230], but

specific data supporting this assertion is limited. In contrast with this, I show that inhibition of cysteine cathepsins actually drove a subtle but significant increase in necroptosis within macrophages. The minimal effect observed in zVAD necroptosis is likely due to the fact that zVAD already inhibits cathepsins[352], and this may not be a limiting factor in the cell death observed. In contrast to the subtle effects on zVAD-induced death, cathepsin inhibitors resulted in significant macrophage necroptosis when combined with a specific caspase-8 inhibitor. Taken together, these data lead to the surprising conclusion that cathepsins function to actively suppress necroptosis through cleavage of Rip1 kinase.

In our western blot analysis, Rip1 cleavage products appear to be predominantly formed by cathepsins, raising the question of how caspase-8 contributes to regulating necroptosis in macrophages. Caspase-8 is undoubtedly linked to control of necroptosis in hematopoiesis during fetal development [106]. Cleavage of Rip1-kinase by caspase-8 was identified before the role of Rip1 in non-apoptotic cell death was discovered [309], and has since been repeatedly confirmed[360]. Given that FADD is thought to recruit caspase-8 to the necrosome after activation[150], I hypothesize that caspase-8 may act as more downstream regulator of necroptosis after Rip1 phosphorylation. In contrast, I observe cathepsin mediated cleavage in macrophages under steady-state conditions, indicating that this may be a more upstream mode of regulating Rip1 activity. Given that the cleavage sites are after the kinase domain and that these cleaved forms persist within the cells, it seems plausible that Rip1 cleaved forms may interact with and inhibit the formation of the necrosome. Further work will be needed to elucidate how proteolysis by cathepsins and caspase-8 regulates necroptosis (see Figure 46 for model).

The idea of cathepsins acting as anti-necroptotic factors is a surprising finding, yet given a newly defined role of cathepsins in the apoptotic program, it seems to fit well into the paradigm of

Figure 46: *The positive and negative regulators of necroptosis.* Through the experiments reported in this thesis we have uncovered a number of novel positive and negative regulators of necroptosis. Signaling through TNFR, IFNAR and TLR4 have all been demonstrated to be competent inducers of Rip1 activation. Caspase-8 is a key inhibitor of necroptosis, preventing the activation of Rip3 kinase by Rip1. We have also shown that cIAPs appear to regulate TNFR mediated activation of necroptosis. We have also demonstrated that cathepsins appear to cleave and regulate the function of Rip1 kinase.

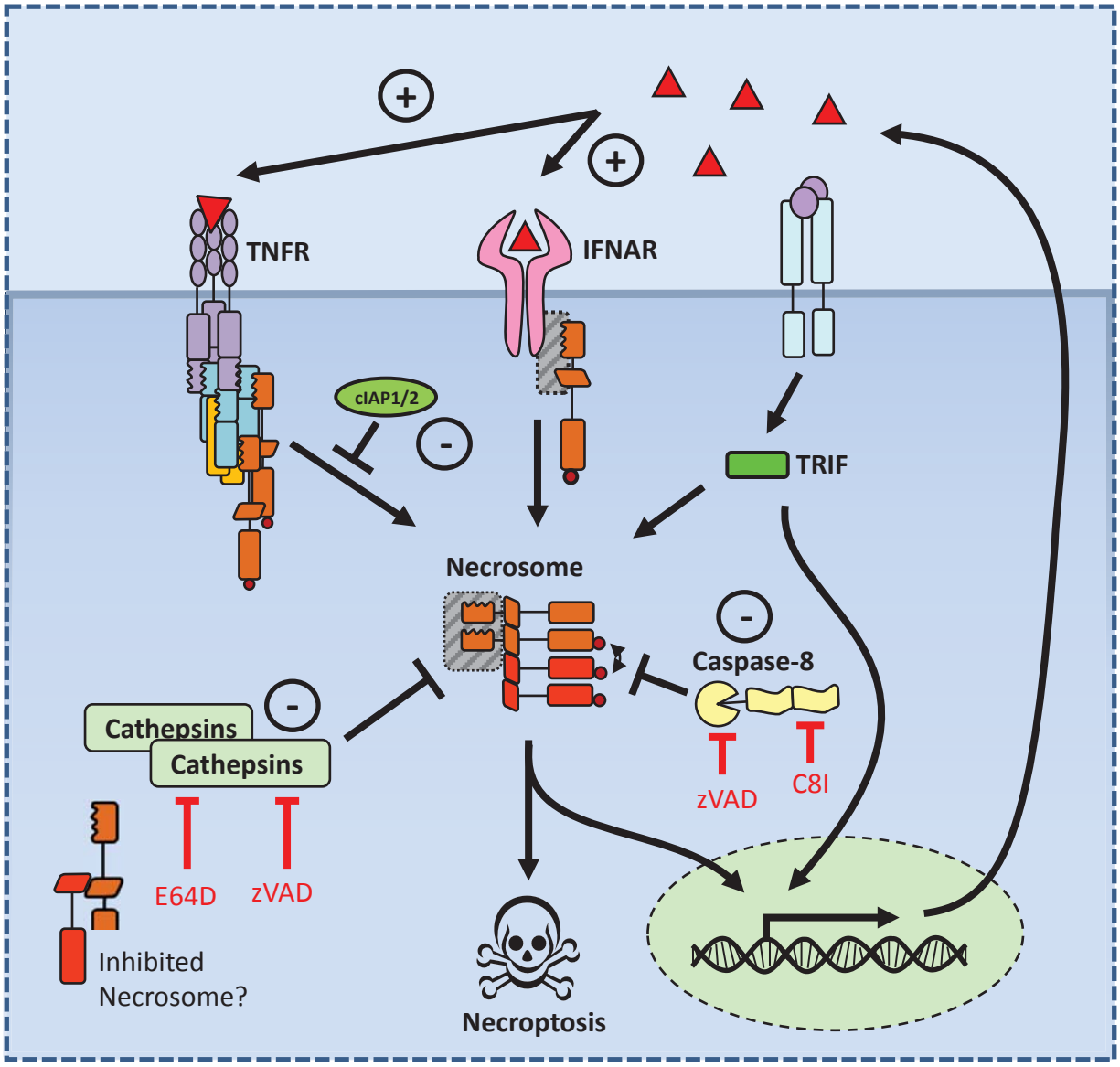
TNFR
IFNAR
cIAP1/2
TRIF
Necrosome
Caspase-8
zVAD
C8I
Cathepsins
Cathepsins
E64D
zVAD
Inhibited
Necrosome?
Necroptosis

pro-apoptotic factors acting to inhibit necroptosis. Interestingly, expression of both cathepsin S and B has been well documented at inflammatory sites in various disease models including pancreatitis [361], inflammatory bowel disease[362], and atherosclerosis[363]. It seems plausible that cathepsin mediated cleavage of Rip1 kinase could play a role in perpetuating macrophage survival and function within inflammatory sites. In addition to this, elevated expression of cathepsins has repeatedly been shown to be a marker for enhanced tumourigenicity and poor prognosis[289]. Given the novel role I have identified for cathepsins in cleaving Rip1 kinase and limiting macrophage necroptosis, it is an exciting possibility that cathepsins may function similarly to enhance resistance to necrotic cell death within cancer cells. Furthermore, using cathepsin inhibition to target macrophage function may represent a novel treatment modality for both cancer and inflammatory diseases.

6.0 CONCLUSION

In this doctoral work I have presented novel insights into the regulation of cell death mechanisms across different cell types, and different models of cell death *in vivo* and *in vitro*. In $CD8^+$ T cells, we show that caspase-3 is activated by antigen presentation. We also show that elevated expression of active caspase-3 is progressively lost throughout proliferation and differentiation of antigen stimulated $CD8^+$ T cells both *in vitro* and *in vivo*. We also support a model wherein caspase-3 does not play a significant role in the removal of antigen specific T cells during contraction. At this time, it remains unclear what the exact purpose of caspase activation is in the process of T cell activation, but it appears that inhibition of caspases does lead to increased cell death. **This work was published in 2010 in *PLoS One*[364].** While we realized that interaction with necroptosis was likely an important factor at the time, understanding of the mechanisms that regulated necroptosis were relatively naïve at the time, and still remain somewhat so.

Thus, in order to learn more about how Rip1 and Rip3 were regulated, we launched a project to investigate necroptosis in the much better characterized system of macrophage cell death. In studying this model, we provided novel evidence for the regulation of the necrosome by cIAPs. We show that cIAP1 and cIAP2 redundantly regulate necroptosis in macrophage cells. Through inducing a constitutive degradation of Rip1 and Rip3, the cIAPs limit the activation of the necrosome, cytokine production and cell death. We finally showed that loss of cIAP1 or cIAP2 activity leads to enhanced death of macrophages *in vivo*, and compromises immune responses to intracellular bacteria. **This work was published in *Cell Death and Differentiation* in 2012**[365]. This work has important implications for the understanding of SMAC mimetics, which are being hotly pursued as

cancer therapies. Better understanding of how cIAPs regulate the necrosome may lead to new synergistic strategies to kill cancer cells.

We next investigated the role of necroptosis in *Salmonella typhimurium*, quickly realizing that necroptotic cell death of macrophages might be a significant consideration in this infection model as well. Rebecca Mulligan and Dr. Nirmal Robinson were working on the role of IFNAR in *Salmonella* infection at this time. The realization that type-I interferon can induce necroptosis in macrophages was instantly a very exciting proposition. Key work to show the specific role of IFNAR in activating Rip1 phosphorylation was performed in collaboration with Dr. Robinson. **We published the paper "Type I interferon induces necroptosis in macrophages during infection with *Salmonella enterica* serovar typhimurium" in 2012 in *Nature Immunology***[285].

The work showing that IFNAR is also required for LPS/zVAD-induced necroptosis is very recent work. *In vivo* work showing a stark difference in reaction to LPS/zVAD treatment in IFNAR and WT mice led us to recognize that interferon-induced necroptosis may be a key mechanism in the pathology of septic shock. This work is currently ongoing in collaboration with Justyna Startek and Erin Cessford, graduate students in the lab of Dr.Sad. We have made several key discoveries in regards to the regulation of necrosome activity by type-I interferon signaling, and we hope to publish this work in the near future. This work not only has the exciting potential to transform the current understanding of sepsis, but will also lead to new understanding of the mechanism of type-I interferons in general, as outlined in the discussion section.

The final section of the project was initiated in late 2011, following my observation of key cleavage bands of Rip1, which disappeared with zVAD treatment. We provide highly novel evidence that cysteine cathepsins are implicated in the regulatory cleavage of Rip1 kinase activity. Only by inhibiting both caspase-8 and cathepsins can necroptosis be-induced efficiently within

macrophages. The work to show that recombinant Rip1 can be directly cleaved by cathepsins was performed in collaboration with Dr. Bojan Shutinoski. Significant technical help was also received from Susan Thurston for this project. We are currently making efforts to identify the specific cleavage sites targeted by the cathepsin proteases. We have prepared the manuscript for this project and hope to submit it soon. This work may have important implications for the understanding of inflammation and cancer, as elevated expression of cathepsins has been consistently associated with these pathologies.

In follow up to the project presented here, I feel it would be highly interesting to return to the model of CD8+ T cell activation. Having become relatively adept at identifying the phosphorylation states of Rip1 and Rip3 kinases, it would be intriguing to examine what effect various stimuli have on Rip activity within CD8+ T cells. The application of specific inhibitors of caspases and other pathways could also be helpful in interrogating the glaring question – Why are caspases activated in proliferating and differentiating cells? There are also interesting connections between caspases, the necrosome and cellular metabolism, which could lead to interesting work.

Immune cells have the ability to rapidly proliferate in response to pathogens or cellular damage. At the same time immune cells must maintain a balance to prevent their own overgrowth, and remove cells if and when they are no longer needed. This is why immune cells have evolved a specialized balance of cell death, not typically seen in other cells of the body. It is for this reason that my own study of cell death in immune cells has so often led to unexpected and surprising results. While this paradoxical nature has often been confounding, it has also made for an exciting scientific project. Through my work with Dr. Sad, I hope that we have been able to add some small pieces to scientific understanding of cell death and immune function.

REFERENCES

1. Engelberg-Kulka, H., Amitai, S., Kolodkin-Gal, I. & Hazan, R. Bacterial Programmed Cell Death and Multicellular Behavior in Bacteria. *PLoS Genet* **2,** e135 (2006).
2. Lewis, K. Programmed Death in Bacteria. *Microbiol. Mol. Biol. Rev.* **64,** 503–514 (2000).
3. Rock, K. L. & Kono, H. The inflammatory response to cell death. *Annu Rev Pathol* **3,** 99–126 (2008).
4. Falk, M. *et al.* Caspase inhibition blocks human T cell proliferation by suppressing appropriate regulation of IL-2, CD25, and cell cycle-associated proteins. *Journal of Immunology* **173,** 5077–5085 (2004).
5. Lamkanfi, M., Festjens, N., Declercq, W., Berghe, T. V. & Vandenabeele, P. Caspases in cell survival, proliferation and differentiation. *Cell Death and Differentiation* **14,** 44–55 (2007).
6. Badovinac, V. P., Porter, B. B. & Harty, J. T. Programmed contraction of CD8+ T cells after infection. *Nature Immunology* **3,** 619–626 (2002).
7. Weant, A. E. *et al.* Apoptosis Regulators Bim and Fas Function Concurrently to Control Autoimmunity and CD8+ T Cell Contraction. *Immunity* **28,** 218–230 (2008).
8. Janeway, C. A. & Medzhitov, R. Innate Immune Recognition. *Annu. Rev. Immunol.* **20,** 197–216 (2002).
9. Murphy, K. P., Travers, P., Walport, M. & Janeway, C. *Janeway's immunobiology*. (Garland Science, 2008).
10. Champion, J. A., Walker, A. & Mitragotri, S. Role of particle size in phagocytosis of polymeric microspheres. *Pharm. Res.* **25,** 1815–1821 (2008).
11. Aderem, A. & Underhill, D. M. Mechanisms of Phagocytosis in Macrophages. *Annual Review of Immunology* **17,** 593–623 (1999).
12. Takeuchi, O. & Akira, S. Pattern Recognition Receptors and Inflammation. *Cell* **140,** 805–820 (2010).
13. Murray, P. J. & Wynn, T. A. Protective and pathogenic functions of macrophage subsets. *Nat Rev Immunol* **11,** 723–737 (2011).
14. Soehnlein, O. & Lindbom, L. Phagocyte partnership during the onset and resolution of inflammation. *Nature Reviews Immunology* **10,** 427–439 (2010).
15. LeVine, A. M., Reed, J. A., Kurak, K. E., Cianciolo, E. & Whitsett, J. A. GM-CSF-deficient mice are susceptible to pulmonary group B streptococcal infection. *J. Clin. Invest.* **103,** 563–569 (1999).
16. Zhan, Y., Lieschke, G. J., Grail, D., Dunn, A. R. & Cheers, C. Essential roles for granulocyte-macrophage colony-stimulating factor (GM-CSF) and G-CSF in the sustained hematopoietic response of Listeria monocytogenes-infected mice. *Blood* **91,** 863–869 (1998).
17. Burnett, S. H. *et al.* Conditional macrophage ablation in transgenic mice expressing a Fas-based suicide gene. *J Leukoc Biol* **75,** 612–623 (2004).
18. O'Brien, A. D., Metcalf, E. S. & Rosenstreich, D. L. Defect in macrophage effector function confers Salmonella typhimurium susceptibility on C3H/HeJ mice. *Cellular Immunology* **67,** 325–333 (1982).
19. O'Brien, A. D., Scher, I. & Formal, S. B. Effect of silica on the innate resistance of inbred mice to Salmonella typhimurium infection. *Infect. Immun.* **25,** 513–520 (1979).
20. Hamano, S. *et al.* Role of macrophages in acute murine cytomegalovirus infection. *Microbiol. Immunol.* **42,** 607–616 (1998).

21. Roscic-Mrkic, B. *et al.* Roles of Macrophages in Measles Virus Infection of Genetically Modified Mice. *J Virol* **75,** 3343–3351 (2001).
22. Fink, K. *et al.* Depletion of macrophages in mice results in higher dengue virus titers and highlights the role of macrophages for virus control. *Eur. J. Immunol.* **39,** 2809–2821 (2009).
23. Mishalian, I. *et al.* Recruited macrophages control dissemination of group A Streptococcus from infected soft tissues. *J. Immunol.* **187,** 6022–6031 (2011).
24. Salcedo, S. P., Noursadeghi, M., Cohen, J. & Holden, D. W. Intracellular replication of Salmonella typhimurium strains in specific subsets of splenic macrophages in vivo. *Cell. Microbiol.* **3,** 587–597 (2001).
25. Drevets, D. A. Dissemination of Listeria monocytogenes by infected phagocytes. *Infect. Immun.* **67,** 3512–3517 (1999).
26. Moazed, T. C., Kuo, C. C., Grayston, J. T. & Campbell, L. A. Evidence of systemic dissemination of Chlamydia pneumoniae via macrophages in the mouse. *J. Infect. Dis.* **177,** 1322–1325 (1998).
27. Kimura, T., Sasaki, M., Okumura, M., Kim, E. & Sawa, H. Flavivirus Encephalitis Pathological Aspects of Mouse and Other Animal Models. *Vet Pathol* **47,** 806–818 (2010).
28. Short, K. R., Brooks, A. G., Reading, P. C. & Londrigan, S. L. The fate of influenza A virus after infection of human macrophages and dendritic cells. *J. Gen. Virol.* **93,** 2315–2325 (2012).
29. Koppensteiner, H., Brack-Werner, R. & Schindler, M. Macrophages and their relevance in Human Immunodeficiency Virus Type I infection. *Retrovirology* **9,** 82 (2012).
30. Monack, D. M., Bouley, D. M. & Falkow, S. Salmonella typhimurium persists within macrophages in the mesenteric lymph nodes of chronically infected Nramp1+/+ mice and can be reactivated by IFNgamma neutralization. *J. Exp. Med.* **199,** 231–241 (2004).
31. Peyron, P. *et al.* Foamy Macrophages from Tuberculous Patients' Granulomas Constitute a Nutrient-Rich Reservoir for M. tuberculosis Persistence. *PLoS Pathog* **4,** e1000204 (2008).
32. Cailhier, J. F. *et al.* Conditional Macrophage Ablation Demonstrates That Resident Macrophages Initiate Acute Peritoneal Inflammation. *J Immunol* **174,** 2336–2342 (2005).
33. Stoneman, V. *et al.* Monocyte/Macrophage Suppression in CD11b Diphtheria Toxin Receptor Transgenic Mice Differentially Affects Atherogenesis and Established Plaques. *Circulation Research* **100,** 884–893 (2007).
34. Sone, Y., Serikov, V. B. & Staub, N. C., Sr. Intravascular macrophage depletion attenuates endotoxin lung injury in anesthetized sheep. *J. Appl. Physiol.* **87,** 1354–1359 (1999).
35. Salkowski, C. A. *et al.* Effect of liposome-mediated macrophage depletion on LPS-induced cytokine gene expression and radioprotection. *J Immunol* **155,** 3168–3179 (1995).
36. Barrera, P. *et al.* Synovial macrophage depletion with clodronate-containing liposomes in rheumatoid arthritis. *Arthritis Rheum.* **43,** 1951–1959 (2000).
37. Ren, W. *et al.* Macrophage depletion diminishes implant-wear-induced inflammatory osteolysis in a mouse model. *J Biomed Mater Res A* **85,** 1043–1051 (2008).
38. Monie, T. P. Activating immunity: lessons from the TLRs and NLRs. *Trends in Biochemical Sciences* **34,** 553–561 (2009).
39. Wesche, H., Henzel, W. J., Shillinglaw, W., Li, S. & Cao, Z. MyD88: an adapter that recruits IRAK to the IL-1 receptor complex. *Immunity* **7,** 837–847 (1997).
40. Li, S., Strelow, A., Fontana, E. J. & Wesche, H. IRAK-4: A novel member of the IRAK family with the properties of an IRAK-kinase. *PNAS* **99,** 5567–5572 (2002).

41. Sun, L., Deng, L., Ea, C.-K., Xia, Z.-P. & Chen, Z. J. The TRAF6 ubiquitin ligase and TAK1 kinase mediate IKK activation by BCL10 and MALT1 in T lymphocytes. *Mol. Cell* **14,** 289–301 (2004).
42. Bettermann, K. *et al.* TAK1 Suppresses a NEMO-Dependent but NF-κB-Independent Pathway to Liver Cancer. *Cancer Cell* **17,** 481–496 (2010).
43. Perkins, N. D. Integrating cell-signalling pathways with NF-κB and IKK function. *Nature Reviews Molecular Cell Biology* **8,** 49–62 (2007).
44. Akira, S., Uematsu, S. & Takeuchi, O. Pathogen Recognition and Innate Immunity. *Cell* **124,** 783–801 (2006).
45. Smale, S. T. Hierarchies of NF-κB target-gene regulation. *Nature Immunology* **12,** 689–694 (2011).
46. Honda, K. & Taniguchi, T. IRFs: master regulators of signalling by Toll-like receptors and cytosolic pattern-recognition receptors. *Nature Reviews Immunology* **6,** 644–658 (2006).
47. Hanada, T. & Yoshimura, A. Regulation of cytokine signaling and inflammation. *Cytokine Growth Factor Rev.* **13,** 413–421 (2002).
48. Feldmann, M. & Saklatvala, J. Proinflammatory cytokines. *Cytokine Ref* **1,** 291–305 (2001).
49. Yoshimura, A., Naka, T. & Kubo, M. SOCS proteins, cytokine signalling and immune regulation. *Nature Reviews Immunology* **7,** 454–465 (2007).
50. Murdoch, C., Muthana, M. & Lewis, C. E. Hypoxia Regulates Macrophage Functions in Inflammation. *The Journal of Immunology* **175,** 6257 –6263 (2005).
51. Dehne, N. & Brüne, B. HIF-1 in the inflammatory microenvironment. *Experimental Cell Research* **315,** 1791–1797 (2009).
52. Ando, M. *et al.* Interleukin 6 enhances glycolysis through expression of the glycolytic enzymes hexokinase 2 and 6-phosphofructo-2-kinase/fructose-2,6-bisphosphatase-3. *J Nippon Med Sch* **77,** 97–105 (2010).
53. Berg, S., Sappington, P. L., Guzik, L. J., Delude, R. L. & Fink, M. P. Proinflammatory cytokines increase the rate of glycolysis and adenosine-5'-triphosphate turnover in cultured rat enterocytes. *Crit. Care Med* **31,** 1203–1212 (2003).
54. Ben-Shlomo, I. *et al.* Interleukin (IL)-1beta increases glucose uptake and induces glycolysis in aerobically cultured rat ovarian cells: evidence that IL-1beta may mediate the gonadotropin-induced midcycle metabolic shift. *Endocrinology* **138,** 2680–2688 (1997).
55. Kominsky, D. J., Campbell, E. L. & Colgan, S. P. Metabolic Shifts in Immunity and Inflammation. *The Journal of Immunology* **184,** 4062 –4068 (2010).
56. Matarese, G. & La Cava, A. The intricate interface between immune system and metabolism. *Trends in Immunology* **25,** 193–200 (2004).
57. Vander Heiden, M. G., Cantley, L. C. & Thompson, C. B. Understanding the Warburg Effect: The Metabolic Requirements of Cell Proliferation. *Science* **324,** 1029–1033 (2009).
58. Buchakjian, M. R. & Kornbluth, S. The engine driving the ship: metabolic steering of cell proliferation and death. *Nat Rev Mol Cell Biol* **11,** 715–727 (2010).
59. Forman, H. J. & Torres, M. Reactive Oxygen Species and Cell Signaling: Respiratory Burst in Macrophage Signaling. *Am. J. Respir. Crit. Care Med.* **166,** S4–8 (2002).
60. Thannickal, V. J. & Fanburg, B. L. Reactive oxygen species in cell signaling. *American Journal of Physiology - Lung Cellular and Molecular Physiology* **279,** L1005 –L1028 (2000).
61. Halliwell, B. in *eLS* (John Wiley & Sons, Ltd, 2001). at <http://onlinelibrary.wiley.com/doi/10.1038/npg.els.0003913/abstract>

62. Naik, E. & Dixit, V. M. Mitochondrial reactive oxygen species drive proinflammatory cytokine production. *J Exp Med* **208,** 417–420 (2011).
63. Wen, H., Ting, J. P.-Y. & O'Neill, L. A. J. A role for the NLRP3 inflammasome in metabolic diseases—did Warburg miss inflammation? *Nature Immunology* **13,** 352–357 (2012).
64. Henninger, D. D. *et al.* Cytokine-induced VCAM-1 and ICAM-1 expression in different organs of the mouse. *J Immunol* **158,** 1825–1832 (1997).
65. Osiak, A., Utermöhlen, O., Niendorf, S., Horak, I. & Knobeloch, K.-P. ISG15, an interferon-stimulated ubiquitin-like protein, is not essential for STAT1 signaling and responses against vesicular stomatitis and lymphocytic choriomeningitis virus. *Mol. Cell. Biol.* **25,** 6338–6345 (2005).
66. Lenschow, D. J. *et al.* Identification of interferon-stimulated gene 15 as an antiviral molecule during Sindbis virus infection in vivo. *J. Virol.* **79,** 13974–13983 (2005).
67. Silverman, R. H. Viral encounters with 2',5'-oligoadenylate synthetase and RNase L during the interferon antiviral response. *J. Virol.* **81,** 12720–12729 (2007).
68. Sadler, A. J. & Williams, B. R. G. Interferon-inducible antiviral effectors. *Nat. Rev. Immunol.* **8,** 559–568 (2008).
69. Chawla-Sarkar, M. *et al.* Apoptosis and interferons: role of interferon-stimulated genes as mediators of apoptosis. *Apoptosis* **8,** 237–249 (2003).
70. Fuertes Marraco, S. A. *et al.* Type I Interferon Drives Dendritic Cell Apoptosis via Multiple BH3-Only Proteins following Activation by PolyIC In Vivo. *PLoS ONE* **6,** e20189 (2011).
71. Lokshin, A., Mayotte, J. E. & Levitt, M. L. Mechanism of Interferon Beta-Induced Squamous Differentiation and Programmed Cell Death in Human Non—Small—Cell Lung Cancer Cell Lines. *JNCI J Natl Cancer Inst* **87,** 206–212 (1995).
72. Juang, S.-H. *et al.* IFN-beta induces caspase-mediated apoptosis by disrupting mitochondria in human advanced stage colon cancer cell lines. *J. Interferon Cytokine Res.* **24,** 231–243 (2004).
73. Zychlinsky, A. & Sansonetti, P. Perspectives series: host/pathogen interactions. Apoptosis in bacterial pathogenesis. *J Clin Invest* **100,** 493–495 (1997).
74. Hilbi, H., Zychlinsky, A. & Sansonetti, P. J. Macrophage apoptosis in microbial infections. *Parasitology* **115 Suppl,** S79–87 (1997).
75. Sansonetti, P. J. *et al.* Caspase-1 activation of IL-1beta and IL-18 are essential for Shigella flexneri-induced inflammation. *Immunity* **12,** 581–590 (2000).
76. Monack, D. M., Detweiler, C. S. & Falkow, S. Salmonella pathogenicity island 2-dependent macrophage death is mediated in part by the host cysteine protease caspase-1. *Cell. Microbiol.* **3,** 825–837 (2001).
77. Franchi, L., Eigenbrod, T., Muñoz-Planillo, R. & Nuñez, G. The inflammasome: a caspase-1-activation platform that regulates immune responses and disease pathogenesis. *Nat Immunol* **10,** 241–247 (2009).
78. Fink, S. L. & Cookson, B. T. Apoptosis, Pyroptosis, and Necrosis: Mechanistic Description of Dead and Dying Eukaryotic Cells. *Infect Immun* **73,** 1907–1916 (2005).
79. D M Monack, D. H. Salmonella exploits caspase-1 to colonize Peyer's patches in a murine typhoid model. *The Journal of experimental medicine* **192,** 249–58 (2000).
80. Lara-Tejero, M. *et al.* Role of the caspase-1 inflammasome in Salmonella typhimurium pathogenesis. *J. Exp. Med.* **203,** 1407–1412 (2006).

81. Raupach, B., Peuschel, S.-K., Monack, D. M. & Zychlinsky, A. Caspase-1-Mediated Activation of Interleukin-1? (IL-1?) and IL-18 Contributes to Innate Immune Defenses against Salmonella enterica Serovar Typhimurium Infection. *Infect Immun* **74,** 4922–4926 (2006).
82. Bergsbaken, T., Fink, S. L. & Cookson, B. T. Pyroptosis: host cell death and inflammation. *Nat Rev Microbiol* **7,** 99–109 (2009).
83. Ichinohe, T., Lee, H. K., Ogura, Y., Flavell, R. & Iwasaki, A. Inflammasome recognition of influenza virus is essential for adaptive immune responses. *J Exp Med* **206,** 79–87 (2009).
84. Broz, P. *et al.* Caspase-11 increases susceptibility to Salmonella infection in the absence of caspase-1. *Nature* **490,** 288–291 (2012).
85. Hueffer, K. & Galán, J. E. Salmonella-induced macrophage death: multiple mechanisms, different outcomes. *Cellular Microbiology* **6,** 1019–1025 (2004).
86. Hsu, L.-C. *et al.* The protein kinase PKR is required for macrophage apoptosis after activation of Toll-like receptor 4. *Nature* **428,** 341–345 (2004).
87. Stockinger, S. *et al.* Production of type I IFN sensitizes macrophages to cell death induced by Listeria monocytogenes. *J. Immunol.* **169,** 6522–6529 (2002).
88. Rayamajhi, M., Humann, J., Penheiter, K., Andreasen, K. & Lenz, L. L. Induction of IFN-αβ enables Listeria monocytogenes to suppress macrophage activation by IFN-γ. *J Exp Med* **207,** 327–337 (2010).
89. Haring, J. S., Badovinac, V. P. & Harty, J. T. Inflaming the CD8+ T cell response. *Immunity* **25,** 19–29 (2006).
90. Russell, J. H. & Ley, T. J. Lymphocyte-Mediated Cytotoxicity. *Annual Review of Immunology* **20,** 323–370 (2002).
91. Porter, B. B. & Harty, J. T. The Onset of CD8+-T-Cell Contraction Is Influenced by the Peak of Listeria monocytogenes Infection and Antigen Display. *Infect Immun* **74,** 1528–1536 (2006).
92. Harrington, L. E., Most Rv, R. van der, Whitton, J. L. & Ahmed, R. Recombinant vaccinia virus-induced T-cell immunity: quantitation of the response to the virus vector and the foreign epitope. *J. Virol.* **76,** 3329–3337 (2002).
93. Flynn, K. J. *et al.* Virus-specific CD8+ T cells in primary and secondary influenza pneumonia. *Immunity* **8,** 683–691 (1998).
94. Butz, E. A. & Bevan, M. J. Massive expansion of antigen-specific CD8+ T cells during an acute virus infection. *Immunity* **8,** 167–175 (1998).
95. Huster, K. M. *et al.* Unidirectional development of CD8+ central memory T cells into protective Listeria-specific effector memory T cells. *Eur. J. Immunol.* **36,** 1453–1464 (2006).
96. Cohen, P. L. & Eisenberg, R. A. Lpr and gld: single gene models of systemic autoimmunity and lymphoproliferative disease. *Annu. Rev. Immunol.* **9,** 243–269 (1991).
97. Salmena, L. *et al.* Essential role for caspase 8 in T-cell homeostasis and T-cell-mediated immunity. *Genes Dev.* **17,** 883–895 (2003).
98. Zhang, J., Kabra, N. H., Cado, D., Kang, C. & Winoto, A. FADD-deficient T cells exhibit a disaccord in regulation of the cell cycle machinery. *J. Biol. Chem.* **276,** 29815–29818 (2001).
99. Chun, H. J. *et al.* Pleiotropic defects in lymphocyte activation caused by caspase-8 mutations lead to human immunodeficiency. *Nature* **419,** 395–399 (2002).
100. Kuranaga, E. & Miura, M. Nonapoptotic functions of caspases: caspases as regulatory molecules for immunity and cell-fate determination. *Trends in Cell Biology* **17,** 135–144 (2007).

101. Fernando, P., Kelly, J. F., Balazsi, K., Slack, R. S. & Megeney, L. A. Caspase 3 activity is required for skeletal muscle differentiation. *PNAS* **99,** 11025–11030 (2002).
102. Sordet, O. *et al.* Specific involvement of caspases in the differentiation of monocytes into macrophages. *Blood* **100,** 4446–4453 (2002).
103. Zermati, Y. *et al.* Caspase Activation Is Required for Terminal Erythroid Differentiation. *J Exp Med* **193,** 247–254 (2001).
104. Ch'en, I. L. *et al.* Antigen-mediated T cell expansion regulated by parallel pathways of death. *Proceedings of the National Academy of Sciences of the United States of America* **105,** 17463–17468 (2008).
105. Ch'en, I. L., Tsau, J. S., Molkentin, J. D., Komatsu, M. & Hedrick, S. M. Mechanisms of necroptosis in T cells. *J Exp Med* **208,** 633–641 (2011).
106. Kaiser, W. J. *et al.* RIP3 mediates the embryonic lethality of caspase-8-deficient mice. *Nature* **471,** 368–372 (2011).
107. Kennedy, N. J., Kataoka, T., Tschopp, J. & Budd, R. C. Caspase activation is required for T cell proliferation. *J. Exp. Med.* **190,** 1891–1896 (1999).
108. Sabbagh, L., Bourbonnière, M., Sékaly, R.-P. & Cohen, L. Y. Selective up-regulation of caspase-3 gene expression following TCR engagement. *Mol. Immunol.* **42,** 1345–1354 (2005).
109. Nussbaum, A. K. & Whitton, J. L. The contraction phase of virus-specific CD8+ T cells is unaffected by a pan-caspase inhibitor. *J. Immunol.* **173,** 6611–6618 (2004).
110. Prlic, M. & Bevan, M. J. Exploring regulatory mechanisms of CD8+ T cell contraction. *PNAS* **105,** 16689–16694 (2008).
111. Pellegrini, M., Belz, G., Bouillet, P. & Strasser, A. Shutdown of an acute T cell immune response to viral infection is mediated by the proapoptotic Bcl-2 homology 3-only protein Bim. *PNAS* **100,** 14175–14180 (2003).
112. Erlacher, M. *et al.* Puma cooperates with Bim, the rate-limiting BH3-only protein in cell death during lymphocyte development, in apoptosis induction. *J Exp Med* **203,** 2939–2951 (2006).
113. Hughes, P. D. *et al.* Apoptosis Regulators Fas and Bim Cooperate in Shutdown of Chronic Immune Responses andÂ Prevention of Autoimmunity. *Immunity* **28,** 197–205 (2008).
114. Hutcheson, J. *et al.* Combined Deficiency of Proapoptotic Regulators Bim and Fas Results in the Early Onset of Systemic Autoimmunity. *Immunity* **28,** 206–217 (2008).
115. Majno, G. & Joris, I. Apoptosis, oncosis, and necrosis. An overview of cell death. *Am J Pathol* **146,** 3–15 (1995).
116. Oke, W. S. Practical Observations on Necrosis in the Long Bones. *Prov Med Surg J* **8,** 248–250 (1844).
117. Partington, C. F. *The British cyclopædia of the arts and sciences*. (Orr & Smith, 1835).
118. Heubner, O. *Experimental diphtheria*. (G.S. Davis, 1885).
119. Majno, G. & Joris, I. Apoptosis, oncosis, and necrosis. An overview of cell death. *Am J Pathol* **146,** 3–15 (1995).
120. Flemming, W. Flemming W: Uber die Bildung von Richtungsfiguren in Saugethiereiern beim Untergang Graaf'scher Follikel. *Arch Anat EntwGesch* 221–244 (1885).
121. Kerr, J. F. R., Wyllie, A. H. & Currie, A. R. Apoptosis: A Basic Biological Phenomenon with Wide-ranging Implications in Tissue Kinetics. *Br J Cancer* **26,** 239–257 (1972).
122. Festjens, N., Vanden Berghe, T. & Vandenabeele, P. Necrosis, a well-orchestrated form of cell demise: signalling cascades, important mediators and concomitant immune response. *Biochim. Biophys. Acta* **1757,** 1371–1387 (2006).

123. Kroemer, G. *et al.* Classification of cell death: recommendations of the Nomenclature Committee on Cell Death 2009. *Cell Death Differ* **16,** 3–11 (2008).
124. Elmore, S. Apoptosis: A Review of Programmed Cell Death. *Toxicol Pathol* **35,** 495–516 (2007).
125. Zhang, J. H. & Xu, M. DNA fragmentation in apoptosis. *Cell Research* **10,** 205–211 (2000).
126. Silva, M. T. Secondary necrosis: The natural outcome of the complete apoptotic program. *FEBS Letters* **584,** 4491–4499 (2010).
127. Guicciardi, M. E. & Gores, G. J. Life and death by death receptors. *FASEB J* **23,** 1625–1637 (2009).
128. Ashkenazi, A. Targeting death and decoy receptors of the tumour-necrosis factor superfamily. *Nature Reviews Cancer* **2,** 420–430 (2002).
129. Valmiki, M. G. & Ramos, J. W. Death effector domain-containing proteins. *Cell. Mol. Life Sci.* **66,** 814–830 (2009).
130. Scott, F. L. *et al.* The Fas–FADD death domain complex structure unravels signalling by receptor clustering. *Nature* **457,** 1019–1022 (2008).
131. Dickens, L. S., Powley, I. R., Hughes, M. A. & MacFarlane, M. The 'complexities' of life and death: Death receptor signalling platforms. *Experimental Cell Research* **318,** 1269–1277 (2012).
132. Varfolomeev, E. *et al.* Molecular determinants of kinase pathway activation by Apo2 ligand/tumor necrosis factor-related apoptosis-inducing ligand. *J. Biol. Chem.* **280,** 40599–40608 (2005).
133. Kang, T.-B. *et al.* Mutation of a Self-Processing Site in Caspase-8 Compromises Its Apoptotic but Not Its Nonapoptotic Functions in Bacterial Artificial Chromosome-Transgenic Mice. *J Immunol* **181,** 2522–2532 (2008).
134. Yang, S., Thor, A. D., Edgerton, S. & Yang, X. Caspase-3 mediated feedback activation of apical caspases in doxorubicin and TNF-α induced apoptosis. *Apoptosis* **11,** 1987–1997 (2006).
135. Kominami, K. *et al.* In Vivo Imaging of Hierarchical Spatiotemporal Activation of Caspase-8 during Apoptosis. *PLoS ONE* **7,** e50218 (2012).
136. Baud, V. & Karin, M. Signal transduction by tumor necrosis factor and its relatives. *Trends Cell Biol.* **11,** 372–377 (2001).
137. Micheau, O. & Tschopp, J. Induction of TNF Receptor I-Mediated Apoptosis via Two Sequential Signaling Complexes. *Cell* **114,** 181–190 (2003).
138. Festjens, N., Vanden Berghe, T., Cornelis, S. & Vandenabeele, P. RIP1, a kinase on the crossroads of a cell's decision to live or die. *Cell Death Differ* **14,** 400–410
139. Ea, C.-K., Deng, L., Xia, Z.-P., Pineda, G. & Chen, Z. J. Activation of IKK by TNFalpha requires site-specific ubiquitination of RIP1 and polyubiquitin binding by NEMO. *Mol. Cell* **22,** 245–257 (2006).
140. Zhang, H. *et al.* Functional complementation between FADD and RIP1 in embryos and lymphocytes. *Nature* **471,** 373–376 (2011).
141. Wong, W. W.-L. *et al.* RIPK1 is not essential for TNFR1-induced activation of NF-kappaB. *Cell Death Differ* **17,** 482–487 (2010).
142. Varfolomeev, E. *et al.* IAP Antagonists Induce Autoubiquitination of c-IAPs, NF-[kappa]B Activation, and TNF[alpha]-Dependent Apoptosis. *Cell* **131,** 669–681 (2007).
143. Vince, J. E. *et al.* IAP Antagonists Target cIAP1 to Induce TNFα-Dependent Apoptosis. *Cell* **131,** 682–693 (2007).

144. Petersen, S. L. *et al.* Autocrine TNFα Signaling Renders Human Cancer Cells Susceptible to Smac-Mimetic-Induced Apoptosis. *Cancer Cell* **12,** 445–456 (2007).
145. Gyrd-Hansen, M. & Meier, P. IAPs: from caspase inhibitors to modulators of NF-kappaB, inflammation and cancer. *Nat. Rev. Cancer* **10,** 561–574 (2010).
146. Annunziata, C. M. *et al.* Frequent Engagement of the Classical and Alternative NF-κB Pathways by Diverse Genetic Abnormalities in Multiple Myeloma. *Cancer Cell* **12,** 115–130 (2007).
147. Zhang, S. Q., Kovalenko, A., Cantarella, G. & Wallach, D. Recruitment of the IKK signalosome to the p55 TNF receptor: RIP and A20 bind to NEMO (IKKgamma) upon receptor stimulation. *Immunity* **12,** 301–311 (2000).
148. Wang, L., Du, F. & Wang, X. TNF-α Induces Two Distinct Caspase-8 Activation Pathways. *Cell* **133,** 693–703 (2008).
149. Chang, D. W. *et al.* c-FLIPL is a dual function regulator for caspase-8 activation and CD95-mediated apoptosis. *EMBO J* **21,** 3704–3714 (2002).
150. Dillon, C. P. *et al.* Survival function of the FADD-CASPASE-8-cFLIPL complex. *Cell Rep* **1,** 401–407 (2012).
151. Oberst, A. *et al.* Inducible Dimerization and Inducible Cleavage Reveal a Requirement for Both Processes in Caspase-8 Activation. *Journal of Biological Chemistry* **285,** 16632–16642 (2010).
152. Roos, W. P. & Kaina, B. DNA damage-induced cell death by apoptosis. *Trends in Molecular Medicine* **12,** 440–450 (2006).
153. Amaral, J. D., Xavier, J. M., Steer, C. J. & Rodrigues, C. M. The Role of p53 in Apoptosis. *Discovery Medicine* **9,** 145–152 (2010).
154. Tissue and cell-specific expression of the p53-target genes: bax, fas, mdm2 and waf1/p21, before and following ionising irradiation in mice. *Oncogene* **19,** (2000).
155. Reed, J. C. *et al.* BCL-2 family proteins: Regulators of cell death involved in the pathogenesis of cancer and resistance to therapy. *Journal of Cellular Biochemistry* **60,** 23–32 (1996).
156. Taylor, R. C., Cullen, S. P. & Martin, S. J. Apoptosis: controlled demolition at the cellular level. *Nat Rev Mol Cell Biol* **9,** 231–241 (2008).
157. Nomura, M. *et al.* 14-3-3 Interacts Directly with and Negatively Regulates Pro-apoptotic Bax. *J. Biol. Chem.* **278,** 2058–2065 (2003).
158. Strasser, A. The role of BH3-only proteins in the immune system. *Nature Reviews Immunology* **5,** 189–200 (2005).
159. Walensky, L. D. *et al.* A Stapled BID BH3 Helix Directly Binds and Activates BAX. *Molecular Cell* **24,** 199–210 (2006).
160. Martinez-Caballero, S. *et al.* Assembly of the Mitochondrial Apoptosis-induced Channel, MAC. *Journal of Biological Chemistry* **284,** 12235–12245 (2009).
161. Chipuk, J. E. & Green, D. R. How do BCL-2 proteins induce mitochondrial outer membrane permeabilization? *Trends Cell Biol* **18,** 157–164 (2008).
162. Jiang, X. CYTOCHROME C -MEDIATED APOPTOSIS. *Annual Review of Biochemistry* **73,** 87–106 (2004).
163. Qin, H. *et al.* Structural basis of procaspase-9 recruitment by the apoptotic protease-activating factor 1. *Nature* **399,** 549–557 (1999).
164. Stennicke, H. R. *et al.* Caspase-9 Can Be Activated without Proteolytic Processing. *J. Biol. Chem.* **274,** 8359–8362 (1999).

165. Malladi, S., Challa-Malladi, M., Fearnhead, H. O. & Bratton, S. B. The Apaf-1•procaspase-9 apoptosome complex functions as a proteolytic-based molecular timer. *EMBO J* **28,** 1916–1925 (2009).
166. Ellis, H. M. & Horvitz, H. R. Genetic control of programmed cell death in the nematode C. elegans. *Cell* **44,** 817–829 (1986).
167. Yuan, J., Shaham, S., Ledoux, S., Ellis, H. M. & Horvitz, H. R. The C. elegans cell death gene ced-3 encodes a protein similar to mammalian interleukin-1β-converting enzyme. *Cell* **75,** 641–652 (1993).
168. Alnemri, E. S. *et al.* Human ICE/CED-3 Protease Nomenclature. *Cell* **87,** 171 (1996).
169. Le, D. A. *et al.* Caspase activation and neuroprotection in caspase-3- deficient mice after in vivo cerebral ischemia and in vitro oxygen glucose deprivation. *Proc. Natl. Acad. Sci. U.S.A.* **99,** 15188–15193 (2002).
170. Leonard, J. R., Klocke, B. J., D'Sa, C., Flavell, R. A. & Roth, K. A. Strain-dependent neurodevelopmental abnormalities in caspase-3-deficient mice. *J. Neuropathol. Exp. Neurol.* **61,** 673–677 (2002).
171. Zheng, T. S. *et al.* Caspase-3 controls both cytoplasmic and nuclear events associated with Fas-mediated apoptosis in vivo. *PNAS* **95,** 13618–13623 (1998).
172. Lakhani, S. A. *et al.* Caspases 3 and 7: key mediators of mitochondrial events of apoptosis. *Science* **311,** 847–851 (2006).
173. Fischer, U., Jänicke, R. U. & Schulze-Osthoff, K. Many cuts to ruin: a comprehensive update of caspase substrates. *Cell Death Differ.* **10,** 76–100 (2003).
174. Enari, M. *et al.* A caspase-activated DNase that degrades DNA during apoptosis, and its inhibitor ICAD. *Nature* **391,** 43–50 (1998).
175. Chay, K.-O., Park, S. S. & Mushinski, J. F. Linkage of caspase-mediated degradation of paxillin to apoptosis in Ba/F3 murine pro-B lymphocytes. *J. Biol. Chem.* **277,** 14521–14529 (2002).
176. Mashima, T. *et al.* Actin cleavage by CPP-32/apopain during the development of apoptosis. *Oncogene* **14,** 1007–1012 (1997).
177. Yi, C. H. & Yuan, J. The Jekyll and Hyde Functions of Caspases. *Dev Cell* **16,** 21–34 (2009).
178. D'Amelio, M., Cavallucci, V. & Cecconi, F. Neuronal caspase-3 signaling: not only cell death. *Cell Death & Differentiation* **17,** 1104–1114 (2010).
179. Snigdha, S., Smith, E. D., Prieto, G. A. & Cotman, C. W. Caspase-3 activation as a bifurcation point between plasticity and cell death. *Neurosci. Bull.* **28,** 14–24 (2012).
180. Du, C., Fang, M., Li, Y., Li, L. & Wang, X. Smac, a Mitochondrial Protein that Promotes Cytochrome c–Dependent Caspase Activation by Eliminating IAP Inhibition. *Cell* **102,** 33–42 (2000).
181. Verhagen, A. M. *et al.* Identification of DIABLO, a Mammalian Protein that Promotes Apoptosis by Binding to and Antagonizing IAP Proteins. *Cell* **102,** 43–53 (2000).
182. Hay, B. A., Wassarman, D. A. & Rubin, G. M. Drosophila homologs of baculovirus inhibitor of apoptosis proteins function to block cell death. *Cell* **83,** 1253–1262 (1995).
183. Chai, J. *et al.* Structural and biochemical basis of apoptotic activation by Smac/DIABLO. *Nature* **406,** 855–862 (2000).
184. Yang, Q.-H. & Du, C. Smac/DIABLO Selectively Reduces the Levels of c-IAP1 and c-IAP2 but Not That of XIAP and Livin in HeLa Cells. *J. Biol. Chem.* **279,** 16963–16970 (2004).

185. Roy, N., Deveraux, Q. L., Takahashi, R., Salvesen, G. S. & Reed, J. C. The c-IAP-1 and c-IAP-2 proteins are direct inhibitors of specific caspases. *EMBO J* **16,** 6914–6925 (1997).
186. Deveraux, Q. L., Takahashi, R., Salvesen, G. S. & Reed, J. C. X-linked IAP is a direct inhibitor of cell-death proteases. *Nature* **388,** 300–304 (1997).
187. Wei, Y., Fan, T. & Yu, M. Inhibitor of apoptosis proteins and apoptosis. *Acta Biochimica et Biophysica Sinica* **40,** 278–288 (2008).
188. Bertrand, M. J. M. *et al.* cIAP1 and cIAP2 Facilitate Cancer Cell Survival by Functioning as E3 Ligases that Promote RIP1 Ubiquitination. *Molecular Cell* **30,** 689–700 (2008).
189. Mahoney, D. J. *et al.* Both cIAP1 and cIAP2 regulate TNFα-mediated NF-κB activation. *PNAS* **105,** 11778–11783 (2008).
190. Huang, H. k *et al.* The inhibitor of apoptosis, cIAP2, functions as a ubiquitin-protein ligase and promotes in vitro monoubiquitination of caspases 3 and 7. *J. Biol. Chem.* **275,** 26661–26664 (2000).
191. Lin, W.-W. & Karin, M. A cytokine-mediated link between innate immunity, inflammation, and cancer. *Journal of Clinical Investigation* **117,** 1175–1183 (2007).
192. LaCasse, E. C. *et al.* IAP-targeted therapies for cancer. *Oncogene* **27,** 6252–6275 (2008).
193. Gaither, A. *et al.* A Smac Mimetic Rescue Screen Reveals Roles for Inhibitor of Apoptosis Proteins in Tumor Necrosis Factor-α Signaling. *Cancer Res* **67,** 11493–11498 (2007).
194. Christofferson, D. E. & Yuan, J. Necroptosis as an alternative form of programmed cell death. *Curr. Opin. Cell Biol* **22,** 263–268 (2010).
195. Proskuryakov, S. Y., Konoplyannikov, A. G. & Gabai, V. L. Necrosis: A specific form of programmed cell death? *Experimental Cell Research* **283,** 1–16 (2003).
196. Slee, E. A. *et al.* Benzyloxycarbonyl-Val-Ala-Asp (OMe) fluoromethylketone (Z-VAD.FMK) inhibits apoptosis by blocking the processing of CPP32. *Biochem J* **315,** 21–24 (1996).
197. Vercammen, D. *et al.* Inhibition of Caspases Increases the Sensitivity of L929 Cells to Necrosis Mediated by Tumor Necrosis Factor. *J Exp Med* **187,** 1477–1485 (1998).
198. Matsumura, H. *et al.* Necrotic death pathway in Fas receptor signaling. *J. Cell Biol.* **151,** 1247–1256 (2000).
199. Chautan, M., Chazal, G., Cecconi, F., Gruss, P. & Golstein, P. Interdigital cell death can occur through a necrotic and caspase-independent pathway. *Current Biology* **9,** 967–S1 (1999).
200. Khwaja, A. & Tatton, L. Resistance to the cytotoxic effects of tumor necrosis factor alpha can be overcome by inhibition of a FADD/caspase-dependent signaling pathway. *J. Biol. Chem.* **274,** 36817–36823 (1999).
201. Lüschen, S., Ussat, S., Scherer, G., Kabelitz, D. & Adam-Klages, S. Sensitization to death receptor cytotoxicity by inhibition of fas-associated death domain protein (FADD)/caspase signaling. Requirement of cell cycle progression. *J. Biol. Chem.* **275,** 24670–24678 (2000).
202. Mocarski, E. S., Upton, J. W. & Kaiser, W. J. Viral infection and the evolution of caspase 8-regulated apoptotic and necrotic death pathways. *Nature Reviews Immunology* **12,** 79–88 (2012).
203. Holler, N. *et al.* Fas triggers an alternative, caspase-8-independent cell death pathway using the kinase RIP as effector molecule. *Nat. Immunol.* **1,** 489–495 (2000).
204. Degterev, A. *et al.* Chemical inhibitor of nonapoptotic cell death with therapeutic potential for ischemic brain injury. *Nature chemical biology* **1,** 112–119 (2005).
205. Degterev, A. *et al.* Identification of RIP1 kinase as a specific cellular target of necrostatins. *Nature Chemical Biology* **4,** 313–321 (2008).

206. Cho, Y. *et al.* Phosphorylation-Driven Assembly of the RIP1-RIP3 Complex Regulates Programmed Necrosis and Virus-Induced Inflammation. *Cell* **137,** 1112–1123 (2009).
207. Feoktistova, M. *et al.* cIAPs Block Ripoptosome Formation, a RIP1/Caspase-8 Containing Intracellular Cell Death Complex Differentially Regulated by cFLIP Isoforms. *Mol Cell* **43,** 449–463 (2011).
208. O'Donnell, M. A. *et al.* Caspase 8 inhibits programmed necrosis by processing CYLD. *Nature Cell Biology* **13,** 1437–1442 (2011).
209. Declercq, W., Vanden Berghe, T. & Vandenabeele, P. RIP Kinases at the Crossroads of Cell Death and Survival. *Cell* **138,** 229–232 (2009).
210. Hitomi, J. *et al.* Identification of a Molecular Signaling Network that Regulates a Cellular Necrotic Cell Death Pathway. *Cell* **135,** 1311–1323 (2008).
211. Vandenabeele, P., Galluzzi, L., Vanden Berghe, T. & Kroemer, G. Molecular mechanisms of necroptosis: an ordered cellular explosion. *Nat Rev Mol Cell Biol* **11,** 700–714 (2010).
212. Vanlangenakker, N., Bertrand, M. J. M., Bogaert, P., Vandenabeele, P. & Vanden Berghe, T. TNF-induced necroptosis in L929 cells is tightly regulated by multiple TNFR1 complex I and II members. *Cell Death Dis* **2,** e230 (2011).
213. Tenev, T. *et al.* The Ripoptosome, a Signaling Platform that Assembles in Response to Genotoxic Stress and Loss of IAPs. *Molecular Cell* **43,** 432–448 (2011).
214. Moujalled, D. M. *et al.* TNF can activate RIPK3 and cause programmed necrosis in the absence of RIPK1. *Cell Death Dis* **4,** e465 (2013).
215. Moquin, D. & Chan, F. K.-M. The molecular regulation of programmed necrotic cell injury. *Trends Biochem. Sci.* **35,** 434–441 (2010).
216. Li, J. *et al.* The RIP1/RIP3 necrosome forms a functional amyloid signaling complex required for programmed necrosis. *Cell* **150,** 339–350 (2012).
217. Wang, Z., Jiang, H., Chen, S., Du, F. & Wang, X. The Mitochondrial Phosphatase PGAM5 Functions at the Convergence Point of Multiple Necrotic Death Pathways. *Cell* **148,** 228–243 (2012).
218. Temkin, V., Huang, Q., Liu, H., Osada, H. & Pope, R. M. Inhibition of ADP/ATP Exchange in Receptor-Interacting Protein-Mediated Necrosis. *Mol. Cell. Biol.* **26,** 2215–2225 (2006).
219. Nakagawa, T. *et al.* Cyclophilin D-dependent mitochondrial permeability transition regulates some necrotic but not apoptotic cell death. *Nature* **434,** 652–658 (2005).
220. Schinzel, A. C. *et al.* Cyclophilin D is a component of mitochondrial permeability transition and mediates neuronal cell death after focal cerebral ischemia. *PNAS* **102,** 12005–12010 (2005).
221. Berghe, T. V. *et al.* Necroptosis, necrosis and secondary necrosis converge on similar cellular disintegration features. *Cell Death Differ* **17,** 922–930 (2010).
222. Xu, X. *et al.* Necrostatin-1 protects against glutamate-induced glutathione depletion and caspase-independent cell death in HT-22 cells. *J. Neurochem.* **103,** 2004–2014 (2007).
223. Lin, Y. *et al.* Tumor necrosis factor-induced nonapoptotic cell death requires receptor-interacting protein-mediated cellular reactive oxygen species accumulation. *J. Biol. Chem.* **279,** 10822–10828 (2004).
224. He, S. *et al.* Receptor Interacting Protein Kinase-3 Determines Cellular Necrotic Response to TNF-[alpha]. *Cell* **137,** 1100–1111 (2009).
225. Jouan-Lanhouet, S. *et al.* TRAIL induces necroptosis involving RIPK1/RIPK3-dependent PARP-1 activation. *Cell Death Differ.* **19,** 2003–2014 (2012).

226. He, S., Liang, Y., Shao, F. & Wang, X. Toll-Like Receptors Activate Programmed Necrosis in Macrophages Through a Receptor-Interacting Kinase-3–Mediated Pathway. *PNAS* **108,** 20054–20059 (2011).
227. Rebsamen, M. *et al.* DAI/ZBP1 recruits RIP1 and RIP3 through RIP homotypic interaction motifs to activate NF-[kappa]B. *EMBO Rep* **10,** 916–922 (2009).
228. Upton, J. W., Kaiser, W. J. & Mocarski, E. S. DAI/ZBP1/DLM-1 Complexes with RIP3 to Mediate Virus-Induced Programmed Necrosis that Is Targeted by Murine Cytomegalovirus vIRA. *Cell Host & Microbe* **11,** 290–297 (2012).
229. Biton, S. & Ashkenazi, A. NEMO and RIP1 control cell fate in response to extensive DNA damage via TNF-α feedforward signaling. *Cell* **145,** 92–103 (2011).
230. Vanlangenakker, N., Vanden Berghe, T. & Vandenabeele, P. Many stimuli pull the necrotic trigger, an overview. *Cell Death Differ* **19,** 75–86 (2012).
231. Andersson, U. & Erlandsson-Harris, H. HMGB1 is a potent trigger of arthritis. *Journal of Internal Medicine* **255,** 344–350 (2004).
232. Pisetsky, D. S. HMGB1: A Dangerous Player in Lupus Pathogenesis. *J Rheumatol* **37,** 689–691 (2010).
233. Andersson, U. & Tracey, K. J. HMGB1 in sepsis. *Scand. J. Infect. Dis.* **35,** 577–584 (2003).
234. Raucci, A., Palumbo, R. & Bianchi, M. E. HMGB1: A signal of necrosis. *Autoimmunity* **40,** 285–289 (2007).
235. Zwaferink, H., Stockinger, S., Reipert, S. & Decker, T. Stimulation of Inducible Nitric Oxide Synthase Expression by Beta Interferon Increases Necrotic Death of Macrophages upon Listeria monocytogenes Infection. *Infect. Immun.* **76,** 1649–1656 (2008).
236. Amantea, D., Nappi, G., Bernardi, G., Bagetta, G. & Corasaniti, M. T. Post-ischemic brain damage: pathophysiology and role of inflammatory mediators. *FEBS Journal* **276,** 13–26 (2009).
237. Kim, J.-B. *et al.* HMGB1, a Novel Cytokine-Like Mediator Linking Acute Neuronal Death and Delayed Neuroinflammation in the Postischemic Brain. *J. Neurosci.* **26,** 6413–6421 (2006).
238. Liu, K. *et al.* Anti-high mobility group box 1 monoclonal antibody ameliorates brain infarction induced by transient ischemia in rats. *FASEB J* **21,** 3904–3916 (2007).
239. Smith, C. *et al.* Necrostatin: A Potentially Novel Cardioprotective Agent? *Cardiovascular Drugs and Therapy* **21,** 227–233 (2007).
240. Andrassy, M. *et al.* High-Mobility Group Box-1 in Ischemia-Reperfusion Injury of the Heart. *Circulation* **117,** 3216–3226 (2008).
241. Yu, M. *et al.* HMGB1 SIGNALS THROUGH TOLL-LIKE RECEPTOR (TLR) 4 AND TLR2. *Shock* **26,** 174–179 (2006).
242. Yang, H. *et al.* A critical cysteine is required for HMGB1 binding to Toll-like receptor 4 and activation of macrophage cytokine release. *Proc. Natl. Acad. Sci. U.S.A.* **107,** 11942–11947 (2010).
243. Andersson, U. *et al.* High mobility group 1 protein (HMG-1) stimulates proinflammatory cytokine synthesis in human monocytes. *J. Exp. Med.* **192,** 565–570 (2000).
244. Schiraldi, M. *et al.* HMGB1 promotes recruitment of inflammatory cells to damaged tissues by forming a complex with CXCL12 and signaling via CXCR4. *J Exp Med* **209,** 551–563 (2012).
245. Yang, D. *et al.* High mobility group box-1 protein induces the migration and activation of human dendritic cells and acts as an alarmin. *J. Leukoc. Biol.* **81,** 59–66 (2007).

246. Bianchi, M. E. DAMPs, PAMPs and alarmins: all we need to know about danger. *J Leukoc Biol* **81,** 1–5 (2007).
247. Kaczmarek, A., Vandenabeele, P. & Krysko, D. V. Necroptosis: The Release of Damage-Associated Molecular Patterns and Its Physiological Relevance. *Immunity* **38,** 209–223 (2013).
248. Lee, T. H., Shank, J., Cusson, N. & Kelliher, M. A. The kinase activity of Rip1 is not required for tumor necrosis factor-alpha-induced IkappaB kinase or p38 MAP kinase activation or for the ubiquitination of Rip1 by Traf2. *J. Biol. Chem.* **279,** 33185–33191 (2004).
249. Christofferson, D. E. *et al.* A novel role for RIP1 kinase in mediating TNFα production. *Cell Death & Disease* **3,** e320 (2012).
250. Cusson-Hermance, N., Khurana, S., Lee, T. H., Fitzgerald, K. A. & Kelliher, M. A. Rip1 Mediates the Trif-dependent Toll-like Receptor 3- and 4-induced NF-κB Activation but Does Not Contribute to Interferon Regulatory Factor 3 Activation. *J. Biol. Chem.* **280,** 36560–36566 (2005).
251. Kang, T.-B., Yang, S.-H., Toth, B., Kovalenko, A. & Wallach, D. Caspase-8 Blocks Kinase RIPK3-Mediated Activation of the NLRP3 Inflammasome. *Immunity* **38,** 27–40 (2013).
252. Meylan, E. *et al.* RIP1 is an essential mediator of Toll-like receptor 3-induced NF-[kappa]B activation. *Nat Immunol* **5,** 503–507 (2004).
253. Newton, K., Sun, X. & Dixit, V. M. Kinase RIP3 is dispensable for normal NF-kappa Bs, signaling by the B-cell and T-cell receptors, tumor necrosis factor receptor 1, and Toll-like receptors 2 and 4. *Mol. Cell. Biol.* **24,** 1464–1469 (2004).
254. Vince, J. E. *et al.* Inhibitor of apoptosis proteins limit RIP3 kinase-dependent interleukin-1 activation. *Immunity* **36,** 215–227 (2012).
255. Petersen, S. L. *et al.* Autocrine TNFα Signaling Renders Human Cancer Cells Susceptible to Smac-Mimetic-Induced Apoptosis. *Cancer Cell* **12,** 445–456 (2007).
256. Wu, Y.-T. *et al.* zVAD-induced necroptosis in L929 cells depends on autocrine production of TNFα mediated by the PKC-MAPKs-AP-1 pathway. *Cell Death Differ.* **18,** 26–37 (2011).
257. Wallach, D., Kovalenko, A. & Kang, T.-B. 'Necrosome'-induced inflammation: must cells die for it? *Trends in Immunology* **32,** 505–509 (2011).
258. Duprez, L. *et al.* RIP Kinase-Dependent Necrosis Drives Lethal Systemic Inflammatory Response Syndrome. *Immunity* **35,** 908–918 (2011).
259. Linkermann, A. *et al.* Dichotomy between RIP1- and RIP3-Mediated Necroptosis in Tumor Necrosis Factor-α–Induced Shock. *Mol Med* **18,** 577–586 (2012).
260. Yang, H. *et al.* Reversing established sepsis with antagonists of endogenous high-mobility group box 1. *PNAS* **101,** 296–301 (2004).
261. Qin, S. *et al.* Role of HMGB1 in apoptosis-mediated sepsis lethality. *J Exp Med* **203,** 1637–1642 (2006).
262. Lin, J. *et al.* A Role of RIP3-Mediated Macrophage Necrosis in Atherosclerosis Development. *Cell Rep* **3,** 200–210 (2013).
263. Andrassy, M. *et al.* HMGB1 Is Associated with Atherosclerotic Plaque Composition and Burden in Patients with Stable Coronary Artery Disease. *PLoS ONE* **7,** e52081 (2012).
264. Kalinina, N. *et al.* Increased Expression of the DNA-Binding Cytokine HMGB1 in Human Atherosclerotic Lesions Role of Activated Macrophages and Cytokines. *Arterioscler Thromb Vasc Biol* **24,** 2320–2325 (2004).

265. Chan, F. K.-M. *et al.* A role for tumor necrosis factor receptor-2 and receptor-interacting protein in programmed necrosis and antiviral responses. *J. Biol. Chem.* **278,** 51613–51621 (2003).
266. Mack, C., Sickmann, A., Lembo, D. & Brune, W. Inhibition of proinflammatory and innate immune signaling pathways by a cytomegalovirus RIP1-interacting protein. *PNAS* **105,** 3094–3099 (2008).
267. Conze, D. B. *et al.* Posttranscriptional downregulation of c-IAP2 by the ubiquitin protein ligase c-IAP1 in vivo. *Mol. Cell. Biol.* **25,** 3348–3356 (2005).
268. Conte, D. *et al.* Inhibitor of Apoptosis Protein cIAP2 Is Essential for Lipopolysaccharide-Induced Macrophage Survival. *Mol. Cell. Biol.* **26,** 699–708 (2006).
269. Kolumam, G. A., Thomas, S., Thompson, L. J., Sprent, J. & Murali-Krishna, K. Type I interferons act directly on CD8 T cells to allow clonal expansion and memory formation in response to viral infection. *J Exp Med* **202,** 637–650 (2005).
270. Müller, U. *et al.* Functional role of type I and type II interferons in antiviral defense. *Science* **264,** 1918–1921 (1994).
271. Shen, L., Sigal, L. J., Boes, M. & Rock, K. L. Important role of cathepsin S in generating peptides for TAP-independent MHC class I crosspresentation in vivo. *Immunity* **21,** 155–165 (2004).
272. Luu, R. A. *et al.* Delayed expansion and contraction of CD8+ T cell response during infection with virulent Salmonella typhimurium. *J. Immunol.* **177,** 1516–1525 (2006).
273. Dudani, R. *et al.* Multiple mechanisms compensate to enhance tumor-protective CD8(+) T cell response in the long-term despite poor CD8(+) T cell priming initially: comparison between an acute versus a chronic intracellular bacterium expressing a model antigen. *J. Immunol.* **168,** 5737–5745 (2002).
274. Monnack, D. Preparation of Bone-marrow-derived macrophages. at <http://monacklab.stanford.edu/protocols.html#bmd>
275. Lu, J. *et al.* SM-164: A Novel, Bivalent Smac Mimetic That Induces Apoptosis and Tumor Regression by Concurrent Removal of the Blockade of cIAP-1/2 and XIAP. *Cancer Research* **68,** 9384–9393 (2008).
276. Wu, C.-J., Conze, D. B., Li, T., Srinivasula, S. M. & Ashwell, J. D. Sensing of Lys 63-linked polyubiquitination by NEMO is a key event in NF-kappaB activation [corrected]. *Nat. Cell Biol.* **8,** 398–406 (2006).
277. Unger, T., Jacobovitch, Y., Dantes, A., Bernheim, R. & Peleg, Y. Applications of the Restriction Free (RF) cloning procedure for molecular manipulations and protein expression. *J. Struct. Biol.* **172,** 34–44 (2010).
278. Albaghdadi, H., Robinson, N., Finlay, B., Krishnan, L. & Sad, S. Selectively reduced intracellular proliferation of Salmonella enterica serovar typhimurium within APCs limits antigen presentation and development of a rapid CD8 T cell response. *J. Immunol.* **183,** 3778–3787 (2009).
279. Sad, S. *et al.* Pathogen proliferation governs the magnitude but compromises the function of CD8 T cells. *J. Immunol.* **180,** 5853–5861 (2008).
280. Wrone-Smith, T. *et al.* Keratinocytes derived from psoriatic plaques are resistant to apoptosis compared with normal skin. *Am. J. Pathol.* **151,** 1321–1329 (1997).
281. Kaech, S. M., Wherry, E. J. & Ahmed, R. Effector and memory T-cell differentiation: implications for vaccine development. *Nat Rev Immunol* **2,** 251–262 (2002).

282. Prakash, H. *et al.* cIAP-1 Controls Innate Immunity to C. pneumoniae Pulmonary Infection. *PLoS ONE* **4,** e6519 (2009).
283. Lu, J. *et al.* SM-164: A Novel, Bivalent Smac Mimetic That Induces Apoptosis and Tumor Regression by Concurrent Removal of the Blockade of cIAP-1/2 and XIAP. *Cancer Research* **68,** 9384–9393 (2008).
284. Suzuki, Y., Nakabayashi, Y., Nakata, K., Reed, J. C. & Takahashi, R. X-linked Inhibitor of Apoptosis Protein (XIAP) Inhibits Caspase-3 and -7 in Distinct Modes. *Journal of Biological Chemistry* **276,** 27058 –27063 (2001).
285. Robinson, N. *et al.* Type I interferon induces necroptosis in macrophages during infection with Salmonella enterica serovar Typhimurium. *Nature Immunology* **13,** 954–962 (2012).
286. Vadiveloo, P. K., Vairo, G., Hertzog, P., Kola, I. & Hamilton, J. A. Role of type I interferons during macrophage activation by lipopolysaccharide. *Cytokine* **12,** 1639–1646 (2000).
287. Sung Ouk Kim & Jiahuai Han. Pan-caspase inhibitor zVAD enhances cell death in RAW246.7 macrophages. *Journal of Endotoxin Research* **7,** 292 –296 (2001).
288. Rozman-Pungercar, J. *et al.* Inhibition of papain-like cysteine proteases and legumain by caspase-specific inhibitors: when reaction mechanism is more important than specificity. *Cell Death Differ.* **10,** 881–888 (2003).
289. Mohamed, M. M. & Sloane, B. F. Cysteine cathepsins: multifunctional enzymes in cancer. *Nature Reviews Cancer* **6,** 764–775 (2006).
290. Chwieralski, C., Welte, T. & Bühling, F. Cathepsin-regulated apoptosis. *Apoptosis* **11,** 143–149 (2006).
291. Matloubian, M., Concepcion, R. J. & Ahmed, R. CD4+ T cells are required to sustain CD8+ cytotoxic T-cell responses during chronic viral infection. *J. Virol.* **68,** 8056–8063 (1994).
292. Gorantla, S. *et al.* CD8+ cell depletion accelerates HIV-1 immunopathology in humanized mice. *J Immunol* **184,** 7082–7091 (2010).
293. Serbina, N. V. & Flynn, J. L. CD8(+) T cells participate in the memory immune response to Mycobacterium tuberculosis. *Infect. Immun.* **69,** 4320–4328 (2001).
294. Mastroeni, P., Villarreal-Ramos, B. & Hormaeche, C. E. Role of T cells, TNF alpha and IFN gamma in recall of immunity to oral challenge with virulent salmonellae in mice vaccinated with live attenuated aro- Salmonella vaccines. *Microb. Pathog.* **13,** 477–491 (1992).
295. Harty, J. T., Schreiber, R. D. & Bevan, M. J. CD8 T cells can protect against an intracellular bacterium in an interferon gamma-independent fashion. *Proc Natl Acad Sci U S A* **89,** 11612–11616 (1992).
296. Perez-Liz, G., Del Valle, L., Gentilella, A., Croul, S. & Khalili, K. Detection of JC virus DNA fragments but not proteins in normal brain tissue. *Ann. Neurol.* **64,** 379–387 (2008).
297. White, F. A., 3rd, Ishaq, M., Stoner, G. L. & Frisque, R. J. JC virus DNA is present in many human brain samples from patients without progressive multifocal leukoencephalopathy. *J. Virol.* **66,** 5726–5734 (1992).
298. Blomgren, K. *et al.* Synergistic Activation of Caspase-3 by m-Calpain after Neonatal Hypoxia-Ischemia A MECHANISM OF 'PATHOLOGICAL APOPTOSIS'? *J. Biol. Chem.* **276,** 10191–10198 (2001).
299. Sharma, A. K. & Rohrer, B. Calcium-induced calpain mediates apoptosis via caspase-3 in a mouse photoreceptor cell line. *J. Biol. Chem.* **279,** 35564–35572 (2004).
300. Berridge, M. J., Lipp, P. & Bootman, M. D. The versatility and universality of calcium signalling. *Nat Rev Mol Cell Biol* **1,** 11–21 (2000).

301. Puga, I., Rao, A. & Macian, F. Targeted Cleavage of Signaling Proteins by Caspase 3 Inhibits T Cell Receptor Signaling in Anergic TÂ Cells. *Immunity* **29,** 193–204 (2008).
302. Ma, S., Ochi, H., Cui, L. & He, W. FasL-induced downregulation of CD28 expression on jurkat cells in vitro is associated with activation of caspases. *Cell Biol. Int.* **27,** 959–964 (2003).
303. Grayson, J. M., Laniewski, N. G., Lanier, J. G. & Ahmed, R. Mitochondrial Potential and Reactive Oxygen Intermediates in Antigen-Specific CD8+ T Cells During Viral Infection. *J Immunol* **170,** 4745–4751 (2003).
304. Harty, J. T. & Badovinac, V. P. Shaping and reshaping CD8+ T-cell memory. *Nat Rev Immunol* **8,** 107–119 (2008).
305. Snow, A. L. *et al.* Critical role for BIM in T cell receptor restimulation-induced death. *Biology Direct* **3,** (2008).
306. Masson, F., Kupresanin, F., Mount, A., Strasser, A. & Belz, G. T. Bid and Bim collaborate during induction of T cell death in persistent infection. *J. Immunol.* **186,** 4059–4066 (2011).
307. Osborn, S. L. *et al.* Fas-associated death domain (FADD) is a negative regulator of T-cell receptor–mediated necroptosis. *Proceedings of the National Academy of Sciences* **107,** 13034 – 13039 (2010).
308. Lu, J. V. *et al.* Complementary roles of Fas-associated death domain (FADD) and receptor interacting protein kinase-3 (RIPK3) in T-cell homeostasis and antiviral immunity. *PNAS* **108,** 15312–15317 (2011).
309. Lin, Y., Devin, A., Rodriguez, Y. & Liu, Z. Cleavage of the death domain kinase RIP by Caspase-8 prompts TNF-induced apoptosis. *Genes Dev* **13,** 2514–2526 (1999).
310. Zhu, L. *et al.* Real-time monitoring of caspase cascade activation in living cells. *J Control Release* **163,** 55–62 (2012).
311. Ferreira, K. S. *et al.* Caspase-3 feeds back on caspase-8, Bid and XIAP in type I Fas signaling in primary mouse hepatocytes. *Apoptosis* **17,** 503–515 (2012).
312. Fischer, K. *et al.* Antigen recognition induces phosphatidylserine exposure on the cell surface of human CD8+ T cells. *Blood* **108,** 4094–4101 (2006).
313. Koenig, A. *et al.* Proliferating γδ T cells manifest high and spatially confined caspase-3 activity. *Immunology* **135,** 276–286 (2012).
314. Koenig, A., Russell, J. Q., Rodgers, W. A. & Budd, R. C. Spatial differences in active caspase-8 defines its role in T-cell activation versus cell death. *Cell Death and Differentiation* **15,** 1701–1711 (2008).
315. Kamada, S., Kikkawa, U., Tsujimoto, Y. & Hunter, T. Nuclear Translocation of Caspase-3 Is Dependent on Its Proteolytic Activation and Recognition of a Substrate-like Protein(s). *J. Biol. Chem.* **280,** 857–860 (2005).
316. Harlin, H., Reffey, S. B., Duckett, C. S., Lindsten, T. & Thompson, C. B. Characterization of XIAP-Deficient Mice. *Mol Cell Biol* **21,** 3604–3608 (2001).
317. Rigaud, S. *et al.* XIAP deficiency in humans causes an X-linked lymphoproliferative syndrome. *Nature* **444,** 110–114 (2006).
318. Mangan, D. & Wahl, S. Differential regulation of human monocyte programmed cell death (apoptosis) by chemotactic factors and pro-inflammatory cytokines. *J Immunol* **147,** 3408–3412 (1991).
319. Busca, A., Saxena, M., Kryworuchko, M. & Kumar, A. Anti-Apoptotic Genes in the Survival of Monocytic Cells During Infection. *Curr Genomics* **10,** 306–317 (2009).

320. Cui, X. *et al.* Lipopolysaccharide induces the expression of cellular inhibitor of apoptosis protein-2 in human macrophages. *Biochim. Biophys. Acta* **1524,** 178–182 (2000).
321. Prakash, H., Albrecht, M., Becker, D., Kuhlmann, T. & Rudel, T. Deficiency of XIAP Leads to Sensitization for Chlamydophila pneumoniae Pulmonary Infection and Dysregulation of Innate Immune Response in Mice. *Journal of Biological Chemistry* **285,** 20291 –20302 (2010).
322. Müller-Sienerth, N. *et al.* SMAC Mimetic BV6 Induces Cell Death in Monocytes and Maturation of Monocyte-Derived Dendritic Cells. *PLoS ONE* **6,** e21556 (2011).
323. Vanlangenakker, N. *et al.* cIAP1 and TAK1 protect cells from TNF-induced necrosis by preventing RIP1/RIP3-dependent reactive oxygen species production. *Cell Death Differ* **18,** 656–665 (2011).
324. Choi, Y. E. *et al.* The E3 Ubiquitin Ligase cIAP1 Binds and Ubiquitinates Caspase-3 and -7 via Unique Mechanisms at Distinct Steps in Their Processing. *Journal of Biological Chemistry* **284,** 12772 –12782 (2009).
325. Bertrand, M. J. M. *et al.* cIAP1/2 Are Direct E3 Ligases Conjugating Diverse Types of Ubiquitin Chains to Receptor Interacting Proteins Kinases 1 to 4 (RIP1–4). *PLoS ONE* **6,** e22356 (2011).
326. Kearney, C. J. *et al.* IAPs and their Antagonists Regulate Spontaneous and TNF-Induced Pro-Inflammatory Cytokine and Chemokine production. *J. Biol. Chem.* (2012). doi:10.1074/jbc.M112.422410
327. Geserick, P. *et al.* Cellular IAPs inhibit a cryptic CD95-induced cell death by limiting RIP1 kinase recruitment. *J Cell Biol* **187,** 1037–1054 (2009).
328. Upton, J. W., Kaiser, W. J. & Mocarski, E. S. Virus inhibition of RIP3-dependent necrosis. *Cell host & microbe* **7,** 302–313 (2010).
329. Lara-Tejero, M. *et al.* Role of the caspase-1 inflammasome in Salmonella typhimurium pathogenesis. *J Exp Med* **203,** 1407–1412 (2006).
330. Velden, A. W. M. van der, Lindgren, S. W., Worley, M. J. & Heffron, F. Salmonella Pathogenicity Island 1-Independent Induction of Apoptosis in Infected Macrophages bySalmonella enterica Serotype Typhimurium. *Infect. Immun.* **68,** 5702–5709 (2000).
331. Guilloteau, L. A. *et al.* The Salmonella virulence plasmid enhances Salmonella-induced lysis of macrophages and influences inflammatory responses. *Infect. Immun.* **64,** 3385–3393 (1996).
332. Brennan, M. A. & Cookson, B. T. Salmonella induces macrophage death by caspase-1-dependent necrosis. *Mol. Microbiol* **38,** 31–40 (2000).
333. Sato, M. *et al.* Distinct and essential roles of transcription factors IRF-3 and IRF-7 in response to viruses for IFN-alpha/beta gene induction. *Immunity* **13,** 539–548 (2000).
334. Lazear, H. M. *et al.* IRF-3, IRF-5, and IRF-7 Coordinately Regulate the Type I IFN Response in Myeloid Dendritic Cells Downstream of MAVS Signaling. *PLoS Pathog* **9,** e1003118 (2013).
335. Karaghiosoff, M. *et al.* Central role for type I interferons and Tyk2 in lipopolysaccharide-induced endotoxin shock. *Nat Immunol* **4,** 471–477 (2003).
336. Pena, G., Cai, B., Deitch, E. A. & Ulloa, L. JAK2 inhibition prevents innate immune responses and rescues animals from sepsis. *J Mol Med (Berl)* **88,** 851–859 (2010).
337. Kim, H. S. & Lee, M.-S. Essential role of STAT1 in caspase-independent cell death of activated macrophages through the p38 mitogen-activated protein kinase/STAT1/reactive oxygen species pathway. *Mol. Cell. Biol.* **25,** 6821–6833 (2005).

338. Huys, L. *et al.* Type I interferon drives tumor necrosis factor-induced lethal shock. *J. Exp. Med.* **206,** 1873–1882 (2009).
339. Kelly-Scumpia, K. M. *et al.* Type I interferon signaling in hematopoietic cells is required for survival in mouse polymicrobial sepsis by regulating CXCL10. *J. Exp. Med.* **207,** 319–326 (2010).
340. Mahieu, T. *et al.* The wild-derived inbred mouse strain SPRET/Ei is resistant to LPS and defective in IFN-beta production. *Proc. Natl. Acad. Sci. U.S.A.* **103,** 2292–2297 (2006).
341. Sakaguchi, S. *et al.* Essential role of IRF-3 in lipopolysaccharide-induced interferon-β gene expression and endotoxin shock. *Biochemical and Biophysical Research Communications* **306,** 860–866 (2003).
342. Hoebe, K. *et al.* Identification of Lps2 as a key transducer of MyD88-independent TIR signalling. *Nature* **424,** 743–748 (2003).
343. Amiot, F., Fitting, C., Tracey, K. J., Cavaillon, J. M. & Dautry, F. Lipopolysaccharide-induced cytokine cascade and lethality in LT alpha/TNF alpha-deficient mice. *Mol. Med.* **3,** 864–875 (1997).
344. Mahieu, T. & Libert, C. Should We Inhibit Type I Interferons in Sepsis? *Infect Immun* **75,** 22–29 (2007).
345. Sundén-Cullberg, J. *et al.* Persistent elevation of high mobility group box-1 protein (HMGB1) in patients with severe sepsis and septic shock. *Crit. Care Med.* **33,** 564–573 (2005).
346. Lamkanfi, M. *et al.* Inflammasome-dependent release of the alarmin HMGB1 in endotoxemia. *J. Immunol.* **185,** 4385–4392 (2010).
347. Husak, L. *et al.* National analysis of sepsis hospitalizations and factors contributing to sepsis in-hospital mortality in Canada. *Healthc Q* **13 Spec No,** 35–41 (2010).
348. Gaieski, D. F. *et al.* Impact of time to antibiotics on survival in patients with severe sepsis or septic shock in whom early goal-directed therapy was initiated in the emergency department. *Crit. Care Med.* **38,** 1045–1053 (2010).
349. Okazaki, Y. & Matsukawa, A. Pathophysiology of sepsis and recent patents on the diagnosis, treatment and prophylaxis for sepsis. *Recent Pat Inflamm Allergy Drug Discov* **3,** 26–32 (2009).
350. Friedman, R. M. Clinical uses of interferons. *Br J Clin Pharmacol* **65,** 158–162 (2008).
351. Zhang, D.-W. *et al.* RIP3, an Energy Metabolism Regulator That Switches TNF-Induced Cell Death from Apoptosis to Necrosis. *Science* **325,** 332–336 (2009).
352. Rozman-Pungercar, J. *et al.* Inhibition of papain-like cysteine proteases and legumain by caspase-specific inhibitors: when reaction mechanism is more important than specificity. *Cell Death Differ.* **10,** 881–888 (2003).
353. Felbor, U. *et al.* Neuronal loss and brain atrophy in mice lacking cathepsins B and L. *PNAS* **99,** 7883–7888 (2002).
354. Verspurten, J., Gevaert, K., Declercq, W. & Vandenabeele, P. SitePredicting the cleavage of proteinase substrates. *Trends Biochem. Sci.* **34,** 319–323 (2009).
355. Guicciardi, M. E., Leist, M. & Gores, G. J. Lysosomes in cell death. *Oncogene* **23,** 2881–2890 (2004).
356. Yamashima, T. & Oikawa, S. The role of lysosomal rupture in neuronal death. *Prog. Neurobiol.* **89,** 343–358 (2009).
357. Repnik, U., Stoka, V., Turk, V. & Turk, B. Lysosomes and lysosomal cathepsins in cell death. *Biochim. Biophys. Acta* **1824,** 22–33 (2012).

358. Guicciardi, M. E. *et al.* Cathepsin B contributes to TNF-alpha-mediated hepatocyte apoptosis by promoting mitochondrial release of cytochrome c. *J. Clin. Invest.* **106,** 1127–1137 (2000).
359. Cirman, T. *et al.* Selective disruption of lysosomes in HeLa cells triggers apoptosis mediated by cleavage of Bid by multiple papain-like lysosomal cathepsins. *J. Biol. Chem.* **279,** 3578–3587 (2004).
360. Rajput, A. *et al.* RIG-I RNA Helicase Activation of IRF3 Transcription Factor Is Negatively Regulated by Caspase-8-Mediated Cleavage of the RIP1 Protein. *Immunity* **34,** 340–351 (2011).
361. Lyo, V. *et al.* Active cathepsins B, L, and S in murine and human pancreatitis. *Am J Physiol Gastrointest Liver Physiol* **303,** G894–G903 (2012).
362. Menzel, K. *et al.* Cathepsins B, L and D in inflammatory bowel disease macrophages and potential therapeutic effects of cathepsin inhibition in vivo. *Clin. Exp. Immunol.* **146,** 169–180 (2006).
363. Li, X., Liu, Z., Cheng, Z. & Cheng, X. Cysteinyl Cathepsins: Multifunctional Enzymes in Cardiovascular Disease. *Chonnam Med J* **48,** 77–85 (2012).
364. McComb, S., Mulligan, R. & Sad, S. Caspase-3 Is Transiently Activated without Cell Death during Early Antigen Driven Expansion of CD8+ T Cells In Vivo. *PLoS ONE* **5,** e15328 (2010).
365. McComb, S. *et al.* cIAP1 and cIAP2 limit macrophage necroptosis by inhibiting Rip1 and Rip3 activation. *Cell Death Differ.* **19,** 1791–1801 (2012).

CONTRIBUTIONS OF COLLABORATORS

Collaborator	Affiliation(s)	Contribution
Dr. Subash Sad	University of Ottawa	Supervisor
Dr. Katherine Wright	University of Ottawa	Thesis Advisory Committee Member
Dr. Robert G Korneluk	Children's Hospital of Eastern Ontario	Thesis Advisory Committee Member, Provided some reagents and cIAP knockout mice utilized in experiments within this thesis
Dr. Lakshmi Krishnan	National Research Council	Close Collaborator, provided advice and discussion in the expereimental development and analysis. Editing of manuscripts
Renu Dudani	National Research Council	Former technical officer in the Sad lab. Provided extensive technical support throughout experiments outlined in this thesis.
Dr. Nirmal Robinson	National Research Council, Universität Köln	Former postdoctoral researcher in the Sad lab. Necroptosis work in Salmonella model was performed in collaboration with Dr. Robinson.
Dr. Bojan Shutinoski	University of Ottawa	Current postdoctoal researcher in Sad lab. Molecular biology work for recombinant Rip1 kinase was performed by Dr. Shutinoski (Figure 40)
Dr. Herman Cheung	Children's Hospital of Eastern Ontario	Probed samples for xIAP expression (Figure 19D).
Susan Thurston	National Research Council	Performed western blot experiments under my direct supervision to examine cleavage of Rip1 kinase. Provided extensive technical support for inhibitor experiments (Figure 36, 37)
Erin Cessford	University of Ottawa	Current Masters student in the Sad Lab. Work investigating necroptosis in IFNAR-/- macrophages was performed in collaboration with Erin under my direct supervision (Figure 32)
Edmund Yao	McGill University, NRC	Former summer student in the Sad lab. Aided in analyzing cytokine release following necroptosis of macrophages under my direct supervision (Figure 20)
Shalini Sahi	University of Ottawa	Former summer student in the Sad lab. Aided in the development of the protocol for generation of BMDM cells.
Dr Shaomeng Wang	University of Michigan	External collaborator. Synthesized SMAC mimetics utilized in this thesis

Scott McComb

Relevant Experience

Spring 2007-Present National Research Council

Doctoral Student

- PhD in Immunology at the University of Ottawa to be completed in early 2013
- Currently working on an investigation of the role of necroptosis in regulation of innate immunity, particularly in the response to intracellular bacterial infections.
- Techniques used include flow cytometry, cell culture, fluorescence/confocal microscopy, bacterial pathogen models, general biochemical techniques and animal work (mouse model).

Honours Research Project *(2006-2007)*

- Honours project focused on the importance of apoptotic mediators in the CD8 T cell response to intracellular bacteria. Techniques included ELISA, microscopy, flow cytometry, and cell sorting. Work published in PLoS One

2005 Health Canada - Vaccines Division

Co-op Student Research Assistant

- Responsibilities included planning and performing experiments related to assigned projects. Projects were technical investigations of an HPLC approach to detect reversion of *Vibrio cholera* toxin in vaccines, and an ELISA based screen for potency of Diphtheria/Tetanus vaccines.

Publications

2013

- Krishnan L, Nguyen T, **McComb S**. (2013) From mice to women: the conundrum of immunity to infection during pregnancy, Journal of Reproductive Immunology, Journal of Reproductive Immunology 97 (1), 62-73 doi: 10.1016/j.jri.2012.10.015

2012

- **McComb S**, Cheung HH, Korneluk RG, Wang S, Krishnan L, Sad S, (2012) cIAP1 and cIAP2 Limit Macrophage Necroptosis by Inhibiting Rip1 and Rip3 Activation. Cell Death and Differentiation, 11 May 2012; doi:10.1038/cdd.2012.59
- Robinson N, **McComb S,** Mulligan R, Dudani R, Krishnan L, Sad S, (2012) Type I interferon induces necroptosis in macrophages during infection with *Salmonella enterica* serovar Typhimurium, Nature Immunology 13, 954–962 (2012) doi:10.1038/ni.2397

2010

- **McComb S**, Mulligan R, Sad S (2010) Caspase-3 Is Transiently Activated without Cell Death during Early Antigen Driven Expansion of $CD8^+$ T Cells *In Vivo*. PLoS ONE 5(12): e15328. doi:10.1371/journal.pone.0015328

Manuscripts in Preparation

- **McComb S**, Cessford E, Startek J, Sad S (2013) Autocrine Type-I Interferon Signaling is a Key Inducer of Inflammatory Necroptosis *Manuscript in Preparation*
- **McComb S**, Shutinoski B, Thurston S, Sad, S. (2013) Cathepsins Limit Macrophage Necroptosis through Cleavage of Rip1 Kinase *Manuscript in Preparation*

Presentations

2013

- **Poster presentation** at Canadian Society for Immunology conference held in Whistler, BC. Title: "Cathepsins Limit Macrophage Necroptosis through Cleavage of Rip1 Kinase"

2012

- **Poster presentation** at Keystone conference Pathways of Cell Death: Beyond apoptosis held in Banff Ab. Title: "cIAP1 and cIAP2 Limit Macrophage Necroptosis By Inhibiting Rip1 And Rip3 Activation"

2011

- **Oral presentation** in the Innate Immunity workshop at the Canadian Society for Immunology conference held in Banff, Ab. Title: "cIAP1 and cIAP2 Limit Macrophage Cell Death by Inhibiting Necrosome Formation"

2010

- **Poster presentation** at the Canadian Society for Immunology Annual Conference at Niagara Falls, On. Title: "cIAP-1 and cIAP-2 Protect Antigen Presenting Cells from Inflammatory Rip1 Dependent Necroptotic Cell Death"

2008

- **Poster presentation** at the Canadian Society for Immunology Annual Conference at Mt Tremblant, QC. Title: "Intensity of Antigen-Presentation Influences the Up-Regulation of Apoptotic Mediators During Activation of CD8+ T-Cells"

2006-2013

- Numerous poster and oral presentations at the University of Ottawa

Other Experience and Involvement

- Served as the **student representative of the Animal Care Committee** for the Institute for Biological Sciences (NRC)
- **Mentored multiple graduate and undergraduate students** in the Sad lab 2008-2013
  - Tasks included teaching technical and academic skills, experimental design, delegation, and managing work for multiple students
- 2+ years as **Laboratory Teaching Assistant**
  - Teaching classes on a range of biochemistry topics for both practical and theoretical skills
  - Grade students and provide feedback to aid in their development

Education

Fall 2007-Present University of Ottawa

- **Currently pursuing a Doctoral degree in Immunology** under the BMI department. Transfer from Masters to PhD program in 2009

2002-2007 University of Ottawa

- **B. Sc in Biopharmaceutical Science** (Genomics Option) with Honours and Co-op
- Graduated cum laude.

Awards

- **Ontario Graduate Scholarship - Doctoral Student Scholarship**
- **Ontario Graduate Student Scholarship in Master's Scholarship 2008**
- Travel Award CSI Conference 2013
- Microbiology and Immunology Program Award of Excellence 2012
- Travel Award Keystone Cell Death Conference 2012
- Microbiology and Immunology Program Award of Excellence 2011
- Travel Award CSI Conference 2011
- University of Ottawa Graduate Admission Scholarship (May 2009)
- Winner – BMIGSA Award for Best Poster – PhD Poster Competition
- Award Winner Graduate Poster Competition - Immunology 2008
- NRC Teamwork and Group Achievement Award
- Dean's List for final 2 years of Undergraduate Degree
- Award Winner Honours Poster Competition Immunology section
- University of Ottawa undergraduate entrance scholarship - $2500
- Lo-Ellen Secondary School Graduation Faculty Award